# HEIFER INTERNATIONAL CENTER
**LITTLE ROCK, ARKANSAS**

**THE PENNSYLVANIA STATE UNIVERSITY**
**SCHREYER HONORS COLLEGE**

**DEPARTMENT OF ARCHITECTURAL ENGINEERING**

SIKANDAR PORTER-GILL
SPRING 2014

A thesis submitted in
partial fulfillment of the requirements for a Bachelor degree of Architectural Engineering
with honors in Architectural Engineering

Reviewed and approved* by the following:

Thomas Boothby
Professor
Thesis Supervisor

Richard Mistrick
Associate Professor
Honors Advisor

*Signatures are on file in the Schreyer Honors College

# HEIFER INTERNATIONAL CENTER

## LITTLE ROCK, ARKANSAS

## General Building Data

Construction dates | February 2004 to January 2006
Construction method | Construction Management at Risk
Height | 4 stories, 65 ft.
Size | 98,000 GSF
Cost | $18 million

PASS ON THE GIFT HEIFER® INTERNATIONAL

POLK STANLEY WILCOX ARCHITECTS

CROMWELL

## LEED Platinum Building

## Architecture

The semi-circular shape is influenced by Heifer International's goal to reduce world hunger and help communities in need. The circular form stems from the "ripple effect" produced from a community helped by the charity's donation of livestock. The LEED Platinum Building occupies a previously contaminated industrial site, that reclaimed wetland areas. An open floor plan maximizes day lighting gain and minimizes energy usage through light and occupancy sensors. The unique form of the roof diverts water to a five-story 20,000 gallon rainwater retention tank.

## Lighting/Electrical

Building provided with 480Y/277V system, with a total of 2000A.

- 1600A transferred to MDP, running at 3-phase, 4 wire

The L/E systems save approximately 57% over conventional buildings, due to:

- Natural day lighting
- Space occupancy sensors
- T5 lamps

## Structure

- Geopier™ Foundation System, with traditional piers and grade beams, supporting a slab on grade
- Framing consists mostly of 2'-0" diameter HSS, supporting a 2 ½" concrete slab on 3" composite deck, supported by a beam and girder system
- Wind and seismic loading is resisted by a steel plate shear wall system acting in both directions, for both the floor and roof diaphragms

## MEP Systems

- Ventilation units provide outside air
- VAV Underfloor Air Delivery for heating and cooling system on all floors, at 14,500 CFM
    - High efficient underfloor system due to limited pressure required
- MEP controlled by temperature, humidity, carbon dioxide and pressure sensors

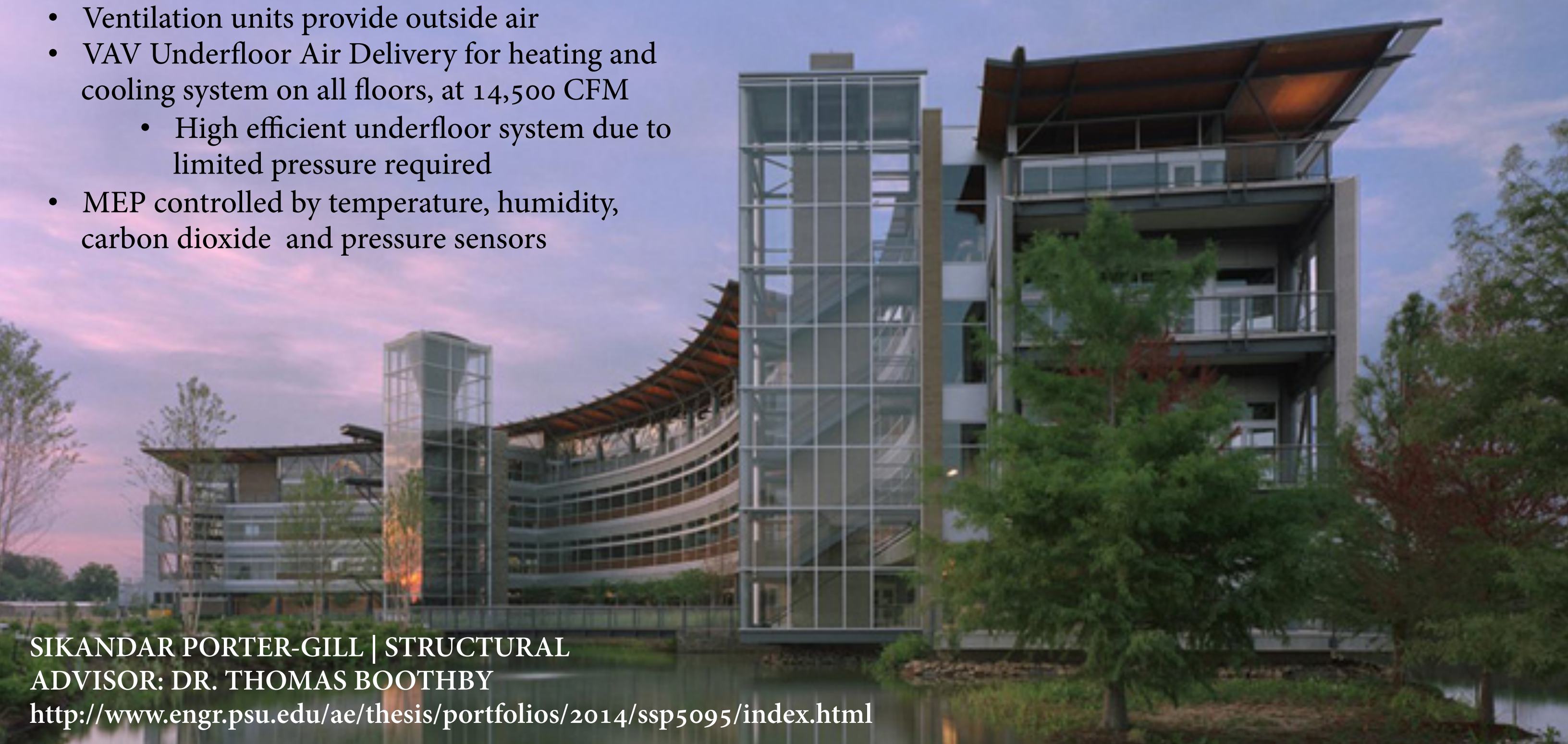

SIKANDAR PORTER-GILL | STRUCTURAL
ADVISOR: DR. THOMAS BOOTHBY
http://www.engr.psu.edu/ae/thesis/portfolios/2014/ssp5095/index.html

# ABSTRACT

Heifer International Center is located in Little Rock, Arkansas, and is the primary headquarters for Heifer International, a non-profit whose goal is to reduce world hunger and poverty. The architect wishes to pursue a new aesthetic look through the use of a different structural material, as the system is exposed. The new hybrid system of glulam and steel causes a reclassification of the building as Type IV, per the International Building Code 2009 §602.4, and prevents the use of the current Underfloor Air Distribution System. This obstacle leads to a new overhead VAV system, with new sizing of the supply and return ductwork required. A thermal bridge on the fourth level was also extensively studied and eliminated in a redesign involving new structural and wall components.

An architectural study was performed on the new exposed structural system. A guideline was established to aide with the design of not just the architectural components of the building, but to also positively lead the design of the engineering systems of the building. The desire to enhance the architecture by changing the structural material influenced mechanical, electrical and the interior aesthetic of the building. The use of glulam in the design provided a unique opportunity to investigate a queen post truss, which lends to integration between the mechanical and structural disciplines. Mechanical and electrical equipment was also incorporated into and hung from the truss.

The non-profit's goal is to reduce world hunger and help communities in need. This astonishing, semi-circular glass clad building is four stories high and roughly 490 feet by 62 feet wide, with a 98,000 gross square footage. It overlooks downtown Little Rock and the Arkansas River. The semi-circular shape of the building stems from the "ripple effect" produced from a community helped by the charity's donation of livestock. Heifer International Center is one of the few Platinum Certified LEED Buildings in the Southern United States. The building is oriented in the east-west direction, to maximize natural lighting. An inverted roof is used to divert rainwater to a five story tower, capable of storing 20,000 gallons of water. An additional goal of the project was to infuse the non-profit's core beliefs into the redesigned engineering systems.

# TABLE OF CONTENTS

# INDEX OF FIGURES

# INDEX OF TABLES

# INDEX OF KEY WORDS

## ACKNOWLEDGEMENTS

I wish to take a moment to express my gratitude towards the many people that took time out of their busy professional lives to help me with my thesis project. Of special importance, with without this project would not be possible are Heifer International, Polk Stanley Wilcox Architects and Cromwell Architects Engineers, Inc.

Additionally, the hours of dedication from the Pennsylvania State University's Architectural Engineering faculty warrants huge thanks. Especially,

- Dr. Thomas Boothby
- Prof. Heather Sustersic
- Dr. Walter G. M. Schneider III
- Prof. Kevin Parfitt
- Dr. Linda Hanagan
- Mr. Issa J. Ramaji
- Dr. Ryan Solnosky
- Dr. Richard Mistrick

Moreover, my friends whom inspired me to continue my work; as we each helped each other through the hardest parts of thesis,

| | |
|---|---|
| Natasha Beck | Macenzie Ceglar |
| Chris Cioffi | Angela Mincemoyer |
| Kristin Sliwinski | Alyssa Stangl |
| John Vais | |

In addition, I would like to thank Chelsea Billotte, Kieran Carlisle, Jeff Martin, Matt Neal and Faye Poon for their valuable input and patience throughout the semester.

Lastly, I would like to thank Prof. Moses Ling, Dr. Andrés Lepage, Prof. Robert Holland and Mr. Corey Wilkinson who encouraged me and dealt with my many questions over the past several years.

Heifer International | Polk Stanley Wilcox Architects | Cromwell Architects Engineers, Inc.

# CHAPTER 1

## THE HEIFER INTERNATIONAL CENTER

## 1.1 Introduction to the Building

Heifer International's headquarters mirrors Heifer's goal of reaching out to a community in need. Heifer International wished their headquarters to match what they were teaching to the world. The shape of the building and campus were inspired by Heifer International's founder Dan West who expressed, "In all my travels around the world, the important decisions were made where people sat in a circle, facing each other as equals." This was extended to show the ripple effect Heifer has on needy communities, through their donation of livestock. These communities agree to pass on the offspring of the animal to others—thus creating a ripple effect throughout the community.


Photo courtesy Timothy Hursley

Figure 1: Exterior view of Heifer International Center

Heifer International Center, shown in Figure 1, is a four-story office building, standing 65 feet tall, with 98,000 square feet. It was constructed between February 2004 and January 2006, at a cost of approximately $18 million. The design team from Polk Stanley Wilcox Architects and Cromwell Architects Engineers, Inc. were faced with the large challenge of providing an open office plan, in a semi-circular shape, while concurrently offering educational and visual interactions, and sustainable features that would express Heifer International's mission of ending world hunger and poverty. This was certainly a challenge for the design team—expressing the abstract meanings of the charity through the physical form of the building.

Heifer International Center continues Heifer's mission of teaching—the public is allowed access to the facility through tours provided by Heifer personnel, showcasing the sustainable features of the office building. This form of interaction with the building not only educates the community about sustainability, but attracts volunteers and workers to Heifer International — aiding in their desire to help needy communities.

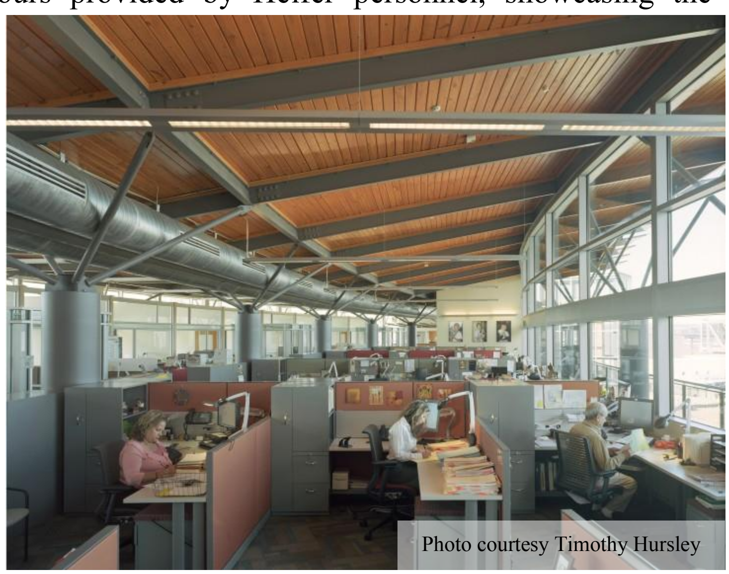
Photo courtesy Timothy Hursley

Figure 2: Interior view of Heifer International Center

The building has an open floor plan that allows natural light to penetrate to the center of each level, provides views of the river and cityscape, and offers extensive community exchange points with easy access to exterior balconies on each level. This is shown in Figure 2.

A unique feature of the building includes the use of a custom tree-column design that supports the inverted roof at both exterior and interior points. The tree column allows the inverted roof to cantilever over the fourth floor office. The roof is inverted for two reasons. The first is to direct rainwater toward the large silo-tower for storage and greywater use, while the second is to provide the ideal angle for a possible future solar panel array.

Heifer International Center is placed in an industrial section of Little Rock, Arkansas, that is currently being revitalized. This led to many advantages that the design team used to the building and site's benefit. The site that Heifer International Center occupies was contaminated with industrial waste, and through land reclamation, the soil was removed from the site and taken to a facility to be treated and used elsewhere in the Arkansas region. The site offered more than just the ability to help reclaim natural land—many bricks and other materials were found during the cleanup process. Most of these reclaimed materials were incorporated into the landscape, and a few were crushed down

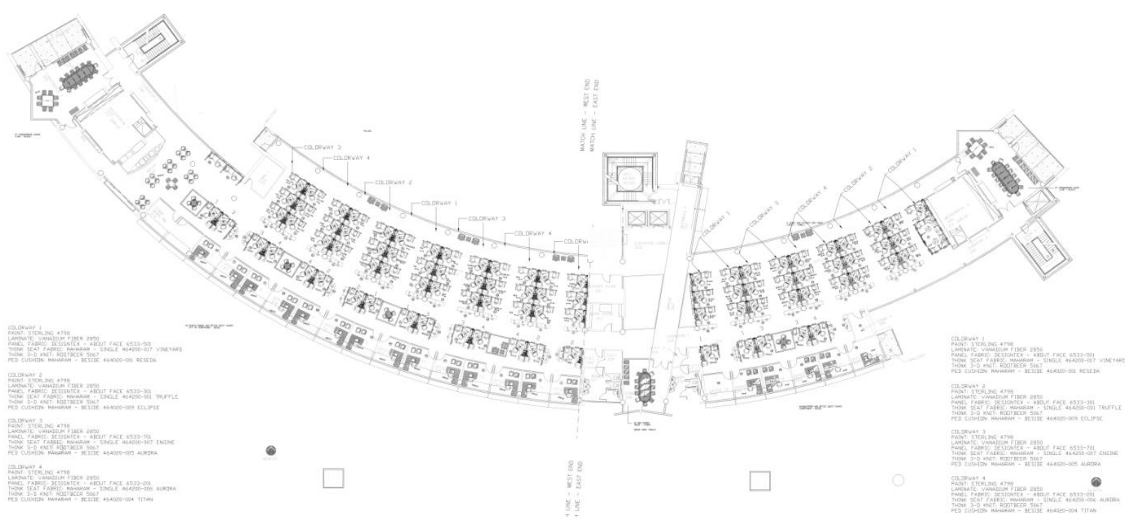

**Figure 3: Typical floor plan**

and used in the footings for the building. The industrial section of the city also housed the steel mill that manufactured Heifer International's steel structure—AFCO Steel Inc. is located only a few blocks away from Heifer's site. Additionally, the mostly glass-clad building is built using Ace Glass Co Inc. as the fabricator of the glass, located less than 100 yards from the building.

## 1.2 Existing Structural Information

Heifer International Center is a four story steel structure that is laterally supported by steel plate shear walls. The floor system is a composite decking system, which is supported with large HSS pipes for the framing system. The framing system bears onto a system of piers and footings. Grade beams also bear onto the system of piers and footings but support the slab-on-grade instead. A section of the Ground Level is recessed into the ground 2'-0" to accommodate a larger mechanical room.

## Foundation System

### *Geotechnical Report*

Grubbs, Hoskyn, Barton & Wyatt, Inc. performed a geotechnical survey of the site in January of 2003. The survey[1] encountered expansive clays on the east side of the building and soft and compressible soils on the west side of the building. Expansive clays expand when they gain water, and contract when they lose water—potentially heaving, or raising, the site elevation four and eight inches. On the east side, the report recommended that the weak soils should be undercut during site grading—approximately 4'-0" to 6'-0". Undercutting involves removing the soil to the specified depth and replacing it with compacted engineered soil. The soil removed would be replaced with low-plasticity clayey sand, sandy clay or gravelly clay. The geotechnical engineer stated that undercutting would allow the use of a slab-on-grade system; however, the use of two potential systems to increase the bearing capacity of the soil would have to be implemented.

The geotechnical engineer recommended either Rammed Aggregate Piers or Drilled Piers, for the foundation system. A Rammed Aggregate Pier® (RAP) System by Geopier Foundation Company, Inc., is used to mechanically improve the soil conditions of the site. The RAP system uses "vertical ramming energy" to add layers of crushed aggregate to the site. Generally, Geopiers™ are formed by drilling 30-inch diameter holes and ramming aggregate into the hole, until a "very stiff, high-density aggregate pier[s]" are formed. This crushed aggregate increased the soil's capacity to between 5 to 7 ksf for the Heifer International Center. Additional Geopiers™ were provided per structural drawings, due to larger loads or the higher potential for uplift at certain sections of the building. The geotechnical engineer stated, "Total settlement of shallow footings on Geopier™ elements would be expected to be less than about 1.0 inch and differential settlement less than about 0.5 inch."

### *Foundation Design*

The design teams chose a RAP® System, which allowed the use of conventional slab-on-grade, footings and grade beams. The RAP® System had the added benefit of increasing the bearing capacity and decreasing the size of the footing.

Heifer International Center also is provided with grade beams to distribute loads to column piers and footings. These grade beams support the slab and prevent the slab from deflecting or settling. The design uses various sizes of grade beam, which are reinforced using #4 stirrups at 24" O.C. #5 and #8 longitudinal reinforcing bars are also used.

[1] Geotechnical survey provided by Polk Stanley Wilcox Architects with permission from owner.

## Gravity Systems

### *Floor System*

Heifer International Center's floor system is composed of girders and beams supporting composite steel deck filled with a concrete slab. The greater part of the beams supporting the floor system are W16x26s and W14x22s, shown in yellow and orange in Figure 4. Each beam has a camber ranging from ¾" to 1". The framing nearer the center of the building is irregular due to the large interior architectural opening, walkway bridge and lobby space, shown in blue on Figure 4. The framing at each end of the building, on the east and west, is also irregular due to the large mechanical spaces, cantilevered balconies and stairwells, shown in blue on Figure 4. The mechanical spaces are generally supported by W16 beams.

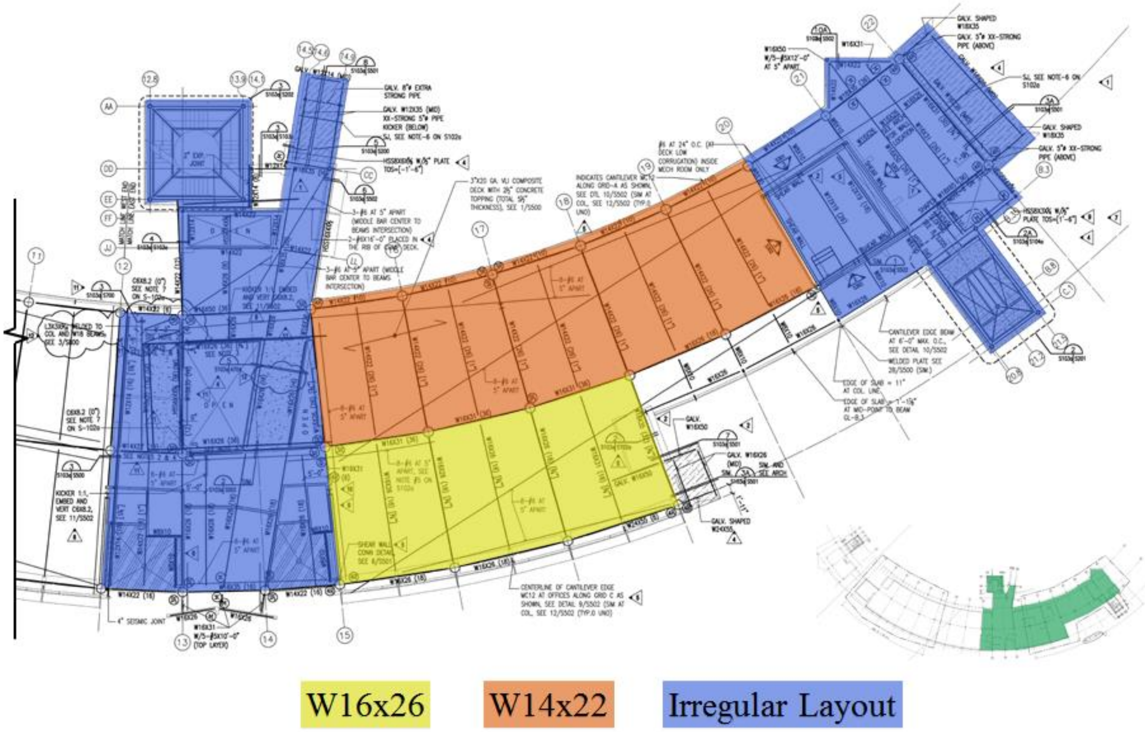


**Figure 4: Comparison of typical framing layout**

Each floor of the Heifer International Center has a similar layout to that shown in the half-plan in Figure 4 above.

A typical bay is 20'-0" x 30'-0", where the floor is supported by a system of beams and girders. The beams and girders collect the loads of the 3VLI 20 gauge composite deck with 2 ½" of normal weight concrete topping for a total thickness of 5 ½". The decking compositely acts with the framing members to take advantage of concrete in compression and steel in tension. A detail showing the composite deck configuration with a wide-flange is shown in Figure 5. In addition, at the edges of the building (or the interior sections that are open to below) the composite deck is ended with a bent edge plate.

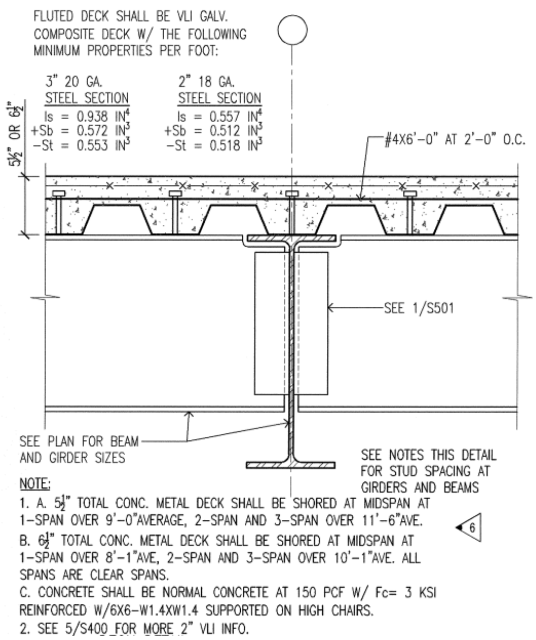


**Figure 5: Interior composite decking detail**

It should be noted that all of the floor slabs, although they are supported by the composite decking, are also reinforced with #4 at 6" O.C. in order to control cracks that occur naturally over the girders. This cracking occurs when the slab tries to take tension to make the beam continuous over the girder. A reason for the insertion of this reinforcement is to reduce the magnitude of the deflection occurring at each level due to the use of under-floor air distribution plenums for the mechanical system.

### *Framing System*

The framing system consists of large round HSS shapes, which continue from the ground level to the fourth floor. Originally concrete columns were considered; however, the contractor and steel fabricator where particularly concerned about tolerances maintaining tolerances on concrete columns, and the attendant difficulty of connecting to the beams. Due to these concerns, the design was changed to round steel, HSSs, which vary from 10" to 24" in diameter. A photograph of the HSS during the erection process is shown in Figure 6.

### *Roof System*

The roof-framing plan varies from the floor framing plans—due to the tree-column designs that flare out on the fourth level and attach to the roof girders. These girders support steel beams, which in turn support a timber wood roof deck. The roof cantilevers approximately 8'-0" beyond the edge of the building, while simultaneously inverting the roof to form a valley. A Thermoplastic Membrane topped with a 4" glued laminated wood decking makes up the first two layers of the roof, Figure 8. The wood decking has a tongue-and-groove assembly and is connected to 3" of continuous wood lumber using 8d nails at 6" O.C. This system is bolted to the top flange of the roof steel members. The roof system is shown in Figure 8 and connects to the flare connection shown in Figure 7.


**Figure 6: Photograph during erection of HSS framing**

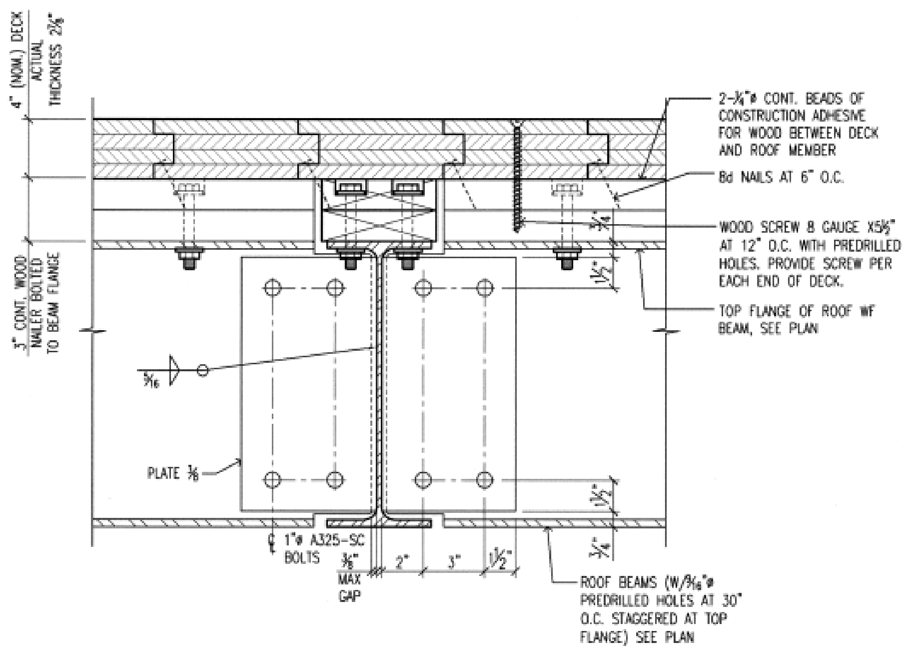


Figure 8: Detail connection of roof wide flange to T&G

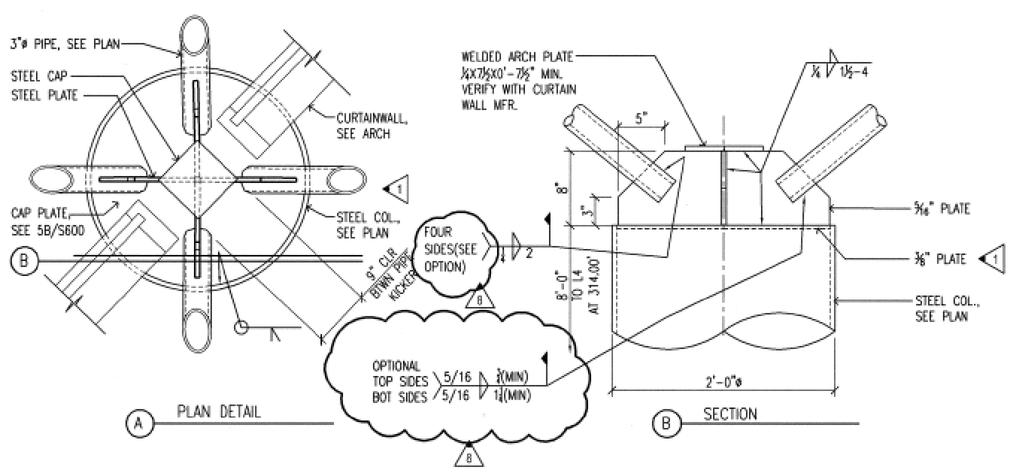


Figure 7: Roof tree-flare connection detail

## Lateral System

Heifer International Center is a four story steel structure and is laterally supported by steel plate shear walls. The floor system is a composite decking system, which is supported with large HSS pipes for the framing system. The framing system bears onto a system of piers and footings. A section of the Ground Level is recessed into the ground 2'-0" to accommodate a larger mechanical room.

A typical steel plate shear wall (SPSW) is shown in Figure 9, which shows the continuous shear plates that are installed into the wall system. For clarity, the shear plates are shown in red, in both section and plan. These plates are reinforced with C-channels spaced at 24" O.C., welded perpendicular to the shear plates attached to the wall. The C-channels are shown in blue in Figure 9 below. Several shear walls along the ground floor use a composite steel plate shear wall and CMU masonry back wall, which is approximately 6" thick.

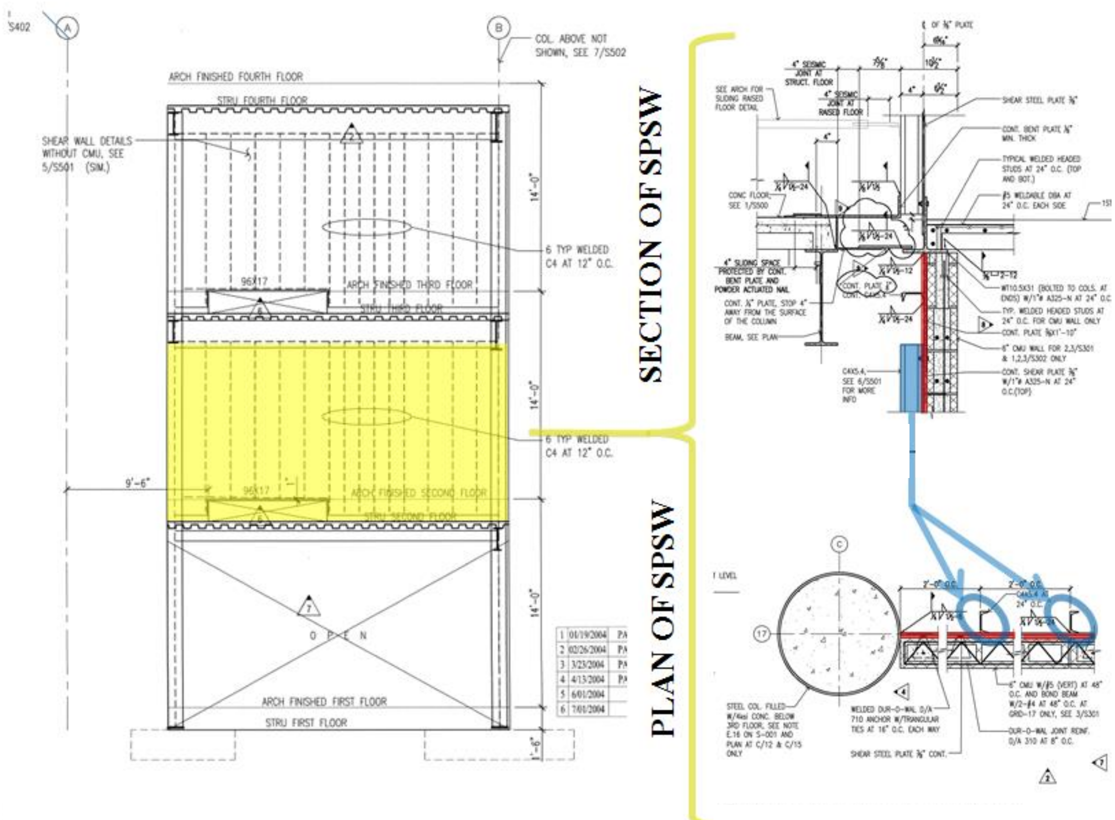


Figure 9: Typical SPSW elevation, section and plan

Lateral stability is ensured in part by the floor deck, which acts as a rigid diaphragm spanning between SPSWs. SPSWs resist horizontal shear, and effectively act as a vertical girder—the columns act as the flanges and the steel plate acts as the web. The SPSWs span from the foundation to the bottom of the fourth floor. The floor slab is also reinforced with additional #6 at 5" O.C. to assist with diaphragm action of lateral loads during a seismic event. According to the design team, this reinforcement is very important around floor openings—analogous to reinforcing openings in the flange of a beam.

Lateral loads at the roof are collected by the roof deck diaphragm and then transferred to the round steel columns, passing through the flare out connections of the tree-columns. This lateral load from the columns is transferred to the fourth floor diaphragm, and the lateral load is collected by the SPSWs.

Due to the irregularities of the building's shape and the 440'-0" length, the semi-circular building was divided into two approximately even sections with a seismic joint. These two halves were analyzed separately for lateral loads, using both static and dynamic methods. Essentially, two separate structures, with separate lateral systems, are joined together to act as one unit. For this technical report, only the east side of the building was analyzed.

## Joint Details

### *Bolted Connections*

Most of the connections are shear connections in Heifer International Center, and are bolted in three or four rows. This is shown in Figure 10 below.

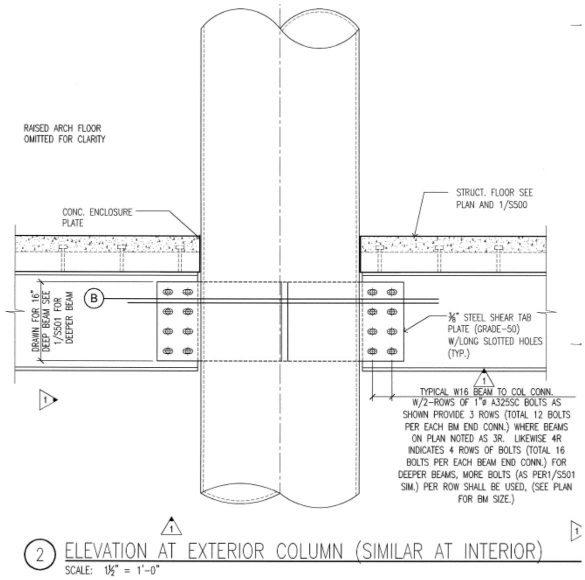


**Figure 10: Typical shear connection**

### *Moment Connections*

Small, cantilevered balconies are anchored to the building using moment connections, which is shown in Figure 11.

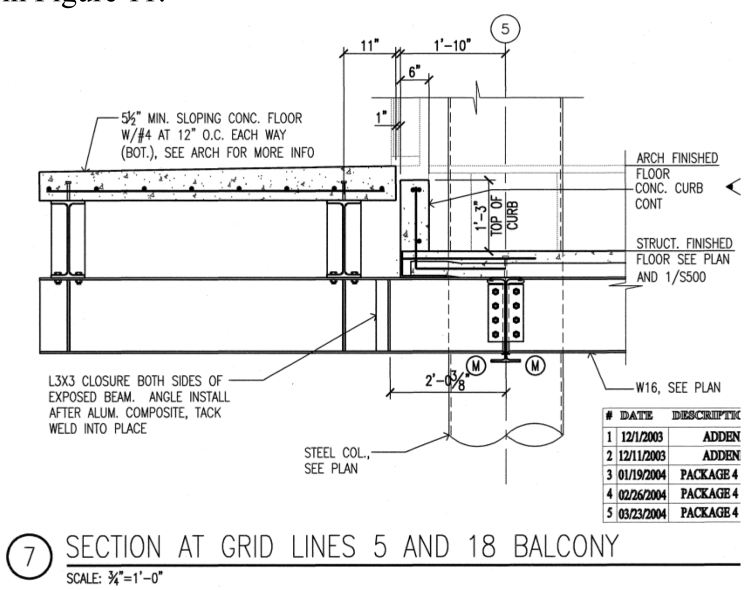


| # | DATE | DESCRIPTIO |
|---|---|---|
| 1 | 12/1/2003 | ADDEN |
| 2 | 12/11/2003 | ADDEN |
| 3 | 01/19/2004 | PACKAGE 4 |
| 4 | 02/26/2004 | PACKAGE 4 |
| 5 | 03/23/2004 | PACKAGE 4 |

**Figure 11: Typical moment connection supporting**

### *East and West End Balconies*

Heifer International Center has large balconies on the east and west that use a shear connection to attach to the building. These balconies are also supported by tension members, HSS pipes. Figure 12 shows a detail section of how the balcony is supported by the shear connection and pipes.

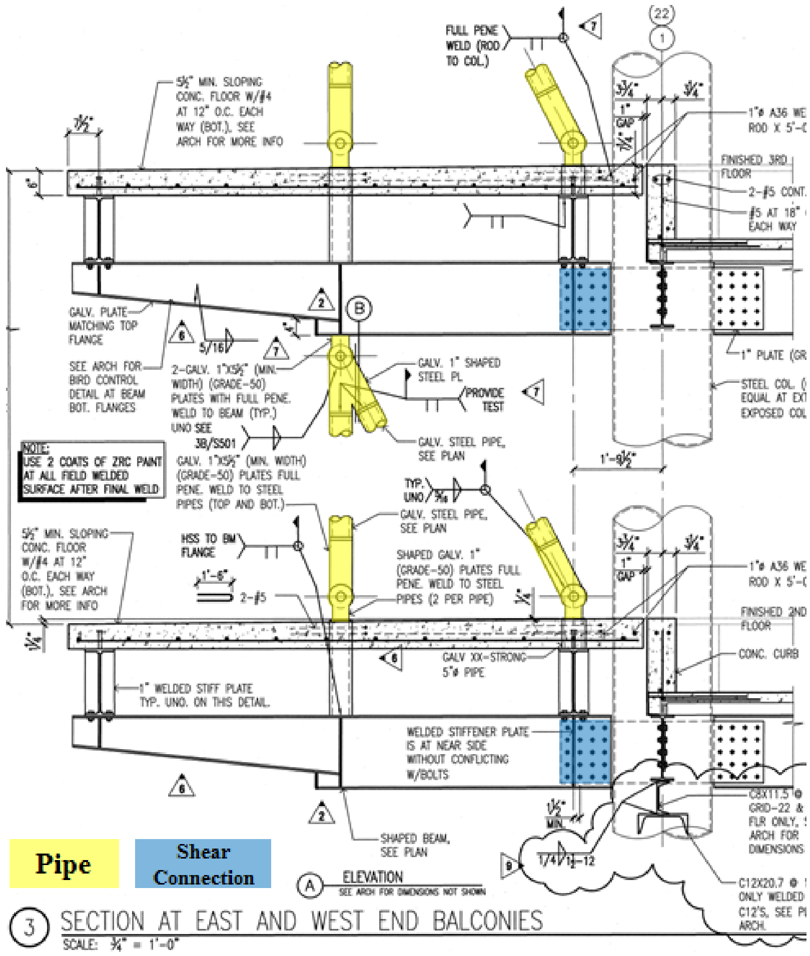


Figure 12: Typical balcony section

### *Seismic Joint*

Due to Heifer International Center's semi-circular shape and the extreme length of the building, a seismic joint was installed at each level between the second and fourth stories. A seismic joint is placed between the abutments of the two halves of the building—in order to moderate damage during an earthquake. A seismic joint is similar to an expansion joint; however, it can accommodate movement in both perpendicular and parallel directions. The design for the seismic joint used at each level is shown in Figure 13 and the actual seismic joint during construction is shown in Figure 14.

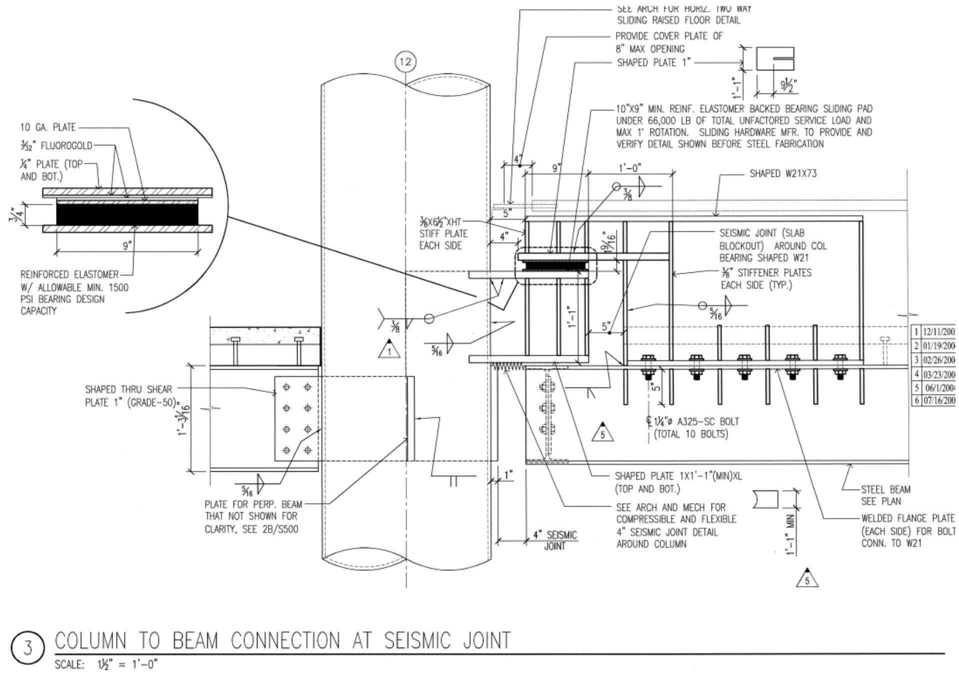


**Figure 13: Seismic joint detail**


**Figure 14: Photograph of seismic joint**

## 1.3 MATERIALS

Heifer International Center used the following materials. Their respective stress and strength properties are provided below.

### Concrete

| | Minimum Strength (ksi) | Air Entraining | Water Reducing Admix Required |
|---|---|---|---|
| Reinforced Footing | 3 | None | Yes |
| Reinforced Walls, Grade Beams and Columns | 4 | 5% AIR | Yes |
| Interior Slab on Grade | 3 | None | Yes |
| Typical Floor Slab | 3 | None | Yes |
| Walkway | 3 | 5% AIR | Yes |
| Precast Column, Plank | 5 | 5% AIR | Yes |

Table 1: Concrete properties used in original design

### Steel

| Shape | ASTM | Grade | Fy (ksi) |
|---|---|---|---|
| Beams and Girders | A992 or A572 | 50 | 50 |
| Hollow Round Columns | A252 | 3 | 45 |
| Columns | A992 or A572 | 50 | 50 |
| Tube Members | A-500 | B | 46 |
| Plates | A-36 | 5% | 36 |
| Misc. Steel | A-36 | None | 36 |
| Connection Bolts | A325-SC | - | - |

Table 2: Steel properties used in original design

### Other Material

| Material | ASTM | Notes |
|---|---|---|
| Concrete Masonry Units | C-90 | Lightweight, Type I<br>Moisture Controlled<br>$f'_m = 1500$ psi |
| Mortar | C-270 | Type S<br>$f'_m = 1800$ psi |
| Grout | | $f'_c = 2500$ psi |
| Reinforcing Bars | A-615 | Fy = 60 |

Table 3: Other material properties used in original design

## 1.4 DETERMINATION OF DESIGN LOADS

This piece of the report reviews the loads used in the design of Heifer International Center, and other local Arkansas laws that influenced the design and construction. It should be noted that these may not be the same values used in the redesign of the building, discussed further in the report.

### National Code for Live Load and Lateral Loads

| Live Load | ASCE-7 1998 Chapter 4 |
|---|---|
| Wind Load | ASCE-7 1998 Chapter 6 |

### Gravity Loads

#### *Live Loads*

Live loads used in the design of Heifer International Center were referenced using ASCE-7 1998 Chapter 4.

#### *Dead Loads*

Dead load allowances were assumed for the typical floor at 95 PSF and roof at 30 PSF. The 95 PSF floor load takes into account the composite decking, potential ponding of concrete, computer technology, mechanical and sprinkler infrastructure.

### Snow Loads

Ground snow loads for Pulaski County Arkansas are 10 PSF, according to ASCE-7 1998 Chapter 7; however, the timber roof loads increased the design load to 30 PSF due to the high possibility of snow drift into the valley of the roof.

### Rain Loads

Rain loads were calculated for Heifer International Center using ASCE-7 1998 Chapter 8.

### Lateral Loads

#### *Wind Loads*

Loads due to wind were calculated using ASCE 7 1998 Chapter 6. The design team used an Exposure Category C (§ 6.5.6.1), with a 90mph wind speed.

#### *Seismic Loads*

The geotechnical report states that the "…site is located in Seismic Zone 1," according to the Pulaski County Arkansas State criteria—an "area of low anticipated seismic damage." The design team referenced ASCE-7 1998 Chapter 9 and the Arkansas Act 1100, Zone 1, of 1991.

### Load Paths

#### *Gravity Load Path*

The composite deck will carry a load on a floor and transfer it to the beams and girders framing each level. As the floor system collects the load, the load is shifted to the framing system composed of large HSS pipes. This is transferred down to the ground level and is resolved onto piers, footings and grade beams. The foundation system dissipates this load into the soil that has been engineered using Geopier™ technology.

Roof loads follow a similar path, except the roof diaphragm is composed of wood timber instead of a concrete composite deck. The timber transfers the loads to steel beams and girders, which in turn distribute the loads to tree-column connections. These intricate connections dissipate the energy down to the foundation using the large HSS pipes that compose the framing system.

### *Lateral Load Path*

The façade of the building picks up the distributed load of the wind and transfers this to the floor diaphragm. The steel plate shear wall collects this horizontal force from the diaphragm and generates a vertical force down, towards the foundation system. The foundation system is then allowed to dissipate the base shear generated by the lateral loads.

## 1.5 Gravity Loads

The dead and live load used in the original design are tabulated below in Table 4 and Table 5, and were taken from the structural drawings. Table 5 references the total dead load used on the project. During analysis and redesign portions of this project, it was advantageous to have a breakdown of the floor dead loads. This breakdown is shown in Table 6[2].

| Live Loads | |
|---|---|
| **Occupancy or Use** | **Load (psf)** |
| Floors (typical) | 80 |
| Balcony | 100 |
| Stairs | 100 |
| Mechanical | 150 |
| Sidewalk | 250 |
| Roof Minimum | 20 |
| Snow Load | 10 |
| Ground Snow Load | 10 |

**Table 4: Live loads used in original design**

| Dead Loads | |
|---|---|
| **Occupancy or Use** | **Load (psf)** |
| Floors (typical) | 95 |
| Roof | 30 |

**Table 5: Dead loads used in original design**

| Breakdown of Floor Dead Loads | |
|---|---|
| **Occupancy or Use** | **Load (psf)** |
| Concrete and steel deck | 63 |
| Concrete ponding | 8 |
| Computers | 12 |
| Lights | 4 |
| Mechanical | 4 |
| Sprinkler | 3 |
| Miscellaneous | 1 |

**Table 6: Breakdown of floor dead loads used in original design**

[2] Breakdown of floor dead loads provided by Cromwell Architects Engineers, Inc.

## 1.6 Lateral System and Loads – Simplified Model

The Heifer International Center is laterally supported by steel plate shear walls. Due to the irregularities of the building's shape and the roughly 440'-0" length, the semi-circular building was divided into two approximately even sections with a seismic joint. These two halves were analyzed separately for lateral loads, using both static and dynamic methods. Essentially, two separate structures, with separate lateral systems, are joined together to act as one unit. For this technical report, only the east side of the building was analyzed.

Lateral stability is ensured in part by the floor deck, which acts as a diaphragm spanning between SPSWs. SPSWs resist horizontal shear, and effectively act as a vertical girder—the columns act as the flanges and the steel plate acts as the web. The SPSWs span from the foundation to the bottom of the fourth floor. The floor slab is also reinforced with additional #6 at 5" O.C. to assist with diaphragm action of lateral loads during a seismic event. According to the design team, this reinforcement is very important around floor openings—analogous to reinforcing openings in the flange of a beam.

Lateral loads at the roof are collected by the roof deck diaphragm and then transferred to the round steel columns, passing through the flare out connections of the tree-columns. This lateral load from the columns is transferred to the fourth floor diaphragm, and the lateral load is collected by the SPSWs.

Please see Lateral System on page 8 for further details.

## ETABS Model

The lateral system for Heifer International Center was modeled in CSi ETABS 2013. This structural modeling program was introduced in AE 530, Computer Modeling of Buildings. The complex geometry of the building was modeled in ETABS, and found to incorrectly execute. The building was simplified to a rectangle 64'-0" x 225'-0" long. The full length of the building was not used because of the seismic joint that splits the building at approximately its midpoint. It should be noted that in the redesign section of this project a model was developed which accounted for the full shape of the building.

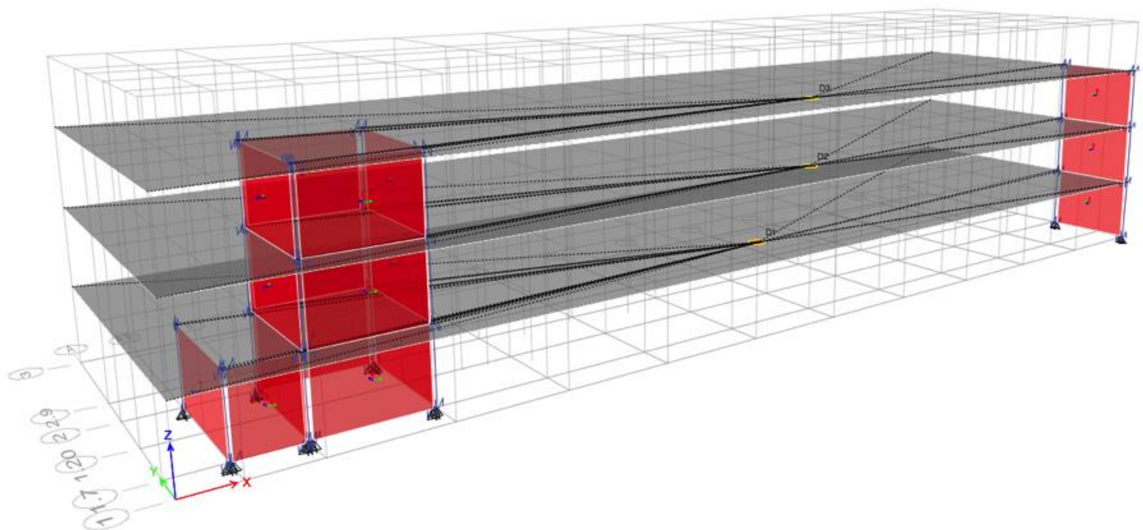

Figure 15: 3D view of ETABS model

### *Effective Steel Plate Shear Wall Depth*

Steel plate shear walls were converted to an effective depth of concrete, due to an instability error that occurred in the model. The simplified rectangular building was modeled with concrete shear walls, which were 2.98" thick. This workaround was possible using the stiffness equation for a shear wall that is assumed fixed-fixed at the top and bottom.

$$k = \frac{1}{\frac{h^3}{12EI} + \frac{1.2h}{AG}}, \qquad where\ I = {}^{tb^3}/_{12}\ and\ A = b \cdot t$$

Equation 1: Stiffness equation for fixed-fixed shear wall

The stiffness of the SPSW was calculated for the various base dimensions, and converted into an effective depth of a concrete shear wall (assuming $f'c = 4000\,psi$). These calculations can be found in Appendix A.1 - Existing Lateral System Modeling.

### *Computer Modeling Assumptions*

The gravity system of the building was not modeled in this technical report, only the lateral system. The floors were modeled as rigid diaphragms, to transfer the lateral load applied at each level. Heifer International Center has a composite deck and slab floor system, making it a good approximation of a rigid diaphragm performance. The base condition of the columns and walls were pinned, based on structural documents.

Structural documents indicated that the columns supporting the steel plate shear walls assisted with lateral interactions. An ETABS link was established between the modeled walls and columns, which were able to ensure the column and wall acted as one. A link was established between each column and floor, at each story level.

### *ETABS Model Validity*

The ETABS model proved to calculate forces that where within reasonable engineering judgment. This was based on the transfer of shear forces through the model, for a dummy load of 1000 kips at the top level, in the x-direction. The observed deflections and forces in each of the walls were realistic. This was further established using a built in ETABS shell stress distribution diagram, shown in Figure 16 below.

The dummy load is acting along the length of the building, in the x-direction. This is causing a tensile stress on the left side of the building's shear walls, and a compressive force on the right side of the shear walls.

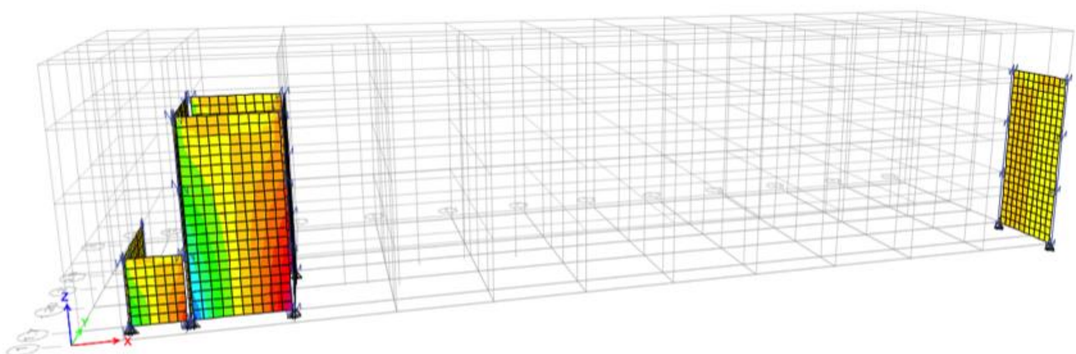

**Figure 16: ETABS shell stress distribution diagram**

The validity of the model was further confirmed by the inherent torsion formed in the shear walls, after a more detailed examination of the forces and the respective direction of force in each wall. Figure 17 depicts the inherent torsional force formed in the three vertical walls, with a dummy 1000 kip x-direction loading.

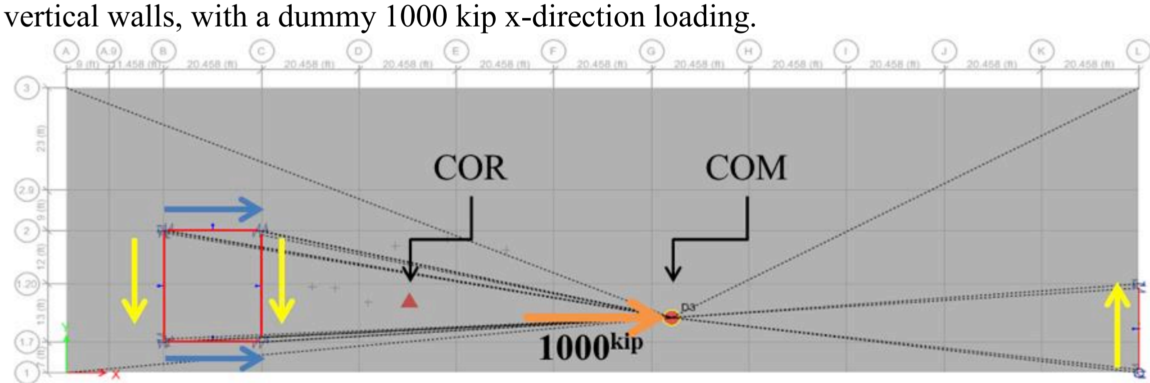


**Figure 17: Inherent torsional force formed in walls**

Seismic and wind loads also followed a conventional load path, further confirming the validity of the model. For a seismic load applied on the y-direction of the model, the shear forces increased as the load transferred down the building—supportive of normal shear transfer in buildings. This is shown in the 3D view of the building to the right, in Figure 18.

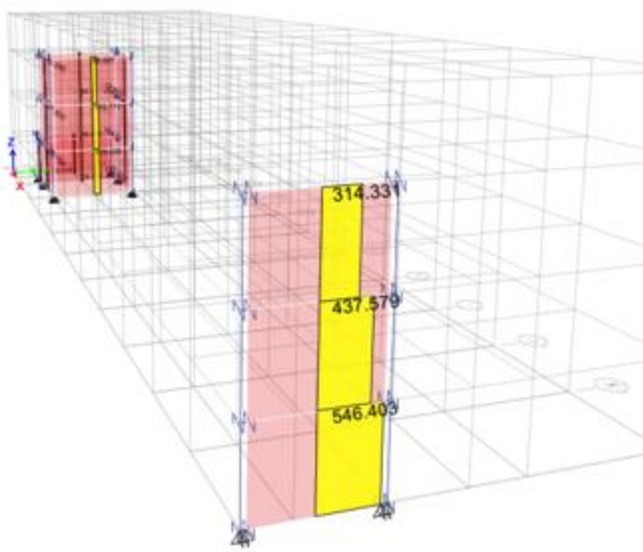


Figure 18: 3D view of shear transfer (seismic y-direction)

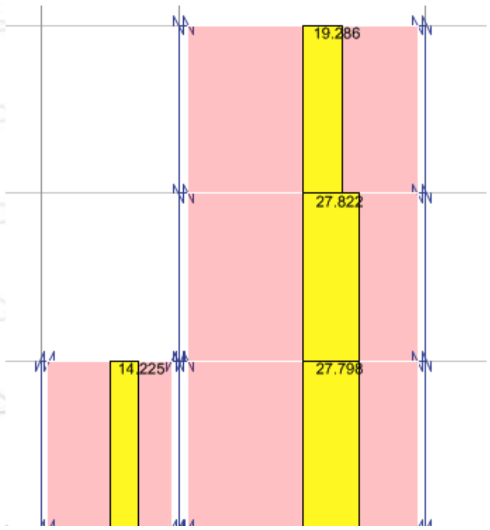


Figure 19: Elevation showing shear decrease on ground floor

A decrease in shear was found in one of the walls, that is explained by the increase in the number of shear walls on this floor. This can be seen on the ground floor of the elevation below, Figure 19, where the shear decreases in the larger shear wall, and is instead picked up by the smaller shear wall offset from the main shear wall on the ground story.

The center of mass and center of rigidity were calculated by the computer, and are shown in Figure 20 below.

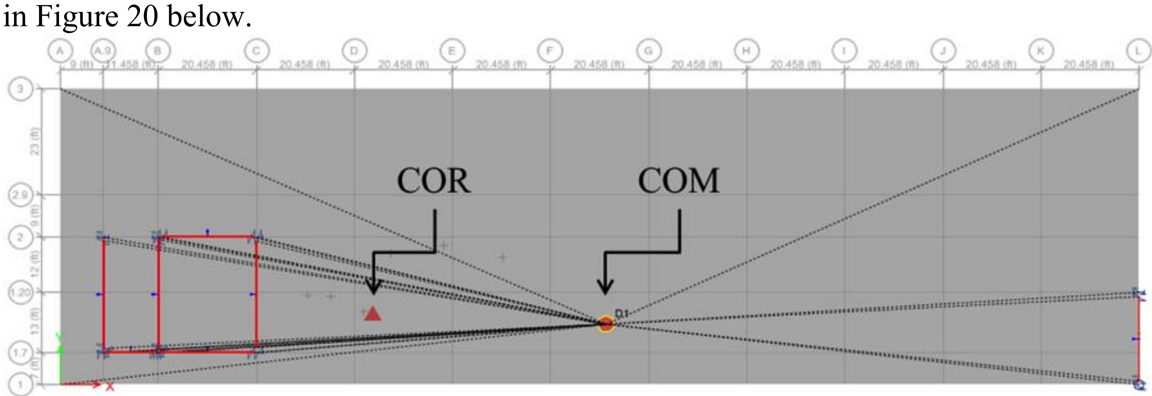


Figure 20: Center of mass and center of rigidity from ETABS

The ETABS model was programmed using pier labeling, and used the convention of Figure 21in referencing shear walls. This pier labeling convention is used throughout this report.

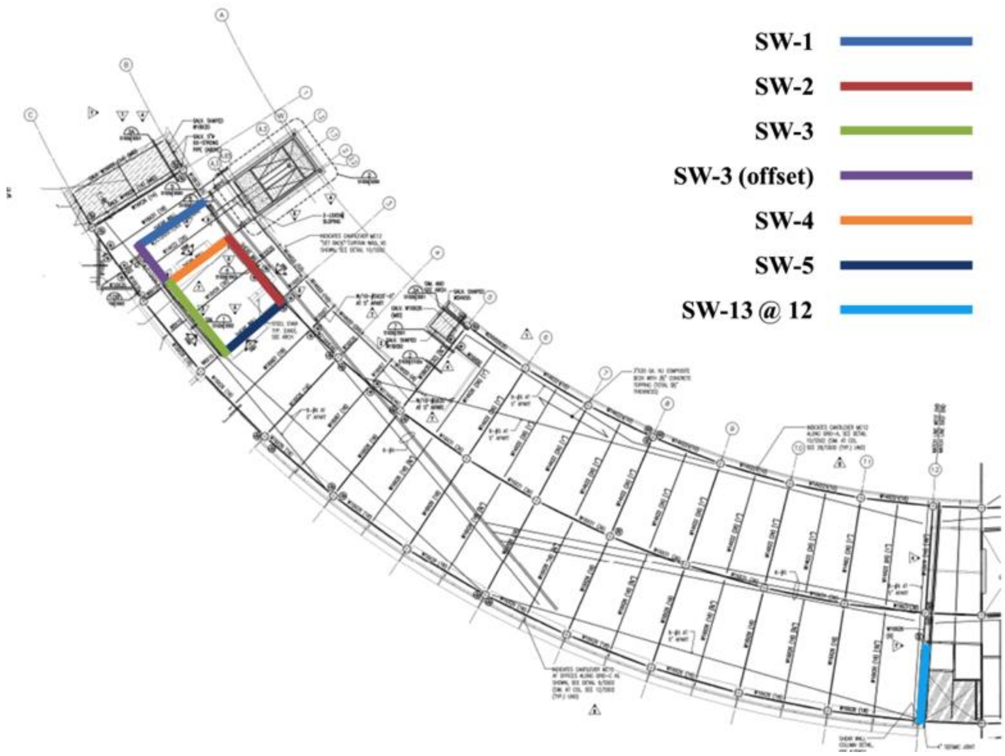


**Figure 21: Shear wall pier labeling convention for east side of the building**

## Seismic Loading

Heifer International Center is located in Little Rock, Arkansas in Seismic Design Category C. The seismic forces experienced by the entire building are summarized below, calculated in compliance with ASCE 7-1998.

| Level | w (kips) | $w*h^k$ | $C_{vx}$ | Story Forces |
|---|---|---|---|---|
| **Stair Tower Top** | 45 | 4025 | 0.008 | 12 |
| **Roof Story** | 2126 | 148691 | 0.307 | 425 |
| **Story 4** | 3436 | 161535 | 0.334 | 462 |
| **Story 3** | 3358 | 106928 | 0.221 | 306 |
| **Story 2** | 3358 | 56404 | 0.117 | 161 |
| **Story 1** | 3225 | 6529 | 0.013 | 19 |

**Table 7: Seismic Forces for Entire Building**

The entire seismic forces were divided by two, to conservatively distribute the forces to the east side of the building, due to the seismic joint. Stair Tower Top, Roof Story and Story 4 each are transferred to the top of the lateral system, which only spans to the base of the fourth floor, as previously discussed in past Technical Assignments. The loads were then analyzed in ETABS 2013 to calculate forces that would be distributed throughout the lateral system. Calculation of the North-South and East-West Seismic Loading can be found in Appendix A.2 - Existing Seismic and Wind Analysis, as well as calculation of inherent and accidental torsions, and the incorporation of amplification factors.

Seismic forces and initial torsional moments, assuming $A_x = 1.0$, were programed into the computer. Deflections at each level were determined for each of the four seismic cases and used to calculate the amplification factor for each respective case. The new amplified torsional moments were then set into the ETABS model, and used to calculate the final shear and moment in each shear wall of the building.

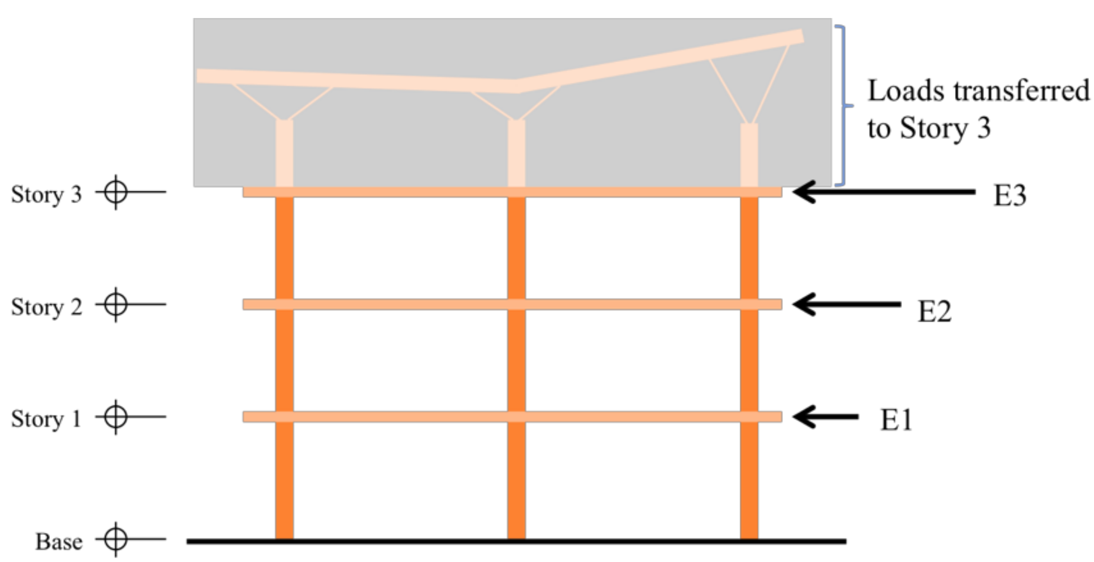


**Figure 22: Seismic loading distribution**

### *North-South Seismic Loading*

**Regular Earthquake Loading (Positive Moment)**

| | Forces | Moments | X Center of Rigidity | Y Center of Rigidity |
|---|---|---|---|---|
| **Story 3** | 449 | 11026.7 | 68.0288 | 17.6914 |
| **Story 2** | 153 | 3752.0 | 69.0701 | 18.2824 |
| **Story 1** | 81 | 1979.2 | 68.933 | 18.5144 |
| A 2.40 amplification factor has been applied to these loads | | | | |

Table 8: NS Regular earthquake loading (positive moment)

**Reverse Earthquake Loading (Negative Moment)**

| | Forces | Moments | X Center of Rigidity | Y Center of Rigidity |
|---|---|---|---|---|
| **Story 3** | 449 | 17592.8 | 68.0288 | 17.6914 |
| **Story 2** | 153 | 5986.2 | 69.0701 | 18.2824 |
| **Story 1** | 81 | 3157.7 | 68.933 | 18.5144 |
| A 1.60 amplification factor has been applied to these loads | | | | |

Table 9: NS Reverse earthquake loading (negative moment)

### *East-West Seismic Loading*

**Regular Earthquake Loading (Positive Moment)**

| | Forces | Moments | X Center of Rigidity | Y Center of Rigidity |
|---|---|---|---|---|
| **Story 3** | 449 | 1437.3 | 68.0288 | 17.6914 |
| **Story 2** | 153 | 489.1 | 69.0701 | 18.2824 |
| **Story 1** | 81 | 258.0 | 68.933 | 18.5144 |
| A 1.0 amplification factor has been applied to these loads | | | | |

Table 10: EW Regular earthquake loading (positive moment)

**Reverse Earthquake Loading (Negative Moment)**

| | Forces | Moments | X Center of Rigidity | Y Center of Rigidity |
|---|---|---|---|---|
| **Story 3** | 449 | 1437.3 | 68.0288 | 17.6914 |
| **Story 2** | 153 | 489.1 | 69.0701 | 18.2824 |
| **Story 1** | 81 | 258.0 | 68.933 | 18.5144 |
| A 1.0 amplification factor has been applied to these loads | | | | |

Table 11: EW Reverse earthquake loading (negative moment)

### *Analysis of Seismic Results*

It was found that the regular earthquake loading in the y-direction had the largest shear development in a steel plate shear wall, particularly; SW-13 at column line 12, with a shear of 546.403 kips. Calculations also showed that overturning due to earthquake controlled the design. An overturning moment of 24,276 kip-ft was found in both directions, because of the same story forces used in both directions.

Seismic drift was calculated by ETABS, and compared to the maximum allowable drift by code. Each inter-story drift, for each seismic load direction, passed. A tabulation of these results can be found on page 25.

### *Seismic Story Drift*

Drift induced by seismic loading was tabulated in ETABS, and compared to the maximum allowable drift, per ASCE 7-1998.

Seismic story drift from the computer model was amplified using the Deflection Amplification Factor, $C_d$, and the importance factor, $I_e$, using §9.5.3.7.1. This was then compared to the maximum allowable inter-story drift, calculated from Table 9.5.2.8. Each story, for each seismic load case, passed the allowable drift.

**East-West (EQ_X)**

| Level | Drift (in) | Story Height (ft) | Maximum Drift Allowed (in) | Delta*Cd/I | Pass |
|---|---|---|---|---|---|
| Story3 | 0.451619 | 14 | 3.36 | 1.354857 | PASS |
| Story2 | 0.351024 | 14 | 3.36 | 1.053072 | PASS |
| Story1 | 0.175374 | 14 | 3.36 | 0.526122 | PASS |

**East-West (EQ_X_REVERSE)**

| Level | Drift (in) | Story Height (ft) | Maximum Drift Allowed (in) | Delta*Cd/I | Pass |
|---|---|---|---|---|---|
| Story3 | 0.449367 | 14 | 3.36 | 1.348101 | PASS |
| Story2 | 0.349253 | 14 | 3.36 | 1.047759 | PASS |
| Story1 | 0.174545 | 14 | 3.36 | 0.523635 | PASS |

*Drift calculated using ETABS Model Joint 14, UX Direction

**North-South (EQ_Y)**

| Level | Drift (in) | Story Height (ft) | Maximum Drift Allowed (in) | Delta*Cd/I | Pass |
|---|---|---|---|---|---|
| Story3 | 0.045525 | 14 | 3.36 | 0.136575 | PASS |
| Story2 | 0.030472 | 14 | 3.36 | 0.091416 | PASS |
| Story1 | 0.016139 | 14 | 3.36 | 0.048417 | PASS |

**North-South (EQ_Y_REVERSE)**

| Level | Drift (in) | Story Height (ft) | Maximum Drift Allowed (in) | Delta*Cd/I | Pass |
|---|---|---|---|---|---|
| Story3 | 0.190831 | 14 | 3.36 | 0.572493 | PASS |
| Story2 | 0.144547 | 14 | 3.36 | 0.433641 | PASS |
| Story1 | 0.062941 | 14 | 3.36 | 0.188823 | PASS |

*Drift calculated using ETABS Model Joint 14, UY Direction

**Table 12: Existing seismic story drift**

The maximum drift allowed was calculated using the following table for ASCE 7-1998, for seismic loading.

**TABLE 9.5.2.8. Allowable Story Drift, $\Delta_a$[a]**

| Structure | Seismic Use Group I | Seismic Use Group II | Seismic Use Group III |
|---|---|---|---|
| Structures, other than masonry shear wall or masonry wall frame structures, 4 stories or less with interior walls, partitions, ceilings and exterior wall systems that have been designed to accommodate the story drifts | $0.025h_{sx}$[b] | $0.020h_{sx}$ | $0.015h_{sx}$ |
| Masonary cantilever shear wall structures[c] | $0.010h_{sx}$ | $0.010h_{sx}$ | $0.010h_{sx}$ |
| Other masonry shear wall structures | $0.007h_{sx}$ | $0.007h_{sx}$ | $0.007h_{sx}$ |
| Masonry wall frame structures | $0.013h_{sx}$ | $0.013h_{sx}$ | $0.010h_{sx}$ |
| All other structures | $0.020h_{sx}$ | $0.015h_{sx}$ | $0.010h_{sx}$ |

[a] $h_{sx}$ is the story height below Level $x$.
[b] There shall be no drift limit for single-story structures with interior walls, partitions, ceilings, and exterior wall systems that have been designed to accommodate the story drifts. The structure separation requirement of Section 9.5.2.8 is not waived.
[c] Structures in which the basic structural system consists of masonry shear walls designed as vertical elements cantilevered from their base or foundation support which are so constructed that moment transfer between shear walls (coupling) is negligible.

**Table 13: ASCE 7-1998 Table 9.8.2.8 for maximum story drift**

## Wind Loading

Wind loading on Heifer International Center was calculated using ASCE 7-1998, and simplified to a large rectangle that was 64'-0" x 491'-0". The four story building, with stair tower, results in several distributed loads along the height of the building. These loads can be resolved into point loads at each level. Once again, the Stair Tower, Roof and Fourth story are added to the lateral force on the top of the third story lateral system. ASCE 7-1998 requires tests of the four main wind cases, which are shown below.

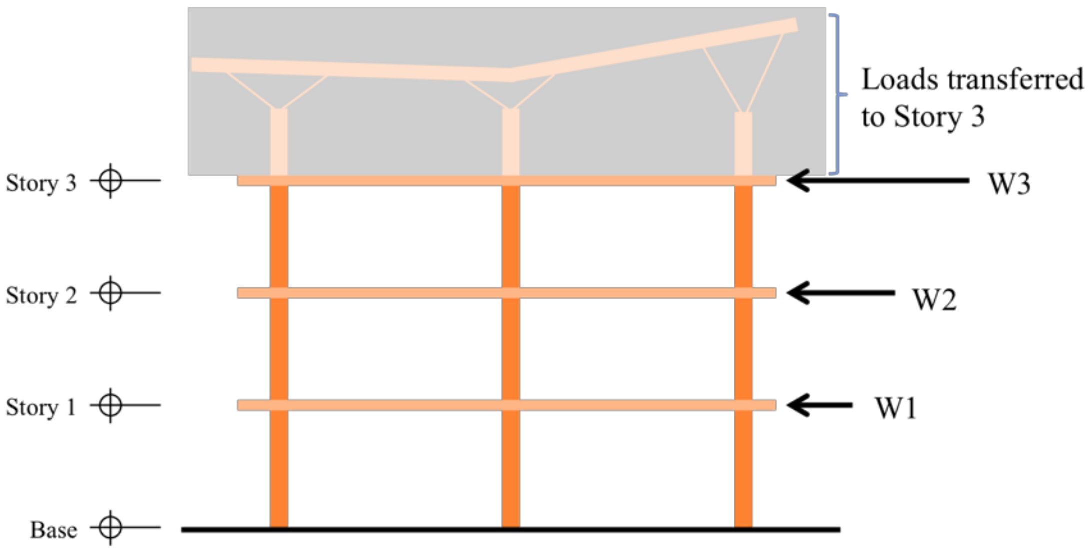


Figure 23: Wind loading distribution

### *Case 1*

A distributed load on each face is applied in the windward and leeward directions. These distributed loads were resolved into a single force in ETABS, for both directions.

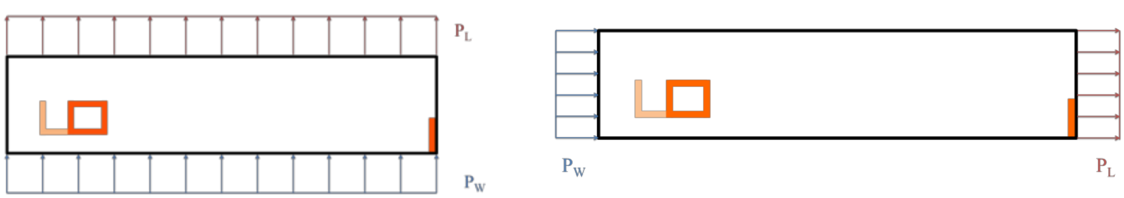


North-South, Y-Direction Loading East-West, X-Direction Loading

Figure 24: Wind analysis, Case 1, NS and EW

| | North-South, Y-Direction | | | East-West, X-Direction | | |
|---|---|---|---|---|---|---|
| | **Forces** | **X** | **Y** | **Forces** | **X** | **Y** |
| **Story3** | 71.46 | 112.519 | 32 | 130.80 | 112.519 | 32 |
| **Story2** | 20.03 | 112.519 | 32 | 38.13 | 112.519 | 32 |
| **Story1** | 18.65 | 112.519 | 32 | 34.99 | 112.519 | 32 |

Table 14: Wind analysis, Case 1

### *Case 2*

An unbalanced distributed load on each face was separated into two separate forces, acting in the X and Y directions. Only the worst case torsional effect on the building was tested. These distributions are shown below.

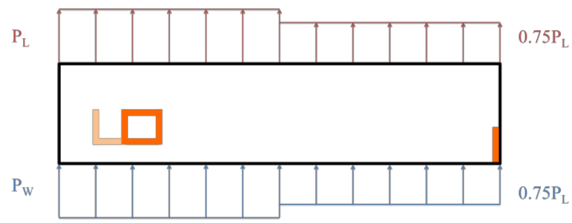


North-South, Y-Direction Loading

Figure 25: Wind analysis, Case 2, NS

**North-South, Y-Direction**

| | 1.0$P_W$ and 1.0$P_L$ | | | 0.75$P_W$ and 0.75$P_L$ | | |
|---|---|---|---|---|---|---|
| | **Forces** | **X** | **Y** | **Forces** | **X** | **Y** |
| **Story3** | 192.22 | 56.25 | 32 | 144.17 | 168.8 | 32 |
| **Story2** | 52.40 | 56.25 | 32 | 39.30 | 168.8 | 32 |
| **Story1** | 47.52 | 56.25 | 32 | 35.64 | 168.8 | 32 |

Table 15: Wind analysis, Case 2, NS

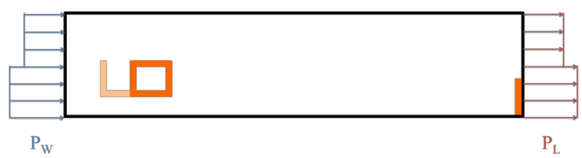


East-West, X-Direction Loading

Figure 26: Wind analysis, Case 2, EW

**East-West, X-Direction**

| | 1.0$P_W$ and 1.0$P_L$ | | | 0.75$P_W$ and 0.75$P_L$ | | |
|---|---|---|---|---|---|---|
| | **Forces** | **X** | **Y** | **Forces** | **X** | **Y** |
| **Story3** | 71.46 | 112.5 | 16 | 53.60 | 112.5 | 48 |
| **Story2** | 20.03 | 112.5 | 16 | 15.02 | 112.5 | 48 |
| **Story1** | 18.65 | 112.5 | 16 | 13.99 | 112.5 | 48 |

Table 16: Wind analysis, Case 2, EW

### *Case 3*

Similar to Case 1, a distributed load on each face is applied in the windward and leeward directions. These distributed loads were resolved into a single force in ETABS, for both directions.

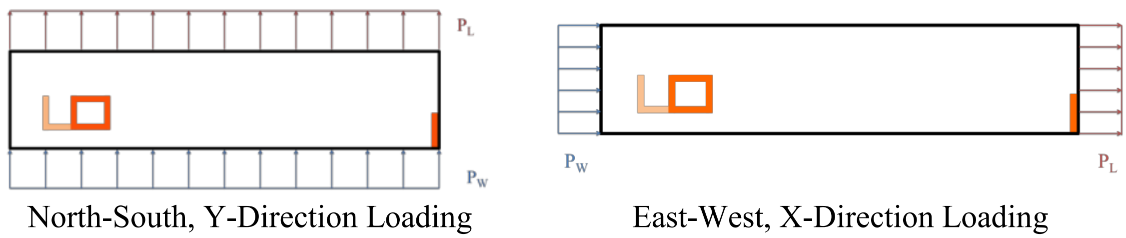


Figure 27: Wind analysis, Case 3, NS and EW

| | North-South, Y-Direction | | | East-West, X-Direction | | |
|---|---|---|---|---|---|---|
| | **Forces** | **X** | **Y** | **Forces** | **X** | **Y** |
| **Story3** | 144.17 | 112.5 | 32.0 | 53.60 | 112.5 | 32.0 |
| **Story2** | 15.02 | 112.5 | 32.0 | 15.02 | 112.5 | 32.0 |
| **Story1** | 13.99 | 112.5 | 32.0 | 13.99 | 112.5 | 32.0 |

Table 17: Wind analysis, Case 3, NS and EW

### *Case 4*

Case 4 is similar to Case 2. An unbalanced distributed load on each face was separated into two separate forces, acting in the X and Y directions. Only the worst case torsional effect on the building was tested. These distributions are shown below.

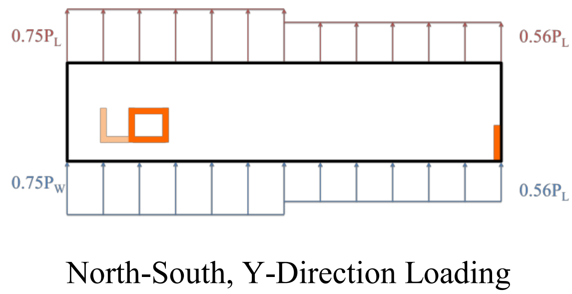


Figure 28: Wind analysis, Case 4, NS

**North-South, Y-Direction**

| | $0.75P_W$ and $0.75P_L$ | | | $0.56P_W$ and $0.56P_L$ | | |
|---|---|---|---|---|---|---|
| | **Forces** | **X** | **Y** | **Forces** | **X** | **Y** |
| **Story3** | 53.60 | 112.5 | 32.0 | 144.17 | 112.5 | 32.0 |
| **Story2** | 15.02 | 112.5 | 32.0 | 39.30 | 112.5 | 32.0 |
| **Story1** | 13.99 | 112.5 | 32.0 | 35.64 | 112.5 | 32.0 |

Table 18: Wind analysis, Case 4, NS

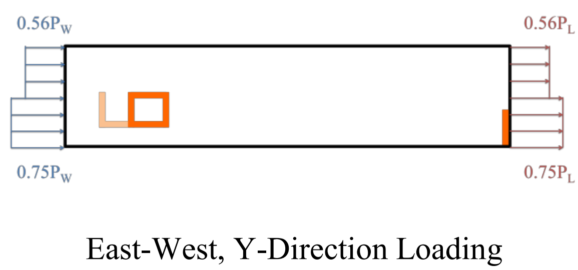


Figure 29: Wind analysis, Case 4, EW

**East-West, X-Direction**

| | $0.75P_W$ and $0.75P_L$ | | | $0.56P_W$ and $0.56P_L$ | | |
|---|---|---|---|---|---|---|
| | **Forces** | **X** | **Y** | **Forces** | **X** | **Y** |
| **Story3** | 64.26 | 112.5 | 16 | 40.02 | 112.5 | 48 |
| **Story2** | 17.84 | 112.5 | 16 | 11.22 | 112.5 | 48 |
| **Story1** | 16.46 | 112.5 | 16 | 10.45 | 112.5 | 48 |

Table 19: Wind analysis, Case 4, EW

### *Analysis of Wind Results*

Analysis of the four cases determined that case 2, in the y-direction would control the design of the lateral system. SW-13 at column line 12 experienced the largest shear, at 208.07 kips. ETABS calculated the drift of the highest level, for each wind case. These drift values were compared to the maximum drift allowed, of $^{l}/_{400}$. Each wind case passed the maximum drift. These results are tabulated below.

While overturning moment was not controlled by wind, it was found the largest moment experienced by the building's base would be 17,860.22 kip-ft due to wind case 2, in the y-direction.

### *Wind Building Drift*

| Load Case | Drift (in) | Maximum Drift Allowed (in) | Pass |
|---|---|---|---|
| WIND_C1_X | 0.258939 | 1.95 | PASS |
| WIND_C1_Y | 0.444476 | 1.95 | PASS |
| WIND_C2_X | 0.452212 | 1.95 | PASS |
| WIND_C2_Y | 1.027321 | 1.95 | PASS |
| WIND_C3_X | 0.194217 | 1.95 | PASS |
| WIND_C3_Y | 0.484402 | 1.95 | PASS |
| WIND_C4_X | 0.376172 | 1.95 | PASS |
| WIND_C4_Y | 0.767836 | 1.95 | PASS |

Table 20: Existing wind building drifts

## Torsional Irregularities

Table 9.5.2.3.2 states that if the maximum story drift is more than 1.2 times the average drift of a particular story, irregularity in the building will exist. It was found the torsional irregularities existed in the Seismic Design Category C structure; however, due to the simplified modeling of the building, this may in fact not be true. Torsional irregularity will be studied more in depth in the future.

**TABLE 9.5.2.3.2. Plan Structural Irregularities**

| Irregularity Type and Description | Reference Section | Seismic Design Category Application |
|---|---|---|
| 1a. Torsional Irregularity | 9.5.2.6.4.3 | D, E, and F |
| Torsional irregularity is defined to exist where the maximum story drift, computed including accidental torsion, at one end of the structure transverse to an axis is more than 1.2 times the average of the story drifts at the two ends of the structure along the axis being considered. Torsional irregularity requirements in the reference sections apply only to structures in which the diaphragms are rigid or semi-rigid. | 9.5.3.5.2 | C, D, E, and F |
| 1b. Extreme Torsional Irregularity | 9.5.2.6.4.3 | D |
| Extreme torsional irregularity is defined to exist where the maximum story drift, computed including accidental torsion, at one end of the structure transverse to an axis is more than 1.4 times the average of the story drifts at the two ends of the structure along the axis being considered. Extreme torsional irregularity requirements in the reference sections apply only to structures in which the diaphragms are rigid or semi-rigid. | 9.5.3.5.2<br>9.5.2.6.5.1 | C and D<br>E and F |
| 2. Re-entrant Corners<br>Plan configurations of a structure and its lateral force-resisting system contain re-entrant corners, where both projections of the structure beyond a re-entrant corner are greater than 15% of the plan dimension of the structure in the given direction. | 9.5.2.6.4.3 | D, E, and F |
| 3. Diaphragm Discontinuity<br>Diaphragms with abrupt discontinuities or variations in stiffness, including those having cutout or open areas greater than 50% of the gross enclosed diaphragm area, or changes in effective diaphragm stiffness of more than 50% from one story to the next. | 9.5.2.6.4.3 | D, E, and F |
| 4. Out-of-Plane Offsets | 9.5.2.6.4.3 | D, E, and F |
| Discontinuities in a lateral force resistance path, such as out-of-plane offsets of the vertical elements. | 9.5.2.6.2.11 | B, C, D, E, or F |
| 5. Nonparallel Systems<br>The vertical lateral force-resisting elements are not parallel to or symmetric about the major orthogonal axes of the lateral force-resisting system. | 9.5.2.6.3.1 | C, D, E, and F |

Table 21: ASCE 7-1998 Table 9.5.2.3.2 Plan Structural Irregularities

## Overturning Moment

The overturning moment of the building was calculated by ETABS for each of the seismic and wind cases tested. The resisting moment that is created by the weight of the building was conservatively calculated using the following assumptions:

1. The weight of the building, 15,549 kips, acted at the Center of Mass of the building, not at the geometric center of the building
2. The shortest moment arm of 13'-2" was used in the resisting moment calculation
3. Worst case moment, seismic loading of 24,279 kip-ft acts in either direction and must be resisted by the weight of the building

With these assumptions, a minimum resisting moment of approximately 136,000 kip-ft was calculated. Comparing this to the worst case overturning moment that the building may experience, a factor of safety of 5.6 exist between the worst case overturning moment and the lowest possible resisting moment. The calculation of the overturning moment and resisting moment can be found on the following page.

### *Foundation Impact*

The overturning moment check confirmed that the foundation was adequate for both wind and seismic loading. Uplift was not considered in these calculations and will have to be explored in more detail in the future.

## *Overturning Moment Calculations*

**Overturning Moment and Base Shear**

Center of Mass
X = 113.8292 feet
Y = 13.1533 feet

Building Effective Weight
$w$ = 15549 kip

**Wind Base Shear and Overturning Moment**

| Load Case | Base Shear Vx (kip) | Base Shear Vy (kip) | Overturning Moment Mx (kip-ft) | Overturning Moment My (kip-ft) |
|---|---|---|---|---|
| EQ_X | -683 | 0 | 0 | -24276 |
| EQ_X_REVERSE | -683 | 0 | 0 | -24276 |
| EQ_Y | 0 | -683 | 24276 | 0 |
| EQ_Y_REVERSE | 0 | -683 | 24276 | 0 |

225 feet

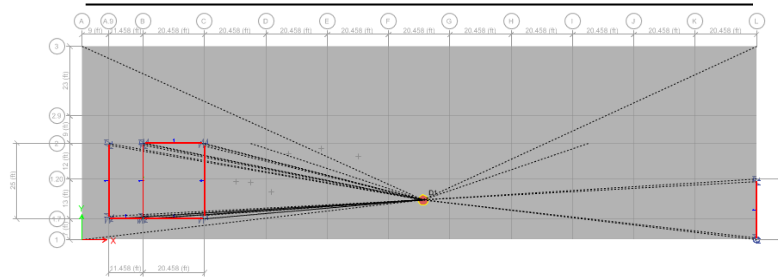

64 feet

**Wind Base Shear and Overturning Moment**

| Load Case | Base Shear Vx (kip) | Base Shear Vy (kip) | Overturning Moment Mx (kip-ft) | Overturning Moment My (kip-ft) |
|---|---|---|---|---|
| WIND_C1_X | -110.14 | 0 | 0 | -3823.26 |
| WIND_C1_Y | -203.92 | -22944.875 | 7051.1 | 0 |
| WIND_C2_X | -192.75 | 0 | 0 | -6690.88 |
| WIND_C2_Y | 0 | -511.25 | 17860.22 | 0 |
| WIND_C3_X | -82.61 | 0 | 0 | -2867.62 |
| WIND_C3_Y | 0 | -219.11 | 7654.5 | 0 |
| WIND_C4_X | -160.25 | 0 | 0 | -5570.18 |
| WIND_C4_Y | 0 | -382.71 | 13369.72 | 0 |

Maximum Moment = 24,276.00 kip-ft experienced by building (assume worst case moment in either direction)
Resisting Moment = 136,346.93 kip-ft from the weight of the building (assuming smallest moment arm and factor of safety of 1.5)

PASS

Factor of Safety = 5.62

## Energy/Virtual Work Diagram

The ETABS computer model was able to calculate the utilization of each member, for each load case. Figure 30 and Figure 31 illustrate how the steel plate shear wall is employed more in resisting lateral loads closer to the base of the building. It should be noted that in Figure 30 the SPSW utilization drops on the first floor, because of the additional shear wall offset on this floor, next to Shear Wall 3.

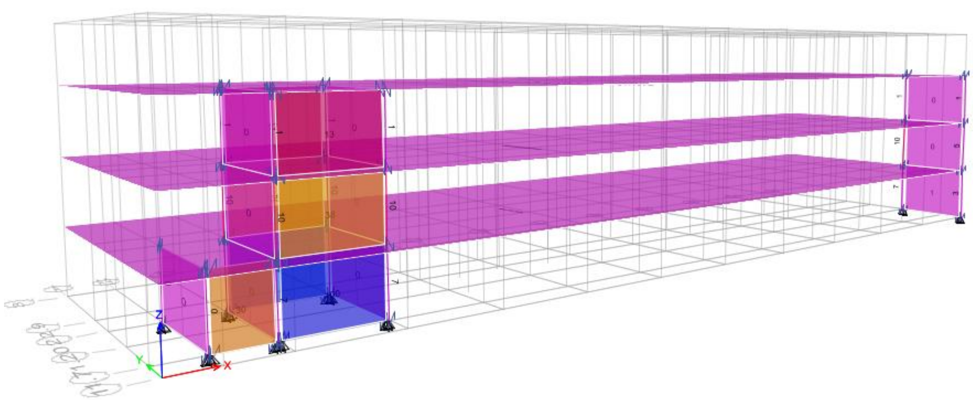

Figure 30: 3D view of member utilization, x-direction loading

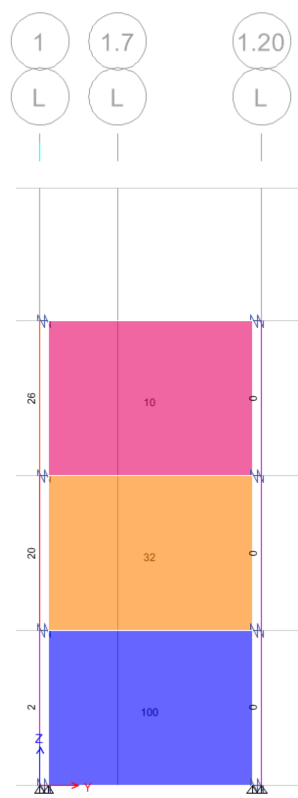


Figure 31: Member utilization of Shear Wall 13 at 12, y-direction loading

## Lateral System Spot Checks

The shear in each steel plate shear wall was calculated and compared, for each seismic and wind load case. The largest shear value was tabulated, and this shear wall was analyzed for shear capacity and deflection. This shear wall, SW-13 at column line 12 was controlled by seismic loads.

The ASCE 7-1998 was referenced for the load combinations, which are shown below in Figure 32.

**2.3.2 Basic Combinations**

Structures, components, and foundations shall be designed so that their design strength equals or exceeds the effects of the factored loads in the following combinations:

1. $1.4(D + F)$
2. $1.2(D + F + T) + 1.6(L + H) + 0.5(L_r \text{ or } S \text{ or } R)$
3. $1.2D + 1.6(L_r \text{ or } S \text{ or } R) + (0.5L \text{ or } 0.8W)$
4. $1.2D + 1.6W + 0.5L + 0.5(L_r \text{ or } S \text{ or } R)$
5. $1.2D + 1.0E + 0.5L + 0.2S$
6. $0.9D + 1.6W + 1.6H$
7. $0.9D + 1.0E + 1.6H$

**Figure 32: Basic Combinations for ASCE 7-1998**

The worst case load combination controlling was load case 5. Load case 7 was eliminated due to the lack of soil loads on Heifer International Center's lateral system. Load case 5 was calculated and applied to the shear walls. These detailed calculations are found on the following pages.

## *SPSW Load Combinations*

PORTER-GILL | | SHEAR WALL CHECK

CONTROLLING SHEAR WALL ⟶ SW-13 @ 12

CONTROLLED BY SEISMIC

$V_{MAX} = 546.403^k$

TRIB. AREA = 110 SF

LOAD CASES

(5) $1.2D + 1.0E + 0.5L + 0.2S$

(7) ~~0.9D + 1.0E + 1.6H~~ → REDUCES DL, ↑'s OT (NO SOIL LOADS)

(5) AXIAL LOADS

$P_U = 1.2D + 0.5L + 0.2S + 1.0E_{VERTICAL}$

$= 1.2[95\text{ PSF} \times 110\text{ SF}]3 + 0.5[80\text{ PSF} \times 110\text{ SF}]3$

$+ 0.2[10\text{ PSF} \times 0\text{ SF}]3 + 1.0[0.2(0.3704)(31.35^k)] \times 1000$

DISCONT. FROM ROOF

$= \boxed{53.14^k \text{ AXIAL}}$

$E_{VERTICAL} = 0.2S_{DS}D$ § 9.5.2.7 eqn. 1

$S_{DS} = 0.3704 > 0.125$ ⟶ YES INCLUDE VERTICAL COMPONENT

$\rho = 1.0$ b/c SDC C § 9.5.2.4.1

$D = 95\text{ PSF} \times 110\text{ SF} \times 3\text{ FLOORS} = 31.35^k$

PORTER-GILL | | SHEAR WALL CHECK

(5) LATERAL

$$L = 1.0\,E_{HORIZONTAL} = \rho Q_E$$

$\rho = 1.0$ b/c SDC C § 9.5.2.4.1

$Q_E = 546.403^k$

So,

$= 1.0(546.403^k) = 546.403^{kips}$

WE CAN CONCLUDE:

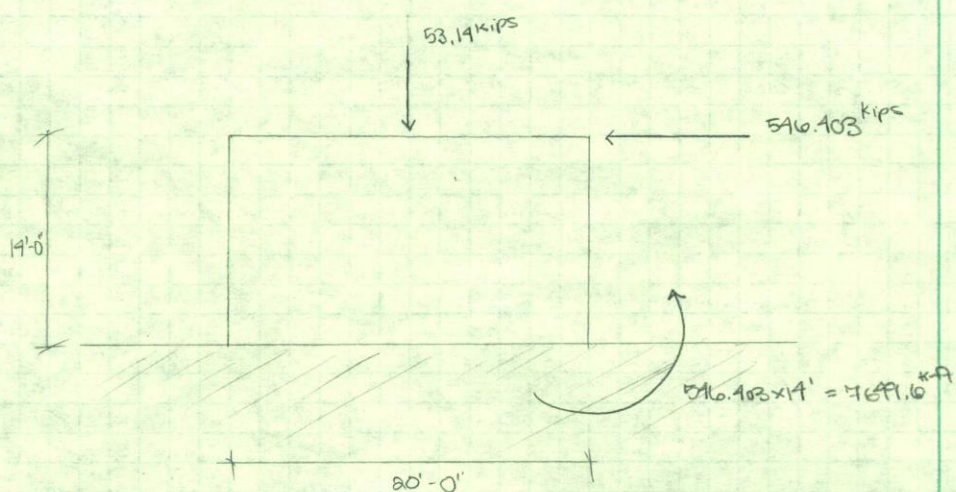

## SPSW Shear Capacity

PORTER-GILL | TECH REPORT 4 | SHEAR WALL CHECK

CHECK SHEAR CAPACITY OF SPSW:

$V_u = V_{max} = 546.403^k$ w/ QUAKE_Y

SPSW DETAILS:

$t_w = 3/8"$
$F_y = 36\text{ksi}$ STEEL, A36
$\phi = 0.9$ FOR SPSW

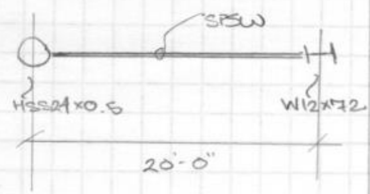


$\phi V_n = \phi \cdot 0.42 \cdot F_y \, t_w \, L_{cf} \sin(2\alpha)$

$L_{cf} = 20' - \left(\underset{W12x24}{12.3"/2} + \underset{HSS24}{24"/2}\right) / 12"/' = 18.4875'$

So, $\phi V_n = 0.9(0.42) \cdot 36 \cdot (3/8")(18.4875) \sin(2 \cdot 30°)$

CONSERVATIVELY ASSUME

$= 980.43^{kip}$

$[\text{if } \alpha = 45°, \ \phi V_n = 1119.9^{kip}]$

$\phi V_n = 980^k \geq 547^{kip} = V_u$ ✓ GOOD

EACH SPSW IS 3/8" THICK → ALL LOADS LOWER

SHEAR CAPACITY GOOD FOR ALL SPSW'S ✓

### *SPSW Deflection Check*

Deflection of the steel plate shear walls were checked at two joints, on each seismic and wind load case. These two joint locations passed the maximum allowed drift for seismic and wind loads. These results are tabulated below, with drift shown with respect to the direction of loading. Please refer to Figure 33 for the location of the two joints measured.

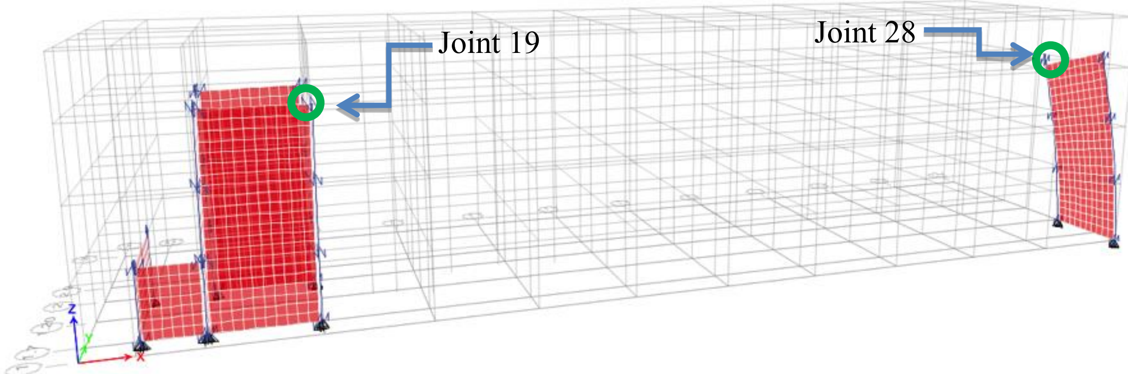


Figure 33: Diagram showing location of joints referenced

**Seismic Loading**

**Joint 19 at Shear Wall 3**

| Level | Drift (in)* | Story Height (ft) | Maximum Drift Allowed (in) | Pass |
|---|---|---|---|---|
| East-West (EQ_X) | 1.64307 | 14 | 3.36 | PASS |
| East-West (EQ_X_REVERSE) | 1.6392 | 14 | 3.36 | PASS |
| North-South (EQ_Y) | 0.40581 | 14 | 3.36 | PASS |
| North-South (EQ_Y_REVERSE) | 0.710209 | 14 | 3.36 | PASS |

**Joint 28 at Shear Wall 13@12**

| Level | Drift (in)* | Story Height (ft) | Maximum Drift Allowed (in) | Pass |
|---|---|---|---|---|
| East-West (EQ_X) | 1.6305 | 14 | 3.36 | PASS |
| East-West (EQ_X_REVERSE) | 1.63101 | 14 | 3.36 | PASS |
| North-South (EQ_Y) | 2.8103 | 14 | 3.36 | PASS |
| North-South (EQ_Y_REVERSE) | 1.10398 | 14 | 3.36 | PASS |

*Drift with respect to direction of loading

Table 22: Steel plate shear wall deflection check (seismic)

## Wind Loading

**Joint 19 at Shear Wall 3**

| Level | Drift (in)* | Story Height (ft) | Maximum Drift Allowed (in) | Pass |
|---|---|---|---|---|
| WIND_C1_X | 0.235866 | 14 | 1.95 | PASS |
| WIND_C1_Y | 0.182638 | 14 | 1.95 | PASS |
| WIND_C2_X | 0.3346 | 14 | 1.95 | PASS |
| WIND_C2_Y | 0.483166 | 14 | 1.95 | PASS |
| WIND_C3_X | 0.189796 | 14 | 1.95 | PASS |
| WIND_C3_Y | 0.199211 | 14 | 1.95 | PASS |
| WIND_C4_X | 0.369934 | 14 | 1.95 | PASS |
| WIND_C4_Y | 0.361898 | 14 | 1.95 | PASS |

**Joint 28 at Shear Wall 13@12**

| Level | Drift (in)* | Story Height (ft) | Maximum Drift Allowed (in) | Pass |
|---|---|---|---|---|
| WIND_C1_X | 0.255909 | 14 | 1.95 | PASS |
| WIND_C1_Y | 0.444476 | 14 | 1.95 | PASS |
| WIND_C2_X | 0.447805 | 14 | 1.95 | PASS |
| WIND_C2_Y | 1.027321 | 14 | 1.95 | PASS |
| WIND_C3_X | 0.191944 | 14 | 1.95 | PASS |
| WIND_C3_Y | 0.484402 | 14 | 1.95 | PASS |
| WIND_C4_X | 0.372965 | 14 | 1.95 | PASS |
| WIND_C4_Y | 0.767836 | 14 | 1.95 | PASS |

*Drift with respect to direction of loading

**Table 23: Steel plate shear wall deflection check (wind)**

### Lateral System Conclusion – Simplified Model

Computer modeling of the lateral system of Heifer International Center was performed for the building. Though the ETABS model of the curved office complex did not properly execute, a simplified version of the building was used in the analysis of the lateral system. Half of the building was modeled in ETABS due to the seismic joint that splits the building at approximately it's midpoint. Spot checks on lateral elements were performed, and the existing lateral system was found to be adequate for the loads anticipated on the structure.

Seismic loading in the North-South direction controlled the design, with a maximum base shear of 550 kips. The controlling case for wind loading was the y-direction, using Case 2, at a base shear of 210 kips. The 550 kip lateral force was used in the verification of the shear capacity of the steel plate shear wall. This maximum lateral force on the ground level, that the steel plate shear wall must endure, passed with over 400 kips of reserve shear capacity. Each shear wall in the model is the same thickness, thus all shear walls in the building are adequate. Deflection of the shear wall was also tested, and found to pass for both seismic and wind loading. The existing lateral system was found to be sufficient for lateral loads for the Heifer International Center.

Inter-story drift and building drift were found to be within the ASCE 7-1998 maximum allowable drift. Furthermore, the overturning moment was found to have no impact on the foundation system.

A more all-inclusive and definitive computer model was developed later in the report, which can be found in section
2.2 Lateral System Redesign, which more accurately modeled the building and its reaction to various lateral loadings.

## 1.7 Problem Statement

The Heifer International Center is currently framed in steel with a composite deck; however, the architect wishes to consider a hybrid system of glulam and steel. Their intention is to see if the architectural features of the Education and Visitor Center, a smaller building next door, may also be applied to the Heifer International Center. In addition, a floor system will need to be researched, compared and selected.

The previous Technical Reports II and IV analyzed the existing building's gravity and lateral systems, under ASCE 7-1998. Technical Report III analyzed alternative floor systems using ASCE 7-2010. Each phase of the redesign will reference ASCE 7-2010.

The redesign will affect mechanical and architectural characteristics of the Heifer International Center. Their affects will need to be considered in a systems investigation through the use of two breadths. Due to the use of combustible material, the glulam, as the structural framing, the new classification of the building is Type IV Construction per the International Building Code 2009 §602.4 (existing structure is classified as Type IIIB). This classification negates the use of the current Underfloor Air Distribution System and a new overhead VAV system will be used. Exposed structural members will be changed and these new features will need to be considered in the revised glulam design.

The gravity system of Heifer International Center will be redesigned in glulam and the current layout of the lateral system will be kept. However, in order to better understand a wider variety of lateral force resisting systems, a concrete shear wall will be studied. It is important to understand why a steel plate shear wall was selected in the original design and examine whether it was crucial for the design.

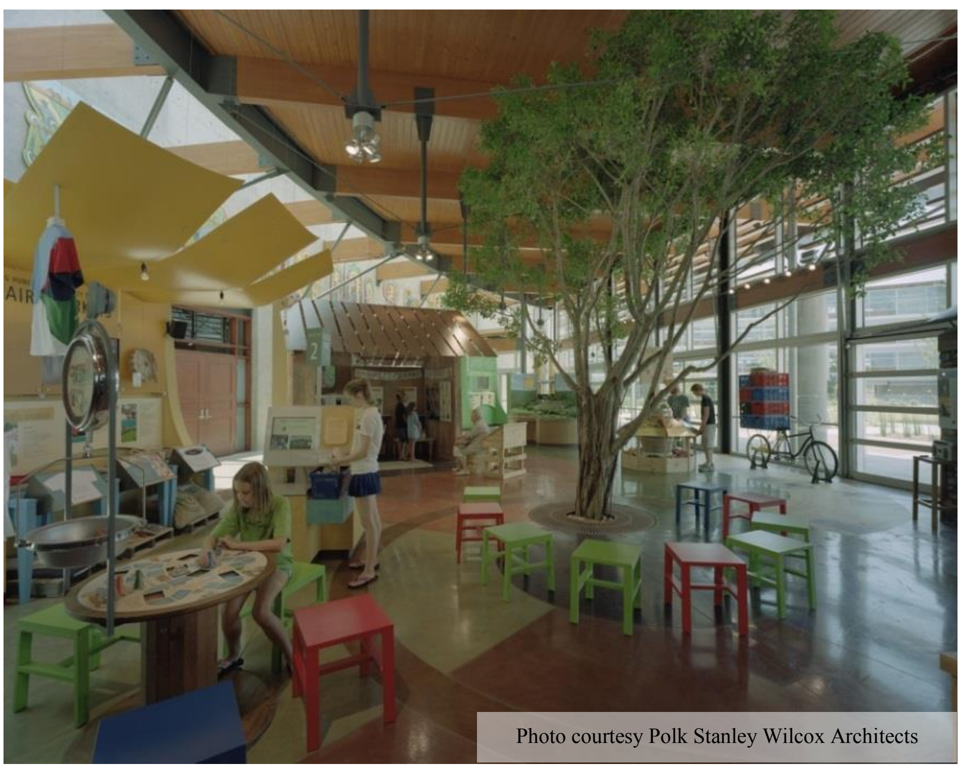

Photo courtesy Polk Stanley Wilcox Architects

Figure 34: Heifer International Education and Visitor Center

## 1.8 Proposed Solution

The selection of the glulam redesign for the gravity system leaves five potential floor systems that must be considered.

1. Tongue and groove wood plank
2. Concrete floor system
3. Composite concrete and wood system
4. Steel decking and concrete system
5. Post tensioned slab system

These five floor systems will be researched and the most practical floor system for the Heifer International Center's glulam beam gravity redesign will be chosen. The glulam beams will be reinforced with tension cables; in a queen post truss design. This advanced modification to a glulam beam may prove beneficial in integration between the structural, mechanical and architectural disciplines. Due to aesthetics and the ease of connection of the glulam beams, the current HSS columns will be kept in the redesign.

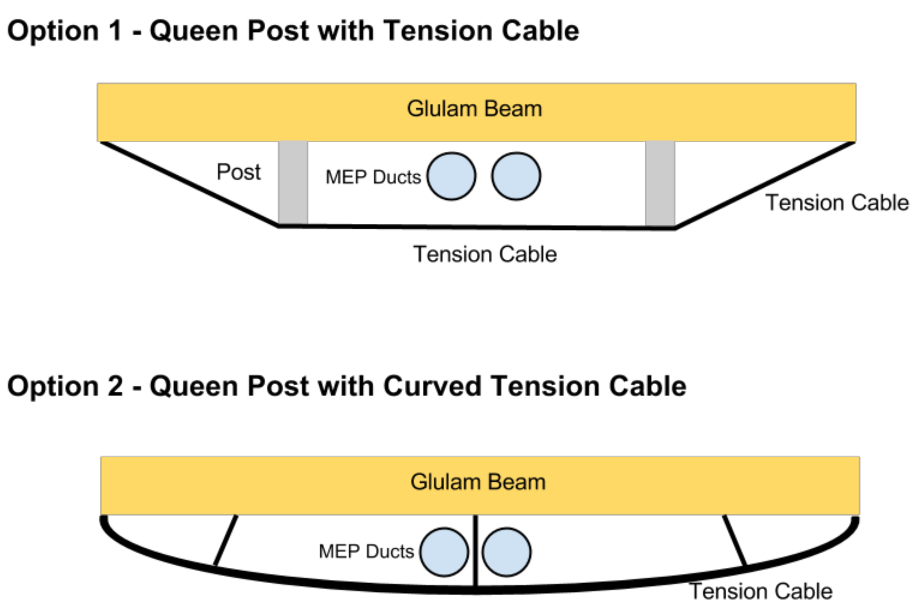


**Figure 35: Potential queen post options**

Figure 35 shows two potential designs of the queen post truss. Each design relies on posts which hold the tension cable out and away from the primary beam. This queen post truss increases the strength of the system and can be designed to add a slight camber into the primary beam. The queen post truss will be analyzed using SAP2000 with a combination of hand calculations.

The lateral system will be redesigned to incorporate concrete shear walls. This new design will be compared to a steel plate shear wall to determine the utility of the steel plate shear wall used in the current building. Due to difficulties previously experienced in Technical Report IV, a RAM Structural System model will be developed for the computer modeling aspect of the project.

Due to the use of combustible framing material, the building must be reclassified as Type IV Construction. This new classification will negate the use of the current Underfloor Air Distribution System because the use of concealed spaces is excluded from Type IV Construction of the International Building Code 2009 §602.4. Exposed structural members will be changed, and these new features will need to be considered in the revised glulam design.

Furthermore, the use of an architectural guideline will aide in the proper development of structural and mechanical systems, in order to respect and expand upon the architectural characteristics of the Visitor and Education Center.

## Breadth Topics

### *Mechanical and Envelope*

A glulam beam system will be used in the redesign of Heifer International Center. Due to the updated construction type, the Underfloor Air Distribution System will be negated. The mechanical system will have to be changed to a new overhead ductwork system. This new system will need to be hung from the ceiling—and it is important that it is incorporated into the revised structural system so it will visually respect other engineering options. The mechanical system will be able to integrate into the queen post, option 1 or 2, previously discussed in this report.

The mechanical breadth will involve generally sizing the building's supply and return ducts and ensuring that the ducts are able to fit through the designed queen post. Due to the open office plan of Heifer International Center, careful consideration will need to be taken in the placement of ductwork and its architectural influence. A study will be performed to understand the new structural system's impact on the thermal envelope, and what may be done to reduce the number of thermal bridges in the current design.

### *Architectural*

Due to the drastic change in structural building materials an architectural study will be performed to understand how the glulam redesign changes the Heifer International Center. The lateral system redesign should not have an effect on architectural considerations. The Education and Visitor Center next door to the Heifer International Center will be used as a design guide to develop architectural characteristics that should be considered during the duration of the structural redesign. This design guide will influence both structural and mechanical disciplines. Revit and AutoCAD will be used to produce renderings of the new architectural features, and the final effect they have on the design.

## MAE Coursework Requirement

Coursework of the Graduate School of the Pennsylvania State University will be incorporated into the redesign of the Heifer International Center. AE 530 – Advanced Computer Modeling of Building Structures will be referenced to develop an advanced Bentley RAM Structural System model of the office building. Additionally, a CSi SAP2000 model may be used to analyze, in detail, the potential queen post that will be used in the redesign. In addition, AE 538 – Earthquake Resistant Design of Buildings will be integrated into the design of the lateral force resisting system.

## Schreyer Honors College Requirement

This thesis work will be submitted in order to fulfill requirements set by the Schreyer Honors College and the Department of Architectural Engineering. An in depth literature review will be performed of a composite concrete and wood floor system. The intent of this research review will be to gain professional experience as a future Engineering of Record having to specify a floor system not referenced in the International Building Code. The Engineer of Record would have to perform an examination of the proposed system, a composite concrete and wood system, to ensure that it will be safe in the building. This will provide a challenging, in depth examination, of a complex system and reference the work of Dr. Walter G.M. Schneider.

## 1.9 Conclusion to Proposed Solution

A scenario has been created, in which the architect is requesting an alternative material for the structure of the Heifer International Center. The architect wishes to explore a different structural material, for aesthetic purposes, due to the fact that the existing system is exposed. A new hybrid system of glulam and steel will be chosen and will provide a unique opportunity to investigate a queen truss. This will lead to integration between the mechanical and structural disciplines. The building will be reclassified as Type IV, per the International Building Code 2009 §602.4, and will prevent the use of the current Underfloor Air Distribution System. This obstacle will lead to a new overhead system, general sizing of ductwork and the careful placement of this ductwork to respect their aesthetic appearance. A study will be performed to understand the new structural system's impact on the thermal envelope, and how this will in turn affect the mechanical system. Mechanical and electrical equipment can be incorporated into and hung from the queen post truss.

The lateral system of the Heifer International Center will be redesigned using concrete shear walls. This new design will be compared to a steel plate shear wall at the end of the spring semester, to determine the utility of the steel plate shear wall used in the current building.

Furthermore, an architectural study will be performed on the new exposed structural system, comparing the designed system to the architectural intent of the Visitor and Education Center, next door to the Heifer International Center.

This project will present a challenging and in depth investigation of a complex structural gravity and floor system, while also expanding the mechanical and architectural breadths. These two breadths will be directly influenced by the designed structural system, and will pose a unique integration between the three disciplines. For this to be evaluated, an architectural model will be created to compare the exiting and redesigned office building.

Graduate level course work will be referenced from AE 530 – Advanced Computer Modeling of Building Structures to develop an advanced CSi ETABS model or a Bentley RAM model of the office building. Knowledge gain in AE 538 – Earthquake Resistant Design of Buildings will be integrated into the design of the lateral force resisting system.

# CHAPTER 2

# STRUCTURAL DEPTH

## 2.1 Gravity System Redesign

This section summarizes the gravity system redesign of the Heifer International Center, in which the primary structural material changed from steel to glulam. Glulam beams were used in conjunction with an engineered queen post girder, specifically designed for the Heifer International Center. The gravity system redesign encompassed a combination of 2D hand calculations and computer analysis, with the additional aide of Microsoft Excel. One of the primary goals of the gravity redesign was to minimize changes to the layout of the Heifer International Center, while still adding a new architectural feature to the interior space. Each skewed bay of the curved building, Figure 37, was idealized as 25’-0” x 29’-0” rectangular bays, shown in Figure 36. With the selection of glulam as the primary gravity structural material, five potential floor systems were investigated.

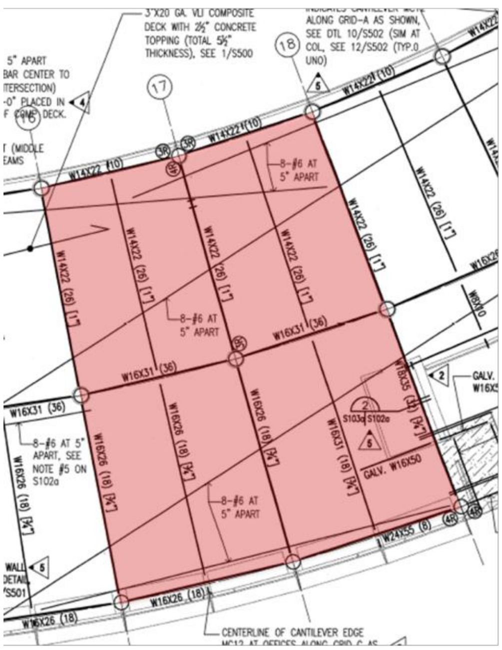


Figure 36: Typical floor plan

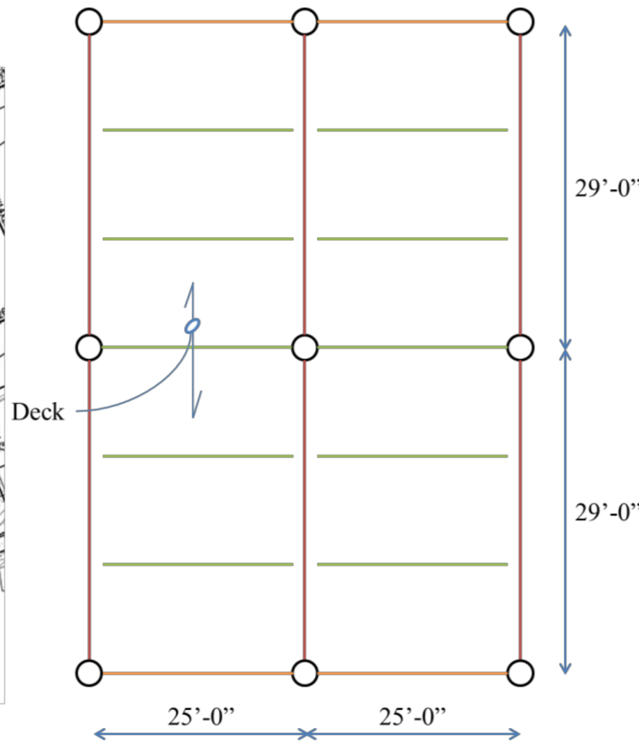


Figure 37: Simplified floor plan

Figure 37 shows the layout of regular glulam beams in green, the designed queen post girder in red and the exterior perimeter beams in orange. The existing HSS24x0.5 columns remained in the redesign and are indicated in black. The conservatively sized 25’-0” x 29’-0” bay was used for the calculation of loads and in the design of member sizes.

## Considerations of the Typical Bay Layout

The redesign concentrated on the typical bays of the office and roof, with the objective of integrating the mechanical, electrical and architectural elements of the building. Due to the complexity of the building, a typical office bay was chosen, which extends from the second to the fourth levels, as well as a typical roof bay. Five potential floors systems were investigated and are summarized in Table 24,

| *Potential Floor System* | *Advantages and Disadvantages* |
|---|---|
| Tongue and groove wood plank | - Spacing will be an issue |
| Concrete floor system | - Additional weight may be of concern<br>- Would not match architectural style of building |
| Composite concrete and wood system | - Intricate calculations required |
| Steel decking and concrete system | + In use in existing building<br>+ Would match redesign of building |
| Post tensioned slab | - Not an economical solution<br>- Would have to span in the short distance thus decreasing the utility of the post tensioning |

**Table 24: Floor system comparison**

After thorough examinations of these floor systems, the steel decking and concrete system was chosen, due to its ability to match up closely with the intended architectural style. This system also offered the possibility of reduced cost by using an industry standard composite decking material.

The preliminary design of a typical office bay only included beams running between columns, with a clear span of 25’-0” between beams. It was found that floor decking would not be able to span this distance, even with the aide of shoring. Intermediary beams had be added to adequately support the decking, causing the beam running between the columns to be converted to a girder. This girder became the queen post that would later be designed to have mechanical and electrical equipment pass through it.

## Composite Decking Selection

A 3VLI 20 gauge composite deck with 2 ½” of normal weight concrete topping, making a total thickness of 5 ½”, was chosen as the decking to span in the 29’-0” direction. The decking will not compositely act with the framing members, due to the lack of shear studs and wide flanges. For this reason the decking is unable to take advantage of concrete in compression and steel in tension (Nucor Corporate, 2013).

## Beam Design of Typical Floor and Roof

The beams spanning between the queen post girders must support a tributary area of approximately 10'-0" of dead and live load, highlighted in yellow on Figure 38. The beam members being designed are in green. This significant load must be carried by the newly designed glulam beam. The final design of the beams called for the two items below,

| | |
|---|---|
| Typical Office Bay | 10 ½" x 19 ¼" 30F-2.1E SP |
| Typical Roof Bay | 8 ½" x 12 ⅜" 30F-2.1E SP |

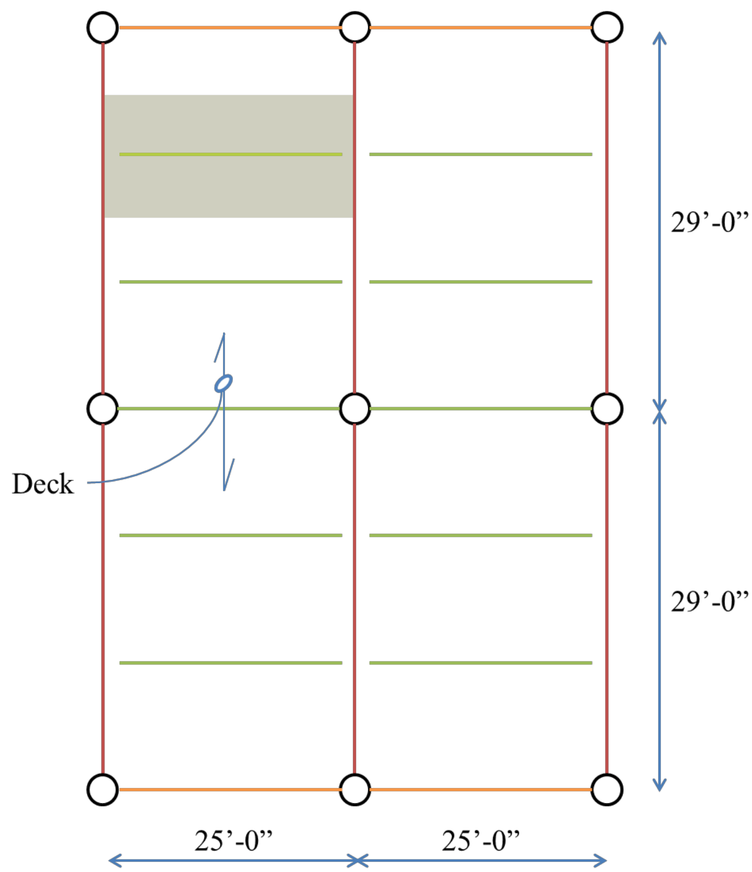


**Figure 38: Beams, girders and perimeter beams of typical office**

Calculations for sizing the beam can be found in Appendix B.1 - Typical Office Beam Design. These members were designed primarily for bending, per Table 5A of the National Design Standard Supplement. Each of these member sizes will have to be produced by a qualified manufacturer and the final member will be subjected to an additional approval by an accredited inspection agency[3]. While the depth of the typical floor bay beam is rather large, it should be noted that the floor to floor height is 14'-0", leaving approximately 9'-6" clear distance when considering the 28" deep clearance space for mechanical and electrical equipment and a 5 ½" deep decking. The beams

[3] Note 8 page 61 National Design Standard Supplement (American Wood Council, 2013)

supporting the roof are sized in Appendix B.4 - Roof Beam Design and are shown in Figure 39. The same roof decking used in the original design was used in the redesign.

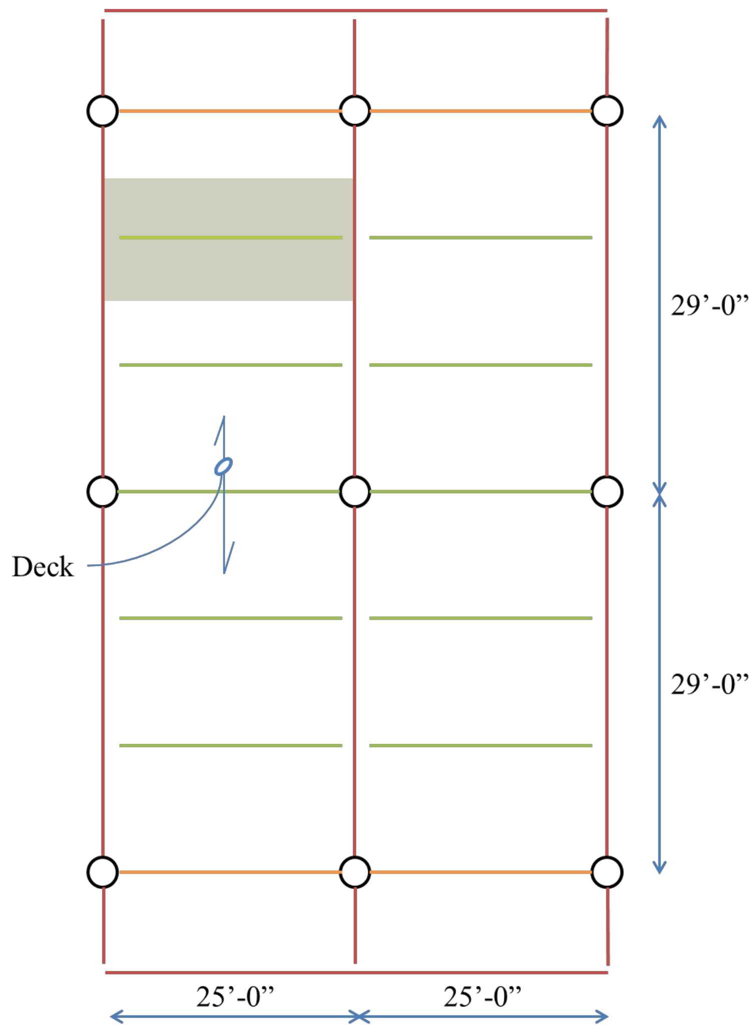


Figure 39: Beams, girders and perimeter beams of roof

The perimeter beams of the typical office bay were designed in both glulam and steel. It was found that the depth of the steel section designed was almost 0'-6" less than the glulam beam sized. These calculations can be found in Appendix B.7 - Typical Office Perimeter Beam, and are shown in orange in Figure 38 and Figure 39 above. The two potential beam size depths vary, allowing more natural light to penetrate the building if the steel wide flange typical office perimeter W14x22 beam is used.

| Typical Office Perimeter Beam | |
|---|---|
| Glulam | 10 ½" x 17 ⅞" 30F-2.1E SP |
| Steel | W14x22 |

The cantilevered section extending past the exterior of the building, on the North and South sides of the typical roof bay were not designed in this exercise. It should be noted that the selection of steel as the perimeter beam material will change the classification of the construction type of the building from Type IV Heavy Timber (HT) to Type IIIB construction, per §602 (International Code Council, 2009).

A reclassification of the building's construction type occurred during the redesign phase and is summarized in Table 25.

| | Existing Structure | Redesign (with glulam perimeter) | Redesign (with steel perimeter) |
|---|---|---|---|
| **IBC Code** | 2000 | 2009 | 2009 |
| **Occupancy Type** | Business – Group B | Business – Group B | Business – Group B |
| **Construction Type** | IIB | IV | IIIB |
| **Max. Height** | 75'-0" | 65'-0" | 75'-0" |
| **Max. Stories** | 5 | 5 | 4 |
| **Max. Allowable Area Per Floor** | 53,438 SF | 36,000 SF | 60,648 SF |
| **Fire Rating** | 0 hours | Min. HT[4] | 0 hours |

**Table 25: IBC 2009 Construction type classification summary**

[4] The minimum width and depth per IBC 2009 was referenced in the design of the HT members.

## Queen Post Girder Design

Several iterations were considered for the queen post girder design. The basic principle of an inverted queen post is to reduce the amount of flexure on the member, thus reducing the required size of the member. This is accomplished by transferring a significant portion of the shear, blue on Figure 40, through a post or posts located along the length of the member. This shear is converted into axial compression in the post, shown in red, which in turn is transferred as tension through the cable, shown in green. This tension force in the cable is transferred up into the top chord of the queen post as an axial force, yellow. This causes the top chord member to act primarily in axial compression, but reduces the moment by approximately one-tenth.

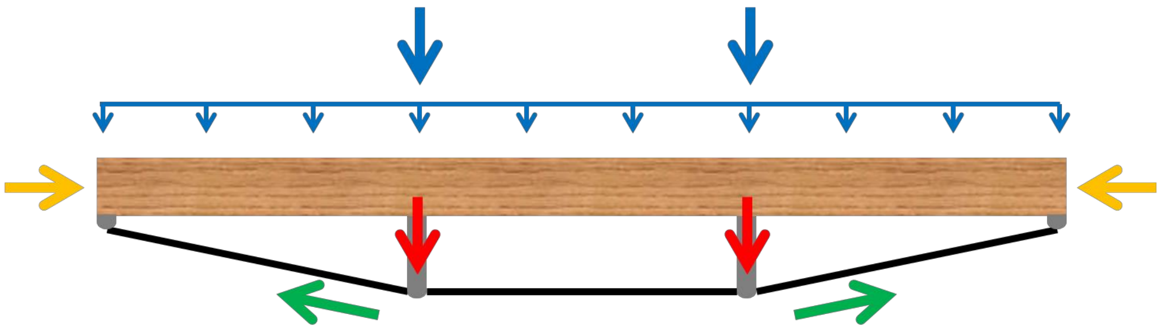

Figure 40: Load path of queen post

A queen post is an indeterminate structure, and was conservatively assumed to be hinged at the post locations. For the design of the queen post, the top chord was composed of glulam, the middle posts were made of square hollow structural steel members, and the bottom chord consisted of several sections of tension cables.

Figure 41: Simplified hinge queen post girder

The assumption of the hinge, shown in Figure 41, allowed for the calculation of the axial load on the posts, the tension in the cables, and the axial load applied to the top chord member. Due to the setup of the typical office and roof bays, each queen post had two point loads acting along its length. To reduce flexure induced by loading, the posts were placed where the incoming beams would frame into the queen post girder. This significantly reduces the moment on the beam and transfers a majority of the loading into the HSS posts.

The sizes chosen for the queen post girders are shown below.

| | |
|---|---|
| Typical Office Bay | 8 ½” x 19 ¼” Stress Class 50 Visual SP<br>3 ½” x 3 ½” x ⅜” Square HSS Post<br>(2) M56 Macalloy 460 Bars |
| Typical Roof Bay | 8 ½” x 12 ⅜” Stress Class 50 Visual SP<br>3 ½” x 3 ½” x ⅜” Square HSS Post<br>(2) M16 Macalloy 460 Bars |

Appendix B.2 - Queen Post Design Hand Calculation and Appendix B.3 - Typical Office Queen Post Design shows calculations for the design of the queen post. In addition, Appendix B.2 - Queen Post Design Hand Calculation walks through a hand calculation of the first iteration of the queen post design of the typical office floor. At the end of this iteration it was found that the queen post design failed due to the interaction between axial and bending on the member. A combination of 2D computer analysis and Microsoft Excel were used to compute the HSS post axial loads, the tension in the cable and the axial load applied to the top chord glulam member. These values were then adapted into a Microsoft Excel spreadsheet that was developed to quickly and accurately arrive at an economical member size of the top chord. Hand calculations were used to size the HSS post and the tension cable (Macalloy Bar & Cable Systems, 2014).

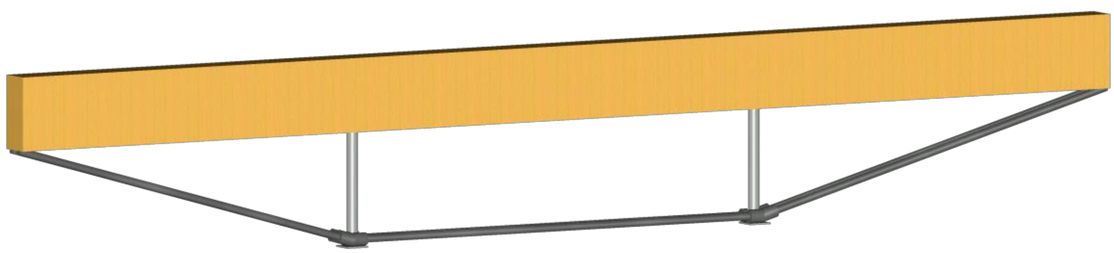

Figure 42: Computer model of queen post girder

A similar iteration was completed for the Typical Roof Bay, shown in Appendix B.5 - Roof Queen Post Design. A SAP2000 model was also developed to confirm the post and cable forces. This data is found in Appendix B.8 - SAP2000 Queen Post Model and shows that an acceptable amount of error was incurred in the assumption of the hinged queen post (Schneider III, 2014).

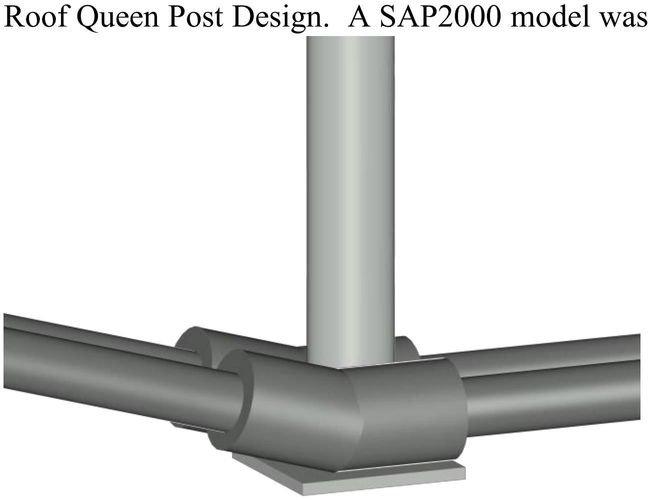

Figure 43: Connection detail for cable of queen post girder

## General Framing Plan

A general framing plan was developed for the east side of the building using Revit. This is shown below in Figure 44 and Figure 45.

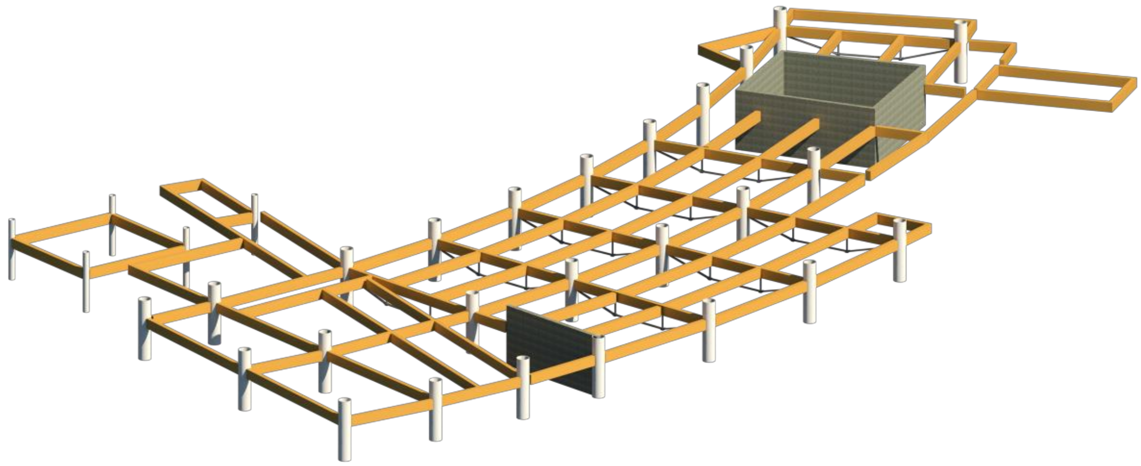

Figure 44: Isometric view of general framing plan

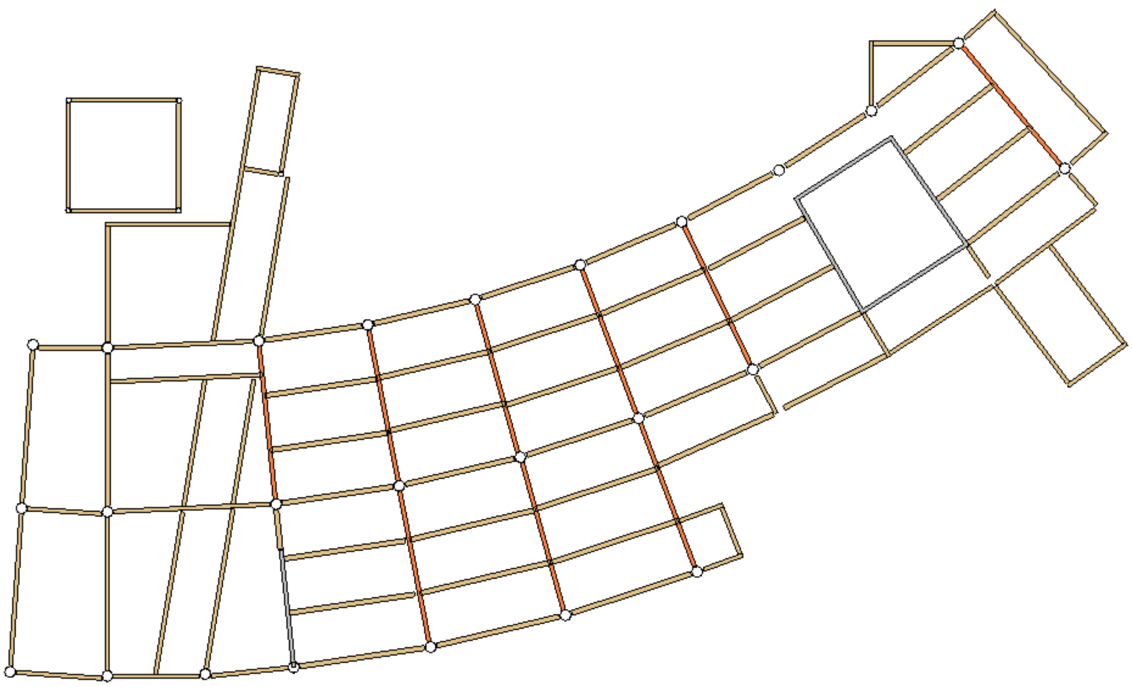

Figure 45: Plan view of general framing plan (East side)

## Fire Rating

Although a fire rating for the building was not required, it was important to understand how long the structure would remain structurally sound during a fire. In order to calculate the fire resistance time, the assumption was made that the queen post girder would act purely in axial compression, such as a column. The fire was assumed to occur on 4 sides of the column, and a fire resistance of approximately 1 hour and 15 minutes was calculated (APA - The Engineered Wood Association, 2009).

$$t = 2.54 \cdot Z \cdot B \left[3 - \frac{B}{D}\right]$$

**Equation 2: Fire rating for a column with a 4 side fire**

## Column Design

Due to aesthetics and the ease of connection of the glulam beams, the current HSS columns will be kept in the redesign. The HSS column sizes are confirmed in Appendix B.9 – Column Sizing

## Foundation Consideration

With the completion of the design of the building, it was found that the axial loads through the columns were reduced, due to the use of glulam. While the design of a new foundation system was not a part of the proposed solution for this thesis project, the foundation system should be considered. Due to the reduced loading, the existing foundation is sufficient to support the building and prevent overturning. This is further investigated in 2.2 Lateral System Redesign and supporting calculations can be found in Appendix C.4 – Building Overturning Check.

## Comparison of Gravity Systems

The change of the structural material to glulam from steel gave the ability to add an aesthetic characteristic to the building, while still adequately supporting the weight of the floors and roof. Below in Table 26 is a comparison of the existing structural system with the redesigned structural system.

| | | Existing | Redesign |
|---|---|---|---|
| | | Steel Wide Flanges | Glulam and Queen Post |
| **System Weight** | | 56 psf | 60 psf |
| **Slab Depth** | | 5.5” | 5.5” |
| **Height** | | | |
| **Floor to Floor** | | 14’-0” | 14’-0” |
| **Option 1** | | 12’-0” | 12’-5”[5] |
| **Option 2** | | 8’-6”[6] | 10’-0”[7] |
| **Constructability** | | Easy | Medium |
| **Fire Protection** | | None | None |
| **Fire Rating** | | - | 1.25 hours |
| **MEP Coordination** | Underfloor Air Distribution (UFAD) System @ 18” depth | MEP runs through the structural queen post girders | |

Table 26: Comparison of existing and redesigned gravity systems

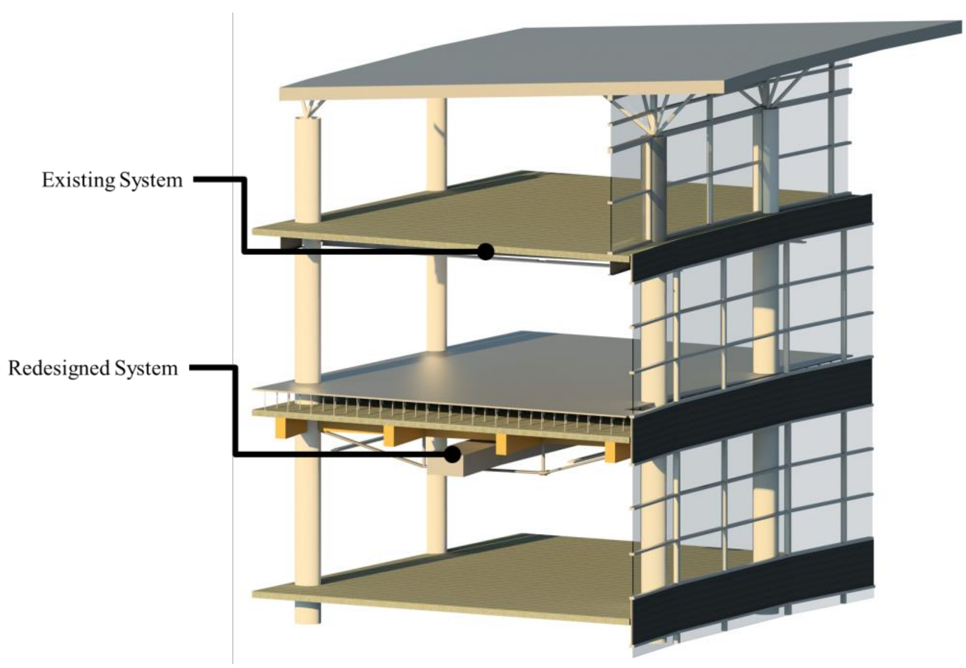


Figure 46: Comparison of existing and redesigned gravity systems

[5] This height is measured from the floor level to the bottom of the structural beams.
[6] This height is measured from the floor level to the bottom of the existing luminaire fixtures.
[7] This height is measured from the floor level to the bottom of the queen post girder’s cable.

## *Existing System Rendering*

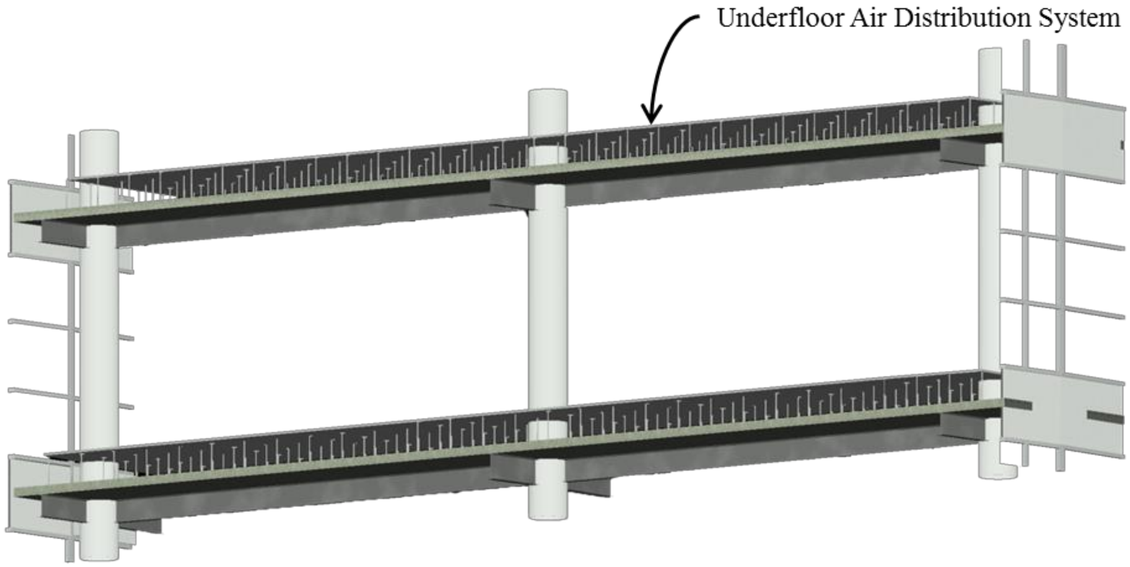


**Figure 47: Existing structural system isometric in view**

## *Redesigned System Rendering*

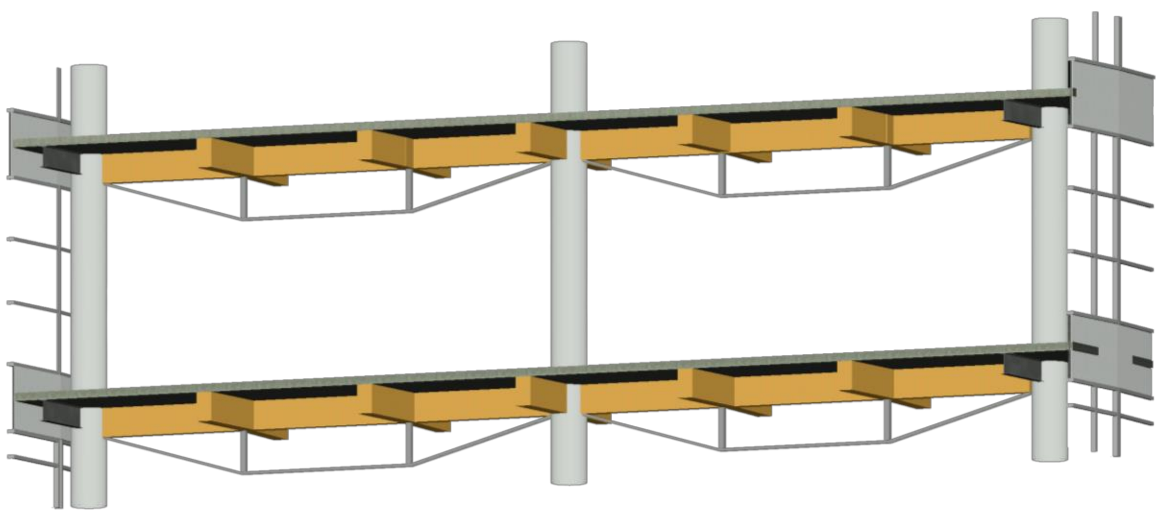

**Figure 48: Redesigned structural system isometric in view**

### *Existing System Dimensions*

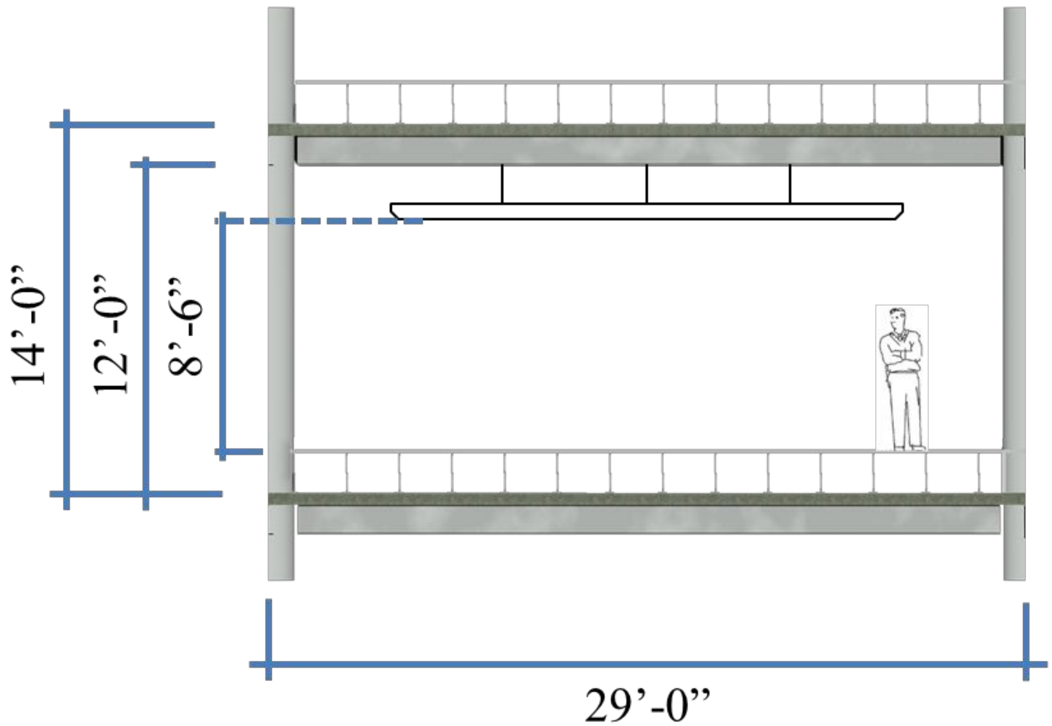


**Figure 49: Existing system typical bay (with dimensions)**

### *Redesigned System Dimensions*

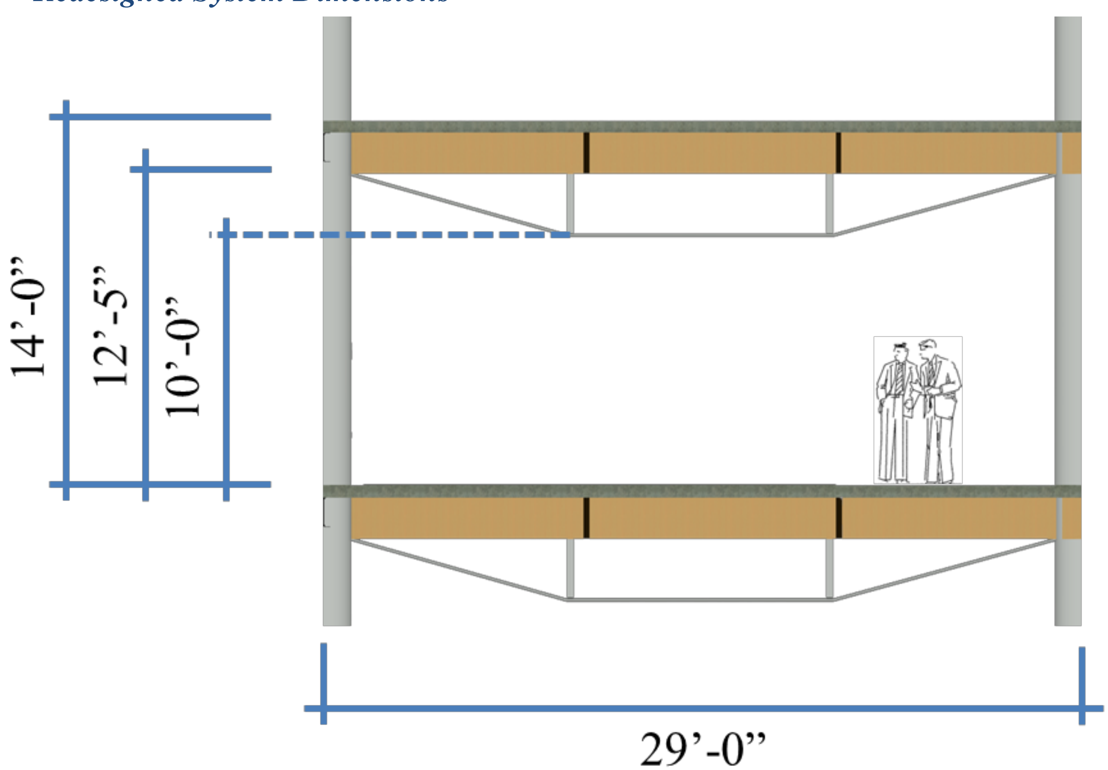


**Figure 50: Redesigned system typical bay (with dimensions)**

A close up of a potential mechanical and electrical layout is shown in Figure 51.

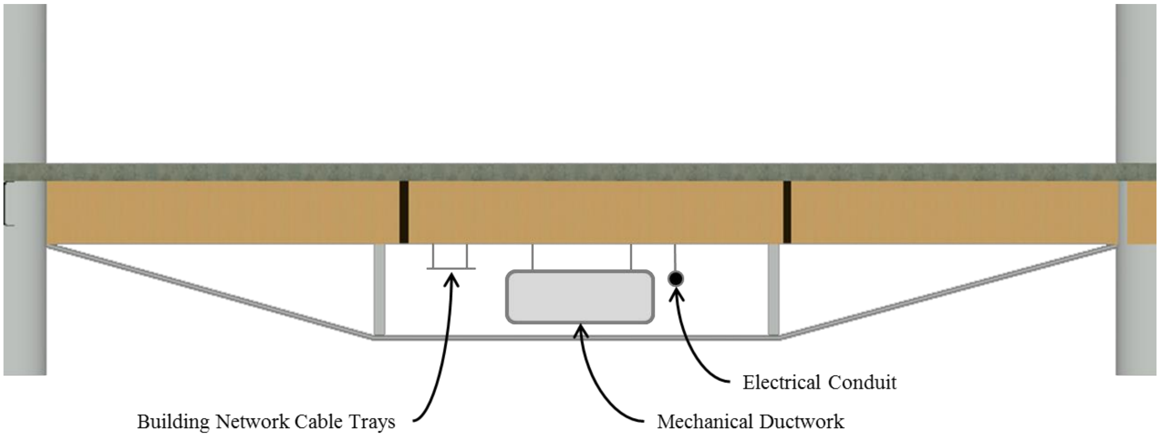


**Figure 51: Redesigned structural system and potential mechanical and electrical**

## 2.2 Lateral System Redesign

The redesign of the gravity system in glulam lessens the likelihood of the use of a steel plate shear wall system. Instead, a cast-in-place concrete shear wall system was designed as the lateral force resisting system of the Heifer International Center. The shear walls kept the same layout as the existing building and were initially designed using the minimum thickness of walls designed by the empirical design method, per §14.5.3.1 (American Concrete Institute, ACI-318, 2011). The building layout was modeled in RAM Structural System (RAM SS) and the shear walls were designed based on the computer generated seismic and wind loadings.

### Computer Modeling Input

The Heifer International Center has a seismic joint at approximately the midpoint of the building, requiring that both sections be modeled separately. The two sections of the building are shown in Figure 52, Figure 53, Figure 54 and Figure 55. Figure 53 and Figure 55 show an isometric of each side of the building from RAM SS. Moreover, the lateral force resisting system does not extend to the fourth level of the building, but instead relies on the fourth level columns and roof diaphragm to transfer lateral load. All mass of the fourth level and roof were applied at the fourth level due to this arrangement.


**Figure 52: LFRS of east end of building**

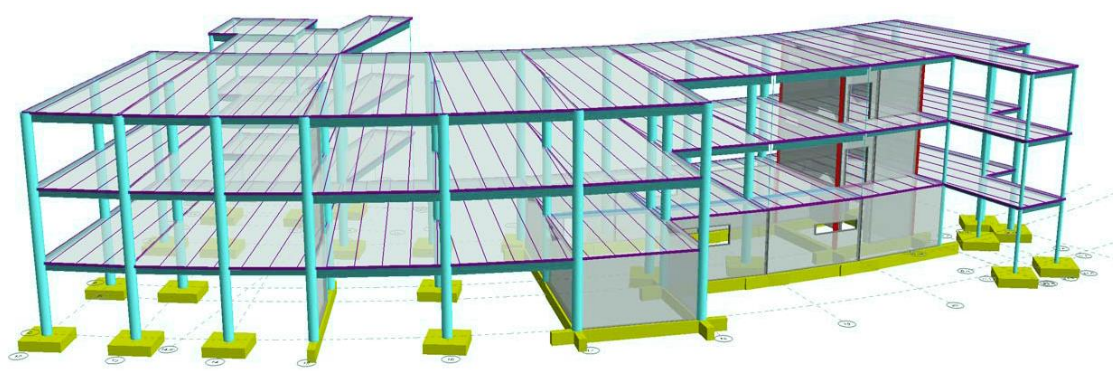

**Figure 53: LFRS of east end of building from RAM SS**


**Figure 54: LFRS of west end of building**

**Figure 55: LFRS of west end of building from RAM SS**

The concrete shear walls were designed as non-bearing shear walls and each level was programmed with the office building's dead and live loads previously calculated in 2.1 Gravity System Redesign. The dead load mass was used in the calculation of computer generated seismic loads. A preliminary size of 8" was chosen using the conservative assumption of a bearing wall which shall have a thickness not "less than 1/25 the supported height or length, whichever is shorter, nor less than 4 in." Each shear wall spans a height of 14'-0" so would have to be a minimum of 6.72", or 8" if a traditional shear wall depth is used (American Concrete Institute, ACI-318, 2011).

The openings in the shear wall were programmed based on the original steel plate shear wall configuration; however, adjustments were made due to the change in the mechanical system. Concrete columns were added at the edges of the shear wall core for stability purposes. In addition, concrete beams were added at the base of the shear walls on level 2, due to a discontinuity of the lateral force resisting system on the ground level.

The following assumptions were made during the modeling process:

- The concrete core wall was modeled as a C-shape (three walls) and a discontinued wall as the fourth wall due to program limitations that do not allow the connection of all four walls.
    - This is a conservative assumption that will make the system less stiff in the computer program, than when compared to the actual monolithic construction pour on the actual site.
- Rigid diaphragm was assumed due to use of composite decking.
- Cracked sections were assumed for the shear walls, per §10.10.4.1, and were assigned moment of inertia property modified of $0.35I_g$ (American Concrete Institute, ACI-318, 2011).

These general steps were used to model the lateral system in RAM Structural System:

- Grid was imported into RAM SS from Autodesk Revit.
- The perimeter of the building was lined with steel beam elements in order for the program to extrapolate an edge of slab.
    - It should be noted that beam self-weight was disabled and did not affect lateral calculations.
- Steel HSS columns were modeled using the HSS24x0.5 of the existing building. This was accomplished by overriding the Master Steel Table of RAM SS and programming in a new HSS size and corresponding properties, seen in Appendix C.1 – HSS24x0.5 Column.
- Shear walls were modeled using the existing building layout.
- RAM Frame was used to program site-specific seismic and wind loads, seen in Appendix C.2 – Seismic and Wind Loading and the two separate sections of the building were then analyzed.
- RAM Concrete was used in the design of the concrete shear walls.

## Torsional Irregularities

Vertical and Horizontal Structural Irregularities had to be considered for the design of the Heifer International Center, per Table 12.3-1 and 12.3-2 of §12.3.2 (ASCE-7 10, Minimum Design Loads for Buildings and Other Structures)

It was possible that a Torsional Irregularity (Type 1a) or Extreme Torsional Irregularity (Type 1b) existed in the structure. After the initial programming and verification of the RAM Structural System model, the torsional amplification factor was calculated and irregularity in each direction was tested. This was achieved by calculating the average and maximum drifts of each floor, at transverse locations of the building, shown in the simplified diagram of Figure 56. Appendix C.6 – Trace Locations visually show the two locations used to test irregularity on each section of the building.

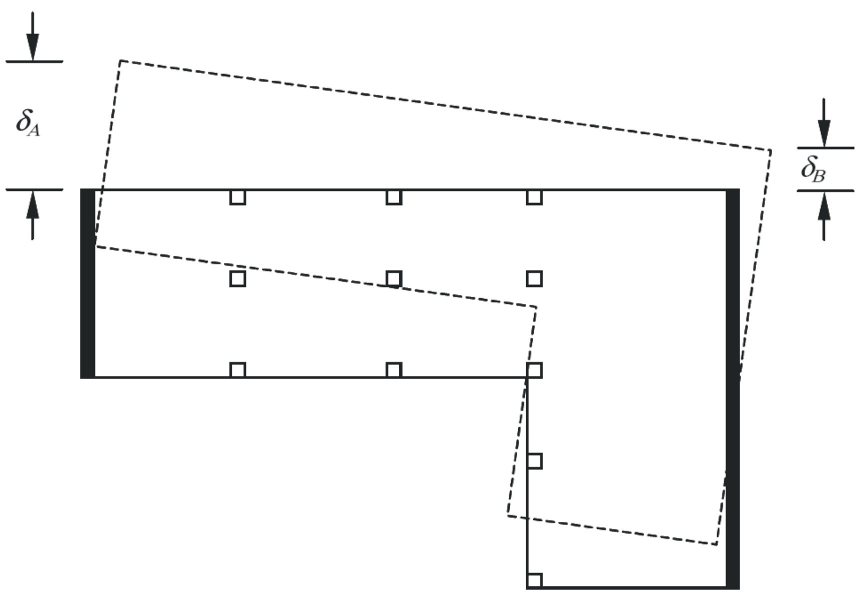


Figure 56: ASCE-7 10 Figure 12.8-1 Torsional Amplification Factor

Due to the seismic joint, the two sections of the building were analyzed separately. Both the x-direction and y-directions were tested for the two sections of the building, east and west sides. The east side of the building was found to have a Type 1b torsional irregularity for all three levels for the x-direction and y-direction. On the other hand, the west side of the building did not have any torsional irregularities in the y-direction; however, had Type 1b irregularity on all levels in the x-direction. This was calculated using Equation 3 below and making a comparison of $1.2\delta_{avg}$ and $1.4\delta_{avg}$. These results are shown in Appendix C.3 – Torsional Irregularity and Seismic Amplification Factor.

$$\delta_{avg} = \frac{\delta_A + \delta_B}{2}$$

Equation 3: Average drift of story

Type 1b is an Extreme Torsional Irregularity and the design of such a building must follow code requirements outlined in Table 12.3-1. These stipulations are summarized below, which are applicable to a Seismic Design Category C building (ASCE-7 10, Minimum Design Loads for Buildings and Other Structures).

- Structural Modeling §12.7.3
  - A 3D computer model incorporating a minimum of three dynamic degrees of freedom was produced for this project.

- Amplification of Accidental Torsional Moment §12.8.4.3
  - The amplification factor, where required, was applied to the accidental torsional moment. Calculations are shown in Appendix C.3 – Torsional Irregularity and Seismic Amplification Factor and references Equation 4.

$$A_x = \left[\frac{\delta_{max}}{1.2\delta_{avg}}\right]^2$$

**Equation 4: Amplification Factor**

- Story Drift Limit §12.12.1
  - The design story drift of the building was maintained below the allowable story drift, $\Delta_a$, provided in Equation 5. Supporting calculations are shown in the Seismic Story Drift section of Appendix C.2 – Seismic and Wind Loading.

$$\Delta_a = 0.020h_x$$

**Equation 5: Allowable story drift**

- Table 12.6-1
  - The Seismic Design Category C building was analyzed using the Equivalent Lateral Force Analysis procedure.

- Modeling §16.2.2
  - Similar stipulations as §12.7.3 above.

In addition to torsional horizontal irregularities, Nonparallel System Irregularity Type 5 existed due to the lateral force resisting system not aligning with the orthogonal application for seismic forces, for both the east and west sides. Type 5 requires the following conditions to be met for Seismic Design Category C and is shown in Figure 57 (ASCE-7 10, Minimum Design Loads for Buildings and Other Structures).

- §12.5.3
  - The orthogonal combination procedure was used in the analysis of the building, requiring 100% of the force in one direction to be combined with 30% of the forces in the orthogonal direction.

- Structural Modeling §12.7.3
  - A 3D computer model incorporating a minimum of three dynamic degrees of freedom was produced for this project.

- Table 12.6-1
  - The Seismic Design Category C building was analyzed using the Equivalent Lateral Force Analysis procedure.

- Structural Modeling §12.7.3 and §16.2.2
  - Please see Type 1b Extreme Torsional Irregularity.

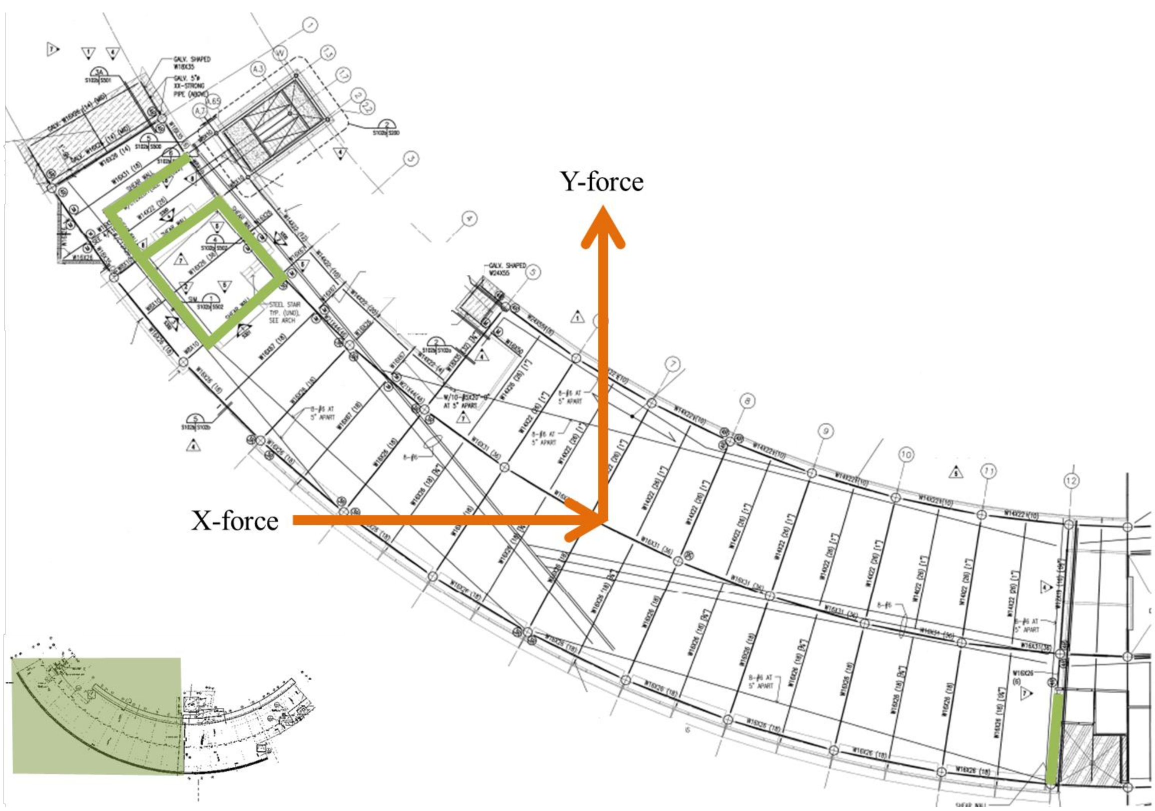


**Figure 57: Type 5 Nonparallel System Irregularity**

Seismic Design Category C has the potential to qualify for two types of vertical irregularity, per Table 12.3-2: In-Plane Discontinuity in Vertical Lateral Force-Resisting Element Irregularity Type 4, and Type 5b Discontinuity in Lateral Strength-Extreme Weak Story Irregularity. Type 4 irregularity was eliminated because there was no shear wall that was discontinuous from the below levels. Type 5b also did not apply to the Heifer International Center, which does not have any levels that have 65% less lateral strength than the levels above.

## Loads Applied to Model

The original analysis of the building used ASCE 7-98; however, the redesign of the building used ASCE 7-10. Due to the drastic change in code requirements only the seismic and wind loadings generated by the computer were used, based on ASCE 7-10. The most up to date wind and seismic data was programmed into the computer and used to generate the loading on each half of the building. The input data can be found in Appendix C.2 – Seismic and Wind Loading. It was previously found in 1.6 Lateral System and Loads of the simplified analysis of the structure, seismic controlled. This was verified for both sections of the building, which were each controlled by a load combination involving seismic loads.

### *Seismic Loads*

Seismic loads were applied to the building and displacements were extracted from the program. These displacements were then used to test if torsional irregularities existed in the building. If Type 1a or Type 1b Horizontal Irregularity existed, the building was checked against and compared to the requirements set forth in Table 12.3-1. In addition, the seismic loads were amplified per the calculated amplification factor. This is shown in Appendix C.3 – Torsional Irregularity and Seismic Amplification Factor and is discussed in greater detail in the Torsional Irregularities section. The torsional moment was first calculated using the original story shear and amplification factor, and then was then resolved into a shear with an eccentricity. This was completed because RAM Frame did not have a function to accept torsional moments, only shear forces.

Seismic drifts were calculated and found to be below the maximum drift allowances for inter-story drift, per §12.12.1 (ASCE-7 10, Minimum Design Loads for Buildings and Other Structures). Seismic forces are summarized below in Table 27 and
Table 28.

**Seismic Shear Summary - West End**

| Level | $V_x$ (kips) | $V_y$ (kips) |
|---|---|---|
| Level 3 | 191.97 | 185.64 |
| Level 2 | 290.03 | 282.97 |
| Level 1 | 341.03 | 331.21 |

**Table 27: Summary of west end seismic forces**

**Seismic Shear Summary - East End**

| Level | $V_x$ (kips) | $V_y$ (kips) |
|---|---|---|
| Level 3 | 221.73 | 180.16 |
| Level 2 | 329.23 | 274.77 |
| Level 1 | 347.62 | 325.55 |

**Table 28: Summary of east end seismic forces**

### *Wind Loads*

The basic wind speed increased from 90 mph to 115 mph, by changing from ASCE 7-98 to ASCE 7-10. Although this increased wind loads, loads still remained below seismic forces. Building drift was calculated and was compared to the industry accepted drift limit of $l/_{400}$. These findings are summarized in the Wind Building Drift section of Appendix C.2 – Seismic and Wind Loading. Wind forces are summarized below in Table 29 and Table 30.

**Wind Shear Summary - West End**

| Level | $V_x$ (kips) | $V_y$ (kips) |
|---|---|---|
| Level 3 | 35.04 | 53.91 |
| Level 2 | 67.36 | 103.94 |
| Level 1 | 63.31 | 98.15 |

Table 29: Summary of west end wind forces

**Wind Shear Summary - East End**

| Level | $V_x$ (kips) | $V_y$ (kips) |
|---|---|---|
| Level 3 | 35.04 | 47.25 |
| Level 2 | 67.36 | 91.1 |
| Level 1 | 63.31 | 86.02 |

Table 30: Summary of east end wind forces

### Building Overturning Moment

The overturning moment of the building was calculated using output from RAM Frame and Microsoft Excel, for wind and seismic cases. This was performed separately for the two sides of the building.

The weight of each side of the building was approximately 4000 kips. The shortest moment arm was calculated to the edge of the building, from each respective side of the building's center of mass, and used in the calculation of the resisting moment. The use of the shortest distance would yield the lowest resisting moment that would prevent the building from overturning. A factor of safety of 1.5 was applied to the calculation of the resisting moment. The worst case moment was calculated for wind and seismic, for both sections of the building and compared to the resisting moment. An overall factor of safety was then calculated for the design, and found to be 5.5 and 3.7, for the west and east ends, respectively. These calculations are shown in Appendix C.4 – Building Overturning Check. Both sides of the building passed for overturning.

## Understanding Load Paths

Due to the Heifer International Center's irregular shape it is important to understand how lateral loads travel through the building's rigid diaphragm and react with the lateral system and are subsequently transferred to the foundation. The west side of the building was visually analyzed for the application of a wind load (this could also apply to seismic loads, too). Fortunately, the layout of the levels and lateral force resisting system are similar for each level, reducing the likelihood of load transfer through the diaphragm creating issues. This is shown below in Figure 58.

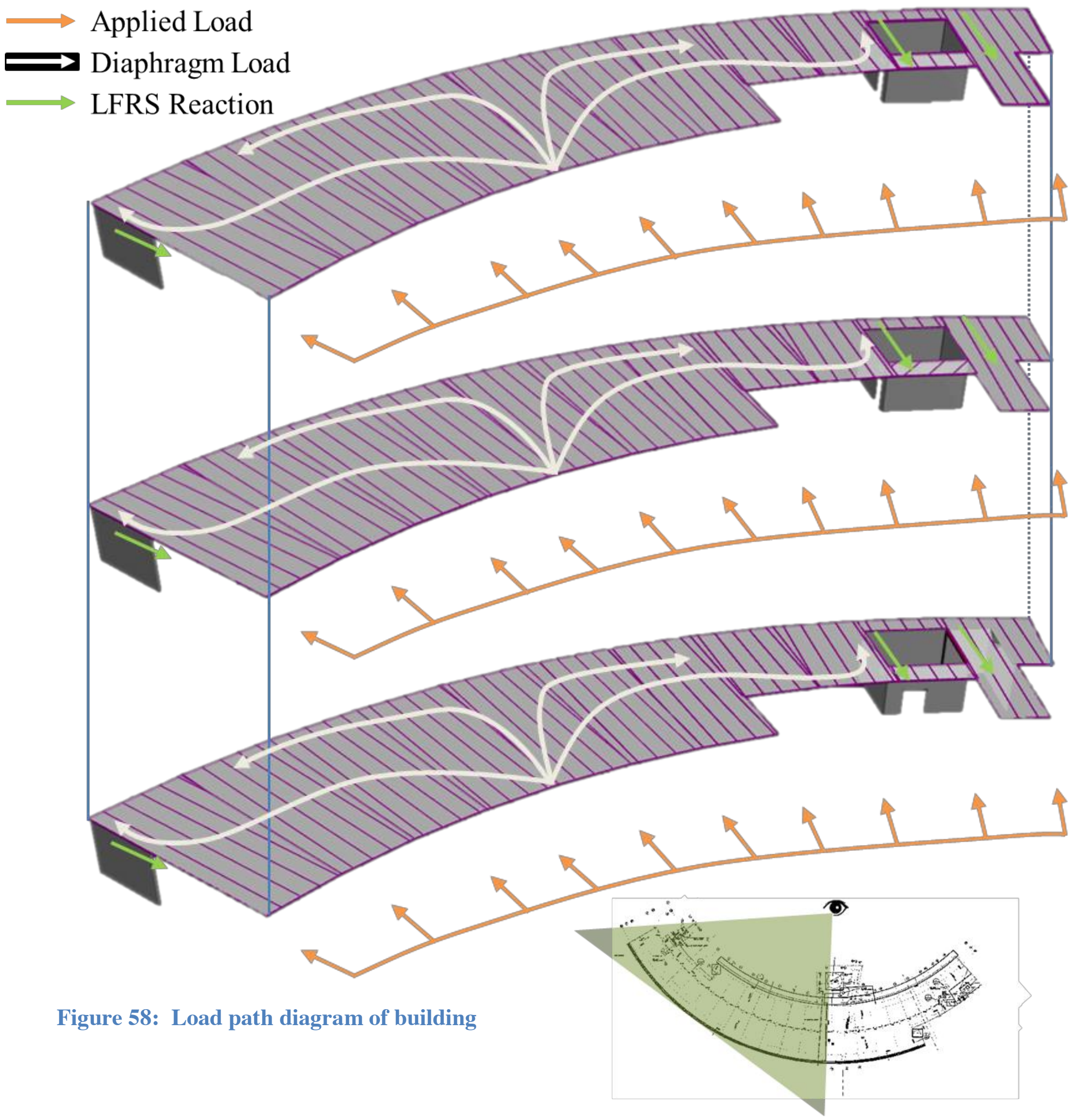


Figure 58: Load path diagram of building

## Shear Wall Design

RAM Concrete was used in the design of the concrete shear walls. The shear wall originally checked, SW-13 @ column line 12, in the Lateral System Spot Checks section of 1.6 Lateral System and Loads, was checked against concrete shear wall requirements. The final design from RAM Concrete for SW-13 @ column line 12 is summarized in Table 31 and shown in Figure 59.

#4 @ 18" O.C. Horizontal

#5 @ 15" O.C. Vertical

Table 31: SW-13 at column line 12 rebar design summary

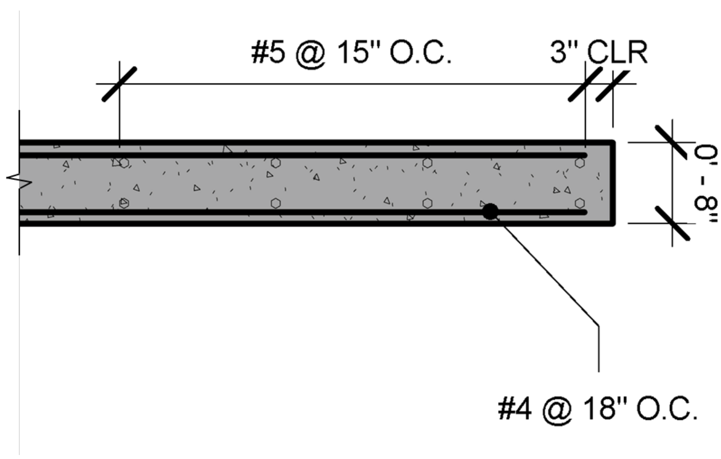


Figure 59: SW-13 at column line 12 section

This shear wall design was manually hand checked using the stipulations outlined for concrete shear walls and reinforcement requirements. These hand checks are shown in Appendix C.5 – Lateral System Hand Checks (American Concrete Institute, ACI-318, 2011), and the RAM Structural System design was found to pass.

The lateral force resisting system concrete shear walls are shown in Figure 60 and Figure 61, which were designed in RAM Structural System. These are shown on the next page. All shear walls in the building were designed to be 8" thick.

## Seismic Joint

Analysis of the maximum deflections from each section of the building verified that the existing 4" seismic joint was adequate for the building deflections. Additional information can be found on the seismic joint in the Seismic Joint section of 1.2 Existing Structural Information.

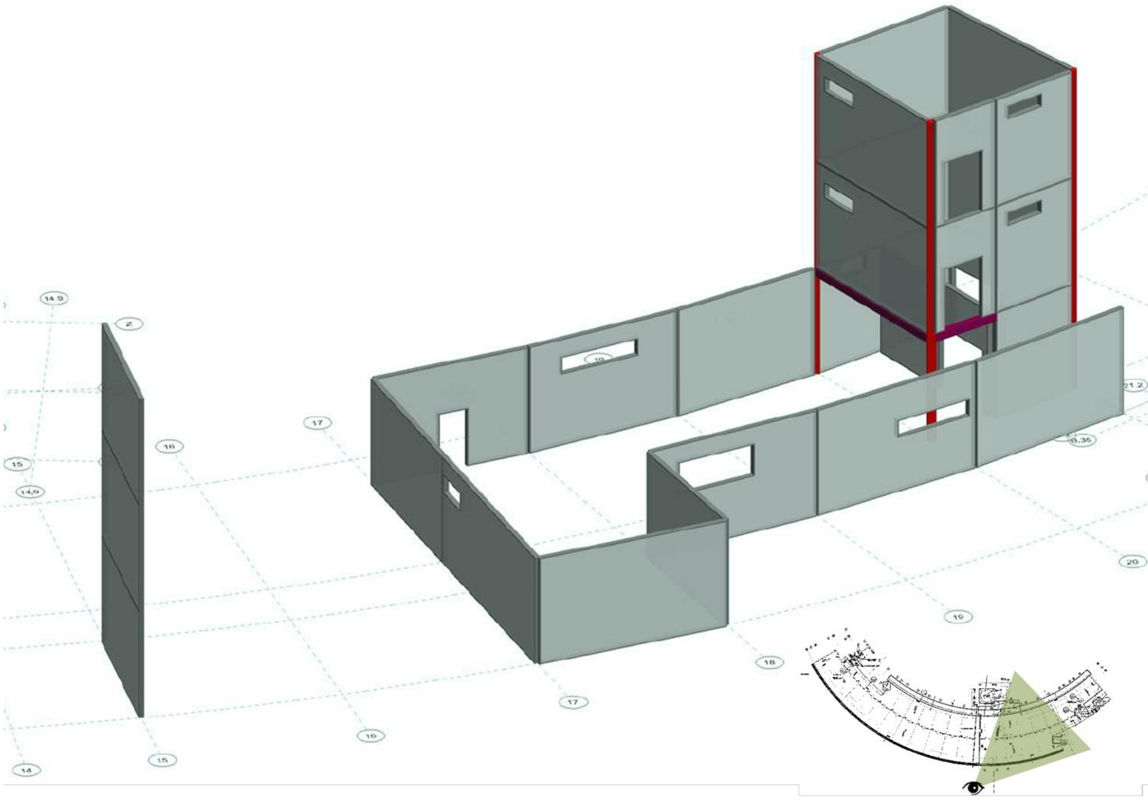

Figure 60: East end of the Heifer International Center

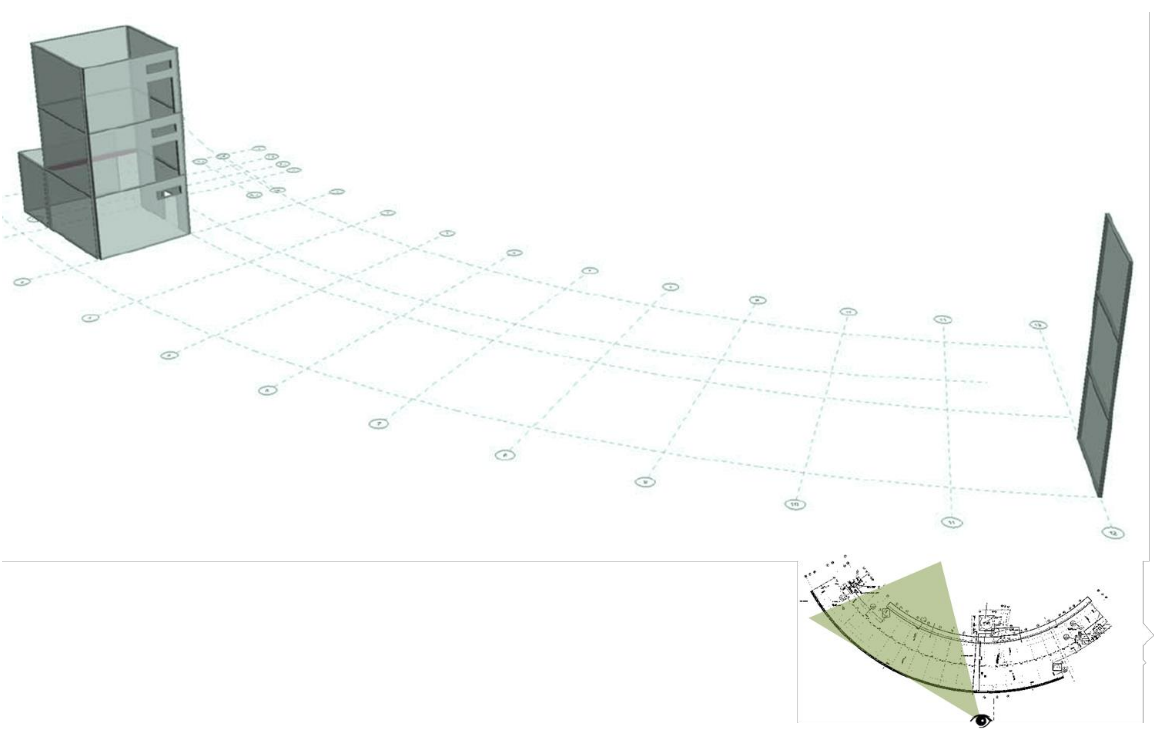

Figure 61: West end of the Heifer International Center

## 2.3 Comparison of Existing and Redesigned Systems

A comparison can be drawn between the existing and redesigned gravity and lateral systems. Each system has advantages over the other system; however, each also has disadvantages. The redesigned gravity system kept the floor-to-floor height the same and also was able to provide over a foot of additional space, immediately over the offices. Space over the girder location, which the typical office level beams frame into, was reduced because of the increased depth of the queen post girder. It should be noted that most of the depth of the queen post girder is for the space between the bottom of the glulam beam and the steel cable. The space is used for mechanical equipment, integrating the structural and mechanical systems in the redesigned queen post.

The main drawback of the redesigned gravity system is cost. The expense of the special order glulam beams and custom made queen post girder will be high—due to materials and labor. However, if the owner and architect wish to achieve the aesthetic look of the glulam and integration of the mechanical and electrical systems into the structural system—then the redesigned gravity is a decent choice. Moreover, the ability to prefabricate the queen post members and ship them to the site, also adds several environmental, cost and labor advantages to the redesigned system. If prefabricated off site, the members can be shipped onto the site and quickly moved into its respective place in the building. There is a disadvantage because the wood is not located as close as the steel manufacturer.

Next the lateral system redesign will be considered. Due to the use of glulam for the gravity redesign, it was found that a concrete shear wall system would be best for the lateral force resisting system in the Heifer International Center. The concrete shear walls were thought to be the best material to connect the glulam beams that would frame into a portion of the shear walls. In addition, the concrete shear wall system would be constructible, due to its ubiquitous use throughout the building industry. After the redesign of the gravity and lateral systems, a connection system between the two was researched. A Simpson Strong-Tie system of High Capacity Girder Hangers for Concrete and Glulam was studied and found to be a potential system to use in the Heifer International Center. This hanger is shown in Figure 62. It was found that the existing industry standard hangers would not be sufficient to support the beams framing into the concrete shear wall assembly; however, if a small portion of the gravity system was redesigned in the future, it would be conceivable to use the Simpson Strong-Tie hangers. Referencing the General Framing Plan of 2.1 Gravity System Redesign and the

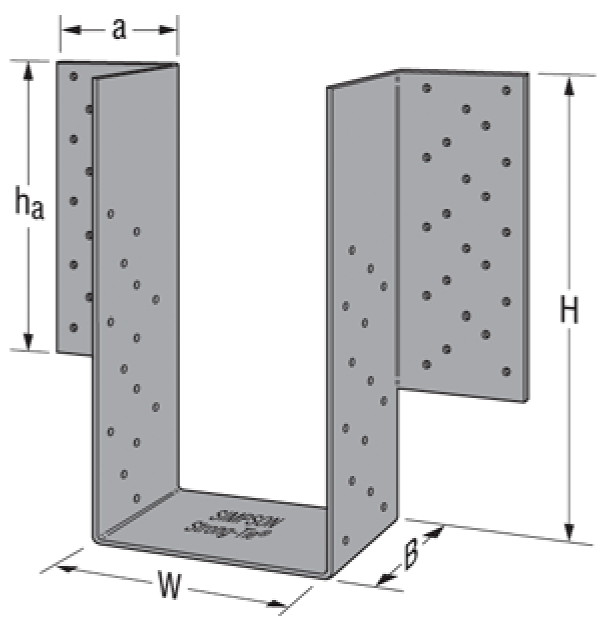


**Figure 62: High capacity girder hangers for glulam**

supporting calculations of Appendix B.1 - Typical Office Beam Design, it is possible to increase the number of beams over the typical bay near shear walls, from three to four or five. If this was completed, then the bearing at the end of the beam would decrease; allowing the use of the High Capacity Girder Hangers for Concrete and Glulam. The hangers are currently capped at approximately 20 kips of downward load; while the system designed calculated a bearing of 21.5 kips. This slight change in the floor plan, highlighted in Figure 63 below, would allow for the use of the Simpson Strong-Tie hanger system (Simpson Strong-Tie, 2014). It is important to prevent contact between the glulam and concrete and provide lateral and uplift resistance to the glulam member. In addition, a slotted connection between the hanger and glulam should be considered to allow longitudinal movement (Showalter, 2012).

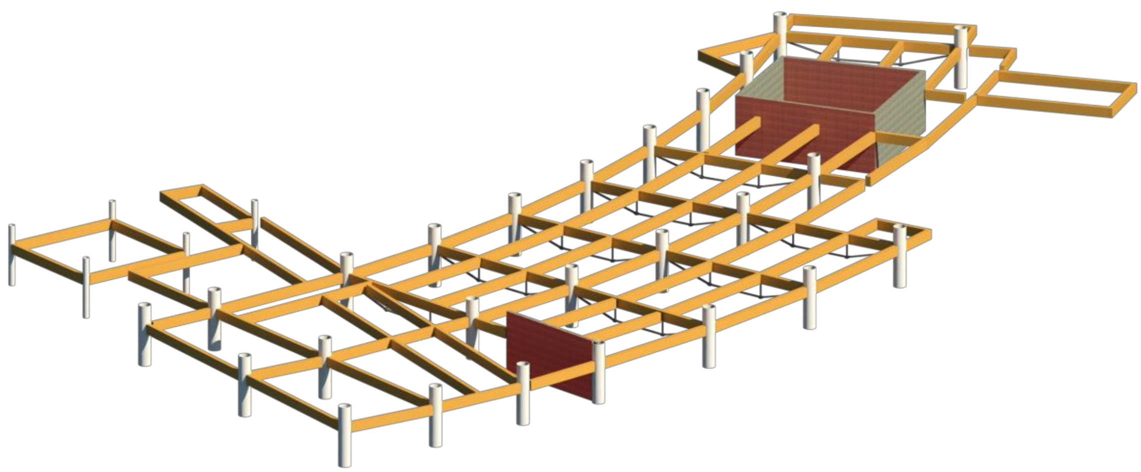

Figure 63: 3D isometric of floor plan highlighting walls to be redesigned

One major question which arose during the project was why the original project used steel plate shear walls. While concrete shear walls are common place in construction, the materials were readily available during the design and construction phases due to a steel manufacturer physically close to the building, making it more economical to use a steel plate shear wall system in the building. In addition, it is possible that the inherent lateral stability of the gravity framing did not require a lateral force resisting system during construction. If this is so, evident by photographs from the time of the construction shown in Figure 64, then it would have been easier to install a steel plate shear wall into


Figure 64: Construction photo with no evident LFRS

the erected structure (Robinson & Ames, 2000).

Another reason why steel plate shear walls may have been chosen is for their utility. It may not have made sense due to the geometrical shape and layout of the building to use concrete shear walls—in other words, an overdesigned system. It was revealed in ETABS SPSW to Concrete Conversion of Appendix A.1 - Existing Lateral System Modeling that the existing steel plate shear walls were equal to approximately 3” of concrete. By code the minimum concrete shear wall thickness would have been 6.72”—a large jump from the equivalent 3” concrete shear wall used for the ⅜” steel plate shear wall.

The lateral force resisting system of the Heifer International Center was redesigned in concrete and found to sufficiently pass code and industry standards. This was achieved without hindering the current layout of the building and also producing an achievable design that can be unified with the redesigned gravity system.

## 2.4 MAE Requirements

The Graduate School curriculum of the Pennsylvania State University wase incorporated into the redesign of the Heifer International Center. Course work of graduate level courses was referenced from AE 530 – Advanced Computer Modeling of Building Structures to develop an advanced Bentley RAM Structural System model of the office building. The powerful design and analysis tools which RAM Structural System offers were used for the lateral design of the building. The gravity system of the Heifer International Center was mostly designed by hand, but was verified using a computer model of the primary structural member, the queen post girder. A CSi SAP2000 model was used to analyze, in detail, the queen post girders. In addition, AE 538 – Earthquake Resistant Design of Buildings was integrated into the design of the lateral force resisting system and the advanced torsional checks required by ASCE 7-10.

# CHAPTER 3

## MECHANICAL AND ENVELOPE

## 3.1 Mechanical and Envelope Breadth

The redesign of the Heifer International Center in glulam led to the removal of the existing underfloor air distribution system. Instead, an overhead ductwork system was introduced and incorporated into the queen post girder designed in section 2.1 Gravity System Redesign. In addition, a thermal bridge was eliminated on each external column of the fourth floor of the office building, by redesigning the fourth floor column.

### Preliminary Duct Sizing

Using provided mechanical drawings, the air handling units for the Heifer International Center were analyzed for an alternative ductwork system. A TRANE Ductulator® was used to preliminary size the ductwork for the new system, using the existing air handling unit's maximum air supply to the various sections of the building. This work is summarized in Table 32 and Table 33. The most important aspect of this research was the determination of the depth of the ductwork. The maximum practical ductwork depth was 25", so the queen post girder was designed at a depth of 28" to easily accommodate the rectangular ductwork.

| Mark | Location | Services | Type | Max Supply (CMU) | Min Outside Air (CMU | Return Air (CMU) |
|---|---|---|---|---|---|---|
| AHU-1E | 1st | East | HOR2 | 6544 | 2452 | 4092 |
| AHU-1W | 1st | West | HOR2 | 8920 | 1715 | 7205 |
| AHU-2E | 2nd | East | HOR2 | 11122 | 1655 | 9467 |
| AHU-2W | 2nd | West | HOR2 | 14403 | 2839 | 11564 |
| AHU-3E | 3rd | East | HOR2 | 11400 | 1655 | 9745 |
| AHU-3W | 3rd | West | HOR2 | 14842 | 2839 | 12003 |
| AHU-4E | 4th | East | HOR2 | 10355 | 2620 | 7736 |
| AHU-4W | 4th | West | HOR2 | 12503 | 2811 | 9692 |
| OSA-1E | - | East | HOR2 | 8400 | 8400 | - |
| OSA-1W | - | West | HOR2 | 10200 | 10200 | - |

Table 32: Air handling unit summary

| Mark | Ductulator® Size (in) | Alternative Ductulator® Size (in) |
|---|---|---|
| AHU-1E | 25x30 | 20x38 |
| AHU-1W | 25x36 | 20x48 |
| AHU-2E | 25x42 | 20x55 |
| AHU-2W | 25x50 | 20x70 |
| AHU-3E | 25x42 | 20x55 |
| AHU-3W | 25x55 | 20x75 |
| AHU-4E | 25x40 | 20x50 |
| AHU-4W | 25x50 | 20x65 |
| OSA-1E | 25x32 | 20x42 |
| OSA-1W | 25x40 | 20x50 |

Table 33: TRANE Ductulator sizing

## Thermal Bridge Elimination

The fourth floor of the office building has several columns that are exposed on the exterior and interior of the building, shown in Figure 65 and Figure 66. This is a direct link between the outside and inside of the building that may cause thermal discomfort in the interior space. In order to eliminate the thermal bridge through the structure, the HSS column, which is continuous from the first to fourth floors, was terminated at the third floor. A wide flange was designed for the fourth floor, which is supported by the concrete-filled HSS below.

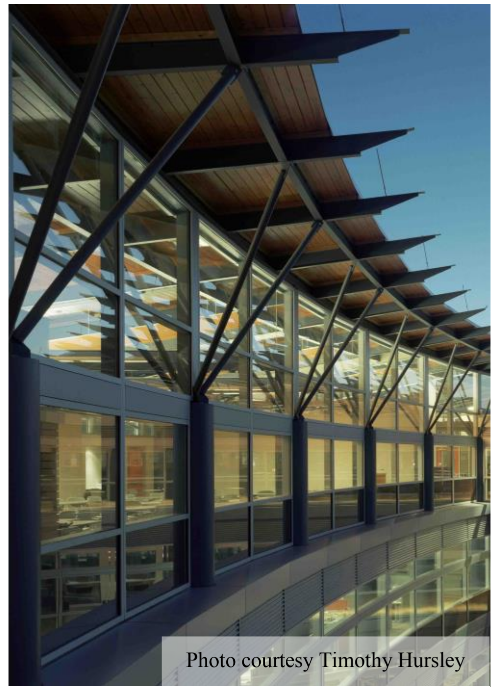


Figure 65: Exterior shot of columns

The final design of the wide flange to support roof and girder loads was a W12x40. It should be noted that a smaller wide flange could have been used; however, smaller wide flanges more easily buckle due to their square shape. These shapes were not considered for the final design. The wide flange would then be covered with an architectural façade, for example aluminum sheathing, on the exterior to give the aesthetic look of the HSS. The cavity would then be filled with insulation and covered on the interior of the building. Calculations for sizing the wide flange can be found in Appendix D.1 – Thermal Bridge Study.

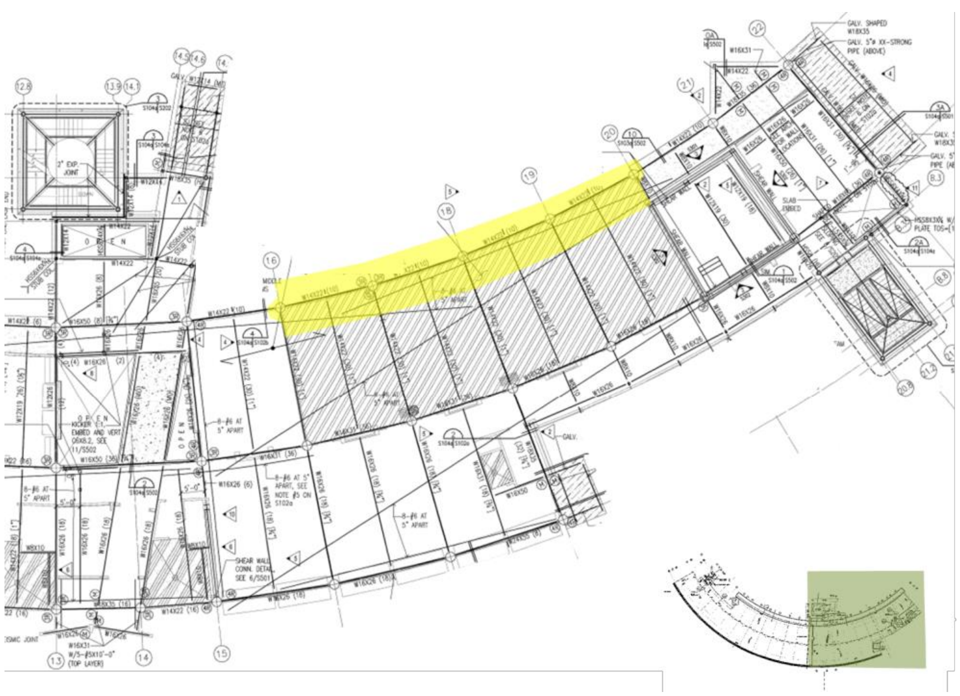

Figure 66: Columns exposed on exterior and interior

### *Thermal Productivity*

A comparison of coefficient of thermal conductivity was drawn between the redesigned system, Table 34 and existing systems, Table 35. The glass façade is summarized in Table 36 and was used for the existing and redesigned systems. The low total U-value of the new system is an improvement over the existing, providing more resistance to temperature change across the system. The worst-case heat travel was considered and is shown in Figure 67.

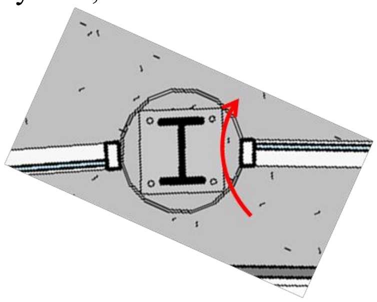

Figure 67: Worst case heat travel

| Material | Depth (in) | R (BTU-in/h-ft$^2$-$^o$F) | U (1/R) |
|---|---|---|---|
| Outside Air Film | - | 0.17 | 5.88 |
| Aluminum Composite | 0.5 | 0.06 | 15.86 |
| Batt Insulation[8] | 3 | 11.45 | 0.09 |
| Aluminum Composite[9] | 0.5 | 0.06 | 15.86 |
| Inside Air Film | - | 0.68 | 1.47 |
| | Sum | 12.43 | 0.08 |

Table 34: Redesigned HSS envelope

| Material | Depth (in) | R (BTU-in/h-ft$^2$-$^o$F) | U (1/R) |
|---|---|---|---|
| Outside Air Film | - | 0.17 | 5.88 |
| HSS Steel | 0.5 | 2.24 | 0.45 |
| Air | 23 | 0.00125 | 802.57 |
| HSS Steel | 0.5 | 2.24 | 0.45 |
| Inside Air Film | - | 0.68 | 1.47 |
| | Sum | 5.33 | 0.19 |

Table 35: Existing HSS envelope

| Material | Depth (in) | R (BTU-in/h-ft$^2$-$^o$F) | U (1/R) |
|---|---|---|---|
| Glass | - | 3.45 | 0.29 |
| | Sum | 3.45 | 0.29 |

Table 36: Glass façade envelope

An approximate 140% increase can be observed between the redesigned and existing systems; showing the added benefit of the redesigned column with batt insulation.

[8] Thermal Batt FIBERGLAS® Insulation (Owens Corning Insultating Systems, LLC, 2007)
[9] Almaxco ACP Mechanical Properties (Almaxco, 2012)

A thermal gradient was developed for the new column-wall system and is shown below in Figure 68, worst case, and Figure 69, middle condition. These calculations are summarized in Worst Case Thermal Gradient and Middle Case Thermal Gradient of Appendix D.1 – Thermal Bridge Study.

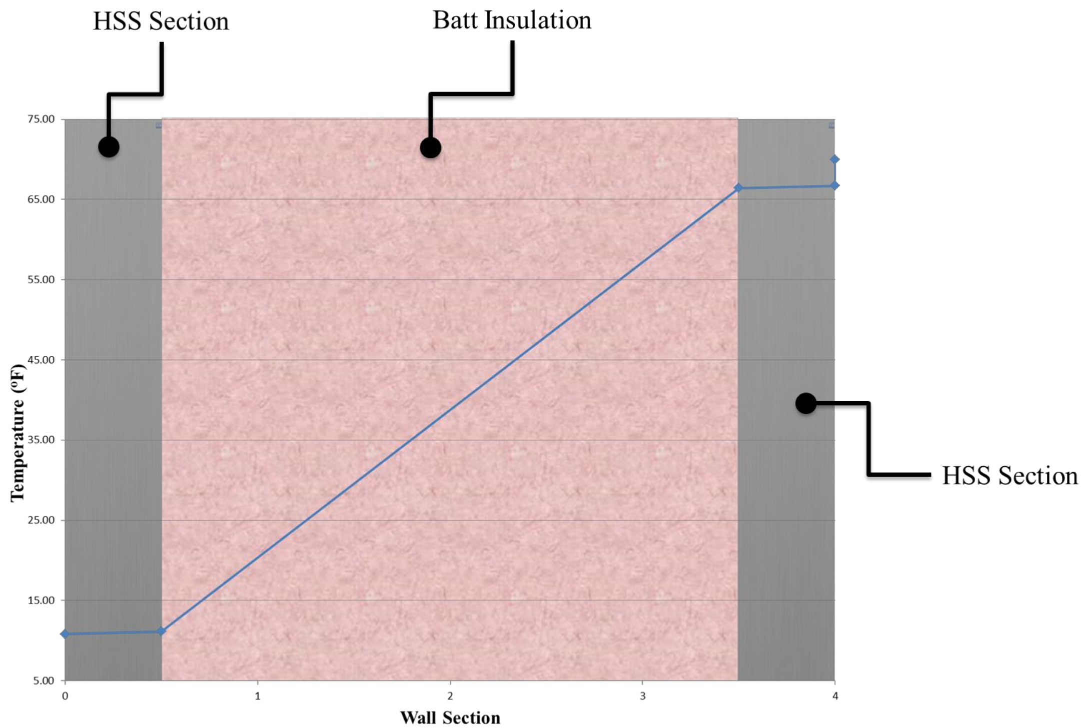


Figure 68: Worst case thermal gradient

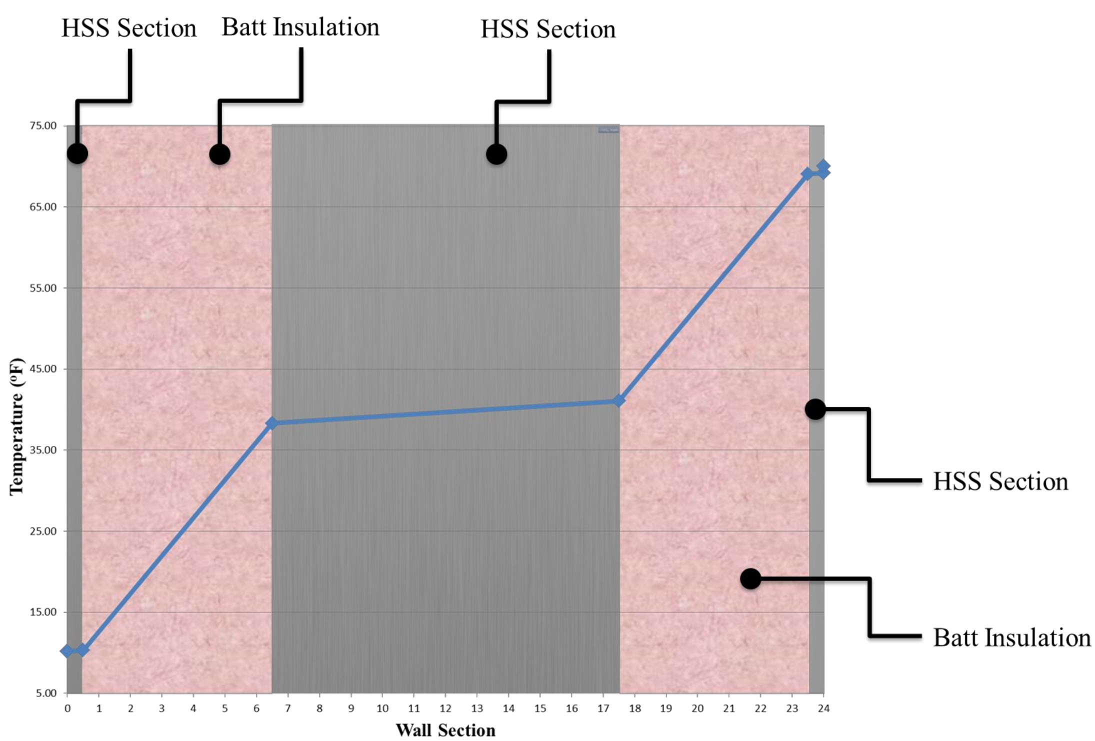


Figure 69: Middle condition thermal gradient

## *Construction Sequence*

A construction sequence for the new design was thoroughly considered and is explained below between Figure 70 and Figure 76.

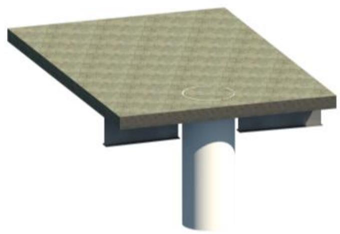

Figure 70: Phase 1 - Column Construction

Construction will begin with the finishing of the fourth floor slab.

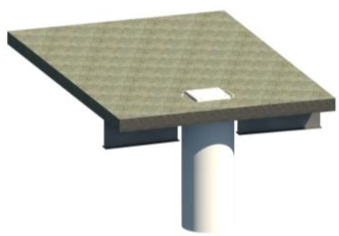

Figure 71: Phase 2 - Column Construction

A base plate will be installed over the third floor concrete filled HSS column.

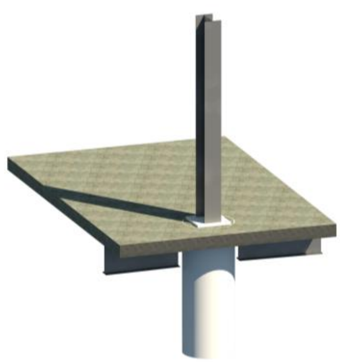

Figure 72: Phase 3 - Column Construction

The W12x40 will be installed to the base plate.

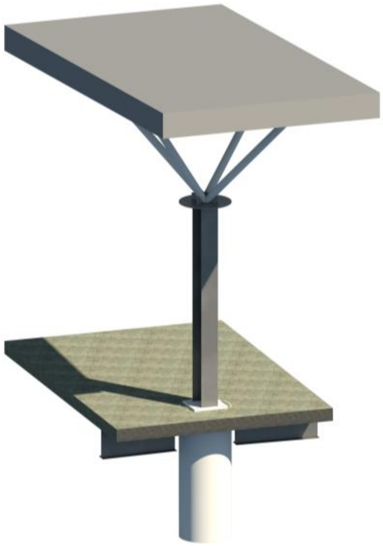

Figure 73: Phase 4 - Column Construction

Installation of inverted roof and tree column connection. The same tree column connection was used as the existing building – a $^{3}/_{8}$" base plate and (2) $^{5}/_{16}$" flange plates.

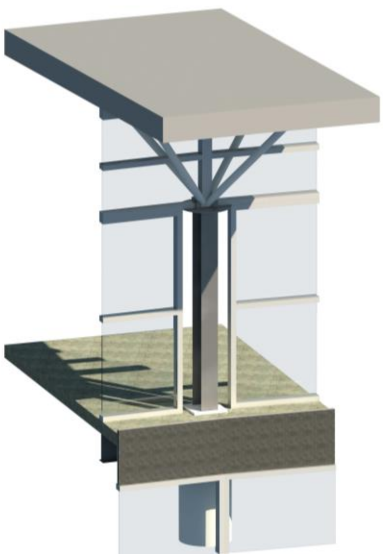

Figure 74: Phase 5 - Column Construction

Glass façade installation.

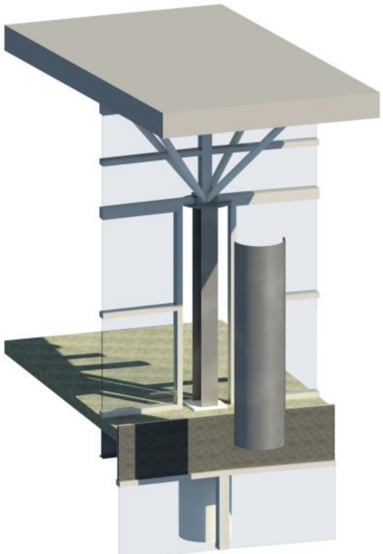

Figure 75: Phase 6 - Column Construction

The aluminum façade sheathing will be placed next, integrating with the glass façade manufacturer's mullion design for easy installation.

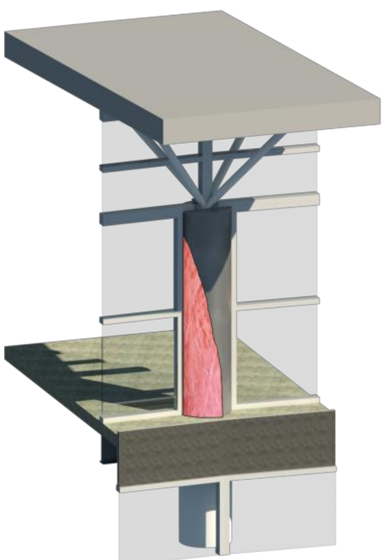

Figure 76: Phase 7 - Column Construction

The void between the aluminum sheathing and wide flange is filled with batt insulation, to properly break the thermal bridge of the original design.

The final design of the new column to prevent the thermal bridge is seen Figure 77.

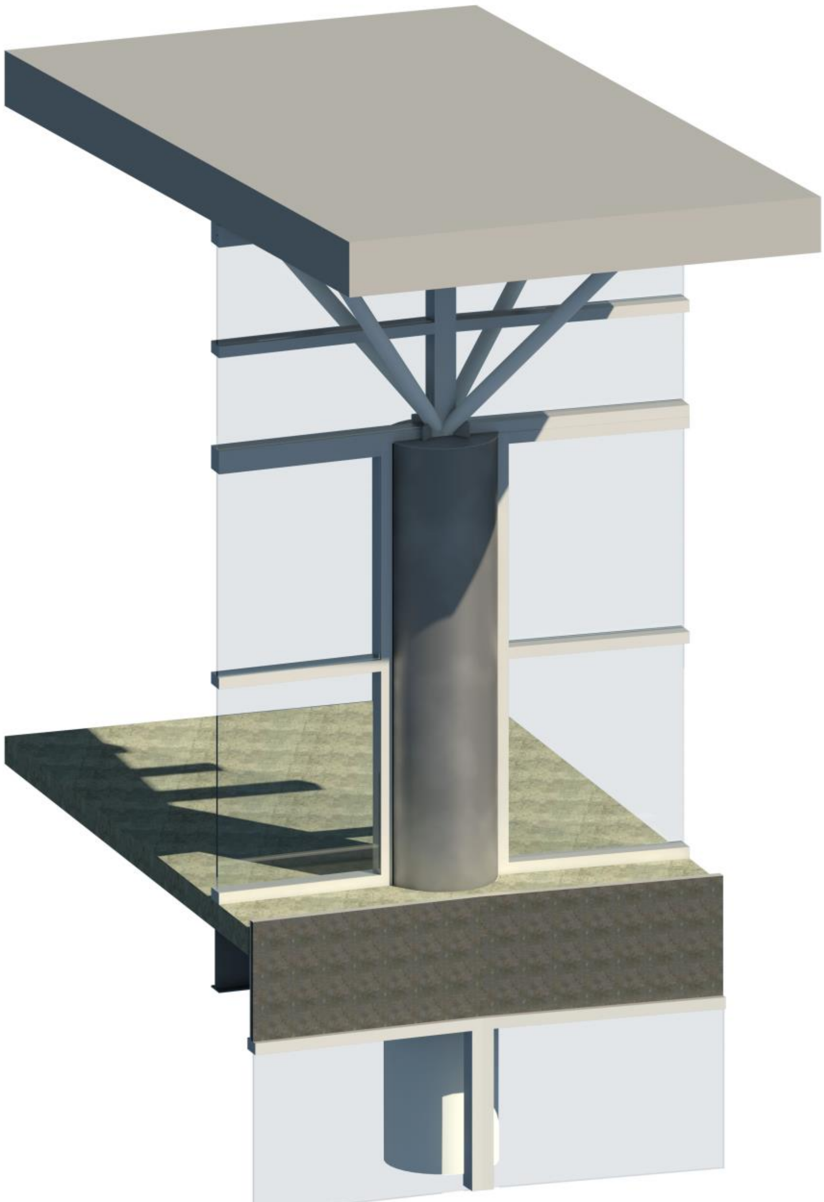

Figure 77: Final column design to prevent thermal bridge

A final rendering of a section of the building is seen below in Figure 78 (level 2 to 4) and also shows a comparison between the existing and redesigned gravity systems. The aluminum façade is shown floating in front of the building to show the new wide flange design.

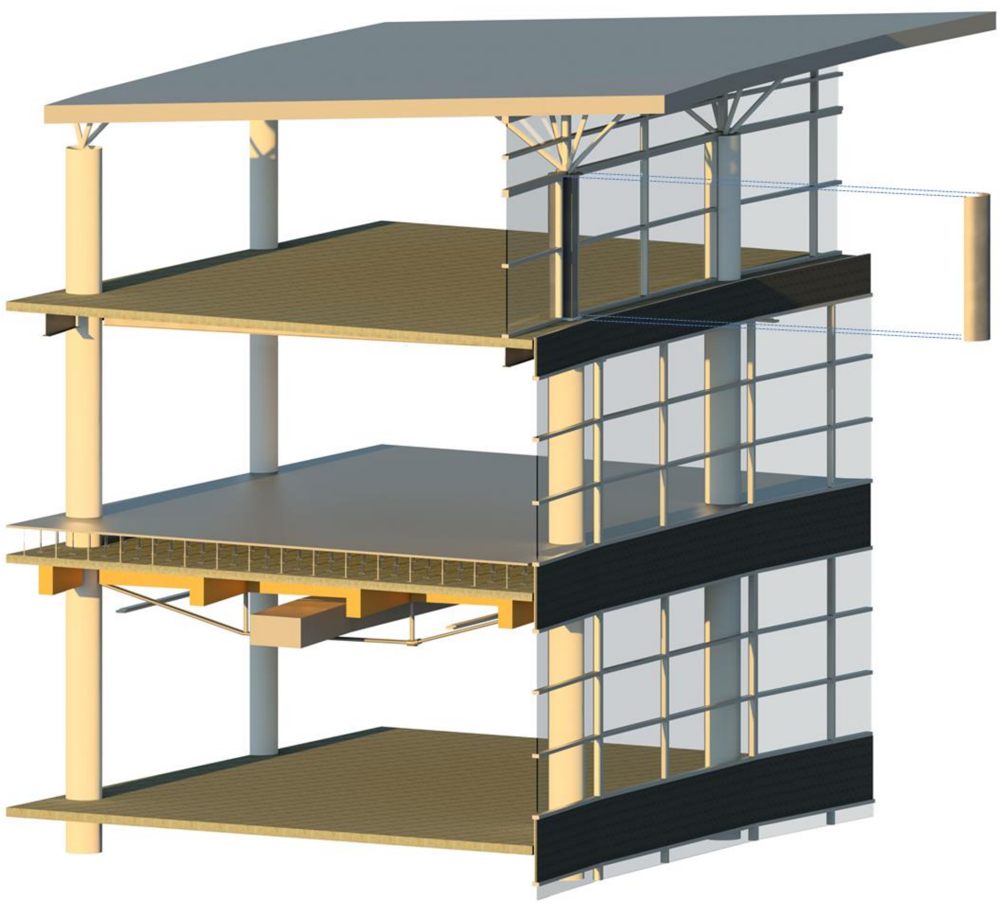

Figure 78: Building section of redesigned column

# CHAPTER 4

## ARCHITECTURE

## 4.1 ARCHITECTURE BREADTH

The drastic change in building materials led to a completely new aesthetic to the interior of the building. Besides the slight change in insulating properties of the fourth level, no other façade changes were made to the envelope. The interior changes can be viewed below in Figure 79, while the existing interior can be seen in Figure 80.

Figure 79: Interior aesthetic changes due to gravity redesign

Figure 80: Interior aesthetic from existing gravity system

## Impacts from Structural Redesign

A primary goal while examining and redesigning the structural depth of the Heifer International Center was to leave the existing layout of the building the same. This was accomplished through an exhaustive design process for the new hybrid glulam and steel gravity systems, and the new cast-in-place concrete lateral force resisting system. The interior aesthetic of the building was successfully changed and fully integrated with the mechanical and structural disciplines of the building. The new structural queen post girders provide the opportunity for occupants to better connect with the building and visually see the elements that are supporting the floors and the engineering systems which interconnect with building, as well as provide comfort to the occupants.

## Architectural Design Guidelines

The following design guideline was established at the inception of the structural depth to aide with the design of, not just the architectural components of the building, but to also positively lead the design of the engineering systems of the building. The desire to enhance the architecture by changing the structural material influenced mechanical, electrical systems and the interior appeal of the building.

These guidelines will aid in the basis for future development of the Heifer International Campus and surrounding area. The standards set forth do not seek to constrain architectural and engineering creativity, but rather to encourage a variety of designs within certain attributes that will ensure to harmonize the campus and encourage public interaction.

The goals of developing these guidelines are:

1. Promote design solutions that lend themselves to educational and visual interactions
2. Express the abstract meanings of charity through the physical form of the building and Heifer International Campus
3. Develop architectural characteristics that should be followed during the duration of the design
4. Lay the foundation for the expansion of the campus in the future and define architectural attributes that should be promoted and which should be discouraged

### *History of Heifer International*

Dan West founded Heifer International almost 70 years ago and the charity has worked tirelessly in the effort to end hunger and poverty throughout the world. By giving power to families to provide for themselves, the organization empowers communities to sustainably support themselves both agriculturally and commercially. This form of dependable food and income is the fundamental ideal of Heifer International, known as *Passing on the Gift* (Heifer International, 2014).

## *Character of the Campus*

### Site Circulation

Pedestrian paths, bicycle paths and personal and commercial vehicular movement will be promoted through the site. East 3rd Street acts as a main street to guide pedestrian and vehicular movement, while World Avenue and Shall Avenue will act as secondary streets. The site is conveniently located near a city light rail station and city bus stop. In addition, an exit off Interstate 30 is located approximately one-third of a mile away from the site. This is shown in Figure 81 below.

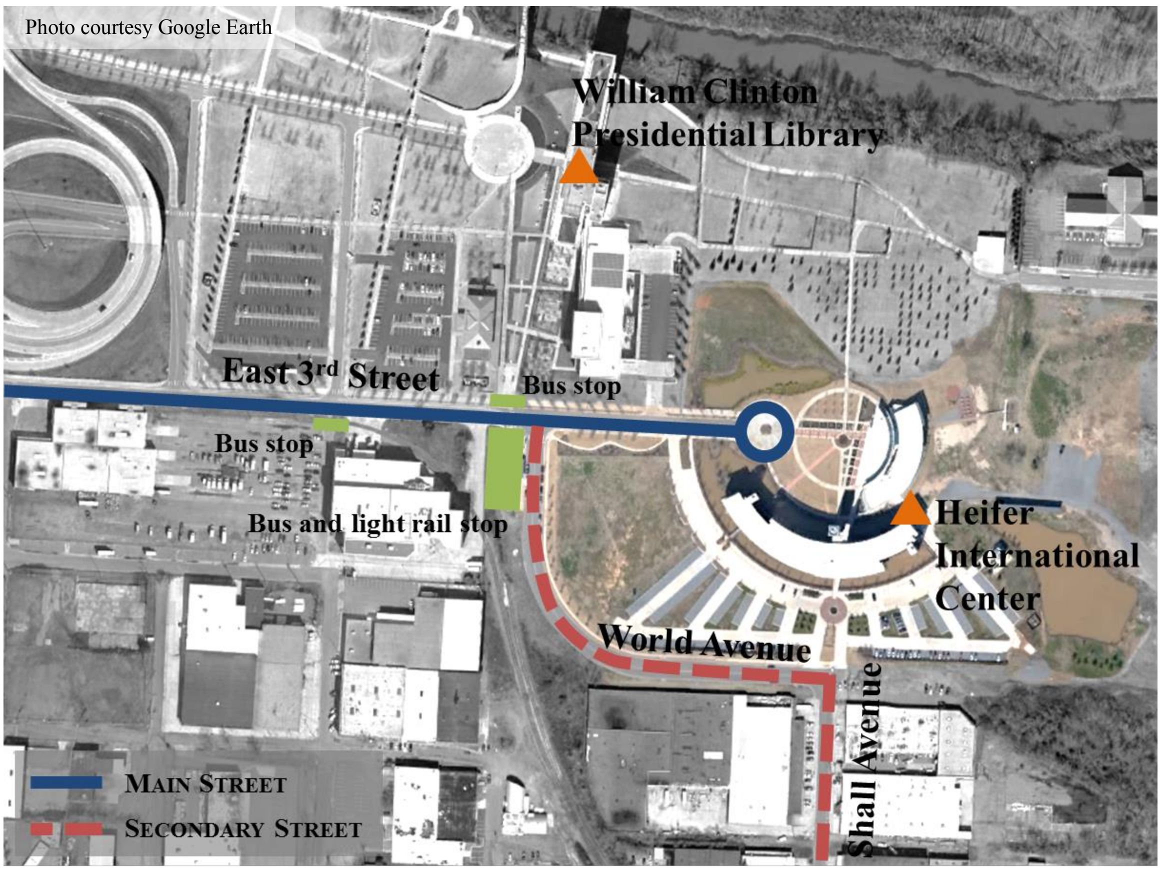


**Figure 81: Site circulation of the Heifer International campus**

Primary movement through the site will act along East 3rd Avenue, and will be the focal point for pedestrian, bicycle and vehicular entrance into the site. From here pedestrians will be able to move through the accessible campus, seen below in Figure 82.

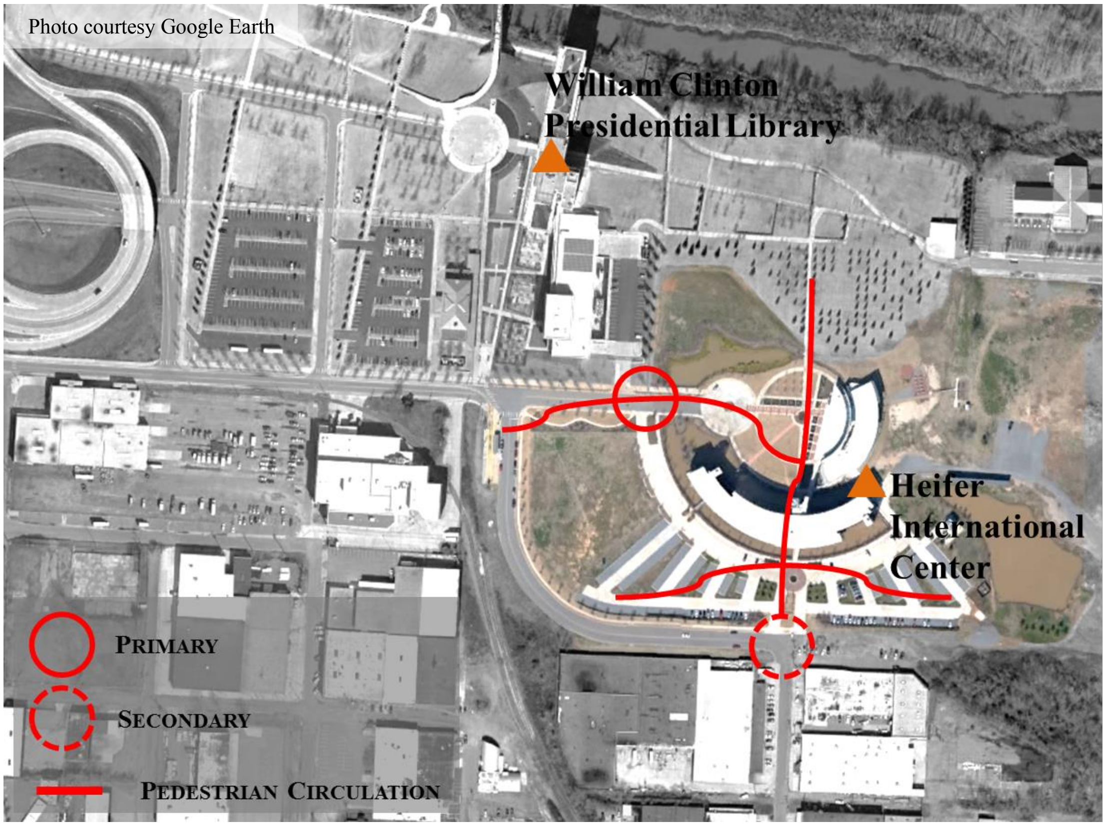


Figure 82: Primary and secondary circulation through Heifer International campus

## Movement on the Site

Buildings should create a defined outdoor space and encourage existing views of the landscape. There should be accessibility between existing and proposed buildings and a uniformity imposed on the campus. The following should be used to accomplish this:

- Roads and Parking Areas
    - Local aggregate to match color and texture of existing drive, Figure 83
    - Porous pavement system shall be used in parking areas, and bioswales shall be used to promote local plant and animal life, Figure 84
    - Parking areas shall accommodate pedestrians and vehicular circulation, Figure 85


Figure 83: Local aggregate to match color and texture

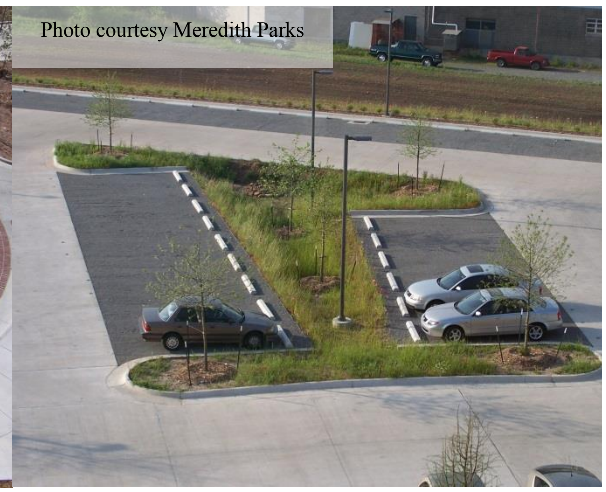


Figure 84: Porous pavement used in parking areas


Figure 85: Pedestrian and vehicular activity accommodated in parking lot

- Integrate site drainage into walkways, Figure 86
- Design of site and campus plantings responsibility of landscape architect
- Specify plants indigenous to central Arkansas to promote plant growth and habitat rehabilitation, Figure 87
- Pedestrian Paths, Figure 88
    - Central Walkway: 13'-6" wide
    - Secondary Walkways: 10' wide
    - Wetland Walkways: 8'-0" wide, concrete and heavy timber

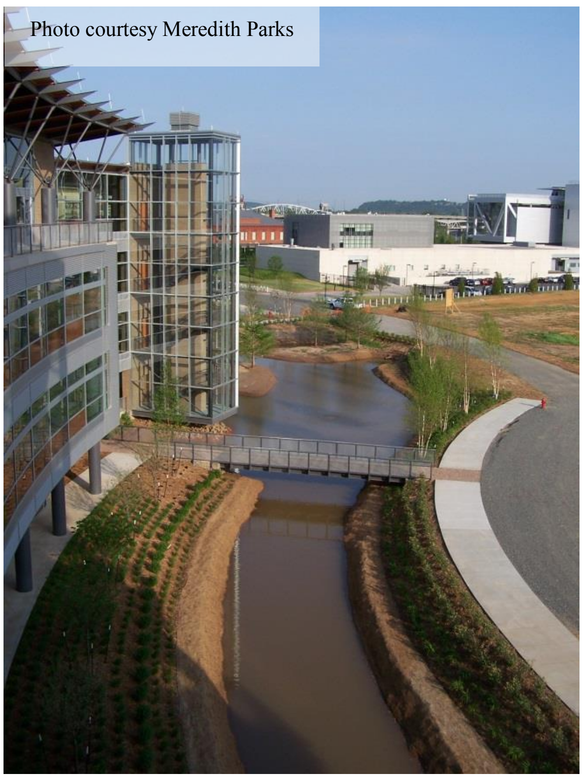


**Figure 86: Integration of walkways and incorporation of drainage system**


**Figure 87: Indigenous plantings used on the campus**

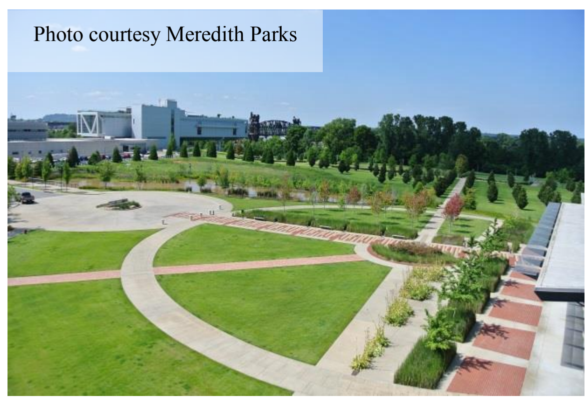


**Figure 88: Central and secondary walkways**

## *Character of Buildings*

- Typology
  - Building profile should incorporate vision of Dan West

*In all my travels around the world, the important decisions were made where people sat in a circle, facing each other as equals. – Dan West*

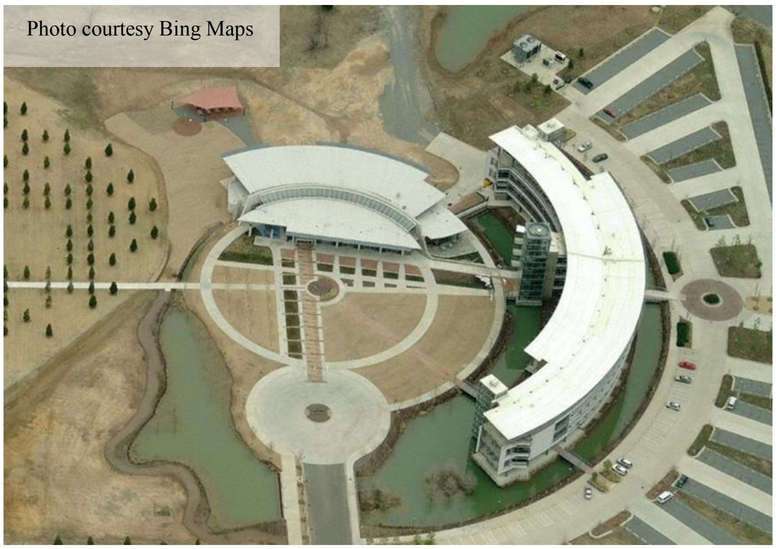


**Figure 89: Circular form of campus**

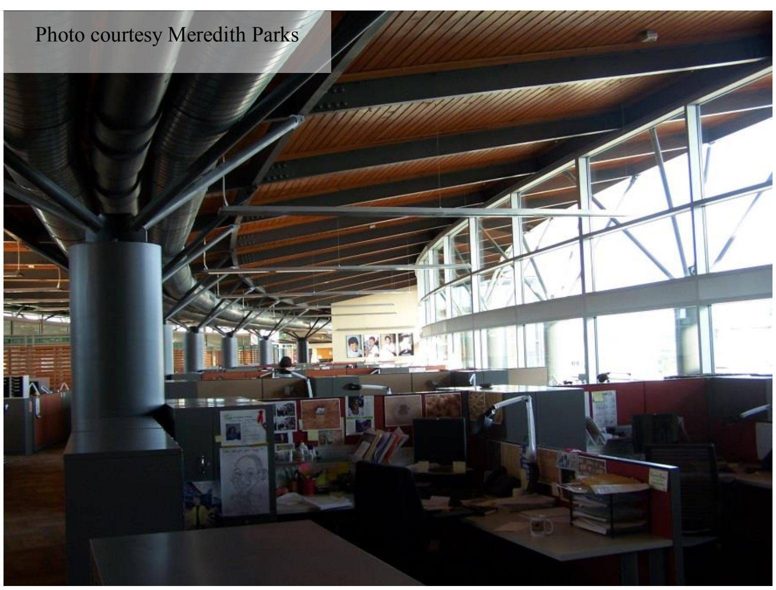


**Figure 90: Circular form of building**

- Roofs
  - Inverted roof system with a slope ranging from 1/12 to 1/6 shall be used, shown in Figure 91
  - Water collection system shall be designed to capture rainfall for use to offset potable water usage, Figure 92
  - Overhangs shall be at the discretion of the architecture, Figure 93
- Entrances and Bridges
  - Weather protected entry way, Figure 93


**Figure 91: Inverted sloped roof**


**Figure 92: Water collection system tower (far left) and local wetland (front right)**

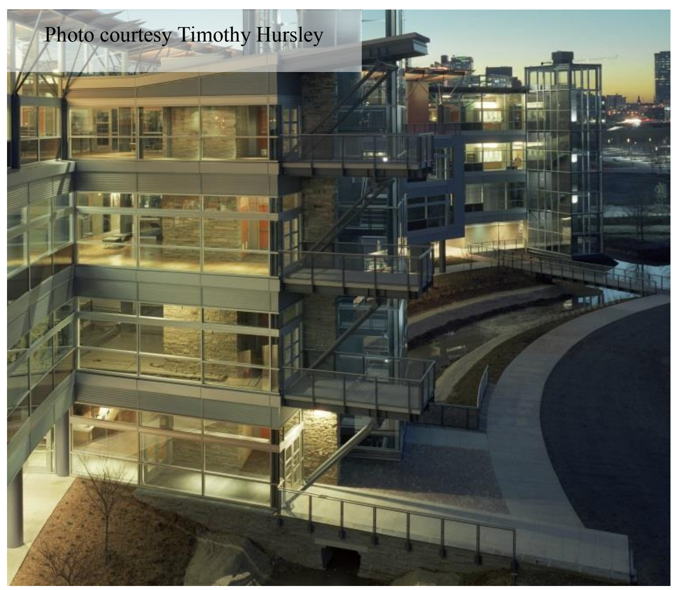


**Figure 93: Covered entrance to building**

- Walls and Windows
  - Glazing system shall promote connection with outdoors and maximize natural day lighting on all floors of the building, Figure 94 and Figure 95


**Figure 94: Natural daylighting in interior of building**


**Figure 95: Exterior shot of natural daylighting penetrating building façade**

## *Character of the Interior Space*

- Fenestration
    - Glazing system shall promote connection with outdoors and maximize natural day lighting, Figure 96 and Figure 97


**Figure 96: Interior natural lighting**


**Figure 97: Exterior view of interior artificial light**

- Spacious interior
    - Large flexible environment for a variety of public and private events, Figure 98

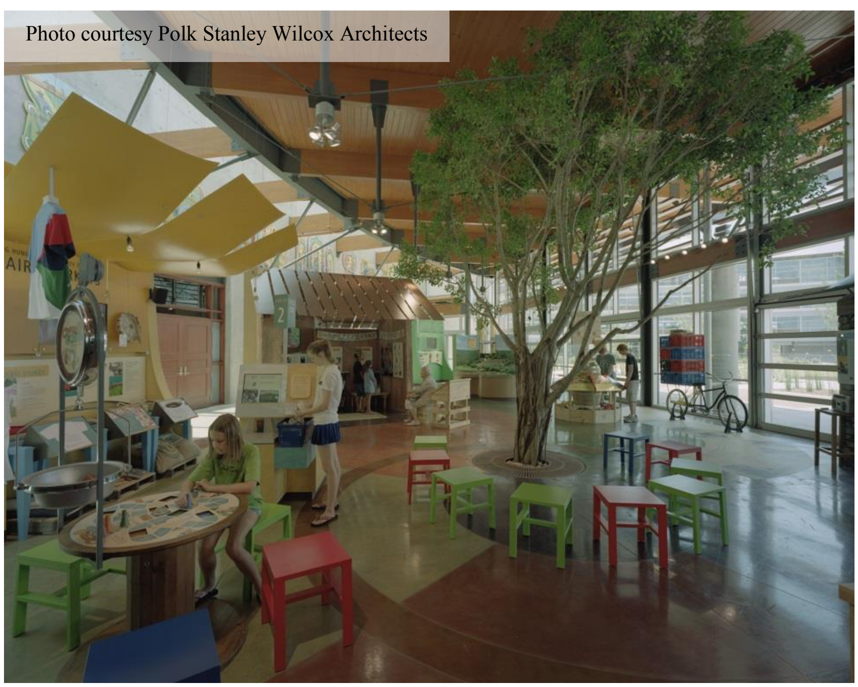


**Figure 98: Interior spacious environment**

- Structural elements
  - Materials
    - Structural materials should focus on glulam, steel and concrete, with the objective of creating a comfortable and homey environment
  - Structural bays
    - A radius should be established and a degree of separation between major structural bays should remain fairly constant
    - A reference point should be located on plans for each circular center, Figure 99

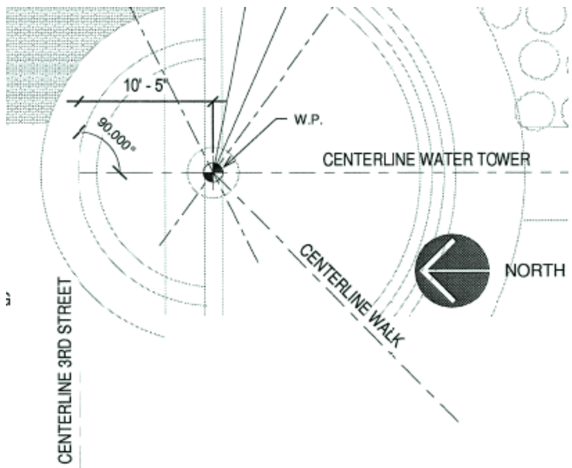


**Figure 99: Reference point on plan to mark circular center**

  - Beams
    - 3 to 4 beam proportions (or sizes) should be used on the project in order to keep a consistent pattern on the gravity system
    - Glulam and steel should be used in the gravity system
    - Steel should be painted with a nature-green color

- Columns
  - An airy atmosphere should be created by the floor to floor heights
  - Steel "tree" column
    - Representation of trees in wetlands surrounding the building and a shelter for each of the charity's employees, Figure 100 and Figure 101
    - Supports inverted roof for rainwater collection
  - 2'-0" wide round columns (steel or concrete material), Figure 102 and Figure 103

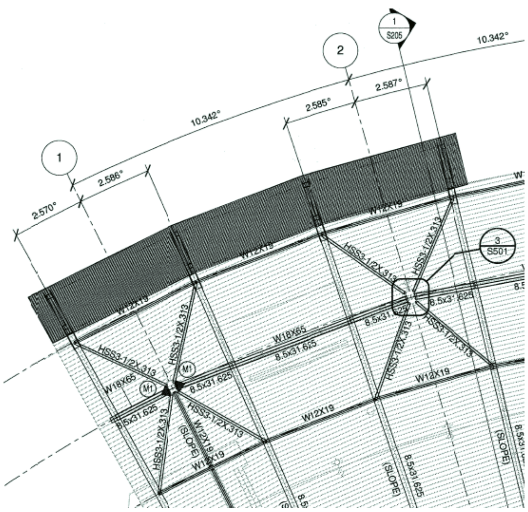


Figure 100: Plan of tree columns

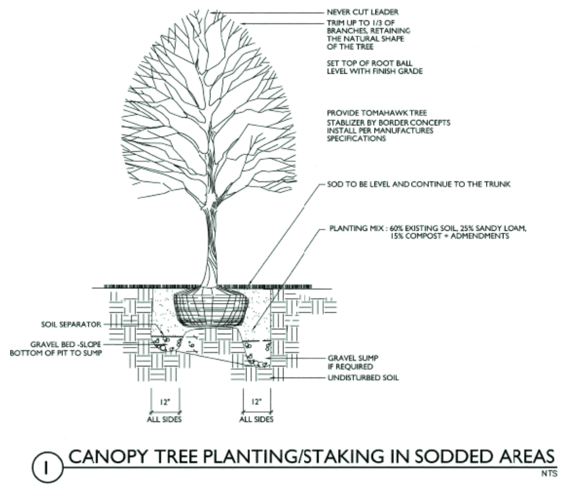


Figure 101: Inspiration for tree column canopy

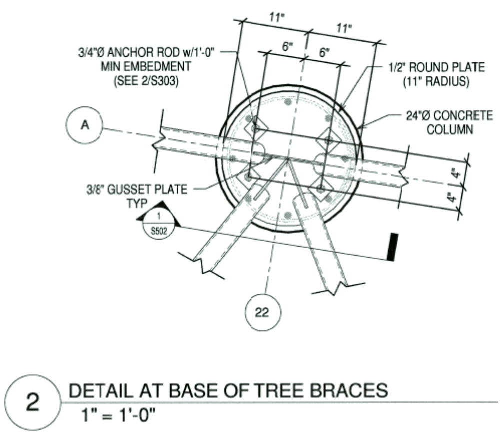


Figure 102: Plan detail of tree column connection

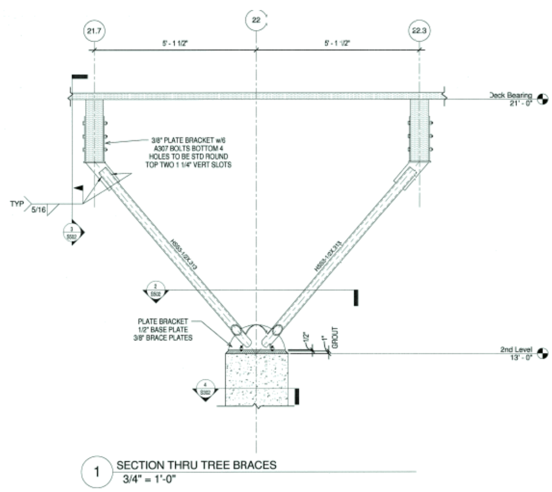


Figure 103: Section detail of tree column connection

# CHAPTER 5

# AN INVESTIGATION OF WOOD-CONCRETE COMPOSITE FLOORING SYSTEMS

Submitted in
partial requirements for degree in Architectural Engineering
with honors in Architectural Engineering

Schreyer Honors College

## 5.1 Composite Wood-Concrete Floor System

A composite wood-concrete system is well matched for the redesigned glulam gravity system of the Heifer International Center. A composite wood-concrete system, also known as a timber-concrete composite (TCC) structure, can be well adapted to the glulam beam and queen post girder system designed for the Heifer International Center. TCC is very useful for restoration work (Gelfii, Giuriani, & Marini, 2002), bridge construction (Yeoh, Fragiacomo, Franceschi, & Boon, 2011) and for new building design and construction. The main advantages of TCC are cost savings and the ability of "replacing nonrenewable resource based concrete and steel with a manageable renewable resource, and reduced energy of material production and construction carbon dioxide emissions." In addition there are technical advantages of using wood and concrete, such as increased fire and acoustical ratings (Gutkowski, Balogh, & To, 2010; Clouston & Schreyer, 2008).

The fundamental design criterion for a TCC system is to keep the neutral axis of the composite cross section close to the boundary of the timber-concrete interface—ensuring that the concrete acts purely in compression and that the timber is mostly subjected to tensile stresses. In addition, a strong and stiff connection system must be in place in order to transfer the shear forces properly and provide an effective cross area for composite action. Lastly, the design criterion calls for a strong timber section, in order to resist bending tensile stresses induced by gravity loads (Yeoh, Fragiacomo, Franceschi, & Boon, 2011).

Due to a shortage of steel in Europe after World War I and World War II, TCC systems began to develop and become popular alternatives in restoration projects of older historical buildings. The existing floor systems of historical buildings were inadequate for sound insulation and fire resistance, and were updated using TCC. This mostly European system expanded throughout the last half century for use in highway bridges and new building construction. As an example, the Vihantasalmi Bridge of Finland was built in 1999 and spans 168 meters. The bridge spans 14 meters wide, 11 meters for the road and 3 meters for a sidewalk. The Vihantasalmi Bridge is shown in Figure 104[10].

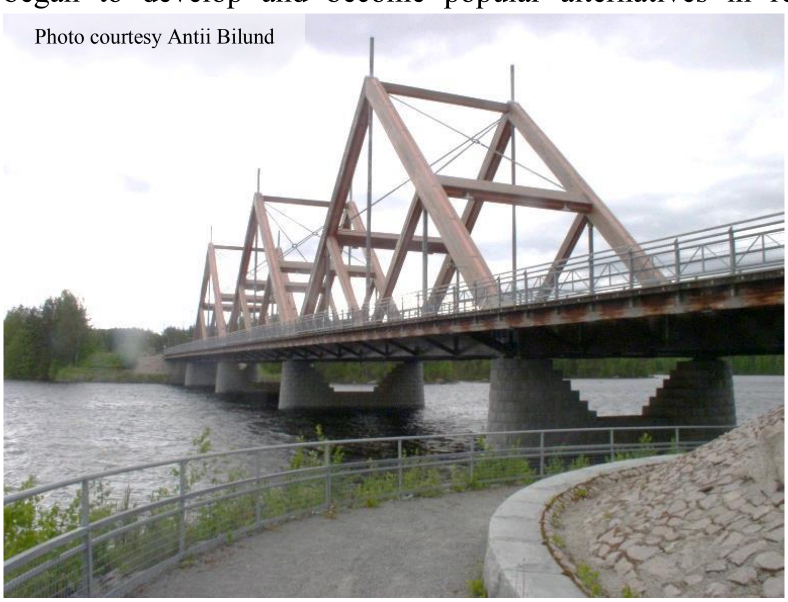


**Figure 104: The Vihantasalmi Bridge of Finland**

[10] Used with permission through the GNU Free Documentation License

## Design Standards of TCC

TCC bridges were considered as far back as 1944 with the specification of the American Association of State Highway Official. TCC is not addressed in most standards throughout the world, except the Eurocode 5, Part 2 for timber bridges. Because the interlayer shear connection is not fully rigid, the assumption of plane sections remaining plane does not apply to this type of composite section. The slip between the bottom fiber of concrete and the upper fiber of timber does not allow for the method of transformed sections.

A designer must be aware that partial composite action is possible due to the flexibility of the shear connection and that there are time-dependent properties of the composite materials. A semi-prefabricated TCC floor system is shown in Figure 105[11], and had to consider these design phenomena (Yeoh, Fragiacomo, Franceschi, & Boon, 2011; European Committee for Standardization, 2004).

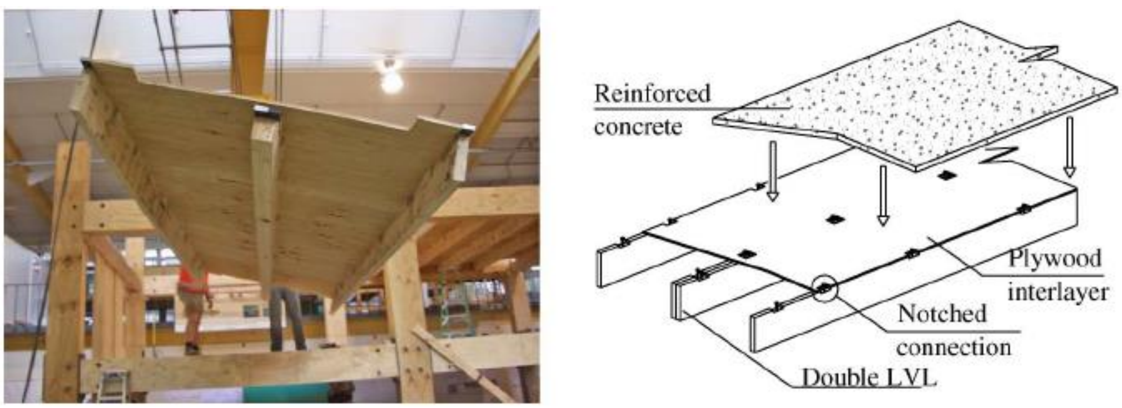


Figure 105: Semi-prefabricated TCC floor system in New Zealand (Yeoh et al.)

A thorough literature review was conducted, limited to the years of 2000 to 2014, to better understand a TCC system and how it may apply to the Heifer International Center. Research of TCC systems have led to the summary of five main systems:

1. Shear connector and wire mesh
2. Shear key connection
3. Hilti and shear key connection
4. Glued composite members
5. Custom lag bolt system

[11] Used with permission from Dr. David Yeoh, Universiti Tun Hussein Onn Malaysia (david@uthm.edu.my)

## Types of TCC Systems

### *Shear connector and wire mesh*

A continuous steel mesh is used in conjunction with a shear connector to join wood and concrete components. One half of a shear connector is embedded in a wood beam, while the other is embedded in concrete (Clouston, Bathon, & Schreyer, 2005), and is shown in Figure 106[12]. This causes composite action between the two materials. This system has been tested in static push-out tests and full scale bending tests, with a span of approximately 33'-0". The wire mesh aids with the composite action, and has performed satisfactorily in adding ductility to the shear connector, but still keeping a stiff connection between the two materials. No design guidelines exist in the United States for TCC systems; however, Eurocode 5 provides formulas which aide in the estimation of design parameters for composite systems with shear connectors (European Committee for Standardization, 2004). Clouston et al. was able to predict failures of the two load test performed on the shear connector and wire mesh composite system using the design parameters of Eurocode 5. Through several iterative tests, it was found that composite action was nearly achieved—"97% effective stiffness and 99% strength of that of a beam with full composite action."

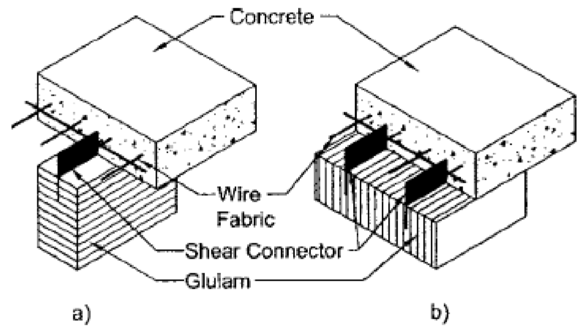


Figure 106: Shear connector and wire mesh (Clouston et al.)

### *Shear key connection*

A second TCC system comprises a construction technique which uses a keyed wood member, shown in the cross section of Figure 107[13]. The beam specimens were monitored during the construction process, and for an overall period of 133 days after the application of the service load. Using a finite element model developed by Department of Civil Engineering of the University of Canterbury, a research team was able to theoretically extend the composite structure through a service life.

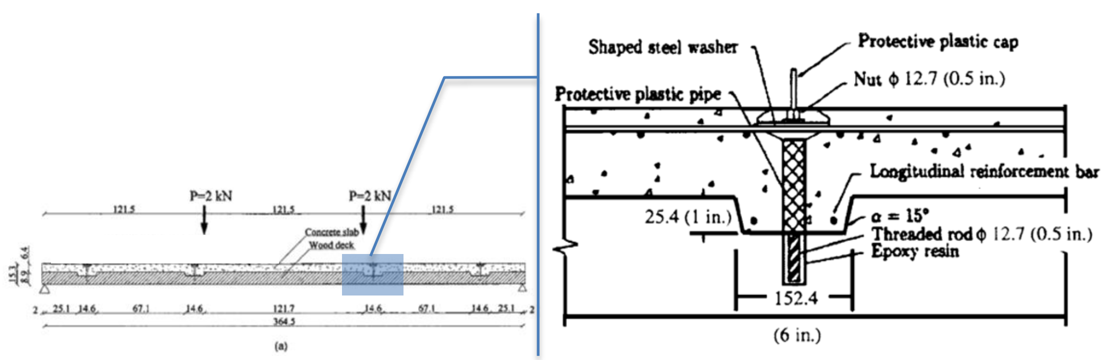


Figure 107: Shear key connection, longitudinal view (Fragiacomo et al.)

[12] Used with permission from Dr. Peggi Clouston, University of Massachusetts (clouston@umass.edu)
[13] Used with permission from Dr. Massimo Fragiacomo, University of Sassari (fragiacomo@uniss.it)

It was found that an increase in moisture from bleeding of the concrete into the timber was "not an issue for the durability of the wood deck" and that the type of construction (shored or unshored) does not affect the structural performance of the system (Fragiacomo, Gutkowski, Balogh, & Fast, 2007). Figure 108[13] shows a cross section of the shear key connection.

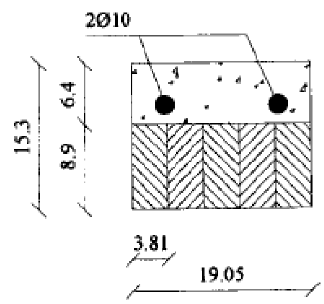


(b)

Figure 108: Shear key connection, cross section, (Fragiacomo et al.)

### *Hilti and shear key connection*

The Hilti and shear connection system is very similar to the shear key connection system just discussed; however, the system uses the proprietary system of Hilti, Inc., and is shown in Figure 109[14]. The construction of offices, hotels and apartments does not typically use light frame wood floor construction. Instead the industry tends towards cast-in-place reinforced concrete slabs or steel composite decking, as previously discussed. Research of this system has been conducted so that the formwork for the traditional concrete slab can be left in place. This allows for the development of composite action (Gutkowski, Balogh, & To, 2010).

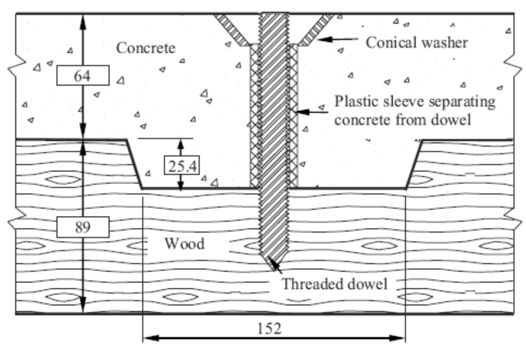


Figure 109: Hilti dowel cross section (Gutkowski et al.)

Research has shown that medium to high composite action is possible for shear key connection solid wood-concrete beam systems. This involves several tests:

- Withdrawal tests of the anchor connector
- Interlayer load-slip tests of the interlayer connection specimens
- Preliminary flexural tests of layered solid wood-concrete beam
- Tests of full scale wood-concrete floors

These tests involved nominal dimension lumber (Brown, Gutkowki, Natterer, & Shigidi, 2008).

[14] Figure from Gutkowski et al. 2010

### *Glued composite members*

The interface of the concrete and wood can be glued. Henrique et al. studied both cast-on-site and prefabricated composite timber-concrete beams, which were produced to simulate the possibility of a partial or full prefabrication composite construction. The glued interface composite members were compared to shear connector timber-concrete beams. A glued interface beam is shown in Figure 110[15].

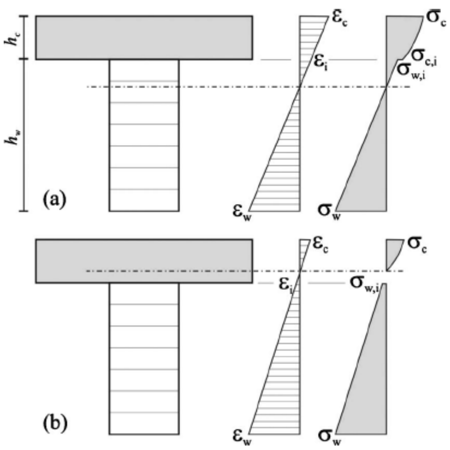


**Figure 110: Glued composite, stress and strain distribution (Henrique et al.)**

Results show that strength is similar between the three groups tested and that a greater stiffness was achieved in the glued composite timber-concrete beams. Due to greater stiffness, less deflection developed in the beam. Under stabilized and dry conditions, the prevailing mode of failure is tension in timber and, when shear failure occurs, it is mostly conditioned by the shear strength of the concrete or timber, not by the adhesive glue. A bending test is shown in Figure 111[15].

Gluing the two sections of the composite wood and concrete beam appear to be a good alternative to a shear connector. The mean and characteristic values of strength are similar for both cases, the glued elements show a stiffer behavior, albeit a small difference under service load. The system was found to have similar results, glued and not glued, for on-site and prefabricated concrete.

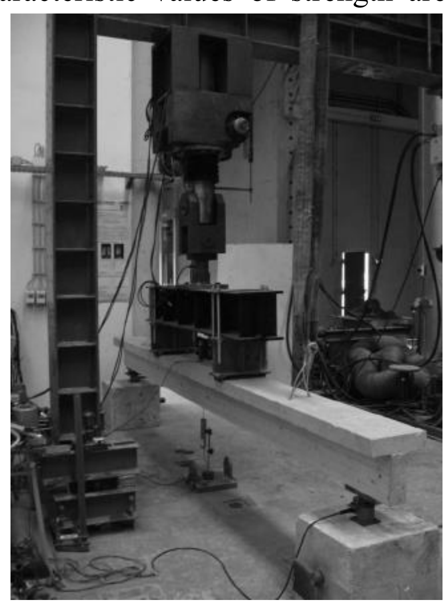

**Figure 111: Bending test of glued composite member (Henrique et al.)**

Prefabricated beams were governed by flexural tension and in the fresh cast on-site concrete the interface shear prevailed as the failure mode, but the observation of the beams has shown that the collapse was dictated by the concrete, not by the adhesive material or timber (according to the author this is odd behavior for the material). Improvement of stiffness and strength is more than 100% compared to a plain solid timber beam. This leads to the conclusion that the system is reliable; however, long-term behavior and the effect of cyclic loads require a further study (Henrique Jorge de Oliveira Negrão, Miguel Maia de Oliveira, Alexandra Leitão de Oliveira, & Barreto Cachim, 2010).

[15] Used with permission from Prof. João Negrão, University of Coimbra (jhnegrao@dec.uc.pt)

### *Custom lag bolt system*

The last system which will be discussed is a custom lag bolt system. This project for the Federal Center South Seattle District Headquarters of the United States Army Corps of Engineers involved reclaiming a substantial amount of wood beams. When paired with reclaimed decking a composite system of timber and concrete could be produced; however, required the use of a lag bolt to sufficiently link the two materials. The lag bolt had to be custom made for the project, increasing costs. The custom lag bolt system is shown in Figure 112[16]. Test assemblies were developed to test load durations and load capacity of the system.

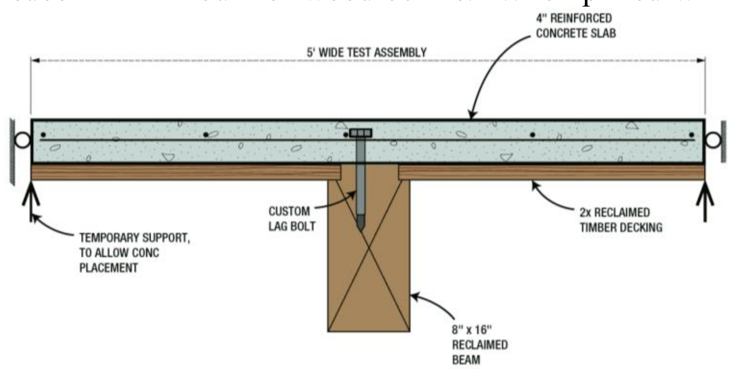

Figure 112: Custom lag bolt system (Swenson et al.)

In order for the design to pass inspection, it had to hold twice the design live load for 24 hours. At the end of the 24 hour period, the deflection of the system would be measured, and then was unloaded. It was required to recover 75% of the measured deflection within the next 24 hour time period. Each test system passed the test. The experiment continued to test failure. It was also found that the system could hold well over 400% of the design dead load and around 550% of the design dead load, with no visible sign of distress to the system. It was not until around 650% of the design live load did cracks appear and "cracking sounds were heard." After approximately 10 minutes of holding the load at 650% above design live load, the beam failed in flexure, and is shown in Figure 113[16] (Swenson & Black, 2013).


Figure 113: Tested beam before failure (Swenson et al.)

[16] Used with permission from Mr. Jim Swenson, KPFF Consulting Engineers (jim.swenson@kpff.com)

## Cyclic Loading Effects to TCC

Repeated and sustained loading have been briefly researched for wood-concrete composite systems. Balogh et al. performed cyclic loading to imitate live loading over a 30 year period for composite beams used for buildings and bridges. After the cyclic imitation loading, the beams were ramp loaded to failure. According to their findings live load cyclic loading led to an "irrecoverable increase in deflection at the end of the 21,600 load cycles on average equal to 18% of the initial elastic deflection." A steady state deflection was almost reached that was comparable to the number of cycles experienced by a major highway bridge. It was found that two types of failures mechanisms formed on the composite beams:

- Shear in the wood between the exterior notch and beam end, Figure 114[17]
- Flexure at midspan of wood member, Figure 115[17]

Figure 114: Shear failure of wood notch (Balogh et al.)

Figure 115: Midspan flexural failure (Balogh et al.)

Shear was characterized by a split from the notch to the end of the beam. This was always followed by bending failure at the midspan. The cyclic loading of the beam increased deflection by 18% and decreased beam stiffness by 9% (on average). Balogh et al. stated that the decrease in stiffness is due to the "progressive damage occurring in the connection detail" (Balogh, Fragiacomo, Gutkowski, & Fast, 2008; Clouston, Bathon, & Schreyer, 2005).

[17] Used with permission from Dr. Jeno Balogh, Metropolitan State University of Denver (jbalogh@msudenver.edu)

## Conclusion to TCC

A timber-concrete composite system offered a unique floor system to study with the new gravity glulam system of the Heifer International Center. While calculations into the design of the floor system were not explored due to time constraints and the challenging design process of TCC systems, a better understanding of the various TCC systems that exist in research and industry was obtained. If the Heifer International Center was in the design phase and a large amount of reclaimed timber was locally available, it should be truly considered as floor system for the building.

## Additional References

The following references were also used in the development of this section of the report.

Loulou, L., Caré, S., Le Roy, R., & Bornert, M. (2010). Damage of Wood-Concrete Composite subjected to variable hygrometric conditions. *EDP Sciences, 6*(28002).

Nawari, N. (2012, June). BIM Standardization and Wood Structures. *Computing in Civil Engineering*, 293-300.

Schneider III, W. G. (2005). *Shear Stud Connection Development for Steel Stringer Highway Bridges with Hardwood Glulam Timber Deck*. The Graduate School, Special Individualized Interidsciplinary Doctoral Majors. The Pennsylvania State University.

# CHAPTER 6

## CONCLUSION

## 6.1 CONCLUSION

Both the gravity and the lateral systems of the Heifer International Center were chosen for redesign. Glulam was used instead of the original steel structure and a cast-in-place concrete shear wall system instead of the steel plate shear wall system. Conceivable systems were devised that could fulfill the request of the architect to explore different structural materials for aesthetic purposes and achieve an integration among the engineering systems. While the potential cost of the system may be greater than the originally designed steel structure, the incorporation of the breadth studies aided with the understanding of how the architectural components of the building could directly tie to the structural, mechanical and electrical systems of the building.

The glulam queen post girder proved to be extremely beneficial to the design, allowing integration between the structural, mechanical, electrical and architectural disciplines. The queen post girder was able to enhance the architectural characteristic of the building by providing a direct visual link between the occupant and the designed engineering systems. Moreover, the floor-to-floor height was unchanged between the existing and redesigned system, which is important to allow for the sense of the open office atmosphere.

The redesigned lateral system, the cast-in-place concrete shear walls, does not impose any variations to the building layout. A potential connection between the glulam gravity beams and the cast-in-place concrete shear walls was studied. Seismic and wind analyses were completed and found to properly pass. Torsional irregularity was studied in depth in this project and was found to not be a significant issue based on the concrete lateral redesign.

It was important to the structural engineer to not impose any changes to the façade system, while still improving the insulating properties of the wall assembly. This was accomplished through a restructuring of the fourth floor columns, which were exposed to the exterior and interior. The U-value of the façade was greatly improved over the existing system, and yet aesthetically appears the same as the existing system.

Overall, the architect was pleased with the results to the redesign as the goals of Mr. Dan West were incorporated and respected. The redesign added a new sense of openness and strength to the building and will allow for the continuation of the charity's *Passing on the Gift*.

## REFERENCES AND WORK CITED

Almaxco. (2012). *Aluminum Composite Panels*. Singapore: Maxgrow Pte Ltd.

American Concrete Institute, ACI-318. (2011). *Building Code Requirements for Structural Concrete and Commentary*. Farmington Hills, MI.

American Institute of Steel Construction. (2011). *Steel Construction Manual* (Fourteenth ed.). American Institute of Steel Construction.

American Society of Civil Engineers. (2010). *ASCE-7 10, Minimum Design Loads for Buildings and Other Structures*. Reston, VA.

American Wood Council. (2013). *National Design Specification (NDS) for Wood Construction with Commentary 2012 Edition*. Leeburg, VA.

APA - The Engineered Wood Association. (2009). *Calculating Fire Resistance of Glulam Beams and Columns*. Tacoma.

Balogh, J., Fragiacomo, M., Gutkowski, R. M., & Fast, R. S. (2008, March). Influence of Repeated and Sustained Loading on the Performance of Layered Wood–Concrete Composite Beams. *Journal of Structural Engineering, 134*(3), 430-439.

Brown, K., Gutkowki, R., Natterer, J., & Shigidi, A. (2008, June). Laboratory tests of composite wood-concrete beams. *Construction and Building Materials, 22*(6), 1059-1066.

Clouston, P., & Schreyer, A. (2008, November). Design and Use of Wood–Concrete Composites. *Practice Periodical on Structural Design and Construction, 13*(4), 167-174.

Clouston, P., Bathon, L. A., & Schreyer, A. (2005, September). Shear and Bending Performance of a Novel Wood–Concrete Composite System. *Journal of Structural Engineers, 131*(9), 1404-1412.

European Committee for Standardization. (2004). *EN 1995: Design of timber structures*. European Committee for Standardization.

Fragiacomo, M., Gutkowski, R. M., Balogh, J., & Fast, R. S. (2007, September). Long-Term Behavior of Wood-Concrete Composite Floor/Deck Systems with Shear Key Connection Detail. *Journal of Structural Engineering, 133*(9), 1307-1315.

Gelfii, P., Giuriani, E., & Marini, A. (2002, December). Stud Shear Connection Design for Composite Concrete Slab and Wood Beams. *Journal of Structural Engineering, 128*(12), 1544-1550.

Gutkowski, R. M., Balogh, J., & To, L. G. (2010, June). Finite-Element Modeling of Short-Term Field Response of Composite Wood-Concrete Floors/Decks. *Journal of Structural Engineering, 136*(6), 707-714.

Heifer International. (2014). *Heifer International | Charity Ending Hunger and Poverty*. Retrieved from Heifer International: http://www.heifer.org/

Henrique Jorge de Oliveira Negrão, J., Miguel Maia de Oliveira, F., Alexandra Leitão de Oliveira, C., & Barreto Cachim, P. (2010, October). Glued Composite Timber-Concrete Beams. II: Analysis and Tests of Beam Specimens. *Journal of Structural Engineering, 136*(10), 1246-1254.

International Code Council. (2009). *International Building Code*. International Code Council.

Macalloy Bar & Cable Systems. (2014, February 6). Macalloy Tensile Structure Systems. Sheffield, South Yorkshire S25, United Kingdom.

Nucor Corporate. (2013). *Vulcraft Deck Catalog*. Retrieved from Vulcraft: http://www.vulcraft.com/

Owens Corning Insultating Systems, LLC. (2007). *Thermal Batt FIBERGLAS Insulation*. Toledo: Owens Corning.

Robinson, K., & Ames, D. (2000, January). Steel Plate Shear Walls: Library Seismic Upgrade. *Modern Steel Construction*.

Schneider III, W. G. (2014). BE 462 - Design of Wood Structures. The Pennsylvania State University.

Showalter, J. (2012). Connection Solutions for Wood-frame Structures. *The American Institute of Architects Continuing Education Systems*. American Wood Council.

Simpson Strong-Tie. (2014). *LGU/MGU/HGU/HHGU High Capacity Girder Hangers for Glulam*. Retrieved from Simpson Strong-Tie: http://www.strongtie.com/

Swenson, J. O., & Black, J. (2013, April). A Worthy Wager. *STRUCTURE magazine*, pp. 26-29.

U.S. Geological Survey. (2013, July). *U.S. Seismic Design Maps*. Retrieved from U.S. Geological Survey: http://www.usgs.gov/

Yeoh, D., Fragiacomo, M., Franceschi, M., & Boon, K. (2011, October). State of the Art on Timber-Concrete Composite Structures: Literature Review. *Journal of Structural Engineering, 137*(10), 1085-1095.

# APPENDIX A

## EXISTING STRUCTURAL ANALYSIS

## APPENDIX A.1 - EXISTING LATERAL SYSTEM MODELING

### Evolution of the ETABS Model

*Model of entire building*

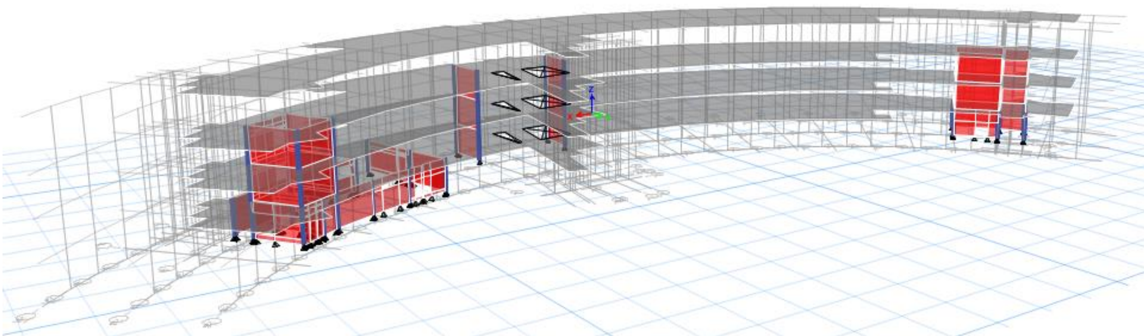

*Model of half of the building, east side*

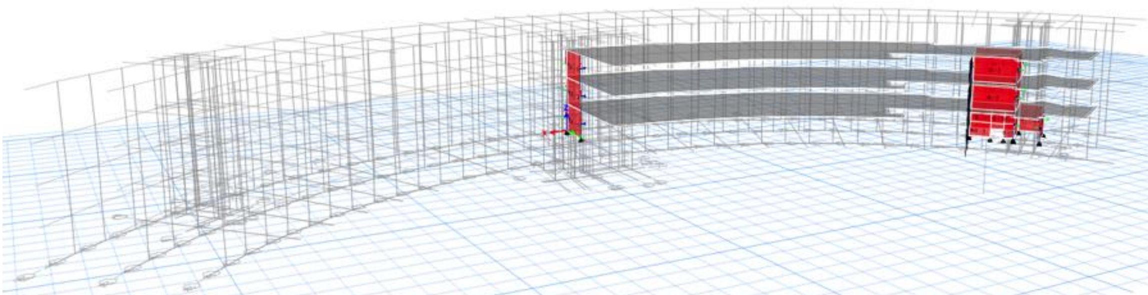

*Simplified model used in this technical report*

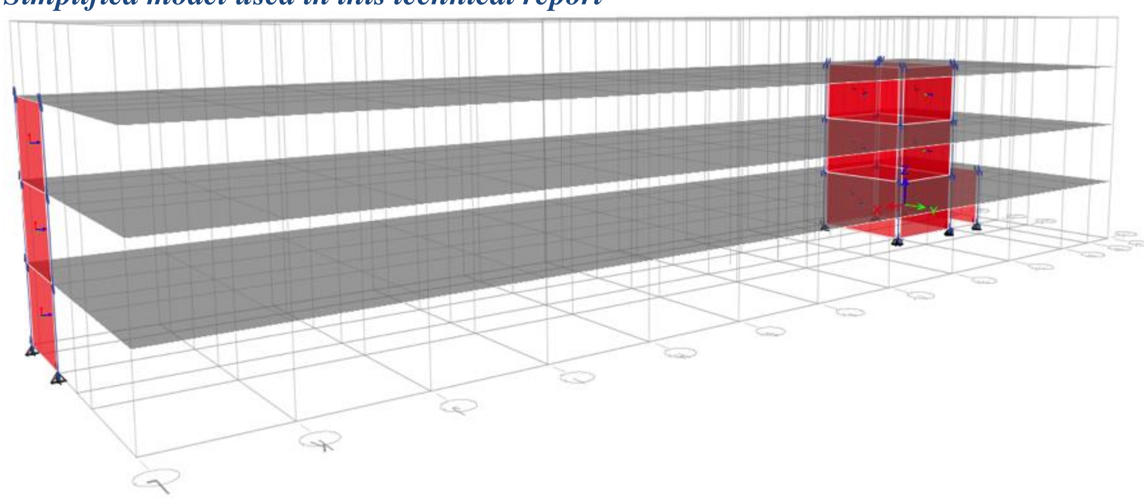

## Elevations of Shear Walls

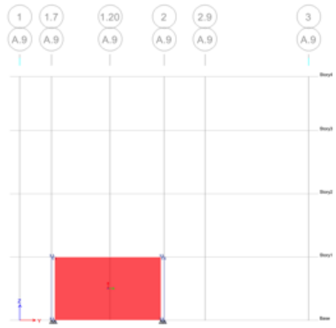

Shear Wall 1

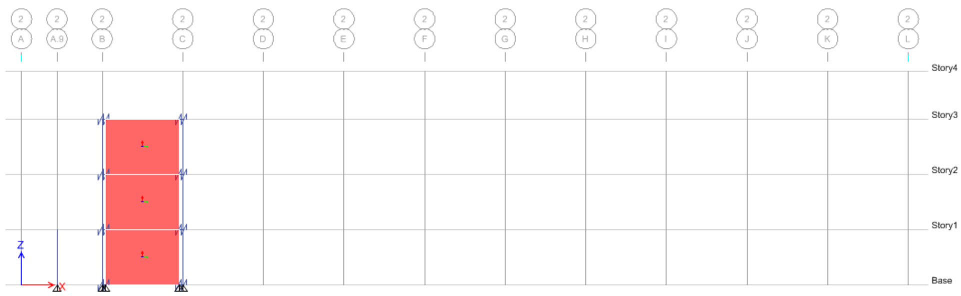


Shear Wall 2, 4, 5, and 13@12

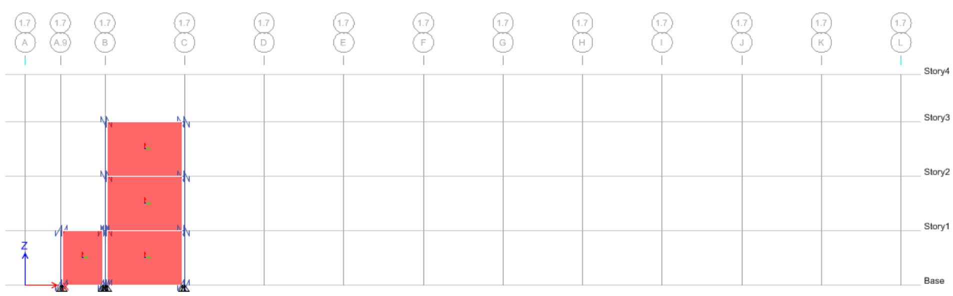


Shear Wall 3 and 3 (offset)

## ETABS SPSW to Concrete Conversion

The steel plate shear wall lateral system was converted into an equivalent concrete shear wall system, using an effective stiffness method. This equates the stiffness of the steel plate shear wall to the stiffness of a concrete shear wall. This allows for an equivalent depth, of the concrete shear wall, to be solved for. It was found an equivalent depth of 2.98" would be used in the model.

Please find the calculations for the conversion of steel to effective concrete on the next page.

The steel plate shear wall lateral system was converted into an equivalent concrete shear wall system, using an effective stiffness method. This equates the stiffness of the steel plate shear wall to the stiffness of a concrete shear wall. This allows for the an equivlanet depth, of the concrete shear wall, to be solved for.

**A36 STEEL**

| | | |
|---|---|---|
| E = | 29000 | ksi |
| G = | 11603 | ksi |
| t = | 0.375 | in |

**CONCRETE**

| | |
|---|---|
| f'c = | 4000 |
| wc = | 145 |
| E = | 3644 |
| G = | 1458 |

| WALL DIMENSIONS | | | | SPSW WALL PROPERTIES | | SPSW STIFFNESS | UPDATED WALL PROPERITES | | CONCRETE SHEAR WALL |
|---|---|---|---|---|---|---|---|---|---|
| h (ft) | h (in) | b (ft) | b (in) | Area (in2) | Inerita (in | $k_{fixed}$ (k/in | Area (in2) | Inerita (in4) | $t_{effective}$ (in) |
| 14 | 168 | 20 | 240 | 90 | 432000 | 4452 | 240 | 1152000 | 2.984901 |
| 14 | 168 | 25 | 300 | 112.5 | 843750 | 5862 | 300 | 2250000 | 2.984936 |
| 14 | 168 | 11.46 | 137.50 | 51.56 | 81230.87 | 1981 | 137.50 | 216615.65 | 2.984752 |
| 14 | 168 | 20.46 | 245.50 | 92.06 | 462363.75 | 4583 | 245.50 | 1232970.01 | 2.984905 |

EQUIVALENT DEPTH = 2.98 inches

## *Hand Calculation of SPSW to Concrete Conversion*

PORTER-GILL | TECH REPORT 4 | EFFECTIVE SPSW

CONVERT SPSW TO EFFECTIVE THICKNESS OF CONCRETE:

$$K = \frac{1}{\frac{h^3}{12EI} + \frac{1.2h}{AG}} \qquad I = \frac{tb^3}{12} \qquad A = bt$$

SPSW

SPSW: $b = 20'$, $h = 14'$, $E = 29000$ ksi, $G = 11\,603$ ksi, $t = 0.375''$

$$K_{SPSW} = \frac{1}{\frac{(14\times12)^3}{12(29000)\cdot\left(\frac{0.375(20\times12)^3}{12}\right)} + \frac{1.2(14\times12)}{(0.375(20\times12))(11603)}}$$

$= 4452.48 \sim 4453$ K/in FOR SPSW

CONC.

CONC: $b = 20'$, $h = 14'$, $E = 3644$, $G = 1458$, $t =$ (SOLVE)

$$4452.48 = \frac{1}{\frac{(14\times12)^3}{12\cdot3644\cdot\left(\frac{t\cdot(20\times12)^3}{12}\right)} + \frac{1.2(14\times12)}{(t\times(20\times12))(1458)}}$$

$t = 2.98''$ THICK CONCRETE WALL FOR COMPARABLE 3/8" THICK SPSW

## Controlling Case Data Output

The controlling case for the building was found to be the earthquake loading in the y-direction.

PORTER-GILL TECH REPORT 4 SHEAR FORCES AND LOAD COMBINATIONS

**Story 1 Shear Forces**

| Pier | Load Case/Combo | V2 | Absolute Value |
|---|---|---|---|
| SW-1 | QUAKE_X | -13.836 | 13.836 |
| SW-1 | QUAKE_X_REV | -3.049 | 3.049 |
| SW-1 | QUAKE_Y | -5.438 | 5.438 |
| SW-1 | QUAKE_Y_REVERSE | 159.8 | 159.795 |
| SW-1 | C1_X | 3.92 | 3.92 |
| SW-1 | C1_Y | 34.435 | 34.435 |
| SW-1 | C2_X | 5.784 | 5.784 |
| SW-1 | C2_Y | 96.926 | 96.926 |
| SW-1 | C1_X | 2.94 | 2.94 |
| SW-1 | C1_Y | 37.213 | 37.213 |
| SW-1 | C4_X_COMBINED | 4.262 | 4.262 |
| SW-1 | C4_Y_COMBINED | 72.673 | 72.673 |

**Max Shear =** **159.795** for **SW-1**
Controlling Load Case = QUAKE_Y_REVERSE
Tributary Area = 125 SF

| Pier | Load Case/Combo | V2 | Absolute Value |
|---|---|---|---|
| SW-13 (12) | QUAKE_X | 25.141 | 25.141 |
| SW-13 (12) | QUAKE_X_REV | 3.689 | 3.689 |
| SW-13 (12) | QUAKE_Y | 546.4 | 546.403 |
| SW-13 (12) | QUAKE_Y_REVERSE | 217.8 | 217.797 |
| SW-13 (12) | C1_X | -8.222 | 8.222 |
| SW-13 (12) | C1_Y | 90.98 | 90.98 |
| SW-13 (12) | C2_X | -12.229 | 12.229 |
| SW-13 (12) | C2_Y | 208.07 | 208.07 |
| SW-13 (12) | C1_X | -6.167 | 6.167 |
| SW-13 (12) | C1_Y | 97.827 | 97.827 |
| SW-13 (12) | C4_X_COMBINED | -9.072 | 9.072 |
| SW-13 (12) | C4_Y_COMBINED | 155.52 | 155.524 |

**Max Shear =** **546.403** for **SW-13 (12)**
Controlling Load Case = QUAKE_Y
Tributary Area = 215 SF

| Pier | Load Case/Combo | V2 | Absolute Value |
|---|---|---|---|
| SW-2 | QUAKE_X | 280.65 | 280.654 |
| SW-2 | QUAKE_X_REV | 282.62 | 282.619 |
| SW-2 | QUAKE_Y | -40.502 | 40.502 |
| SW-2 | QUAKE_Y_REVERSE | -10.397 | 10.397 |
| SW-2 | C1_X | 46.339 | 46.339 |
| SW-2 | C1_Y | -5.434 | 5.434 |
| SW-2 | C2_X | 80.897 | 80.897 |
| SW-2 | C2_Y | -11.833 | 11.833 |
| SW-2 | C1_X | 34.756 | 34.756 |
| SW-2 | C1_Y | -5.865 | 5.865 |
| SW-2 | C4_X_COMBINED | 67.152 | 67.152 |
| SW-2 | C4_Y_COMBINED | -8.837 | 8.837 |

**Max Shear =** **282.619** for **SW-2**
Controlling Load Case = QUAKE_X_REV
Tributary Area = 175 SF

| Pier | Load Case/Combo | V2 | Absolute Value |
|---|---|---|---|
| SW-3 | QUAKE_X | 299.17 | 299.17 |
| SW-3 | QUAKE_X_REV | 297.85 | 297.85 |
| SW-3 | QUAKE_Y | 27.798 | 27.798 |
| SW-3 | QUAKE_Y_REVERSE | 7.573 | 7.573 |
| SW-3 | C1_X | 47.395 | 47.395 |
| SW-3 | C1_Y | 3.847 | 3.847 |
| SW-3 | C2_X | 83.077 | 83.077 |
| SW-3 | C2_Y | 8.428 | 8.428 |
| SW-3 | C1_X | 35.548 | 35.548 |
| SW-3 | C1_Y | 4.147 | 4.147 |
| SW-3 | C4_X_COMBINED | 69.135 | 69.135 |
| SW-3 | C4_Y_COMBINED | 6.295 | 6.295 |

**Max Shear =** **299.17** for **SW-3**
Controlling Load Case = QUAKE_X
Tributary Area = 200 SF

PORTER-GILL TECH REPORT 4 SHEAR FORCES AND LOAD COMBINATIONS

| Pier | Load Case/Combo | V2 | Absolute Value |
|---|---|---|---|
| SW-3 (OFFSET) | QUAKE_X | 155.27 | 155.267 |
| SW-3 (OFFSET) | QUAKE_X_REV | 154.53 | 154.534 |
| SW-3 (OFFSET) | QUAKE_Y | 14.225 | 14.225 |
| SW-3 (OFFSET) | QUAKE_Y_REVERSE | 2.997 | 2.997 |
| SW-3 (OFFSET) | C1_X | 24.213 | 24.213 |
| SW-3 (OFFSET) | C1_Y | 1.731 | 1.731 |
| SW-3 (OFFSET) | C2_X | 42.447 | 42.447 |
| SW-3 (OFFSET) | C2_Y | 3.692 | 3.692 |
| SW-3 (OFFSET) | C1_X | 18.161 | 18.161 |
| SW-3 (OFFSET) | C1_Y | 1.875 | 1.875 |
| SW-3 (OFFSET) | C4_X_COMBINED | 35.364 | 35.364 |
| SW-3 (OFFSET) | C4_Y_COMBINED | 2.756 | 2.756 |
| **Pier** | **Load Case/Combo** | **V2** | **Absolute Value** |
| SW-4 | QUAKE_X | -7.941 | 7.941 |
| SW-4 | QUAKE_X_REV | -0.615 | 0.615 |
| SW-4 | QUAKE_Y | 39.025 | 39.025 |
| SW-4 | QUAKE_Y_REVERSE | 151.24 | 151.243 |
| SW-4 | C1_X | 2.925 | 2.925 |
| SW-4 | C1_Y | 36.319 | 36.319 |
| SW-4 | C2_X | 4.375 | 4.375 |
| SW-4 | C2_Y | 97.667 | 97.667 |
| SW-4 | C1_X | 2.194 | 2.194 |
| SW-4 | C1_Y | 38.888 | 38.888 |
| SW-4 | C4_X_COMBINED | 3.261 | 3.261 |
| SW-4 | C4_Y_COMBINED | 73.191 | 73.191 |
| **Pier** | **Load Case/Combo** | **V2** | **Absolute Value** |
| SW-5 | QUAKE_X | -2.309 | 2.309 |
| SW-5 | QUAKE_X_REV | 0.402 | 0.402 |
| SW-5 | QUAKE_Y | 119.54 | 119.536 |
| SW-5 | QUAKE_Y_REVERSE | 161.07 | 161.068 |
| SW-5 | C1_X | 1.2 | 1.2 |
| SW-5 | C1_Y | 44.728 | 44.728 |
| SW-5 | C2_X | 1.819 | 1.819 |
| SW-5 | C2_Y | 114.53 | 114.53 |
| SW-5 | C1_X | 0.9 | 0.9 |
| SW-5 | C1_Y | 47.967 | 47.967 |
| SW-5 | C4_X_COMBINED | 1.37 | 1.37 |
| SW-5 | C4_Y_COMBINED | 85.765 | 85.765 |

**Max Shear = 155.267 for SW-3 (OFFSET)**
Controlling Load Case = QUAKE_X
Tributary Area = 90 SF

**Max Shear = 151.243 for SW-4**
Controlling Load Case = QUAKE_Y_REVERSE
Tributary Area = 140 SF

**Max Shear = 161.068 for SW-5**
Controlling Load Case = QUAKE_Y_REVERSE
Tributary Area = 200 SF

**OVERALL MAXIMUM SHEAR CONTROLLING = 546.4 kip**

## APPENDIX A.2 - EXISTING SEISMIC AND WIND ANALYSIS

### Seismic Loading Calculations

add large page of calculations

## Seismic Amplification Factor

The seismic amplification factor, $A_x$, was calculated for each story, for each earthquake loading. The worst case of a particular floor, for each case, was applied to calculate the total torsional moment and accidential torsional moment. 9.5.3.5.2 covers the amplification factor that must be applied to these moments.

$$A_x = \left(\frac{\delta_{max}}{1.2\delta_{avg}}\right)^2 \qquad \text{(Eq. 9.5.3.5.2)}$$

**QUAKE_X_REGULAR**

| Level | Maximum Displacement | Average Displacement | Amplification Factor | Updated Amplification Factor |
|---|---|---|---|---|
| Story3 | 1.650297 | 1.633777 | 0.708559251 | 1.0 |
| Story2 | 0.888202 | 0.879394 | 0.708425206 | 1.0 |
| Story1 | 0.295822 | 0.293091 | 0.707446301 | 1.0 |

**QUAKE_X_REVERSE**

| Level | Maximum Displacement | Average Displacement | Amplification Factor | Updated Amplification Factor |
|---|---|---|---|---|
| Story3 | 1.637171 | 1.632025 | 0.698830707 | 1.0 |
| Story2 | 0.881133 | 0.878502 | 0.698610216 | 1.0 |
| Story1 | 0.293522 | 0.29287 | 0.697539891 | 1.0 |

**QUAKE_Y_REGULAR**

| Level | Maximum Displacement | Average Displacement | Amplification Factor | Updated Amplification Factor |
|---|---|---|---|---|
| Story3 | 2.21301 | 1.271017 | 2.105239655 | 2.1 |
| Story2 | 1.212938 | 0.691314 | 2.137784916 | 2.1 |
| Story1 | 0.42688 | 0.229725 | 2.397908479 | 2.4 |

**QUAKE_Y_REVERSE**

| Level | Maximum Displacement | Average Displacement | Amplification Factor | Updated Amplification Factor |
|---|---|---|---|---|
| Story3 | 1.358426 | 0.974261 | 1.350077945 | 1.4 |
| Story2 | 0.744244 | 0.525585 | 1.392458523 | 1.4 |
| Story1 | 0.262932 | 0.173467 | 1.59547742 | 1.6 |

Indicates controlling amplification factor

## Wind Loading Calculations

### *Case 1*

# Case 1 - ASCE-7 1998

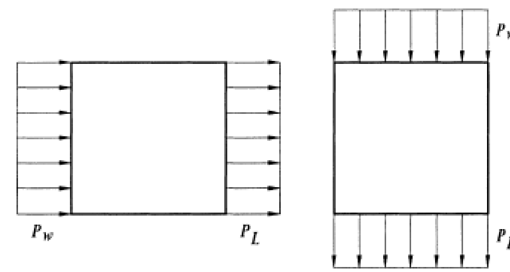


CASE 1

**Case 1, X-Direction**
**East-West**
**L = 64 feet**

| Level | $P_w$ | $P_L$ | |
|---|---|---|---|
| 1 | 10.91 | -9.78 | psf |
| 2 | 11.04 | -9.78 | psf |
| 3 | 12.57 | -9.78 | psf |
| 4 | 13.60 | -9.78 | psf |
| Roof | 14.76 | -9.78 | psf |
| Stair Tower | 15.65 | -9.78 | psf |

| | $P_w$ | $P_L$ | |
|---|---|---|---|
| Stair Tower | 15.65 | -9.78 | psf |
| Roof | 14.76 | -9.78 | psf |
| 4 | 13.60 | -9.78 | psf |
| 3 | 12.57 | -9.78 | psf |
| 2 | 11.04 | -9.78 | psf |

| | Force (k) | Force (k) | |
|---|---|---|---|
| Stair Tower | 0.1409 | -0.088 | klf |
| Roof | 0.2878 | -0.191 | klf |
| 4 | 0.2380 | -0.171 | klf |
| 3 | 0.1760 | -0.137 | klf |
| 2 | 0.1545 | -0.137 | klf |

**Loads Applied to Diaphragm**

| | $P_w$ | $P_L$ | |
|---|---|---|---|
| **lodified Roof** | 0.4286 | -0.2788 | klf |
| **4** | 0.2380 | -0.1712 | klf |
| **3** | 0.17601584 | -0.136955 | klf |
| **2** | 0.1545 | -0.1370 | klf |

**Case 1, Y-Direction**
**North-South**
**L = 225 feet**

| Level | $P_w$ | $P_L$ | |
|---|---|---|---|
| 1 | 11.00 | -3.95 | psf |
| 2 | 11.14 | -3.95 | psf |
| 3 | 12.69 | -3.95 | psf |
| 4 | 13.72 | -3.95 | psf |
| Roof | 14.89 | -3.95 | psf |
| Stair Tower | 15.79 | -3.95 | psf |

| | $P_w$ | $P_L$ | |
|---|---|---|---|
| Stair Tower | 15.79 | -3.95 | psf |
| Roof | 14.89 | -3.95 | psf |
| 4 | 13.72 | -3.95 | psf |
| 3 | 12.69 | -3.95 | psf |
| 2 | 11.14 | -3.95 | psf |

| | Force (k) | Force (k) | |
|---|---|---|---|
| Stair Tower | 0.1422 | -0.036 | klf |
| Roof | 0.1340 | -0.077 | klf |
| 4 | 0.1235 | -0.069 | klf |
| 3 | 0.1142 | -0.055 | klf |
| 2 | 0.1002 | -0.055 | klf |

**Loads Applied to Diaphragm**

| | $P_w$ | $P_L$ | |
|---|---|---|---|
| **Modified Roof** | 0.2762 | -0.1125 | klf |
| **4** | 0.1235 | -0.0691 | klf |
| **3** | 0.114185095 | -0.05528166 | klf |
| **2** | 0.1002 | -0.0553 | klf |

**East-West, X**

| Point Load | Location | |
|---|---|---|
| | X | Y |
| 45.28 | | |
| 71.46 | 112.5 | 32 |
| 20.03 | 112.5 | 32 |
| 18.65 | 112.5 | 32 |

**North-South, Y**

| Point Load | Location | |
|---|---|---|
| | X | Y |
| 87.46 | | |
| 130.80 | 112.5 | 32 |
| 38.13 | 112.5 | 32 |
| 34.99 | 112.5 | 32 |

## *Case 2*

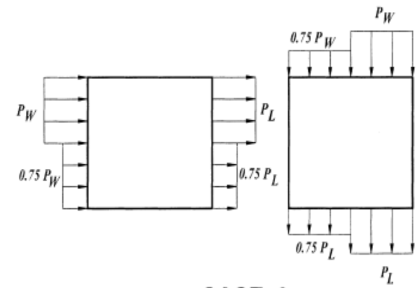


### Case 2 - ASCE-7 1998

**Case 2, X-Direction**
**East-West**
**L = 64 feet**

| Level | $P_w$ | $0.75P_w$ | $P_L$ | $0.75P_L$ | |
|---|---|---|---|---|---|
| 1 | 10.91 | 8.18 | -9.78 | -7.34 | psf |
| 2 | 11.04 | 8.28 | -9.78 | -7.34 | psf |
| 3 | 12.57 | 9.43 | -9.78 | -7.34 | psf |
| 4 | 13.60 | 10.20 | -9.78 | -7.34 | psf |
| Roof | 14.76 | 11.07 | -9.78 | -7.34 | psf |
| Stair Tower | 15.65 | 11.74 | -9.78 | -7.34 | psf |

| | $P_w$ | $0.75P_w$ | $P_L$ | $0.75P_L$ | |
|---|---|---|---|---|---|
| Stair Tower | 15.65 | 11.74 | -9.78 | -7.34 | psf |
| Roof | 14.76 | 11.07 | -9.78 | -7.34 | psf |
| 4 | 13.60 | 10.20 | -9.78 | -7.34 | psf |
| 3 | 12.57 | 9.43 | -9.78 | -7.34 | psf |
| 2 | 11.04 | 8.28 | -9.78 | -7.34 | psf |

| | Force (k) | Force (k) | Force (k) | Force (k) | |
|---|---|---|---|---|---|
| Stair Tower | 0.1409 | 0.106 | -0.0880 | -0.066 | klf |
| Roof | 0.2878 | 0.216 | -0.1908 | -0.143 | klf |
| 4 | 0.2380 | 0.178 | -0.1712 | -0.128 | klf |
| 3 | 0.1760 | 0.132 | -0.1370 | -0.103 | klf |
| 2 | 0.1545 | 0.116 | -0.1370 | -0.103 | klf |

**Loads Applied to Diaphragm**

| | $P_w$ | $0.75P_w$ | $P_L$ | $0.75P_L$ | |
|---|---|---|---|---|---|
| Modified Roof | 0.4286 | 0.3215 | -0.2788 | -0.2091 | klf |
| 4 | 0.2380 | 0.1785 | -0.1712 | -0.1284 | klf |
| 3 | 0.1760 | 0.132 | -0.1370 | -0.103 | klf |
| 2 | 0.1545 | 0.1159 | -0.1370 | -0.1027 | klf |

**Case 2, Y-Direction**
**North-South**
**L = 225 feet**

| Level | $P_w$ | $0.75P_w$ | $P_L$ | $0.75P_L$ | |
|---|---|---|---|---|---|
| 1 | 11.00 | 8.25 | -3.95 | -2.96 | psf |
| 2 | 11.14 | 8.35 | -3.95 | -2.96 | psf |
| 3 | 12.69 | 9.52 | -3.95 | -2.96 | psf |
| 4 | 13.72 | 10.29 | -3.95 | -2.96 | psf |
| Roof | 14.89 | 11.17 | -3.95 | -2.96 | psf |
| Stair Tower | 15.79 | 11.85 | -3.95 | -2.96 | psf |

| | $P_w$ | $0.75P_w$ | $P_L$ | $0.75P_L$ | |
|---|---|---|---|---|---|
| Stair Tower | 15.79 | 11.85 | -3.95 | -2.96 | psf |
| Roof | 14.89 | 11.17 | -3.95 | -2.96 | psf |
| 4 | 13.72 | 10.29 | -3.95 | -2.96 | psf |
| 3 | 12.69 | 9.52 | -3.95 | -2.96 | psf |
| 2 | 11.14 | 8.35 | -3.95 | -2.96 | psf |

| | Force (k) | Force (k) | Force (k) | Force (k) | |
|---|---|---|---|---|---|
| Stair Tower | 0.1422 | 0.107 | -0.0355 | -0.027 | klf |
| Roof | 0.2904 | 0.218 | -0.0770 | -0.058 | klf |
| 4 | 0.2402 | 0.180 | -0.0691 | -0.052 | klf |
| 3 | 0.1776 | 0.133 | -0.0553 | -0.041 | klf |
| 2 | 0.1559 | 0.117 | -0.0553 | -0.041 | klf |

**Loads Applied to Diaphragm**

| | $P_w$ | $0.75P_w$ | $P_L$ | $0.75P_L$ | |
|---|---|---|---|---|---|
| Modified Roof | 0.4325 | 0.3244 | -0.1125 | -0.0844 | klf |
| 4 | 0.2402 | 0.1801 | -0.0691 | -0.0518 | klf |
| 3 | 0.1776 | 0.133 | -0.0553 | -0.041 | klf |
| 2 | 0.1559 | 0.1169 | -0.0553 | -0.0415 | klf |

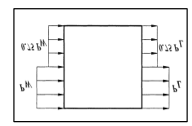

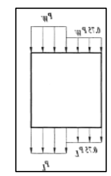

**East-West for 1.0P**

| Point Load | Location X | Location Y |
|---|---|---|
| 45.28 | | |
| 71.46 | 112.5 | 16 |
| 20.03 | 112.5 | 16 |
| 18.65 | 112.5 | 16 |

**North-South for 1.0P**

| Point Load | Location X | Location Y |
|---|---|---|
| 122.64 | | |
| 192.22 | 56.25 | 32 |
| 52.40 | 56.25 | 32 |
| 47.52 | 56.25 | 32 |

**East-West for 0.75P**

| Point Load | Location X | Location Y |
|---|---|---|
| 33.96 | | |
| 53.60 | 112.5 | 48 |
| 15.02 | 112.5 | 48 |
| 13.99 | 112.5 | 48 |

**North-South for 0.75P**

| Point Load | Location X | Location Y |
|---|---|---|
| 91.98 | | |
| 144.17 | 168.75 | 32 |
| 39.30 | 168.75 | 32 |
| 35.64 | 168.75 | 32 |

## *Case 3*

# Case 3 - ASCE-7 1998

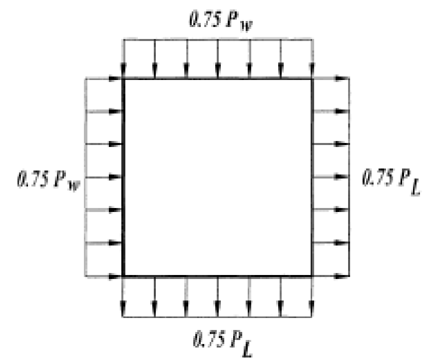


CASE 3

**Case 3, X-Direction**
**East-West**
**L = 64 feet**

| Level | $0.75P_w$ | $0.75P_L$ | |
|---|---|---|---|
| 1 | 8.18 | -7.34 | |
| 2 | 8.28 | -7.34 | |
| 3 | 9.43 | -7.34 | |
| 4 | 10.20 | -7.34 | |
| Roof | 11.07 | -7.34 | |
| Stair Tower | 11.74 | -7.34 | |
| | | | |
| | **$0.75P_w$** | **$0.75P_L$** | |
| Stair Tower | 11.74 | -7.34 | psf |
| Roof | 11.07 | -7.34 | psf |
| 4 | 10.20 | -7.34 | psf |
| 3 | 9.43 | -7.34 | psf |
| 2 | 8.28 | -7.34 | psf |
| | | | |
| | **Force (k)** | **Force (k)** | |
| Stair Tower | 0.1057 | -0.066 | klf |
| Roof | 0.2158 | -0.143 | klf |
| 4 | 0.1785 | -0.128 | klf |
| 3 | 0.1320 | -0.103 | klf |
| 2 | 0.1159 | -0.103 | klf |

**Loads Applied to Diaphragm**

| | $0.75P_w$ | $0.75P_L$ | |
|---|---|---|---|
| **odified Roof** | 0.3215 | -0.2091 | klf |
| **4** | 0.1785 | -0.1284 | klf |
| **3** | 0.1320 | -0.1027 | klf |
| **2** | 0.1159 | -0.1027 | klf |

**Case 3, Y-Direction**
**North-South**
**L = 225 feet**

| Level | $0.75P_w$ | $0.75P_L$ | |
|---|---|---|---|
| 1 | 8.25 | -2.96 | |
| 2 | 8.35 | -2.96 | |
| 3 | 9.52 | -2.96 | |
| 4 | 10.29 | -2.96 | |
| Roof | 11.17 | -2.96 | |
| Stair Tower | 11.85 | -2.96 | |
| | | | |
| | **$0.75P_w$** | **$0.75P_L$** | |
| Stair Tower | 11.85 | -2.96 | psf |
| Roof | 11.17 | -2.96 | psf |
| 4 | 10.29 | -2.96 | psf |
| 3 | 9.52 | -2.96 | psf |
| 2 | 8.35 | -2.96 | psf |
| | | | |
| | **Force (k)** | **Force (k)** | |
| Stair Tower | 0.1066 | -0.027 | klf |
| Roof | 0.2178 | -0.058 | klf |
| 4 | 0.1801 | -0.052 | klf |
| 3 | 0.1332 | -0.041 | klf |
| 2 | 0.1169 | -0.041 | klf |

**Loads Applied to Diaphragm**

| | $0.75P_w$ | $0.75P_L$ | |
|---|---|---|---|
| **Modified Roof** | 0.3244 | -0.0844 | klf |
| **4** | 0.1801 | -0.0518 | klf |
| **3** | 0.1332 | -0.0415 | klf |
| **2** | 0.1169 | -0.0415 | klf |

East-West

| Point Load | Location X | Location Y |
|---|---|---|
| 33.96 | | |
| 53.60 | 112.5 | 32 |
| 15.02 | 112.5 | 32 |
| 13.99 | 112.5 | 32 |

North-South

| Point Load | Location X | Location Y |
|---|---|---|
| 91.98 | | |
| 144.17 | 112.5 | 32 |
| 39.30 | 112.5 | 32 |
| 35.64 | 112.5 | 32 |

## *Case 4*

# Case 4 - ASCE-7 1998

Case 4, X-Direction
East-West
L = 64 feet

| Level | $0.75P_w$ | $0.56P_w$ | $0.75P_L$ | $0.56P_L$ | |
|---|---|---|---|---|---|
| 1 | 8.18 | 6.11 | -7.34 | -5.48 | psf |
| 2 | 11.04 | 6.18 | -7.34 | -5.48 | psf |
| 3 | 12.57 | 7.04 | -7.34 | -5.48 | psf |
| 4 | 13.60 | 7.62 | -7.34 | -5.48 | psf |
| Roof | 14.76 | 8.26 | -7.34 | -5.48 | psf |
| Stair Tower | 15.65 | 8.77 | -7.34 | -5.48 | psf |

| | $0.75P_w$ | $0.56P_w$ | $0.75P_L$ | $0.56P_L$ | |
|---|---|---|---|---|---|
| Stair Tower | 15.65 | 8.77 | -7.34 | -5.48 | psf |
| Roof | 14.76 | 8.26 | -7.34 | -5.48 | psf |
| 4 | 13.60 | 7.62 | -7.34 | -5.48 | psf |
| 3 | 12.57 | 7.04 | -7.34 | -5.48 | psf |
| 2 | 11.04 | 6.18 | -7.34 | -5.48 | psf |

| | Force (k) | Force (k) | Force (k) | Force (k) | |
|---|---|---|---|---|---|
| Stair Tower | 0.1409 | 0.079 | -0.0660 | -0.049 | klf |
| Roof | 0.2878 | 0.161 | -0.1431 | -0.107 | klf |
| 4 | 0.2380 | 0.133 | -0.1284 | -0.096 | klf |
| 3 | 0.1760 | 0.099 | -0.1027 | -0.077 | klf |
| 2 | 0.1545 | 0.087 | -0.1027 | -0.077 | klf |

Loads Applied to Diaphragm

| | $0.75P_w$ | $0.56P_w$ | $0.75P_L$ | $0.56P_L$ | |
|---|---|---|---|---|---|
| **odified Roof** | 0.4286 | 0.2400 | -0.2091 | -0.1561 | klf |
| **4** | 0.2380 | 0.1333 | -0.1284 | -0.0959 | klf |
| **3** | 0.1760 | 0.099 | -0.1027 | -0.077 | klf |
| **2** | 0.1545 | 0.0865 | -0.1027 | -0.0767 | klf |

Case 4, Y-Direction
North-South
L = 225 feet

| Level | $0.75P_w$ | $0.56P_w$ | $0.75P_L$ | $0.56P_L$ | |
|---|---|---|---|---|---|
| 1 | 8.25 | 6.16 | -2.96 | -2.21 | psf |
| 2 | 8.35 | 6.24 | -2.96 | -2.21 | psf |
| 3 | 9.52 | 7.10 | -2.96 | -2.21 | psf |
| 4 | 10.29 | 7.68 | -2.96 | -2.21 | psf |
| Roof | 11.17 | 8.34 | -2.96 | -2.21 | psf |
| Stair Tower | 11.85 | 8.85 | -2.96 | -2.21 | psf |

| | $0.75P_w$ | $0.56P_w$ | $0.75P_L$ | $0.56P_L$ | |
|---|---|---|---|---|---|
| Stair Tower | 11.85 | 8.85 | -2.96 | -2.21 | psf |
| Roof | 11.17 | 8.34 | -2.96 | -2.21 | psf |
| 4 | 10.29 | 7.68 | -2.96 | -2.21 | psf |
| 3 | 9.52 | 7.10 | -2.96 | -2.21 | psf |
| 2 | 8.35 | 6.24 | -2.96 | -2.21 | psf |

| | Force (k) | Force (k) | Force (k) | Force (k) | |
|---|---|---|---|---|---|
| Stair Tower | 0.1066 | 0.080 | -0.0267 | -0.020 | klf |
| Roof | 0.2178 | 0.163 | -0.0577 | -0.043 | klf |
| 4 | 0.1801 | 0.134 | -0.0518 | -0.039 | klf |
| 3 | 0.1332 | 0.099 | -0.0415 | -0.031 | klf |
| 2 | 0.1169 | 0.087 | -0.0415 | -0.031 | klf |

Loads Applied to Diaphragm

| | $0.75P_w$ | $0.56P_w$ | $0.75P_L$ | $0.56P_L$ | |
|---|---|---|---|---|---|
| **Modified Roof** | 0.3244 | 0.2422 | -0.0844 | -0.0630 | klf |
| **4** | 0.1801 | 0.1345 | -0.0518 | -0.0387 | klf |
| **3** | 0.1332 | 0.099 | -0.0415 | -0.031 | klf |
| **2** | 0.1169 | 0.0873 | -0.0415 | -0.0310 | klf |

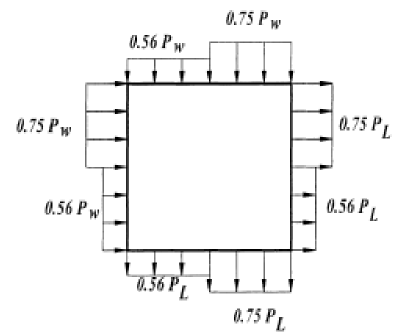


CASE 4

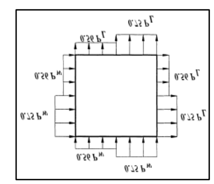

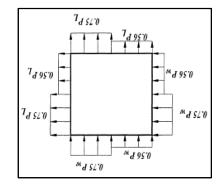

East-West for 0.75P

| Point Load | Location X | Location Y |
|---|---|---|
| 40.81 | | |
| 64.26 | 112.5 | 16 |
| 17.84 | 112.5 | 16 |
| 16.46 | 112.5 | 16 |

North-South for 0.75P

| Point Load | Location X | Location Y |
|---|---|---|
| 91.98 | | |
| 144.17 | 56.25 | 32 |
| 39.30 | 56.25 | 32 |
| 35.64 | 56.25 | 32 |

East-West for 0.56P

| Point Load | Location X | Location Y |
|---|---|---|
| 25.35 | | |
| 40.02 | 112.5 | 48 |
| 11.22 | 112.5 | 48 |
| 10.45 | 112.5 | 48 |

North-South for 0.56P

| Point Load | Location X | Location Y |
|---|---|---|
| 68.68 | | |
| 107.64 | 168.75 | 32 |
| 29.35 | 168.75 | 32 |
| 26.61 | 168.75 | 32 |

# APPENDIX B

## REDESIGN OF GRAVITY SYSTEM

## APPENDIX B.1 - TYPICAL OFFICE BEAM DESIGN

BEAM DESIGN (FRAMING INTO QUEEN POST)

$w = 164.5$ PSF

TRIB. WIDTH : 9'-8" ~ 9.67' → ROUND TO 10'

164.5 PSF × 10' = 1645 PLF or 1.7 KLF ON BEAMS

$$M = \frac{1.7(25')^2}{8} = 133'^k$$

$$R = \frac{1.7(25)}{2} = 21.25^k$$

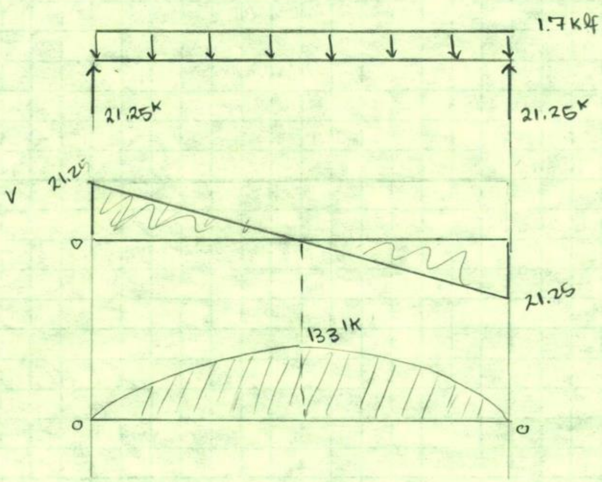


$M_{max} = 133'^K$

GLULAM, PRIMARILY IN BENDING → TABLE 5A

PLEASE SEE EXCEL SHEET FOR INTERPOLATED GLULAM SIZE...

## Loading

Computer analysis loading


## Flexure and Reactions

Computer analysis results, showing the maximum moment is 132.8 kip-ft or 133 kip-ft

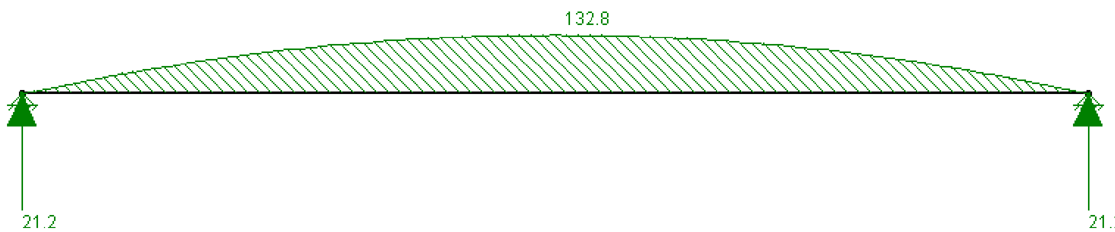

# Computer Analysis Data

Designer : **SIKANDAR PORTER-GILL**

**BEAM ANALYSIS**

February 11, 2014
12:09 PM
Checked By:_____

### Member Data

| Member Label | I Joint | J Joint | Area in^2 | Moment of Inertia in^4 | Elastic Modulus ksi | End Releases I-End | End Releases J-End | Length ft |
|---|---|---|---|---|---|---|---|---|
| M1 | N1 | N2 | 10 | 100 | 29000 | | | 25 |

### Member Distributed Loads

| Member Label | Direction | Start Magnitude (k/ft, F) | End Magnitude (k/ft, F) | Start Location (ft or %) | End Location (ft or %) |
|---|---|---|---|---|---|
| M1 | Y | -1.7 | -1.7 | 0 | 0 |

### Reactions

| Joint Label | X Force (k) | Y Force (k) | Moment (k-ft) |
|---|---|---|---|
| N1 | 0 | 21.25 | 0 |
| N2 | 0 | 21.25 | 0 |
| Totals: | 0 | 42.5 | |

### Member Section Forces

| Member Label | Section | Axial (k) | Shear (k) | Moment (k-ft) |
|---|---|---|---|---|
| M1 | 1 | 0 | 21.25 | 0 |
| | 2 | 0 | 10.625 | 99.609 |
| | 3 | 0 | 0 | 132.812 |
| | 4 | 0 | -10.625 | 99.609 |
| | 5 | 0 | -21.25 | 0 |

## Member Sizing

### Flexure in Beam

Moment 133 kip-ft

$F'_b = F_b \times C_D \times C_M \times C_t \times C_L \times C_V \times C_{fu} \times C_c \times C_i$

Pick a size,

10-1/2" x 19-1/4""

10.5 x 19.25

where the $A_{provided}$ = 202.1 $in^2$

$S_{sect\ modulus}$ = 648.5 $in^3$

| | | | |
|---|---|---|---|
| $C_D$ = | 1.00 | because live load controls | §2.3.2 |
| $C_M$ = | 1.00 | because interior beam in conditioned space | §5.3.3 |
| $C_t$ = | 1.00 | because interior beam in conditioned space | §5.3.4 |
| $C_L$ = | 0.987 | calculated below | §5.3.5 |
| $C_V$ = | 0.934 | calculated below | §5.3.6 |
| $C_{fu}$ = | 1.00 | because not loaded parellel to wide faces of lamin. | §5.3.7 |
| $C_c$ = | 1.00 | because no curvature to beam | §5.3.8 |
| $C_i$ = | 1.00 | because no tapering of beam | §5.3.9 |

Pick a Visually Graded Southern Pine Stress Group Table 5A

Group = 30F-2.1E SP

$F_b$ = 3000 psi

Emin = 1110000 psi

Calculate $C_L$ Adjustment Factor

$l_u$ = 25.00 ft, the unbraced length of the girder

d = 19.25 in, choosen to be consistent with girder depth

$l_u / d$ = 15.58

*so now we can calculate $l_e$,*

$l_e$ = 552 in, or 46.00 ft

reliant on inequality on page 16, Supplem

$R_B$ = 9.82

$$F_{bE} = \frac{1.20 E'_{min}}{(R_B)^2} = 13820.2$$

$F_b* = F_b \times C_D \times C_M \times C_t \times C_c \times C_i =$ 3000 psi

$F_{bE} / F_b* =$ 4.61

$$C_L = \frac{1 + {F_{bE}}/{F_b *}}{1.9} - \sqrt{\left(\frac{1 + {F_{bE}}/{F_b *}}{1.9}\right)^2 - \frac{{F_{bE}}/{F_b *}}{0.95}} = 0.987$$

Calculate $C_V$ Adjustment Factor

$$C_V = \left(\frac{21}{L}\right)^{1/x}\left(\frac{12}{d}\right)^{1/x}\left(\frac{5.125}{b}\right)^{1/x} \leq 1.0$$

| | | | | | |
|---|---|---|---|---|---|
| L = | 25 | ft | x = | 20 | for Southern Pine |
| d = | 19.25 | in | | | |
| b = | 10.5 | in | | | |

$C_V =$ 0.934 < 1.0

Calculate $F_b'$ Using the Minimum of $C_V$ or $C_L$

min | $C_L =$ 0.987
| $C_V =$ 0.934

$F'_b =$ 2802 psi

$f_b = \frac{M}{S} =$ 2461.1 psi < $F'_b$

Calculate $f_b$ and Determine if Selected Beam Passes

$f_b =$ 2461 psi < $F_b' =$ 2802

| **Bending Passes** |
|---|
| Use a 10-1/2" x 19-1/4"" for the beam |

## APPENDIX B.2 - QUEEN POST DESIGN HAND CALCULATION

QUEEN POST DESIGN

LOADS:

- SUPERIMPOSED DL
  - 1.5 CARPET
  - 12 COMPUTER
  - 10 SDW (MECH + LTG + SPRINKLER)
  - 10 FRAMING

33.5 PSF SDL

- LIVE LOADS
  - 80 OFFICE + PARTITIONS

- DEAD LOAD
  - 51 3VLI20 VULCRAFT DECKING

ASD → SDL + LL + DL = 33.5 + 51 + 80 = 164.5 PSF

BEAMS (INTERIOR)

TRIB. WIDTH = 9'-8" ~ 10'

164.5 PSF × 10' = 1645 PLF OR 1.7 KLF ON BEAMS

$M = \frac{wl^2}{8} = \frac{1.7(25')^2}{8} = 133^{1k}$ MAX ON BEAMS (INTERIOR)

$R = \frac{wl}{2} = \frac{1.7(25')}{2} = 21.25$ REACTION AT ENDS

× 2 b/c 2 BEAMS FALL ON EA. GIRDER SECTION

$= 42.5^k$

GENERAL FRAMING LAYOUT

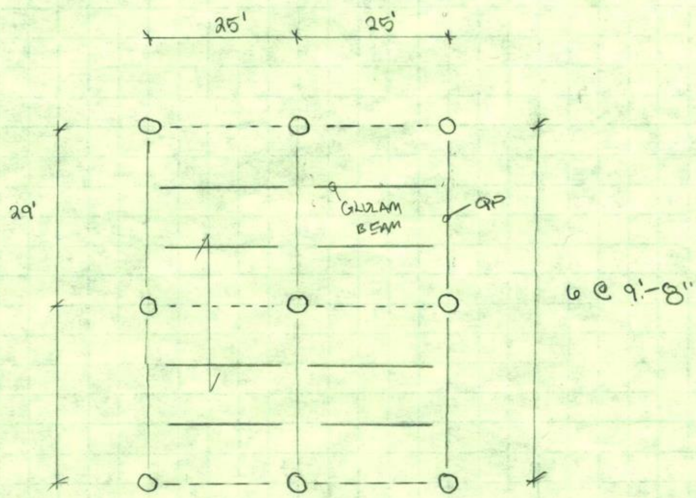

DUE TO ASSUMPTION OF HINGE, ALL 42.5$^K$ WOULD BE TRANSFERED INTO POST

TABULATED IN EXCEL PRINTOUTS

LET'S CHOOSE 9'-8" FROM BEAM END TO POST W/ 2.25' HIGH POST

$f_c = 181.37^K$ AXIAL LOAD (PARALLEL TO BEAM GRAIN)

$f_{c\perp} = 42.5^K$ SHEAR LOAD (PERPENDICULAR TO BEAM GRAIN)

$f_b = \frac{M}{S}$ (BENDING)

SOUTHERN PINE WILL BE USED

COMPRESSION PARALLEL TO BEAM GRAIN

$F_c' = F_c \times C_M \times C_t \times C_P$ TABLE 53.1

ADJUSTMENT FACTORS

$C_D = 1.0$

$C_M = 1.0$

$C_t = 1.0$

$C_P = 0.65$ assumed

$F_c =$ 1900 psi FOR 47 VISUALLY GRADED SOUTHERN PINE
FOR 4 OR MORE LAMINATIONS

So, $F_c' = (2300) \times 1 \times 1 \times 1 \times 0.65$

$= 1235$ psi

we know $f_c = 181.37^{kips} \sim 182^{kips} / AREA$

$f_c \leq F'_c$

$\frac{182^{kips}}{AREA} \times 1000^{lb/k} \leq 1235 psi$

$AREA = 147.36 \; IN^2$

a $10\text{-}1/2" \times 15\text{-}1/8" \rightarrow A = 158.8 \; IN^2$

CHECK $C_p = 0.65$ ASSUMPTION

$$C_p = \frac{1 + F_{cE}/F_c^*}{2c} - \sqrt{\left(\frac{1 + F_{cE}/F_c^*}{2c}\right)^2 - \frac{F_{cE}/F_c^*}{c}}$$

$$F_c^* = F_c \times C_D \times C_M \times C_t$$

$$= 1900 \times 1 \times 1 \times 1 = 1900 \text{ psi}$$

$$\frac{l_e}{d} = \frac{9.67' \times 12''/'}{10.5} = 11.05 < 50 \checkmark \rightarrow \text{CONTROLS}$$

$$= \frac{9.67' \times 12''/'}{15.125} = 7.67 < 50 \checkmark$$

$$E'_{min} = E_{min} \times C_m \times C_t$$

$$= (0.74 \times 10^6) \times 1.0 \times 1.0$$

$$= 0.74 \times 10^6$$

$$F_{cE} = \frac{0.822\, E'_{min}}{(l_e/d)^2} = \frac{0.822\,(0.74 \times 10^6)}{(11.05^2)}$$

$$= 4982$$

$$F_{cE} / F_c^* = 4982/1900 = 2.62 \text{ ratio}$$

$$C_p = \frac{1 + 2.62}{2 \cdot 0.9} - \sqrt{\left(\frac{1 + 2.62}{2 \cdot 0.9}\right)^2 - \frac{2.62}{0.9}}$$

$$C_p = 0.946 > 0.65 = C_{p,assumed}$$

So, member can be smaller...

Lets assume $C_p = 0.9$ instead

$F'_c = 1900 \times 1 \times 1 \times 1 \times 0.9 = 1710$ psi

$\text{AREA} = \frac{182^k \times 1000}{1710} = 106.43 \text{ IN}^2 \longrightarrow$ 8-1/2" × 13-3/4"
$A_{PROV} = 116.9 \text{ IN}^2$

Now CHECK, $C_p = 0.9$

$F_c^* = 1900$ psi (no change)

$l_e/d = \frac{9.67' \times 12''/'}{8.5} = 13.65 < 50$ ✓ → CONTROLS

$= \frac{9.67' \times 12''/'}{13.75} = 8.43 < 50$ ✓

$E'_{min} = 0.74 \times 10^6$ psi (no change)

$F_{cE} = \frac{0.822(0.74 \times 10^6)}{13.65^2} = 3264.6$ psi

$F_{cE}/F_c^* = 3265/1900 = 1.71$

$$C_p = \frac{1 + 1.71}{2 \cdot 0.9} - \sqrt{\left(\frac{1+1.71}{2 \cdot 0.9}\right)^2 - \frac{1.71}{0.9}}$$

$C_p = 0.9067$ ✓ GOOD ASSUMPTION

So, $F'_c = 1710 \times 116.9 \text{ in}^2 / 1000 = 199.89^k$ allowed

$f_c = \frac{182^k \times 1000}{116.9} = 1556$ psi

$f_c = 1556 < F'_c = 1710$ ✓ GOOD
8½ × 13-3/4

SELF WEIGHT OF SELECTED MEMBER

$$D = 62.4\left(\frac{G}{1+G(0.009)(M.C.)}\right)\left(1+\frac{M.C.}{100}\right)$$

G = 0.55 FOR 47 SOUTHERN PINE GLULAM

M.C. = 5% b/c INSIDE
OR 10%

$$D = 62.4\left(\frac{0.55}{1+0.55(0.009)(\underset{\text{or }10}{5})}\right)\left(1+\frac{\overset{\text{or }10}{5}}{100}\right)$$

= 35.17 or 35.97 PCF

we have $8\text{-}1/2 \times 13\text{-}3/4$, $A = 116.9\ IN^2$

$$A = 116.9\ IN^2 \times \frac{1^2\ ft^2}{12^2\ IN^2} = 0.8118\ ft^2$$

$$35.97\ \frac{lb}{ft^3} \times 0.8118\ ft^2 = 29.2\ plf$$

SELF WEIGHT AND POINT LOADS CAUSE MOMENT (MAX) OF $8.819^k \sim 8.9^k$ — COMPUTER ANALYSIS

BENDING ANALYSIS

$F'_b = F_b \times C_D \times C_M \times C_t \times C_L \times C_V \times C_{fu} \times C_c \times C_I$

$F_b = 1400$ psi (about x-x)

ADJUSTMENT FACTORS

$C_D = 1.0$

$C_M = 1.0$

$C_t = 1.0$

$C_L \neq 1.0$

$l_u = 9.67'$

$d = 13.75"$

$l_u/d = \dfrac{9.67' \times 12"/'}{13.75"} = 8.44$

$7 \leq l_u/d \leq 14.3$

$l_e = 1.63 l_u + 3d$

$= 1.63(9.67' \times 12) + 3(13.75")$

$= 230.39"$ or $19.19'$

$R_B = \sqrt{\dfrac{l_e d}{b^2}} = \sqrt{\dfrac{(19.19 \times 12)(13.75)}{(8.5^2)}} = 6.62$

$F_{bE} = \dfrac{1.20 E'_{min}}{R_B^2} = \dfrac{1.2(0.74 \times 10^6)}{(6.62^2)} = 20263$

$F_b^* = F_b \times C_D \times C_M \times C_t \times C_c \times C_I$

$= 1400 \times 1 \times 1 \times 1 \times 1 \times 1 = 1400$ psi

$F_{bE}/F_b^* = 20263/1400 = 14.47$

So,

$$C_L = \frac{1 + F_{bE}/F_b^*}{1.9} - \sqrt{\left(\frac{1 + F_{bE}/F_b^*}{1.9}\right)^2 - \frac{F_{bE}/F_b^*}{0.95}}$$

$$C_L = 0.9963$$

$$C_V = \left(\frac{21}{29'}\right)^{1/20} \cdot \left(\frac{12}{13.75}\right)^{1/20} \cdot \left(\frac{5.125}{8.5}\right)^{1/20} = 0.953$$

$$\min \left| \begin{array}{l} C_L = 0.9963 \\ C_V = 0.953 \end{array} \right. \longrightarrow 0.953 \text{ CONTROLS}$$

$C_{fu} = 1.0$ b/c NOT loaded parallel to wide faces of laminations

$C_c = 1.0$

$C_I = 1.0$

Now, $F_b' = 1400 \times 1 \times 1 \times 1 \times 0.953 \times 1 \times 1 \times 1$

$= 1334.2$ psi

SELF+POINT LOADS

$$f_b = \frac{M}{S} = \frac{8.9^k \times 12}{267.8} = 0.3988\text{ksi} < 1334 \text{ psi allowed}$$

$$f_b = 398.8 \text{ psi} < 1334 \text{ psi} = F_b'$$

✓Good

8-1/2" x 13-3/4"

COMBINED AXIAL AND LOADING

$$\left(\frac{f_c}{F'_c}\right)^2 + \frac{f_{b1}}{F'_{b1}(1 - f_c/F_{cE1})} \leq 1.0$$

$$\left(\frac{1556}{1710}\right)^2 + \frac{398.8}{1334(1 - 1556/8540)} = 1.191 \not\leq 1.0$$

X FAILS INTERACTION

where,

$$F_{cE} = \frac{0.822\,E'_{min}}{(l_{e1}/d_1)^2} = \frac{0.822(6.74 \times 10^6)}{\left(\frac{9.67' \times 12}{13.75}\right)^2} = 8540$$

AN EXCEL SHEET WILL BE USED TO INTERPOLATE THE SIZE OF THE GLULAM BEAM REQUIRED...

## APPENDIX B.3 - TYPICAL OFFICE QUEEN POST DESIGN

### Loading

Computer analysis loading

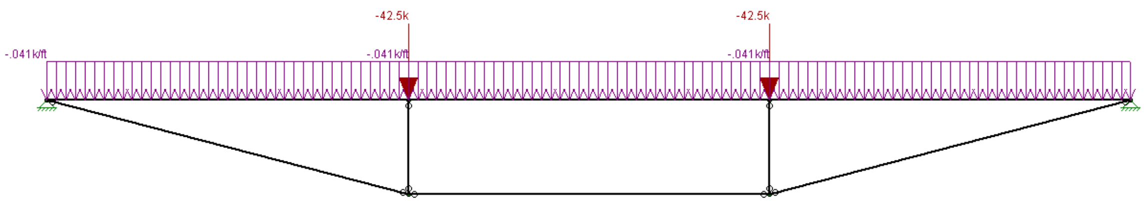


### Flexure and Reactions

Computer analysis results, showing the maximum moment is 8.9 kip-ft

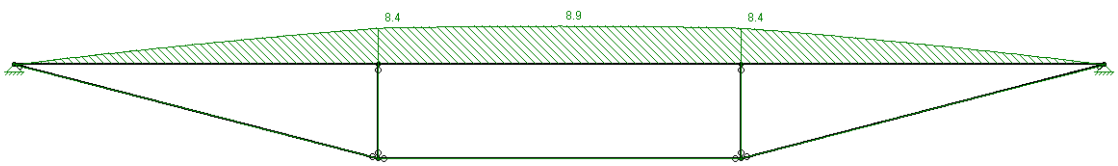


### Axial Cable and Girder Forces

The assumption of the hinged queen post was used to determine the post reactions, cable tension and girder axial forces.

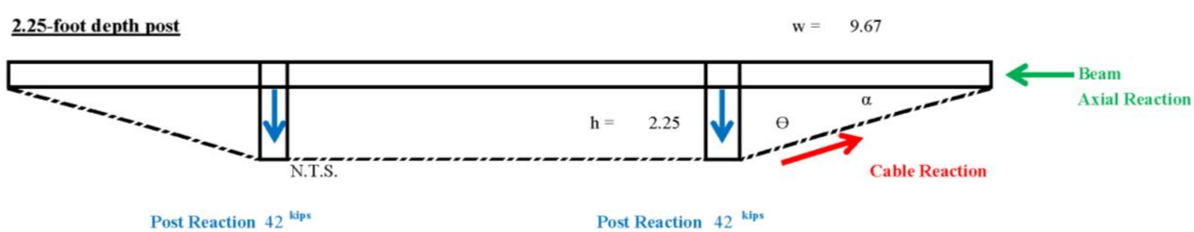


PRELIMINARY CALCULATIONS

Θ = tan-1(w/h) = 1.34 radians

α = 88.66 radians

CALCULATE RESULTANT FORCES IN CABLE AND BEAM

Cable Reaction 186.21 kips

Beam Axial Reaction 181.37 kips

# Computer Analysis Data

Designer : **SIKANDAR PORTER-GILL**

**GIRDER ANALYSIS**

February 11, 2014
12:03 PM
Checked By:_____

## Member Data

| Member Label | I Joint | J Joint | Area in^2 | Moment of Inertia in^4 | Elastic Modulus ksi | End Releases I-End | End Releases J-End | Length ft |
|---|---|---|---|---|---|---|---|---|
| M1 | N1 | N2 | 10 | 100 | 29000 | | | 9.67 |
| M2 | N2 | N3 | 10 | 100 | 29000 | | | 9.66 |
| M3 | N3 | N4 | 10 | 100 | 29000 | | | 9.67 |
| M4 | N1 | N5 | 10 | 100 | 29000 | PIN | PIN | 9.988 |
| M5 | N5 | N6 | 10 | 100 | 29000 | PIN | PIN | 9.66 |
| M6 | N6 | N4 | 10 | 100 | 29000 | PIN | PIN | 9.988 |
| M7 | N2 | N5 | 10 | 100 | 29000 | PIN | PIN | 2.5 |
| M8 | N3 | N6 | 10 | 100 | 29000 | PIN | PIN | 2.5 |

## Joint Loads/Enforced Displacements

| Joint Label | [L]oad or [D]isplacement | Direction | Magnitude (k, k-ft, in, rad) |
|---|---|---|---|
| N2 | L | Y | -42.5 |
| N3 | L | Y | -42.5 |

## Member Distributed Loads

| Member Label | Direction | Start Magnitude (k/ft, F) | End Magnitude (k/ft, F) | Start Location (ft or %) | End Location (ft or %) |
|---|---|---|---|---|---|
| M1 | Y | -.041 | -.041 | 0 | 0 |
| M2 | Y | -.041 | -.041 | 0 | 0 |
| M3 | Y | -.041 | -.041 | 0 | 0 |

## Reactions

| Joint Label | X Force (k) | Y Force (k) | Moment (k-ft) |
|---|---|---|---|
| N1 | -162.565 | 43.095 | 0 |
| N4 | 162.565 | 43.094 | 0 |
| Totals: | 0 | 86.189 | |

## Member Section Forces

| Member Label | Section | Axial (k) | Shear (k) | Moment (k-ft) |
|---|---|---|---|---|
| M1 | 1 | 0 | 1.066 | 0 |
| | 2 | 0 | .967 | 2.458 |
| | 3 | 0 | .868 | 4.676 |
| | 4 | 0 | .769 | 6.655 |
| | 5 | 0 | .67 | 8.394 |
| M2 | 1 | 0 | .198 | 8.394 |
| | 2 | 0 | .099 | 8.752 |
| | 3 | 0 | 0 | 8.872 |
| | 4 | 0 | -.099 | 8.752 |
| | 5 | 0 | -.198 | 8.394 |
| M3 | 1 | 0 | -.67 | 8.394 |
| | 2 | 0 | -.769 | 6.655 |
| | 3 | 0 | -.868 | 4.676 |
| | 4 | 0 | -.967 | 2.458 |
| | 5 | 0 | -1.066 | 0 |
| M4 | 1 | -167.91 | 0 | 0 |
| | 2 | -167.91 | 0 | 0 |
| | 3 | -167.91 | 0 | 0 |

Designer : **SIKANDAR PORTER-GILL** **GIRDER ANALYSIS**
February 11, 2014
12:03 PM
Checked By:_____

## *Member Section Forces*

| Member Label | Section | Axial (k) | Shear (k) | Moment (k-ft) |
|---|---|---|---|---|
| | 4 | -167.91 | 0 | 0 |
| | 5 | -167.91 | 0 | 0 |
| M5 | 1 | -162.565 | 0 | 0 |
| | 2 | -162.565 | 0 | 0 |
| | 3 | -162.565 | 0 | 0 |
| | 4 | -162.565 | 0 | 0 |
| | 5 | -162.565 | 0 | 0 |
| M6 | 1 | -167.91 | 0 | 0 |
| | 2 | -167.91 | 0 | 0 |
| | 3 | -167.91 | 0 | 0 |
| | 4 | -167.91 | 0 | 0 |
| | 5 | -167.91 | 0 | 0 |
| M7 | 1 | 42.028 | 0 | 0 |
| | 2 | 42.028 | 0 | 0 |
| | 3 | 42.028 | 0 | 0 |
| | 4 | 42.028 | 0 | 0 |
| | 5 | 42.028 | 0 | 0 |
| M8 | 1 | 42.028 | 0 | 0 |
| | 2 | 42.028 | 0 | 0 |
| | 3 | 42.028 | 0 | 0 |
| | 4 | 42.028 | 0 | 0 |
| | 5 | 42.028 | 0 | 0 |

## Top Chord Member Sizing

**Compression Parallel to Beam Grain** Axial Compression **181.37** kips

$F'_c = F_c \times C_D \times C_M \times C_t \times C_p$

Adjustment Factors

| | | | |
|---|---|---|---|
| $C_D$ = | 1.00 | because live load controls | §2.3.2 |
| $C_M$ = | 1.00 | because interior beam in conditioned space | §5.3.3 |
| $C_t$ = | 1.00 | because interior beam in conditioned space | §5.3.4 |
| $C_p$ = | 0.92 | assumed value | §3.7.1 |

Pick a Visually Graded Southern Pine Stress Group — Table 5B

| | | |
|---|---|---|
| Group = | 50 | |
| $F_c$ = | 2300 | psi |
| Emin = | 1000000 | psi |

*so,*

$F'_c$ = 2116 psi allowable compression stress

*now the required area would be,*

A = 86 in$^2$ required area of glulam

Pick a,

8-1/2" x 19-1/4"

8.5 x 19.25

where the $A_{provided}$ = 163.6 in$^2$

Is the area greater than required area? Yes

Check the Assumption of the $C_p$ Adjustment Factor

$$C_p = \frac{1 + {F_{CE}}/{F_c *}}{2c} - \sqrt{\left(\frac{1 + {F_{CE}}/{F_c *}}{2c}\right)^2 - \frac{{F_{CE}}/{F_c *}}{c}}$$

$F_C^* = F_c \times C_D \times C_M \times C_t =$ 2300 psi

$l_e / d =$ 13.65 and 6.03 *where* *13.65* *controls*

< 50 < 50

$E_{min}' = E_{min} \times C_M \times C_t =$ 1000000 psi

$$F_{CE} = \frac{0.822 E'_{min}}{\left({l_e}/{d}\right)^2} = \quad 4414 \text{ psi}$$

$F_{CE} / F_C^* =$ 1.92 c = 0.9

*now the $C_P$ adjustment factor can be calculated*

$C_P =$ 0.92 < $C_{P,asummed}$

Calculate $f_c$ and Determine if Selected Beam Passes

$f_c =$ 1108 psi < $F_C' =$ 2116

**Compression Parallel to Grain Passes**

## Moment Induced by Self-Weight of Member

G = 0.55 Table 5B

M.C. = 5 % or 10 %
because interior beam in conditioned space

$D = 62.4\left(\frac{G}{1+G(0.009)(M.C.)}\right)\left(1+\frac{M.C.}{100}\right) =$ 35.17 pcf, or 35.97 pcf

*we will take the maximum,*
D = 35.97 pcf

*we have a* 8-1/2" x 19-1/4" *glulam beam with,*
A = 163.6 $in^2$

*convert to square feet,*
A = 1.1363 $ft^2$

*now calculate the linear load created by its self weight, over a 29' span*
*w* = 40.87 plf

**Flexure in Queen Post Girder** Moment 8.9 kip-ft

$F'_b = F_b \times C_D \times C_M \times C_t \times C_L \times C_V \times C_{fu} \times C_c \times C_i$

Adjustment Factors

| | | | |
|---|---|---|---|
| $C_D$ = | 1.00 | because live load controls | §2.3.2 |
| $C_M$ = | 1.00 | because interior beam in conditioned space | §5.3.3 |
| $C_t$ = | 1.00 | because interior beam in conditioned space | §5.3.4 |
| $C_L$ = | 0.994 | calculated below | §5.3.5 |
| $C_V$ = | 0.937 | calculated below | §5.3.6 |
| $C_{fu}$ = | 1.00 | because not loaded parellel to wide faces of lamin. | §5.3.7 |
| $C_c$ = | 1.00 | because no curvature to beam | §5.3.8 |
| $C_i$ = | 1.00 | because no tapering of beam | §5.3.9 |

Pick a Visually Graded Southern Pine Stress Group — Table 5B

| | | |
|---|---|---|
| Group = | 50 | |
| $F_b$ = | 2100 | psi |
| Emin = | 1000000 | psi |

Calculate $C_L$ Adjustment Factor

$l_u$ = 9.67 ft, the unbraced length of the girder

d = 19.25 in, depth choosen in compression parellel to grain calculation

$l_u / d$ = 6.03

*so now we can calculate $l_e$,*

$l_e$ = 246.83 in, or 20.57 ft

$R_B$ = 8.11

$$F_{bE} = \frac{1.20E'_{min}}{(R_B)^2} = 18247$$

$F_b^* = F_b \times C_D \times C_M \times C_t \times C_c \times C_i$ = 2100 psi

$F_{bE} / F_b^*$ = 8.69

$$C_L = \frac{1 + {F_{bE}}/{F_b*}}{1.9} - \sqrt{\left(\frac{1 + {F_{bE}}/{F_b*}}{1.9}\right)^2 - \frac{{F_{bE}}/{F_b*}}{0.95}} = 0.994$$

Calculate $C_V$ Adjustment Factor

$$C_V = \left(\frac{21}{L}\right)^{1/x}\left(\frac{12}{d}\right)^{1/x}\left(\frac{5.125}{b}\right)^{1/x} \leq 1.0$$

| | | | | | |
|---|---|---|---|---|---|
| L = | 29 | ft | x = | 20 | for Southern Pine |
| d = | 19.25 | in | | | |
| b = | 8.5 | in | | | |

$C_V$ = 0.937 < 1.0

Calculate $F_b'$ Using the Minimum of $C_V$ or $C_L$

min | $C_L$ = 0.994 | $C_V$ = 0.937

Section Modulus (x) = 525 $in^3$

$F'_b$ = 1968 psi

$f_b = \frac{M}{S} =$ 203.4 psi < $F'_b$

Calculate $f_b$ and Determine if Selected Beam Passes

$f_b$ = 203 psi < $F_b'$ = 1968

**Bending Passes**

## Combined Axial and Bending Loading Interaction

$$\left(\frac{f_c}{F_c'}\right)^2 + \frac{f_{b1}}{F_{b1}'\left(1 + {f_c}/{F_{CE1}}\right)} \leq 1.0$$ §3.9.2

| | | | | | |
|---|---|---|---|---|---|
| $f_c$ = | 1108 | psi | $E_{min}'$ = | 1000000 | psi |
| $F_c'$ = | 2116 | psi | | | |
| $f_{b1}$ = | 203 | psi | | | |
| $F_{b1}$ = | 1968 | psi | | | |

$$F_{CE1} = \frac{0.822E_{min}'}{\left({l_{e1}}/{d_1}\right)^2} = 22621.3 \text{ psi}$$

*where,*

$l_{e1}$ = 9.67 ft

$d_1$ = 19.25 in

| | |
|---|---|
| $f_c < F_{CE1}$ | True |

0.274 + 0.099 = 0.373 < 1.0

| **Combined Axial and Bending Pass** |
|---|
| **Use a,** |
| **8-1/2" x 19-1/4"** |
| **for the glulam queen post** |
| **With a,** |
| **Southern Pine Group of 50** |

## Tension Cable Sizing

QUEEN POST - TENSION CABLE

186.21 KIPS ⟶ 190 KIPS

MACALLOY 460 BAR SYSTEM

| | MIN YIELD | MIN BREAK |
|---|---|---|
| M56 | 205 K | 271.8 K |
| M64 | 270.7 K | 358.8 K |

M56 205 K > 190 K TOTAL ✓ GOOD

DESIGN CALLS FOR TWO CABLES
✓ FOR STABILITY
✓ ADDED SAFETY

$\boxed{\text{(2) M56 MACALLOY 460 BARS FOR TENSION WILL BE USED}}$

## Macalloy 460 Bar System

### Table 1 - Tendon Capacities for Carbon Macalloy 460

| | | | | | | | | | | | | | | | | |
|---|---|---|---|---|---|---|---|---|---|---|---|---|---|---|---|---|
| Thread | mm | M10 | M12 | M16 | M20 | M24 | M30 | M36 | M42 | M48 | M56 | M64 | M76 | M85 | M90 | M100 |
| | inch | 3/8 | 1/2 | 5/8 | 3/4 | 1 | 1 1/4 | 1 3/8 | 1 5/8 | 2 | 2 1/4 | 2 1/2 | 3 | 3 3/8 | 3 1/2 | 4 |
| Nominal Bar Dia. | mm | 10 | 11 | 15 | 19 | 22 | 28 | 34 | 39 | 45 | 52 | 60 | 72 | 82 | 87 | 97 |
| | inch | 0.39 | 0.43 | 0.59 | 0.75 | 0.87 | 1.1 | 1.34 | 1.54 | 1.77 | 2.05 | 2.36 | 2.83 | 3.23 | 3.43 | 3.82 |
| Min. Yield Load | kN | 25 | 36 | 69 | 108 | 156 | 249 | 364 | 501 | 660 | 912 | 1204 | 1756 | 2239 | 2533 | 3172 |
| | kip | 5.6 | 8.1 | 15.5 | 24.3 | 35.1 | 56 | 81.8 | 112.6 | 148.4 | 205 | 270.7 | 394.7 | 503.3 | 569.4 | 713.1 |
| Min. Break Load | kN | 33 | 48 | 91 | 143 | 207 | 330 | 483 | 665 | 875 | 1209 | 1596 | 2329 | 2969 | 3358 | 4206 |
| | kip | 7.4 | 10.8 | 20.5 | 32.1 | 46.5 | 74.2 | 108.6 | 149.5 | 196.7 | 271.8 | 358.8 | 523.6 | 667.4 | 754.9 | 945.5 |
| Design Resistance to EC3 | kN | 24 | 35 | 66 | 103 | 149 | 238 | 348 | 479 | 630 | 870 | 1149 | 1677 | 2138 | 2418 | 3029 |
| | kip | 5.4 | 7.87 | 14.84 | 25.16 | 33.5 | 53.5 | 78.23 | 107.7 | 141.63 | 195.58 | 258.31 | 377 | 480.64 | 543.59 | 680.95 |
| Nominal Bar Weight | (kg/m) | 0.5 | 0.75 | 1.4 | 2.2 | 3 | 4.8 | 7.1 | 9.4 | 12.5 | 16.7 | 22.2 | 32 | 41.5 | 46.7 | 58 |
| | (lb/ft) | 0.34 | 0.5 | 0.94 | 1.48 | 2.02 | 3.23 | 4.77 | 6.32 | 8.4 | 11.22 | 14.92 | 21.5 | 27.89 | 31.38 | 38.97 |

### Macalloy 460 in Application

Engineers all over the world have used Macalloy systems in the most diverse of applications. Among these are bridges, government buildings, stadia, airports, and hotels, to name just a few. The longevity and design again reflect the level of innovation and quality, which have become firm components of Macalloy products.

### Macalloy 460 Carbon Bars

Macalloy 460 is a manufactured carbon steel, with excellent mechanical properties. The thread is rolled, rather than cut. This gives rise to the use of smaller diameter bars for a given metric thread, resulting in material cost saving. The carbon Macalloy 460 is also a weldable steel with a maximum carbon equivalent of 0.55%. Arc welding may be carried out using standard techniques and low hydrogen rods.

The Macalloy 460 bar has the following mechanical properties:

| | |
|---|---|
| Minimum Yield Stress | 460 N/mm² |
| Minimum Breaking Stress | 610 N/mm² |
| Minimum Elongation | 19% |
| Minimum charpy Impact Value | 27J @ -20°C |
| Young's Modulus | 205 kN/mm² |

| | |
|---|---|
| Minimum Yield Stress | 66,700 psi |
| Minimum Breaking Stress | 88,400 psi |
| Minimum Elongation | 19% |
| Minimum charpy Impact Value | 20 ft-lb @ 4°F |
| Young's Modulus | 29,700 ksi |

The standard diameter range for this system is from M10 (3/8") to M100 (4"). In addition, other diameters can be supplied but are subject to longer lead times. Tendons up to and including M16 (5/8") diameters can be supplied in lengths of 6m (19'8"). For larger diameters, lengths of up to 11.95m (39'2") are available. Greater lengths are possible using couplers and turnbuckles. These fittings are designed to take the full load of the bar.

### Adjustment

Adjustments within each fork or spade are:
M10 to M56: +/- ½ thread diameter
M64 to M100: +/-25mm / 1"

Turnbuckles give additional adjustments of:
M10 to M24: +/-25mm / 1"
M30 to M100: +/-50mm / 2"

Special turnbuckles, with a greater adjustment, are available on request.

### Fatigue

Threads are rolled on to the bar and are therefore more resistant to fatigue. Testing a range of diameters has been carried out over 2 million cycles, the results of which are available from the Macalloy technical department.

### Corrosion Protection

Macalloy tendons can be supplied in plain carbon steel, primed, or hot dip galvanized finish. If requested at the time of order, hot dip galvanizing can be applied to tendons after the threading process. The threads are then brushed to remove any excess zinc.

Length permitting, galvanized bars are delivered pre-assembled. This procedure ensures that threads are 100% operational. Connected bars, greater than 11.95m (39' 2"), are delivered part assembled. Please note that hot dip galvanizing is not comparable with a paint finish. The visual appearance of forks and spades may differ in appearance from that of the bar, by virtue of the different material compositions.

### Paint

For architectural purposes, it is recommended a painted finish is applied to the galvanizing. The corrosion resistance of the bar can then be enhanced.

Macalloy offers any kind of paint finish (primer, paint or fire protection) for hot dip galvanized, or self color tendons. These finishes will be sourced from certified suppliers.

### European Approval

The Macalloy 460 system has European CE approval under the ETA number 07/0215 for all standard diameters from M10 (3/8") and M100 (4"). When specifying, always ask for CE approved systems.

### Table 2 - Macalloy 460 Gusset Plate Dimensions

| | | | | | | | | | | | | | | | | |
|---|---|---|---|---|---|---|---|---|---|---|---|---|---|---|---|---|
| Thread | mm | M10 | M12 | M16 | M20 | M24 | M30 | M36 | M42 | M48 | M56 | M64 | M76 | M85 | M90 | M100 |
| | inch | 3/8 | 1/2 | 5/8 | 3/4 | 1 | 1 1/4 | 1 3/8 | 1 5/8 | 2 | 2 1/4 | 2 1/2 | 3 | 3 3/8 | 3 1/2 | 4 |
| T (Thickness) | mm | 10 | 10 | 12 | 15 | 20 | 22 | 30 | 35 | 40 | 45 | 55 | 70 | 70 | 80 | 85 |
| | inch | 0.39 | 0.39 | 0.47 | 0.59 | 0.79 | 0.87 | 1.18 | 1.38 | 1.57 | 1.77 | 2.17 | 2.76 | 2.76 | 3.15 | 3.35 |
| D | mm | 11.5 | 13 | 17 | 21.5 | 25.5 | 31.5 | 37.5 | 43.5 | 49.5 | 57.5 | 65.5 | 78.5 | 91.5 | 96.5 | 111.5 |
| | inch | 0.45 | 0.51 | 0.67 | 0.85 | 1 | 1.24 | 1.48 | 1.71 | 1.95 | 2.26 | 2.58 | 3.09 | 3.6 | 3.8 | 4.39 |
| E | mm | 18 | 22 | 30 | 37 | 43 | 56 2.2 | 64 | 74 | 84 | 101 | 112 | 132 | 160 | 166 | 196 |
| | inch | 0.71 | 0.87 | 1.18 | 1.46 | 1.69 | | 2.52 | 2.91 | 3.31 | 3.98 | 4.41 | 5.2 | 6.3 | 6.54 | 7.72 |
| H (min) | mm | 28 | 34 | 48 | 60 | 68 | 90 | 103 | 118 | 135 | 163 | 180 | 211 | 259 | 266 | 317 |
| | inch | 1.1 | 1.34 | 1.89 | 2.36 | 2.68 | 3.54 | 4.06 | 4.65 | 5.31 | 6.42 | 7.09 | 8.31 | 10.2 | 10.47 | 12.48 |

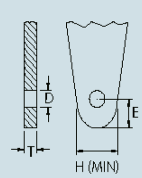


EXPERIENCE INNOVATION QUALITY

## Steel Square HSS Sizing

QUEEN POST - STEEL POST DESIGN

assuming $l_e = 28'' \times 1$ or $\times 2.10$ = 28" or 58.8"

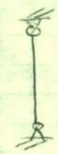

$K_e = 1.0$

$K_e = 2.10$

let's use the more conservative value, assuming the cable offers a "free" constraint.

$l_e = 58.8''$ or 4.9'

CHOOSE 3-1/2" x 3-1/2" x 3/8" SQUARE HSS

| $l_e$ | ASD P (Kips) |
|---|---|
| 4 | 102 |
| 4.9 | 97.2 |
| 5 | 96.7 |

97.2 → INTERPOLATED VALUE (pg. 4-64 OF STL. MANUAL)

$97.2^k > 42.5^k$ MAX. AXIAL FORCE

✓ GOOD

$$\boxed{\therefore \text{ USE } 3\text{-}1/2 \times 3\text{-}1/2'' \times 3/8'' \text{ SQUARE HSS FOR EACH POST}}$$

## Deflection Check

DEFLECTION CHECK - TYP. OFFICE BAY

TYP. OFFICE - BEAM

$$\frac{5wl^4}{384EI} = \frac{5(1.97)(25^4)}{384(2.1E6)(6242)} \times 12^3 = 0.0011 < \frac{l}{600} = \frac{25\times12}{600} = 0.5''$$

30F-2.1ESF    10-1/2" x 19-1/4"

✓ GOOD

TYP OFFICE - QP

$$\frac{5wl^4}{384EI} = \frac{5(0.04087)(29^4)}{384(1.9E6)(5053)} \times 12^3 = 0.000067'' \text{ due to selfweight}$$

TYPE 50SP    8 1/2" x 19-1/4"

$$\frac{Pl^3}{28EI} = \frac{42.5(29^4)}{28(19e6)(5053)} \times 12^3 = 0.193'' \text{ due to point loads}$$

Two point loads

$$0.193067'' < \frac{l}{600} = \frac{29\times12}{600} = 0.58''$$

✓ GOOD

# APPENDIX B.4 - ROOF BEAM DESIGN

## Loading

Computer analysis loading

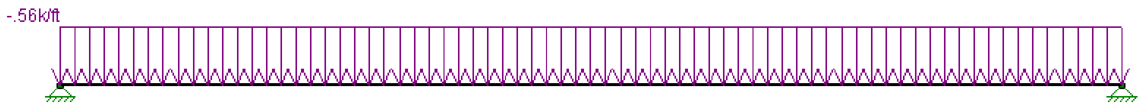


## Flexure and Reactions

Computer analysis results, showing the maximum moment is 43.8 kip-ft, or 44 kip-ft

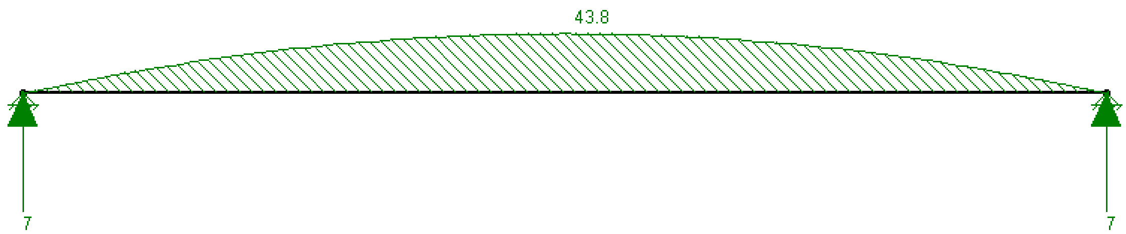

## Computer Analysis Data

Designer : **SIKANDAR PORTER-GILL**

**BEAM ANALYSIS**

February 11, 2014
12:18 PM
Checked By:_____

### *Member Data*

| Member Label | I Joint | J Joint | Area in^2 | Moment of Inertia in^4 | Elastic Modulus ksi | End Releases I-End | End Releases J-End | Length ft |
|---|---|---|---|---|---|---|---|---|
| M1 | N1 | N2 | 10 | 100 | 29000 | | | 25 |

### *Member Distributed Loads*

| Member Label | Direction | Start Magnitude (k/ft, F) | End Magnitude (k/ft, F) | Start Location (ft or %) | End Location (ft or %) |
|---|---|---|---|---|---|
| M1 | Y | -.56 | -.56 | 0 | 0 |

### *Reactions*

| Joint Label | X Force (k) | Y Force (k) | Moment (k-ft) |
|---|---|---|---|
| N1 | 0 | 7 | 0 |
| N2 | 0 | 7 | 0 |
| Totals: | 0 | 14 | |

### *Member Section Forces*

| Member Label | Section | Axial (k) | Shear (k) | Moment (k-ft) |
|---|---|---|---|---|
| M1 | 1 | 0 | 7 | 0 |
| | 2 | 0 | 3.5 | 32.812 |
| | 3 | 0 | 0 | 43.75 |
| | 4 | 0 | -3.5 | 32.813 |
| | 5 | 0 | -7 | 0 |

## Member Sizing

ROOF BEAM DESIGN

LOADS

- SUPERIMPOSED DL

| | |
|---|---|
| 0.29 | ROOF MEMBRANE |
| 6 | 4" RIGID INSULATION |
| 7.3 | T&G WOOD DECK |
| 9 | 3" WOOD NAILER |
| 4 | MECH. |
| 4 | LTG. |
| 3 | SPRINKLER |
| 1 | MISC DL |

34.59 PSF ~ 36 PSF DL

- LIVE LOADS

20 PSF ROOF (PER DRAWINGS) > 10 PSF ASCE-10 SNOW FOR ARKANSAS

ASD → LL + DL = 36 + 20 = 56 PSF

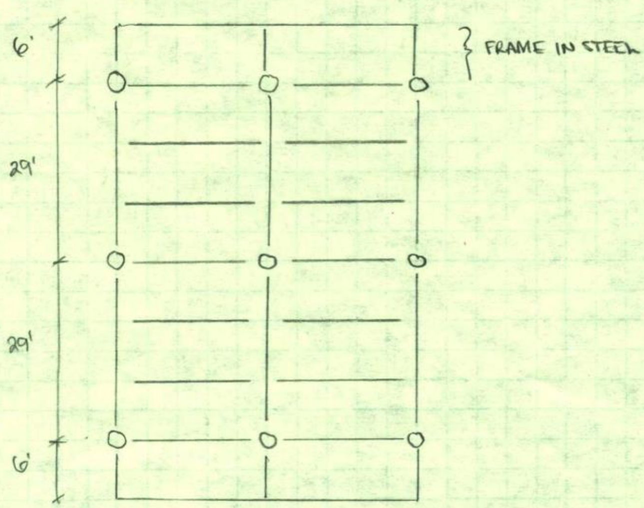

56 PSF x (10') = 560 PLF

APPROX. TRIB WIDTH

$$M = \frac{0.56(25')^2}{8} = 43.75 \text{ kip ft}$$

USING ESTABLISHED EXCEL DESIGN TABLE,
USE 8-1/2" x 12-3/8" BEAM
GROUP 30F-2.1E SP

$$R = \frac{0.56(25')}{2} = 7^{\text{kips}} \quad \times 2 \longrightarrow 14^{\text{kips}}$$

APPLIED TO
GP GIRDER

## Flexure in Beam - Roof

Moment 44 kip-ft

$F'_b = F_b \times C_D \times C_M \times C_t \times C_L \times C_V \times C_{fu} \times C_c \times C_i$

Pick a size,

8-1/2" x 12-3/8""

8.5 x 12.375

where the $A_{provided}$ = 105.2 $in^2$

$S_{sect\ modulus}$ = 216.9 $in^3$

| | | | |
|---|---|---|---|
| $C_D$ = | 1.00 | because live load controls | §2.3.2 |
| $C_M$ = | 1.00 | because interior beam in conditioned space | §5.3.3 |
| $C_t$ = | 1.00 | because interior beam in conditioned space | §5.3.4 |
| $C_L$ = | 0.987 | calculated below | §5.3.5 |
| $C_V$ = | 0.965 | calculated below | §5.3.6 |
| $C_{fu}$ = | 1.00 | because not loaded parellel to wide faces of lamin. | §5.3.7 |
| $C_c$ = | 1.00 | because no curvature to beam | §5.3.8 |
| $C_i$ = | 1.00 | because no tapering of beam | §5.3.9 |

Pick a Visually Graded Southern Pine Stress Group — Table 5A

Group = 30F-2.1E SP

$F_b$ = 3000 psi

Emin = 1110000 psi

Calculate $C_L$ Adjustment Factor

$l_u$ = 25.00 ft, the unbraced length of the girder

d = 12.375 in, choosen to be consistent with girder depth

$l_u$ / d = 24.24

*so now we can calculate $l_e$,*

$l_e$ = 552 in, or 46.00 ft

reliant on inequality on page 16, Supplem

$R_B$ = 9.72

$F_{bE} = \frac{1.20 E'_{min}}{(R_B)^2}$ = 14088.3

$F_b^* = F_b \times C_D \times C_M \times C_t \times C_c \times C_i =$ 3000 psi

$F_{bE} / F_b^* =$ 4.70

$$C_L = \frac{1 + {F_{bE}}/{F_b*}}{1.9} - \sqrt{\left(\frac{1 + {F_{bE}}/{F_b*}}{1.9}\right)^2 - \frac{{F_{bE}}/{F_b*}}{0.95}} = 0.987$$

Calculate $C_V$ Adjustment Factor

$$C_V = \left(\frac{21}{L}\right)^{1/x}\left(\frac{12}{d}\right)^{1/x}\left(\frac{5.125}{b}\right)^{1/x} \leq 1.0$$

| | | | | | |
|---|---|---|---|---|---|
| L = | 25 | ft | x = | 20 | for Southern Pine |
| d = | 12.375 | in | | | |
| b = | 8.5 | in | | | |

$C_V =$ 0.965 < 1.0

Calculate $F_b'$ Using the Minimum of $C_V$ or $C_L$

min | $C_L =$ 0.987
$C_V =$ 0.965

$F'_b =$ 2895 psi

$f_b = \frac{M}{S} =$ 2434.3 psi < $F'_b$

Calculate $f_b$ and Determine if Selected Beam Passes

$f_b =$ 2434 psi < $F_b' =$ 2895

**Bending Passes**

Use a 8-1/2" x 12-3/8"" for the beam

# APPENDIX B.5 - ROOF QUEEN POST DESIGN

## Loading

Computer analysis loading

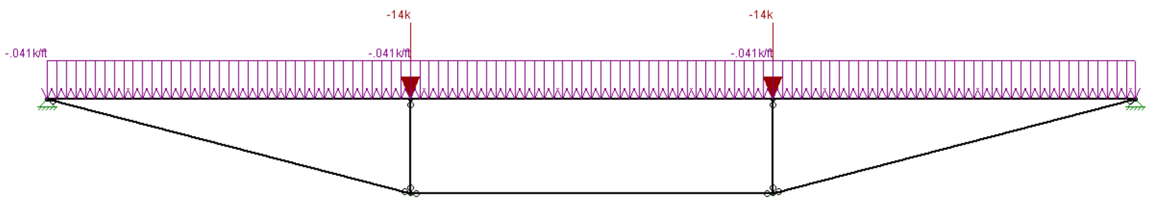


## Flexure and Reactions

Computer analysis results, showing the maximum moment is 3 kip-ft, or 3.1 kip-ft

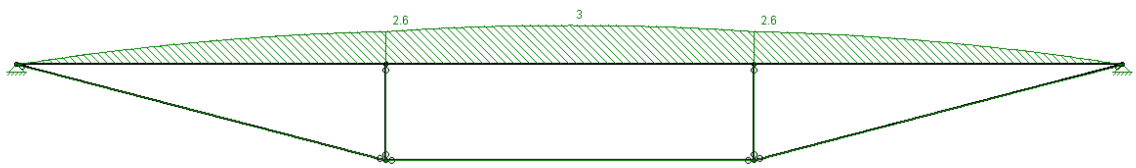


## Axial Cable and Girder Forces

The assumption of the hinged queen post was used to determine the post reactions, cable tension and girder axial forces.

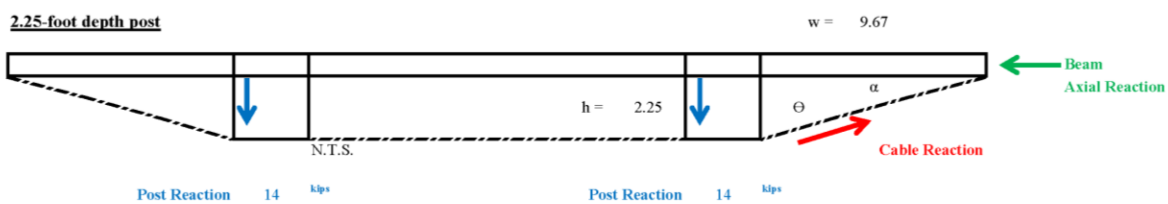


PRELIMINARY CALCULATIONS

Θ = tan-1(w/h) = 1.34 radians

α = 88.66 radians

CALCULATE RESULTANT FORCES IN CABLE AND BEAM

Cable Reaction 61.78 kips

Beam Axial Reaction 60.17 kips

## Computer Analysis Data

Designer : **SIKANDAR PORTER-GILL** **GIRDER ANALYSIS**
February 11, 2014
12:04 PM
Checked By:_____

### *Member Data*

| Member Label | I Joint | J Joint | Area in^2 | Moment of Inertia in^4 | Elastic Modulus ksi | End Releases I-End | End Releases J-End | Length ft |
|---|---|---|---|---|---|---|---|---|
| M1 | N1 | N2 | 10 | 100 | 29000 | | | 9.67 |
| M2 | N2 | N3 | 10 | 100 | 29000 | | | 9.66 |
| M3 | N3 | N4 | 10 | 100 | 29000 | | | 9.67 |
| M4 | N1 | N5 | 10 | 100 | 29000 | PIN | PIN | 9.988 |
| M5 | N5 | N6 | 10 | 100 | 29000 | PIN | PIN | 9.66 |
| M6 | N6 | N4 | 10 | 100 | 29000 | PIN | PIN | 9.988 |
| M7 | N2 | N5 | 10 | 100 | 29000 | PIN | PIN | 2.5 |
| M8 | N3 | N6 | 10 | 100 | 29000 | PIN | PIN | 2.5 |

### *Joint Loads/Enforced Displacements*

| Joint Label | [L]oad or [D]isplacement | Direction | Magnitude (k, k-ft, in, rad) |
|---|---|---|---|
| N2 | L | Y | -14 |
| N3 | L | Y | -14 |

### *Member Distributed Loads*

| Member Label | Direction | Start Magnitude (k/ft, F) | End Magnitude (k/ft, F) | Start Location (ft or %) | End Location (ft or %) |
|---|---|---|---|---|---|
| M1 | Y | -.041 | -.041 | 0 | 0 |
| M2 | Y | -.041 | -.041 | 0 | 0 |
| M3 | Y | -.041 | -.041 | 0 | 0 |

### *Reactions*

| Joint Label | X Force (k) | Y Force (k) | Moment (k-ft) |
|---|---|---|---|
| N1 | -54.658 | 14.595 | 0 |
| N4 | 54.658 | 14.594 | 0 |
| Totals: | 0 | 29.189 | |

### *Member Section Forces*

| Member Label | Section | Axial (k) | Shear (k) | Moment (k-ft) |
|---|---|---|---|---|
| M1 | 1 | 0 | .464 | 0 |
| | 2 | 0 | .365 | 1.001 |
| | 3 | 0 | .266 | 1.763 |
| | 4 | 0 | .166 | 2.285 |
| | 5 | 0 | .067 | 2.568 |
| M2 | 1 | 0 | .198 | 2.568 |
| | 2 | 0 | .099 | 2.927 |
| | 3 | 0 | 0 | 3.046 |
| | 4 | 0 | -.099 | 2.927 |
| | 5 | 0 | -.198 | 2.568 |
| M3 | 1 | 0 | -.067 | 2.568 |
| | 2 | 0 | -.166 | 2.285 |
| | 3 | 0 | -.266 | 1.763 |
| | 4 | 0 | -.365 | 1.001 |
| | 5 | 0 | -.464 | 0 |
| M4 | 1 | -56.455 | 0 | 0 |
| | 2 | -56.455 | 0 | 0 |
| | 3 | -56.455 | 0 | 0 |

Designer : **SIKANDAR PORTER-GILL** **GIRDER ANALYSIS** February 11, 2014
12:04 PM
Checked By:_____

***Member Section Forces***

| Member Label | Section | Axial (k) | Shear (k) | Moment (k-ft) |
|---|---|---|---|---|
| | 4 | -56.455 | 0 | 0 |
| | 5 | -56.455 | 0 | 0 |
| M5 | 1 | -54.658 | 0 | 0 |
| | 2 | -54.658 | 0 | 0 |
| | 3 | -54.658 | 0 | 0 |
| | 4 | -54.658 | 0 | 0 |
| | 5 | -54.658 | 0 | 0 |
| M6 | 1 | -56.455 | 0 | 0 |
| | 2 | -56.455 | 0 | 0 |
| | 3 | -56.455 | 0 | 0 |
| | 4 | -56.455 | 0 | 0 |
| | 5 | -56.455 | 0 | 0 |
| M7 | 1 | 14.131 | 0 | 0 |
| | 2 | 14.131 | 0 | 0 |
| | 3 | 14.131 | 0 | 0 |
| | 4 | 14.131 | 0 | 0 |
| | 5 | 14.131 | 0 | 0 |
| M8 | 1 | 14.131 | 0 | 0 |
| | 2 | 14.131 | 0 | 0 |
| | 3 | 14.131 | 0 | 0 |
| | 4 | 14.131 | 0 | 0 |
| | 5 | 14.131 | 0 | 0 |

## Top Chord Member Sizing

**Compression Parallel to Beam Grain** Axial Compression **60.17** kips

$F'_c = F_c \times C_D \times C_M \times C_t \times C_p$

Adjustment Factors

| | | | |
|---|---|---|---|
| $C_D$ = | 1.00 | because live load controls | §2.3.2 |
| $C_M$ = | 1.00 | because interior beam in conditioned space | §5.3.3 |
| $C_t$ = | 1.00 | because interior beam in conditioned space | §5.3.4 |
| $C_p$ = | 0.92 | assumed value | §3.7.1 |

Pick a Visually Graded Southern Pine Stress Group — Table 5B

| | | |
|---|---|---|
| Group = | 50 | |
| $F_c$ = | 2300 | psi |
| Emin = | 1000000 | psi |

*so,*

$F'_c$ = 2116 psi allowable compression stress

*now the required area would be,*

A = 28 $in^2$ required area of glulam

Pick a,

8-1/2" x 12-3/8"

8.5 x 12.375

where the $A_{provided}$ = 105.2 $in^2$

Is the area greater than required area? Yes

Check the Assumption of the $C_p$ Adjustment Factor

$$C_p = \frac{1 + {F_{CE}}/{F_c *}}{2c} - \sqrt{\left(\frac{1 + {F_{CE}}/{F_c *}}{2c}\right)^2 - \frac{{F_{CE}}/{F_c *}}{c}}$$

$F_C* = F_c \times C_D \times C_M \times C_t =$ 2300 psi

$l_e / d =$ 13.65 and 9.37 *where* *13.65* *controls*

< 50 < 50

$E_{min}' = E_{min} \times C_M \times C_t =$ 1000000 psi

$$F_{CE} = \frac{0.822 E'_{min}}{\left({l_e}/{d}\right)^2} =$$ 4414 psi

$F_{CE} / F_C* =$ 1.92 c = 0.9

*now the $C_P$ adjustment factor can be calculated*

$C_P =$ 0.92 < $C_{P,asummed}$

Calculate $f_c$ and Determine if Selected Beam Passes

$f_c =$ 572 psi < $F_C' =$ 2116

**Compression Parallel to Grain Passes**

## Moment Induced by Self-Weight of Member

G = 0.55 Table 5B

M.C. = 5 % or 10 %
because interior beam in conditioned space

$$D = 62.4\left(\frac{G}{1+G(0.009)(M.C.)}\right)\left(1+\frac{M.C.}{100}\right) = 35.17 \text{ pcf, or } 35.97 \text{ pcf}$$

*we will take the maximum,*
D = 35.97 pcf

*we have a* 8-1/2" x 12-3/8" *glulam beam with,*
A = 105.2 $in^2$

*convert to square feet,*
A = 0.7305 $ft^2$

*now calculate the linear load created by its self weight, over a 29' span*
$w$ = 26.28 plf > 0.041 klf assumed in maximum moment calculation

## Flexure in Queen Post Girder - Roof

Moment 3.1 kip-ft

$F'_b = F_b \times C_D \times C_M \times C_t \times C_L \times C_V \times C_{fu} \times C_c \times C_i$

<u>Adjustment Factors</u>

| | | | |
|---|---|---|---|
| $C_D =$ | 1.00 | because live load controls | §2.3.2 |
| $C_M =$ | 1.00 | because interior beam in conditioned space | §5.3.3 |
| $C_t =$ | 1.00 | because interior beam in conditioned space | §5.3.4 |
| $C_L =$ | 0.996 | calculated below | §5.3.5 |
| $C_V =$ | 0.958 | calculated below | §5.3.6 |
| $C_{fu} =$ | 1.00 | because not loaded parellel to wide faces of lamin. | §5.3.7 |
| $C_c =$ | 1.00 | because no curvature to beam | §5.3.8 |
| $C_i =$ | 1.00 | because no tapering of beam | §5.3.9 |

<u>Pick a Visually Graded Southern Pine Stress Group</u> Table 5B

Group = 50

$F_b =$ 2100 psi

Emin = 1000000 psi

<u>Calculate $C_L$ Adjustment Factor</u>

$l_u =$ 9.67 ft, the unbraced length of the girder

d = 12.375 in, depth choosen in compression parellel to grain calculation

$l_u / d =$ 9.37

*so now we can calculate $l_e$,*

$l_e =$ 226.205 in, or 18.85 ft

$R_B =$ 6.22

$F_{bE} = \frac{1.20 E'_{min}}{(R_B)^2} =$ 30972.2

$F_b{*} = F_b \times C_D \times C_M \times C_t \times C_c \times C_i =$ 2100 psi

$F_{bE} / F_b{*} =$ 14.75

$$C_L = \frac{1 + {F_{bE}}/{F_b *}}{1.9} - \sqrt{\left(\frac{1 + {F_{bE}}/{F_b *}}{1.9}\right)^2 - \frac{{F_{bE}}/{F_b *}}{0.95}} = 0.996$$

Calculate $C_V$ Adjustment Factor

$$C_V = \left(\frac{21}{L}\right)^{1/x}\left(\frac{12}{d}\right)^{1/x}\left(\frac{5.125}{b}\right)^{1/x} \leq 1.0$$

| | | | | | |
|---|---|---|---|---|---|
| L = | 29 | ft | x = | 20 | for Southern Pine |
| d = | 12.375 | in | | | |
| b = | 8.5 | in | | | |

$C_V =$ 0.958 < 1.0

Calculate $F_b$' Using the Minimum of $C_V$ or $C_L$

min | $C_L =$ 0.996
$C_V =$ 0.958

Section Modulus (x) = 267.8 $in^3$

$F'_b =$ 2012 psi

$f_b = \frac{M}{S} =$ 138.9 psi < $F'_b$

Calculate $f_b$ and Determine if Selected Beam Passes

$f_b =$ 139 psi < $F_b' =$ 2012

**Bending Passes**

## Combined Axial and Bending Loading Interaction

$$\left(\frac{f_c}{F_c'}\right)^2 + \frac{f_{b1}}{F_{b1}'\left(1 + {f_c}/{F_{CE1}}\right)} \leq 1.0$$ §3.9.2

| | | | | | |
|---|---|---|---|---|---|
| $f_c$ = | 572 | psi | $E_{min}'$ = | 1000000 | psi |
| $F_c'$ = | 2116 | psi | | | |
| $f_{b1}$ = | 139 | psi | | | |
| $F_{b1}$ = | 2012 | psi | | | |

$$F_{CE1} = \frac{0.822 E_{min}'}{\left({l_{e1}}/{d_1}\right)^2} = 9348.6 \text{ psi}$$

*where,*

$l_{e1}$ = 9.67 ft

$d_1$ = 12.375 in

| | |
|---|---|
| $f_c < F_{CE1}$ | True |

0.073 + 0.065 = 0.138 < 1.0

| **Combined Axial and Bending Pass** |
|---|
| **Use a,** |
| **8-1/2" x 12-3/8"** |
| **for the glulam queen post** |
| **With a,** |
| **Southern Pine Group of 50** |

## Member Summary, Tension Cable and Steel Square HSS Sizing

ROOF QUEEN POST DESIGN

CONSERVATIVELY ASSUME 0.041 K/FT SELF WEIGHT
↳ REFERENCING TYP. FLOOR QP

FROM COMPUTER ANALYSIS: $M_{max}$ qp girder $= 1.615^{kft} \longrightarrow 1.7^{kft}$

AN EXCEL TABLE WILL BE USED TO CALCULATE
THE SUFFICIENT QP GIRDER SIZE...
↳ AFTER DESIGN SUMMARY

$\boxed{\text{8-1/2" x 12-3/8" GLULAM QP, GROUP 50 SP}}$

TENSION CABLE

$61.78^{k} \longrightarrow 62^{kips}$

| | Min. Yield | Min. Break |
|---|---|---|
| M16 | 69 | 91 |
| M20 | 108 | 143 |

M16 $69^{k} > 62^{k}$ TOTAL ✓GOOD

DESIGN CALLS FOR TWO CABLES
✓FOR STABILITY
✓ADDED SAFETY

$\boxed{\text{(2) M16 MACALLOY 460 BARS FOR TENSION WILL BE USED}}$

QP POST (following previously sized post)

$l_e$ = 58.8" or 4.9' with $14^k$ axial

CONSTRUCTIBILITY

USE SAME POST, 3-1/2" x 3-1/2" x 3/8" SQUARE HSS

$97.2^k > 14^k$ MAX. AXIAL FORCE

✓ GOOD

∴ USE 3-1/2" x 3-1/2 x 3/8"

FOR EACH POST

ROOF QUEEN POST DESIGN SUMMARY

8-1/2" x 12-3/8", GLULAM QP
GROUP 50 SP

WITH (2) 460 MACALLOY BARS

WITH 3-1/2" x 3-1/2" x 3/8" POST/S

## Deflection Check

DEFLECTION CHECK - ROOF BAY

BEAM

$$\frac{5(0.56)(25^4)}{384(2.166)(1342)} \times 12^3 = 0.0017 < \frac{l}{600} = \frac{25' \times 12}{600} = 0.5''$$

8 1/2 x 12 3/8

30F.-2.1E SP

✓ GOOD

QUEEN POST

$$\frac{5(0.04087)(29^4)}{384(1.986)(1342)} \times 12^3 = 0.00044$$

TYPE 80

8 1/2 x 12 3/8

$$\frac{14(29^4)}{28(1.986)(1342)} \times 12^3 = 0.23$$

$$= 0.2304'' < \frac{l}{600} = 0.58''$$

✓ GOOD

## APPENDIX B.6 - SUMMARY OF BEAM SIZES

- The typical office beam will be specified as a 10 ½" x 19 ¼" 30F-2.1E Southern Pine.
- The typical office queen post will be specified as an 8 ½" x 19 ¼" Stress Class 50 Visual Southern Pine, with 3 ½" x 3 ½" x ⅜" Square HSS Post and (2) M56 Macalloy 460 Bars
- The typical roof beam will be specified as a 8 ½" x 12 ⅜" 30F-2.1E Southern Pine.
- The typical roof queen post will be specified as a 8 ½" x 12 ⅜" Stress Glass 50 Visual Southern Pine, with 3 ½" x 3 ½" x ⅜" Square HSS Post and (2) M16 Macalloy 460 Bars

## APPENDIX B.7 - TYPICAL OFFICE PERIMETER BEAM

TYPICAL OFFICE - PERIMETER BEAM

FROM PREV. TECH REPORT II: 280 PLF ON EDGE

TRIB. = $\frac{9.67'}{2}$ + 2' = 6.84' ~ 7'-0" x 164.5 PSF OFFICE

edge

= 1151.5 PLF ~ 1.2 KIF

+ 0.28 KIF

1.48 KLF ~ 1.5 KLF

$M = \frac{1.5(25^2)}{8} = 117.18^{kft} \sim 117.2^{'k}$

$R = \frac{1.5(25)}{2} = 18.75^{k}$

GLULAM:

SIZE 10-1/2" x 17-7/8", 30F-2.1E SP d=19.25"

STEEL SIZE W14X22, SAME AS ACTUAL DESIGN d=13.7"
(STL MANUAL, pg. 3-26)

* IT SHOULD BE NOTED THAT THE USE OF STEEL PERIMETER BEAMS WILL CHANGE IBC 2009 CONSTRUCTION TYPE.

## APPENDIX B.8 - SAP2000 QUEEN POST MODEL

### Original Model

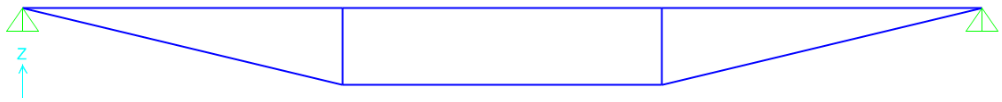


### Member Releases

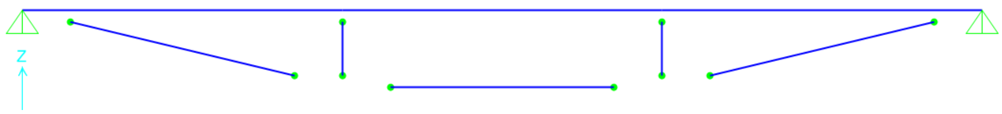


### Loading

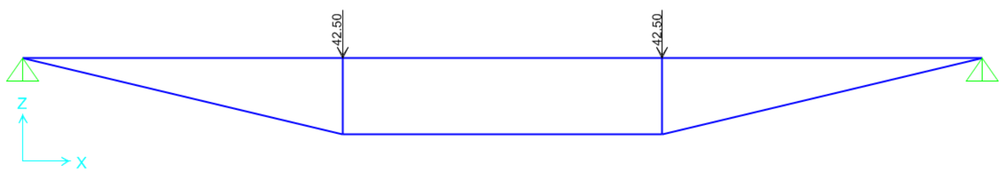


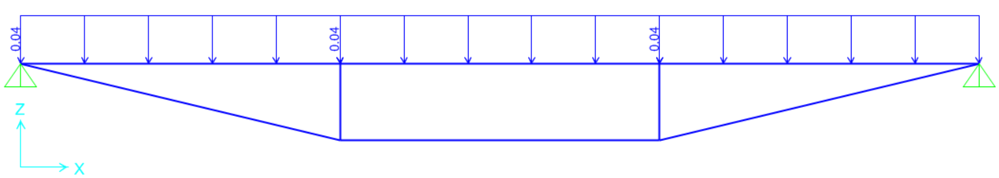


### Axial Loading

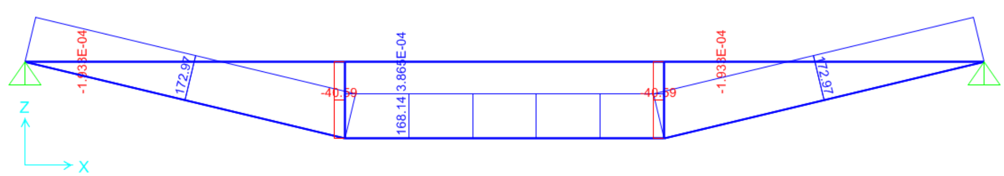


| Member | Force | Percent Error (from actual) |
|---|---|---|
| Cable | 172.97 | 7.1% |
| Cable | 168.141 | 9.7% |
| Cable | 172.97 | 7.1% |
| Post | -40.586 | 3.4% |
| Post | -40.586 | 3.4% |

## APPENDIX B.9 – COLUMN SIZING

COLUMN CONFIRMATION

° FOR EASE OF CONNECTION AND AESTHETICS, THE SAME COLUMNS WILL BE USED FROM EXISTING BUILDING DESIGN

→ 24" DIAMETER, MIN THICKNESS = 0.438" @ 14'-0" effective

PERIMETER BEAM $18.75^k$ × 2 / FLOOR

QUEEN POST (OFF) $43^k$

QUEEN POST (ROOF) $14.5^k$

CONSERVATIVE VALUE ASSUMED

$$P_u = 3\times(18.75(2) + 43) + 1\times(14.5 + 18.75(2))$$

$$= 293.5^k > ASD_{axial} = 691^k$$

@ 14'

for HSS20x20x0.5

(STL. MANUAL 4-68)

HSS 24x24x0.5 > HSS 20x20x0.5 ✓ (GOOD)

# APPENDIX C

## REDESIGN OF LATERAL SYSTEM

## APPENDIX C.1 – HSS24X0.5 COLUMN

The Master Steel Table for RAM SS was modified to account for the larger HSS24x0.5 used in the Heifer International Center (American Institute of Steel Construction, 2011).

RAMAISC.TAB - Notepad

File Edit Format View Help

| | | | | | | | | | | | | | |
|---|---|---|---|---|---|---|---|---|---|---|---|---|---|
| HSS4X2X3/16 | R | 4 | 0.174 | 2 | 0.174 | 1.89 | 3.66 | 1.83 | 2.34 | 1.22 | 1.22 | 1.43 | 3.08 |
| HSS4X2X1/8 | R | 4 | 0.116 | 2 | 0.116 | 1.30 | 2.65 | 1.32 | 1.66 | 0.898 | 0.898 | 1.02 | 2.20 |
| HSS3.5X3.5X3/8 | R | 3.5 | 0.349 | 3.5 | 0.349 | 4.09 | 6.49 | 3.71 | 4.69 | 6.49 | 3.71 | 4.69 | 11.2 |
| HSS3.5X3.5X5/16 | R | 3.5 | 0.291 | 3.5 | 0.291 | 3.52 | 5.84 | 3.34 | 4.14 | 5.84 | 3.34 | 4.14 | 9.89 |
| HSS3.5X3.5X1/4 | R | 3.5 | 0.233 | 3.5 | 0.233 | 2.91 | 5.04 | 2.88 | 3.50 | 5.04 | 2.88 | 3.50 | 8.35 |
| HSS3.5X3.5X3/16 | R | 3.5 | 0.174 | 3.5 | 0.174 | 2.24 | 4.05 | 2.31 | 2.76 | 4.05 | 2.31 | 2.76 | 6.56 |
| HSS3.5X3.5X1/8 | R | 3.5 | 0.116 | 3.5 | 0.116 | 1.54 | 2.90 | 1.66 | 1.93 | 2.90 | 1.66 | 1.93 | 4.58 |
| HSS3.5X2X1/4 | R | 3.5 | 0.233 | 2 | 0.233 | 2.21 | 3.17 | 1.81 | 2.36 | 1.30 | 1.30 | 1.58 | 3.16 |
| HSS3.5X2X3/16 | R | 3.5 | 0.174 | 2 | 0.174 | 1.71 | 2.61 | 1.49 | 1.89 | 1.08 | 1.08 | 1.27 | 2.55 |
| HSS3.5X2X1/8 | R | 3.5 | 0.116 | 2 | 0.116 | 1.19 | 1.90 | 1.09 | 1.34 | 0.795 | 0.795 | 0.912 | 1.83 |
| HSS3.5X1.5X1/4 | R | 3.5 | 0.233 | 1.5 | 0.233 | 1.97 | 2.55 | 1.46 | 1.98 | 0.638 | 0.851 | 1.06 | 1.79 |
| HSS3.5X1.5X3/16 | R | 3.5 | 0.174 | 1.5 | 0.174 | 1.54 | 2.12 | 1.21 | 1.60 | 0.544 | 0.725 | 0.867 | 1.49 |
| HSS3.5X1.5X1/8 | R | 3.5 | 0.116 | 1.5 | 0.116 | 1.07 | 1.57 | 0.896 | 1.15 | 0.411 | 0.548 | 0.630 | 1.09 |
| HSS3X3X3/8 | R | 3 | 0.349 | 3 | 0.349 | 3.39 | 3.78 | 2.52 | 3.25 | 3.78 | 2.52 | 3.25 | 6.64 |
| HSS3X3X5/16 | R | 3 | 0.291 | 3 | 0.291 | 2.94 | 3.45 | 2.30 | 2.90 | 3.45 | 2.30 | 2.90 | 5.94 |
| HSS3X3X1/4 | R | 3 | 0.233 | 3 | 0.233 | 2.44 | 3.02 | 2.01 | 2.48 | 3.02 | 2.01 | 2.48 | 5.08 |
| HSS3X3X3/16 | R | 3 | 0.174 | 3 | 0.174 | 1.89 | 2.46 | 1.64 | 1.97 | 2.46 | 1.64 | 1.97 | 4.03 |
| HSS3X3X1/8 | R | 3 | 0.116 | 3 | 0.116 | 1.30 | 1.78 | 1.19 | 1.40 | 1.78 | 1.19 | 1.40 | 2.84 |
| HSS3X2.5X5/16 | R | 3 | 0.291 | 2.5 | 0.291 | 2.64 | 2.92 | 1.94 | 2.51 | 2.18 | 1.74 | 2.20 | 4.34 |
| HSS3X2.5X1/4 | R | 3 | 0.233 | 2.5 | 0.233 | 2.21 | 2.57 | 1.72 | 2.16 | 1.93 | 1.54 | 1.90 | 3.74 |
| HSS3X2.5X3/16 | R | 3 | 0.174 | 2.5 | 0.174 | 1.71 | 2.11 | 1.41 | 1.73 | 1.59 | 1.27 | 1.52 | 3.00 |
| HSS3X2.5X1/8 | R | 3 | 0.116 | 2.5 | 0.116 | 1.19 | 1.54 | 1.03 | 1.23 | 1.16 | 0.931 | 1.09 | 2.13 |
| HSS3X2X5/16 | R | 3 | 0.291 | 2 | 0.291 | 2.35 | 2.38 | 1.59 | 2.11 | 1.24 | 1.24 | 1.58 | 2.87 |
| HSS3X2X1/4 | R | 3 | 0.233 | 2 | 0.233 | 1.97 | 2.13 | 1.42 | 1.83 | 1.11 | 1.11 | 1.38 | 2.52 |
| HSS3X2X3/16 | R | 3 | 0.174 | 2 | 0.174 | 1.54 | 1.77 | 1.18 | 1.48 | 0.932 | 0.932 | 1.12 | 2.05 |
| HSS3X2X1/8 | R | 3 | 0.116 | 2 | 0.116 | 1.07 | 1.30 | 0.867 | 1.06 | 0.692 | 0.692 | 0.803 | 1.47 |
| HSS2.5X2.5X5/16 | R | 2.5 | 0.291 | 2.5 | 0.291 | 2.35 | 1.82 | 1.46 | 1.88 | 1.82 | 1.46 | 1.88 | 3.20 |
| HSS2.5X2.5X1/4 | R | 2.5 | 0.233 | 2.5 | 0.233 | 1.97 | 1.63 | 1.30 | 1.63 | 1.63 | 1.30 | 1.63 | 2.79 |
| HSS2.5X2.5X3/16 | R | 2.5 | 0.174 | 2.5 | 0.174 | 1.54 | 1.35 | 1.08 | 1.32 | 1.35 | 1.08 | 1.32 | 2.25 |
| HSS2.5X2.5X1/8 | R | 2.5 | 0.116 | 2.5 | 0.116 | 1.07 | 0.998 | 0.799 | 0.947 | 0.998 | 0.799 | 0.947 | 1.61 |
| HSS2.5X2X1/4 | R | 2.5 | 0.233 | 2 | 0.233 | 1.74 | 1.33 | 1.06 | 1.37 | 0.930 | 0.930 | 1.17 | 1.90 |
| HSS2.5X2X3/16 | R | 2.5 | 0.174 | 2 | 0.174 | 1.37 | 1.12 | 0.894 | 1.12 | 0.786 | 0.786 | 0.956 | 1.55 |
| HSS2.5X2X1/8 | R | 2.5 | 0.116 | 2 | 0.116 | 0.956 | 0.833 | 0.667 | 0.809 | 0.589 | 0.589 | 0.694 | 1.12 |
| HSS2.5X1.5X1/4 | R | 2.5 | 0.233 | 1.5 | 0.233 | 1.51 | 1.03 | 0.822 | 1.11 | 0.449 | 0.599 | 0.764 | 1.10 |
| HSS2.5X1.5X3/16 | R | 2.5 | 0.174 | 1.5 | 0.174 | 1.19 | 0.882 | 0.705 | 0.915 | 0.390 | 0.520 | 0.636 | 0.929 |
| HSS2.5X1.5X1/8 | R | 2.5 | 0.116 | 1.5 | 0.116 | 0.840 | 0.668 | 0.535 | 0.671 | 0.300 | 0.399 | 0.469 | 0.687 |
| HSS2.5X1X3/16 | R | 2.5 | 0.174 | 1 | 0.174 | 1.02 | 0.646 | 0.517 | 0.713 | 0.143 | 0.285 | 0.360 | 0.412 |
| HSS2.5X1X1/8 | R | 2.5 | 0.116 | 1 | 0.116 | 0.724 | 0.503 | 0.403 | 0.532 | 0.115 | 0.230 | 0.274 | 0.322 |
| HSS2X2X1/4 | R | 2 | 0.233 | 2 | 0.233 | 1.51 | 0.747 | 0.747 | 0.964 | 0.747 | 0.747 | 0.964 | 1.31 |
| HSS2X2X3/16 | R | 2 | 0.174 | 2 | 0.174 | 1.19 | 0.641 | 0.641 | 0.797 | 0.641 | 0.641 | 0.797 | 1.09 |
| HSS2X2X1/8 | R | 2 | 0.116 | 2 | 0.116 | 0.840 | 0.486 | 0.486 | 0.584 | 0.486 | 0.486 | 0.584 | 0.796 |

PIPE

| | | | | | | | |
|---|---|---|---|---|---|---|---|
| HSS24.000X0.500 | R | 24.000 | 0.465 | 34.400 | 2381.400 | 198.400 | 257.600 |
| HSS20.000X0.500 | R | 20.000 | 0.465 | 28.500 | 1360.000 | 136.000 | 177.000 |
| HSS20.000X0.375 | R | 20.000 | 0.349 | 21.500 | 1040.000 | 104.000 | 135.000 |
| HSS18.000X0.500 | R | 18.000 | 0.465 | 25.600 | 985.000 | 109.000 | 143.000 |
| HSS18.000X0.375 | R | 18.000 | 0.349 | 19.400 | 754.000 | 83.800 | 109.000 |
| HSS16.000X0.625 | R | 16.000 | 0.581 | 28.100 | 838.000 | 105.000 | 138.000 |
| HSS16.000X0.500 | R | 16.000 | 0.465 | 22.700 | 685.000 | 85.700 | 112.000 |
| HSS16.000X0.438 | R | 16.000 | 0.407 | 19.900 | 606.000 | 75.800 | 99.000 |
| HSS16.000X0.375 | R | 16.000 | 0.349 | 17.200 | 526.000 | 65.700 | 85.500 |
| HSS16.000X0.312 | R | 16.000 | 0.291 | 14.400 | 443.000 | 55.400 | 71.800 |
| HSS16.000X0.250 | R | 16.000 | 0.233 | 11.500 | 359.000 | 44.800 | 57.900 |
| HSS14.000X0.625 | R | 14.000 | 0.581 | 24.500 | 552.000 | 78.900 | 105.000 |
| HSS14.000X0.500 | R | 14.000 | 0.465 | 19.800 | 453.000 | 64.800 | 85.200 |
| HSS14.000X0.375 | R | 14.000 | 0.349 | 15.000 | 349.000 | 49.800 | 65.100 |
| HSS14.000X0.312 | R | 14.000 | 0.291 | 12.500 | 295.000 | 42.100 | 54.700 |
| HSS14.000X0.250 | R | 14.000 | 0.233 | 10.100 | 239.000 | 34.100 | 44.200 |
| HSS12.750X0.500 | R | 12.750 | 0.465 | 17.900 | 339.000 | 53.200 | 70.200 |
| HSS12.750X0.375 | R | 12.750 | 0.349 | 13.600 | 262.000 | 41.000 | 53.700 |
| HSS12.750X0.250 | R | 12.750 | 0.233 | 9.160 | 180.000 | 28.200 | 36.500 |
| HSS10.750X0.500 | R | 10.750 | 0.465 | 15.000 | 199.000 | 37.000 | 49.200 |
| HSS10.750X0.375 | R | 10.750 | 0.349 | 11.400 | 154.000 | 28.700 | 37.800 |
| HSS10.750X0.250 | R | 10.750 | 0.233 | 7.700 | 106.000 | 19.800 | 25.800 |
| HSS10.000X0.625 | R | 10.000 | 0.581 | 17.200 | 191.000 | 38.300 | 51.600 |
| HSS10.000X0.500 | R | 10.000 | 0.465 | 13.900 | 159.000 | 31.700 | 42.300 |
| HSS10.000X0.375 | R | 10.000 | 0.349 | 10.600 | 123.000 | 24.700 | 32.500 |
| HSS10.000X0.312 | R | 10.000 | 0.291 | 8.880 | 105.000 | 20.900 | 27.400 |
| HSS10.000X0.250 | R | 10.000 | 0.233 | 7.150 | 85.300 | 17.100 | 22.200 |
| HSS10.000X0.188 | R | 10.000 | 0.174 | 5.370 | 64.800 | 13.000 | 16.800 |
| HSS9.625X0.500 | R | 9.625 | 0.465 | 13.400 | 141.000 | 29.200 | 39.000 |
| HSS9.625X0.375 | R | 9.625 | 0.349 | 10.200 | 110.000 | 22.800 | 30.000 |

# APPENDIX C.2 – SEISMIC AND WIND LOADING

## Seismic ASCE 7-10

### *General Programming Input*

Risk Category II

For ordinary reinforced concrete shear walls, Classification 1.2 of §12.2-1

$C_d = 4.0$

$R = 4.0$

Please review the Summary and Detailed Report on the next page for the following values (U.S. Geological Survey, 2013):

$S_S = 0.410g$

$S_1 = 0.165g$

$TL = 12\ sec$

Site Class C

The Structure Period, $T_a$:

Value calculated by RAM SS using the Standard Equation

$C_t = 0.020$ was used for “all other structural systems” per Table 12.8-2

Orthogonal Effects Considered at 100%/30%

(American Society of Civil Engineers, ASCE-7 10, Minimum Design Loads for Buildings and Other Structures, 2010)

## U.S. Geological Survey Report



# USGS Design Maps Summary Report

**User–Specified Input**

| | |
|---|---|
| **Report Title** | Heifer International Center –2010<br>Thu February 20, 2014 17:15:04 UTC |
| **Building Code Reference Document** | ASCE 7–10 Standard<br>(which utilizes USGS hazard data available in 2008) |
| **Site Coordinates** | 34.74492°N, 92.25781°W |
| **Site Soil Classification** | Site Class C – "Very Dense Soil and Soft Rock" |
| **Risk Category** | I/II/III |


**USGS–Provided Output**

| | | | | | |
|---|---|---|---|---|---|
| $S_S$ = | 0.410 g | $S_{MS}$ = | 0.491 g | $S_{DS}$ = | 0.328 g |
| $S_1$ = | 0.165 g | $S_{M1}$ = | 0.270 g | $S_{D1}$ = | 0.180 g |

For information on how the SS and S1 values above have been calculated from probabilistic (risk–targeted) and deterministic ground motions in the direction of maximum horizontal response, please return to the application and select the "2009 NEHRP" building code reference document.

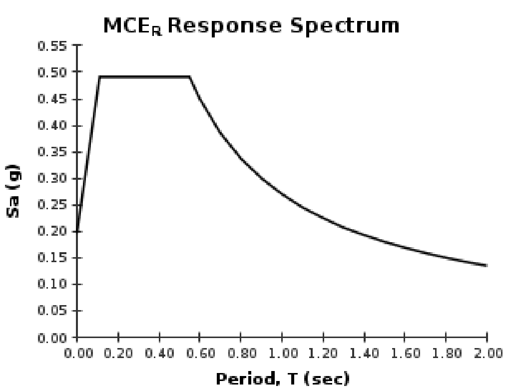


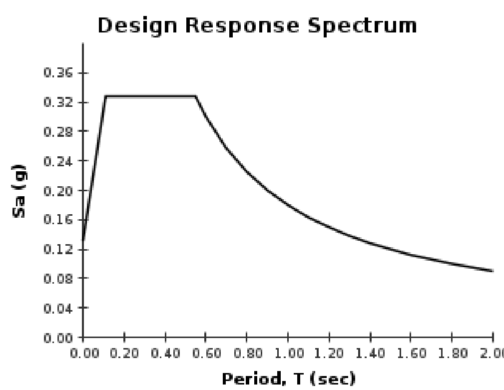


For $PGA_M$, $T_L$, $C_{RS}$, and $C_{R1}$ values, please view the detailed report.

# USGS Design Maps Detailed Report

ASCE 7-10 Standard (34.74492°N, 92.25781°W)

Site Class C – "Very Dense Soil and Soft Rock", Risk Category I/II/III

## Section 11.4.1 — Mapped Acceleration Parameters

Note: Ground motion values provided below are for the direction of maximum horizontal spectral response acceleration. They have been converted from corresponding geometric mean ground motions computed by the USGS by applying factors of 1.1 (to obtain $S_S$) and 1.3 (to obtain $S_1$). Maps in the 2010 ASCE-7 Standard are provided for Site Class B. Adjustments for other Site Classes are made, as needed, in Section 11.4.3.

| | |
|---|---|
| **From Figure 22-1** [1] | $S_S = 0.410$ g |
| **From Figure 22-2** [2] | $S_1 = 0.165$ g |

## Section 11.4.2 — Site Class

The authority having jurisdiction (not the USGS), site-specific geotechnical data, and/or the default has classified the site as Site Class C, based on the site soil properties in accordance with Chapter 20.

Table 20.3–1 Site Classification

| Site Class | $\bar{v}_S$ | $\bar{N}$ or $\bar{N}_{ch}$ | $\bar{s}_u$ |
|---|---|---|---|
| A. Hard Rock | >5,000 ft/s | N/A | N/A |
| B. Rock | 2,500 to 5,000 ft/s | N/A | N/A |
| C. Very dense soil and soft rock | 1,200 to 2,500 ft/s | >50 | >2,000 psf |
| D. Stiff Soil | 600 to 1,200 ft/s | 15 to 50 | 1,000 to 2,000 psf |
| E. Soft clay soil | <600 ft/s | <15 | <1,000 psf |
| | Any profile with more than 10 ft of soil having the characteristics:<br>• Plasticity index $PI > 20$,<br>• Moisture content $w \geq 40\%$, and<br>• Undrained shear strength $\bar{s}_u < 500$ psf | | |
| F. Soils requiring site response analysis in accordance with Section 21.1 | See Section 20.3.1 | | |

For SI: 1ft/s = 0.3048 m/s 1lb/ft² = 0.0479 kN/m²

Section 11.4.3 — Site Coefficients and Risk–Targeted Maximum Considered Earthquake ($MCE_R$) Spectral Response Acceleration Parameters

Table 11.4–1: Site Coefficient $F_a$

| Site Class | Mapped MCE $_R$ Spectral Response Acceleration Parameter at Short Period | | | | |
|---|---|---|---|---|---|
| | $S_S \le 0.25$ | $S_S = 0.50$ | $S_S = 0.75$ | $S_S = 1.00$ | $S_S \ge 1.25$ |
| A | 0.8 | 0.8 | 0.8 | 0.8 | 0.8 |
| B | 1.0 | 1.0 | 1.0 | 1.0 | 1.0 |
| C | 1.2 | 1.2 | 1.1 | 1.0 | 1.0 |
| D | 1.6 | 1.4 | 1.2 | 1.1 | 1.0 |
| E | 2.5 | 1.7 | 1.2 | 0.9 | 0.9 |
| F | See Section 11.4.7 of ASCE 7 | | | | |

Note: Use straight–line interpolation for intermediate values of $S_S$

**For Site Class = C and $S_s$ = 0.410 g, $F_a$ = 1.200**

Table 11.4–2: Site Coefficient $F_v$

| Site Class | Mapped MCE $_R$ Spectral Response Acceleration Parameter at 1–s Period | | | | |
|---|---|---|---|---|---|
| | $S_1 \le 0.10$ | $S_1 = 0.20$ | $S_1 = 0.30$ | $S_1 = 0.40$ | $S_1 \ge 0.50$ |
| A | 0.8 | 0.8 | 0.8 | 0.8 | 0.8 |
| B | 1.0 | 1.0 | 1.0 | 1.0 | 1.0 |
| C | 1.7 | 1.6 | 1.5 | 1.4 | 1.3 |
| D | 2.4 | 2.0 | 1.8 | 1.6 | 1.5 |
| E | 3.5 | 3.2 | 2.8 | 2.4 | 2.4 |
| F | See Section 11.4.7 of ASCE 7 | | | | |

Note: Use straight–line interpolation for intermediate values of $S_1$

**For Site Class = C and $S_1$ = 0.165 g, $F_v$ = 1.635**

| | |
|---|---|
| Equation (11.4–1): | $S_{MS} = F_aS_S = 1.200 \times 0.410 = 0.491$ g |
| Equation (11.4–2): | $S_{M1} = F_vS_1 = 1.635 \times 0.165 = 0.270$ g |

Section 11.4.4 — Design Spectral Acceleration Parameters

| | |
|---|---|
| Equation (11.4–3): | $S_{DS} = ⅔ S_{MS} = ⅔ \times 0.491 = 0.328$ g |
| Equation (11.4–4): | $S_{D1} = ⅔ S_{M1} = ⅔ \times 0.270 = 0.180$ g |

Section 11.4.5 — Design Response Spectrum

| | |
|---|---|
| From Figure 22-12 [3] | $T_L$ = 12 seconds |

Figure 11.4–1: Design Response Spectrum

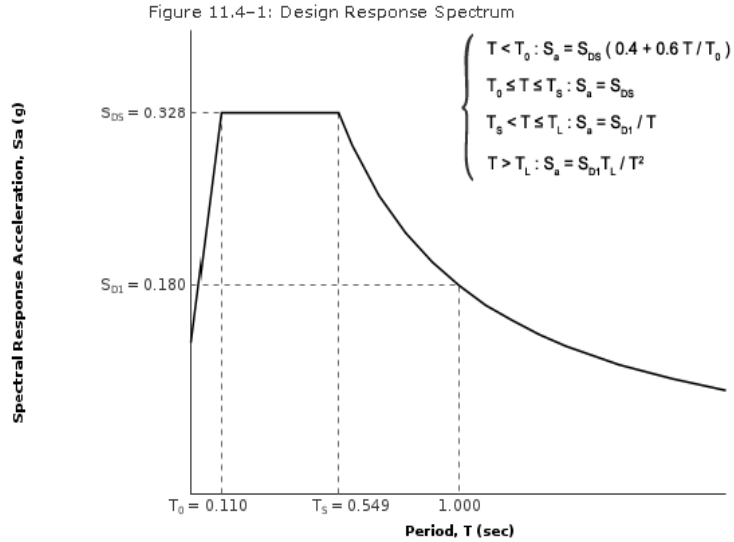

2/20/14 Design Maps Detailed Report

Section 11.4.6 — Risk-Targeted Maximum Considered Earthquake ($MCE_R$) Response Spectrum

The $MCE_R$ Response Spectrum is determined by multiplying the design response spectrum above by 1.5.

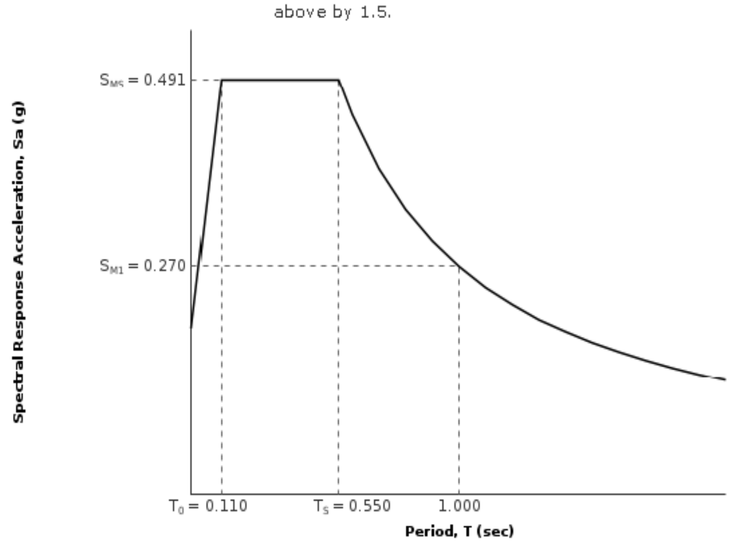


geohazards.usgs.gov/designmaps/us/report.php?template=minimal&latitude=34.7449152&longitude=-92.2578128&siteclass=2&riskcategory=0&edition=asce-2... 4/6

Section 11.8.3 — Additional Geotechnical Investigation Report Requirements for Seismic Design Categories D through F

| | |
|---|---|
| **From Figure 22-7** [4] | PGA = 0.213 |
| **Equation (11.8–1):** | $PGA_M = F_{PGA}PGA = 1.187 \times 0.213 = 0.253$ g |

Table 11.8–1: Site Coefficient $F_{PGA}$

| Site Class | Mapped MCE Geometric Mean Peak Ground Acceleration, PGA | | | | |
|---|---|---|---|---|---|
| | PGA ≤ 0.10 | PGA = 0.20 | PGA = 0.30 | PGA = 0.40 | PGA ≥ 0.50 |
| A | 0.8 | 0.8 | 0.8 | 0.8 | 0.8 |
| B | 1.0 | 1.0 | 1.0 | 1.0 | 1.0 |
| C | 1.2 | 1.2 | 1.1 | 1.0 | 1.0 |
| D | 1.6 | 1.4 | 1.2 | 1.1 | 1.0 |
| E | 2.5 | 1.7 | 1.2 | 0.9 | 0.9 |
| F | See Section 11.4.7 of ASCE 7 | | | | |

Note: Use straight–line interpolation for intermediate values of PGA

**For Site Class = C and PGA = 0.213 g, $F_{PGA}$ = 1.187**

Section 21.2.1.1 — Method 1 (from Chapter 21 – Site-Specific Ground Motion Procedures for Seismic Design)

| | |
|---|---|
| **From Figure 22-17** [5] | $C_{RS}$ = 0.829 |
| **From Figure 22-18** [6] | $C_{R1}$ = 0.816 |

## Section 11.6 — Seismic Design Category

Table 11.6-1 Seismic Design Category Based on Short Period Response Acceleration Parameter

| VALUE OF $S_{DS}$ | RISK CATEGORY | | |
|---|---|---|---|
| | I or II | III | IV |
| $S_{DS} < 0.167g$ | A | A | A |
| $0.167g \le S_{DS} < 0.33g$ | B | B | C |
| $0.33g \le S_{DS} < 0.50g$ | C | C | D |
| $0.50g \le S_{DS}$ | D | D | D |

**For Risk Category = I and $S_{DS}$ = 0.328 g, Seismic Design Category = B**

Table 11.6-2 Seismic Design Category Based on 1-S Period Response Acceleration Parameter

| VALUE OF $S_{D1}$ | RISK CATEGORY | | |
|---|---|---|---|
| | I or II | III | IV |
| $S_{D1} < 0.067g$ | A | A | A |
| $0.067g \le S_{D1} < 0.133g$ | B | B | C |
| $0.133g \le S_{D1} < 0.20g$ | C | C | D |
| $0.20g \le S_{D1}$ | D | D | D |

**For Risk Category = I and $S_{D1}$ = 0.180 g, Seismic Design Category = C**

Note: When $S_1$ is greater than or equal to 0.75g, the Seismic Design Category is **E** for buildings in Risk Categories I, II, and III, and **F** for those in Risk Category IV, irrespective of the above.

Seismic Design Category ≡ "the more severe design category in accordance with Table 11.6-1 or 11.6-2" = C

---

Note: See Section 11.6 for alternative approaches to calculating Seismic Design Category.

### References

1. *Figure 22-1*: http://earthquake.usgs.gov/hazards/designmaps/downloads/pdfs/2010_ASCE-7_Figure_22-1.pdf
2. *Figure 22-2*: http://earthquake.usgs.gov/hazards/designmaps/downloads/pdfs/2010_ASCE-7_Figure_22-2.pdf
3. *Figure 22-12*: http://earthquake.usgs.gov/hazards/designmaps/downloads/pdfs/2010_ASCE-7_Figure_22-12.pdf
4. *Figure 22-7*: http://earthquake.usgs.gov/hazards/designmaps/downloads/pdfs/2010_ASCE-7_Figure_22-7.pdf
5. *Figure 22-17*: http://earthquake.usgs.gov/hazards/designmaps/downloads/pdfs/2010_ASCE-7_Figure_22-17.pdf
6. *Figure 22-18*: http://earthquake.usgs.gov/hazards/designmaps/downloads/pdfs/2010_ASCE-7_Figure_22-18.pdf

## *Seismic Story Drift*

### Seismic Story Drift - West End

**$C_d$ =** 4
**I =** 1

West Side

**X-direction Seismic Loading**

| Level | δ, Actual Displacement (in) | $\delta_x$, Modified Displacement (in) | Story Height (ft) | Δ, Design Story Drift (in) | $\Delta_a$, Allowable Story Drift (in) | Pass |
|---|---|---|---|---|---|---|
| Story3 | 0.3799 | 1.5196 | 14 | 0.6464 | 3.36 | PASS |
| Story2 | 0.2183 | 0.8732 | 14 | 0.5816 | 3.36 | PASS |
| Story1 | 0.0729 | 0.2916 | 14 | 0.2916 | 3.36 | PASS |

@ RAM Frame Location EX A @ (-156.198, -393.277), trace Location 1

**X-direction Seismic Loading**

| Level | δ, Actual Displacement (in) | $\delta_x$, Modified Displacement (in) | Story Height (ft) | Δ, Design Story Drift (in) | $\Delta_a$, Allowable Story Drift (in) | Pass |
|---|---|---|---|---|---|---|
| Story3 | 0.2436 | 0.9744 | 14 | 0.4084 | 3.36 | PASS |
| Story2 | 0.1415 | 0.566 | 14 | 0.3784 | 3.36 | PASS |
| Story1 | 0.0469 | 0.1876 | 14 | 0.1876 | 3.36 | PASS |

@ RAM Frame Location EX B @ (-379.546, -319.250), trace Location 3

**Y-direction Seismic Loading**

| Level | δ, Actual Displacement (in) | $\delta_x$, Modified Displacement (in) | Story Height (ft) | Δ, Design Story Drift (in) | $\Delta_a$, Allowable Story Drift (in) | Pass |
|---|---|---|---|---|---|---|
| Story3 | 0.4542 | 1.8168 | 14 | 0.7776 | 3.36 | PASS |
| Story2 | 0.2598 | 1.0392 | 14 | 0.674 | 3.36 | PASS |
| Story1 | 0.0913 | 0.3652 | 14 | 0.3652 | 3.36 | PASS |

@ RAM Frame Location EX A @ (-156.198, -393.277), trace Location 1

**Y-direction Seismic Loading**

| Level | δ, Actual Displacement (in) | $\delta_x$, Modified Displacement (in) | Story Height (ft) | Δ, Design Story Drift (in) | $\Delta_a$, Allowable Story Drift (in) | Pass |
|---|---|---|---|---|---|---|
| Story3 | 0.1035 | 0.414 | 14 | 0.1736 | 3.36 | PASS |
| Story2 | 0.0601 | 0.2404 | 14 | 0.1744 | 3.36 | PASS |
| Story1 | 0.0165 | 0.066 | 14 | 0.066 | 3.36 | PASS |

@ RAM Frame Location EX B @ (-379.546, -319.250), trace Location 3

Please refer to Appendix C.6 – Trace Locations for a visual location of EX A and EX B

# Seismic Story Drift - East End

**$C_d$ =** 4

**I =** 1

East Side

**X-direction Seismic Loading**

| Level | δ, Actual Displacement (in) | $\delta_x$, Modified Displacement (in) | Story Height (ft) | Δ, Design Story Drift (in) | $\Delta_a$, Allowable Story Drift (in) | Pass |
|---|---|---|---|---|---|---|
| Story3 | 0.2051 | 0.8204 | 14 | 0.3948 | 3.36 | PASS |
| Story2 | 0.1064 | 0.4256 | 14 | 0.38 | 3.36 | PASS |
| Story1 | 0.0114 | 0.0456 | 14 | 0.0456 | 3.36 | PASS |

@ RAM Frame Location EX C @ (-365.149, -844.326), trace location 4

**X-direction Seismic Loading**

| Level | δ, Actual Displacement (in) | $\delta_x$, Modified Displacement (in) | Story Height (ft) | Δ, Design Story Drift (in) | $\Delta_a$, Allowable Story Drift (in) | Pass |
|---|---|---|---|---|---|---|
| Story3 | 0.4083 | 1.6332 | 14 | 0.8188 | 3.36 | PASS |
| Story2 | 0.2036 | 0.8144 | 14 | 0.74 | 3.36 | PASS |
| Story1 | 0.0186 | 0.0744 | 14 | 0.0744 | 3.36 | PASS |

@ RAM Frame Location EX D @ (-556.445, -926.789), trace location 5

**Y-direction Seismic Loading**

| Level | δ, Actual Displacement (in) | $\delta_x$, Modified Displacement (in) | Story Height (ft) | Δ, Design Story Drift (in) | $\Delta_a$, Allowable Story Drift (in) | Pass |
|---|---|---|---|---|---|---|
| Story3 | 0.2524 | 1.0096 | 14 | 0.5116 | 3.36 | PASS |
| Story2 | 0.1245 | 0.498 | 14 | 0.4592 | 3.36 | PASS |
| Story1 | 0.0097 | 0.0388 | 14 | 0.0388 | 3.36 | PASS |

@ RAM Frame Location EX C @ (-365.149, -844.326), trace location 4

**Y-direction Seismic Loading**

| Level | δ, Actual Displacement (in) | $\delta_x$, Modified Displacement (in) | Story Height (ft) | Δ, Design Story Drift (in) | $\Delta_a$, Allowable Story Drift (in) | Pass |
|---|---|---|---|---|---|---|
| Story3 | -0.219 | -0.876 | 14 | -0.472 | 3.36 | PASS |
| Story2 | -0.101 | -0.404 | 14 | -0.376 | 3.36 | PASS |
| Story1 | -0.007 | -0.028 | 14 | -0.028 | 3.36 | PASS |

@ RAM Frame Location EX D @ (-556.445, -926.789), trace location 5

Please refer to Appendix C.6 – Trace Locations for a visual location of EX C and EX D

## Wind ASCE 7-10

Exposure C

Mean roof height = 65'-0" (conservatively assumed)

$k_{zt} = 0$ due to no hills near building

Use calculated n for x and y for natural frequency

$V = 115\ mph$ for basic wind speed

$G = 0.85$ (conservatively assumed)

(American Society of Civil Engineers, ASCE-7 10, Minimum Design Loads for Buildings and Other Structures, 2010)

## *Wind Building Drift*

### Wind Building Drift - West End

$h_{building}$ = 65 ft

**X-direction, Wind Loading**

| Load Case | Total Building Displacement (in) | Maximum Building Drift Allowed (in) | Pass |
|---|---|---|---|
| W1 | 0.211 | 1.95 | PASS |
| W2 | 0.067 | 1.95 | PASS |
| W3 | 0.139 | 1.95 | PASS |
| W4 | 0.178 | 1.95 | PASS |
| W5 | 0.093 | 1.95 | PASS |
| W6 | 0.007 | 1.95 | PASS |
| W7 | 0.208 | 1.95 | PASS |
| W8 | 0.108 | 1.95 | PASS |
| W9 | 0.109 | 1.95 | PASS |
| W10 | 0.203 | 1.95 | PASS |
| W11 | 0.034 | 1.95 | PASS |
| W12 | 0.128 | 1.95 | PASS |

**Y-direction, Wind Loading**

| Load Case | Total Building Displacement (in) | Maximum Building Drift Allowed (in) | Pass |
|---|---|---|---|
| W1 | 0.109 | 1.95 | PASS |
| W2 | 0.346 | 1.95 | PASS |
| W3 | 0.032 | 1.95 | PASS |
| W4 | 0.131 | 1.95 | PASS |
| W5 | 0.369 | 1.95 | PASS |
| W6 | 0.149 | 1.95 | PASS |
| W7 | 0.340 | 1.95 | PASS |
| W8 | -0.178 | 1.95 | PASS |
| W9 | 0.136 | 1.95 | PASS |
| W10 | 0.375 | 1.95 | PASS |
| W11 | -0.253 | 1.95 | PASS |
| W12 | -0.014 | 1.95 | PASS |

EX A @ (-156.198, -393.277), trace Location 1

## Wind Building Drift - West End

$h_{building}$ = 65 ft

**X-direction, Wind Loading**

| Load Case | Total Building Displacement (in) | Maximum Building Drift Allowed (in) | Pass |
|---|---|---|---|
| W1 | 0.159 | 1.95 | PASS |
| W2 | -0.001 | 1.95 | PASS |
| W3 | 0.126 | 1.95 | PASS |
| W4 | 0.113 | 1.95 | PASS |
| W5 | -0.015 | 1.95 | PASS |
| W6 | 0.014 | 1.95 | PASS |
| W7 | 0.119 | 1.95 | PASS |
| W8 | 0.120 | 1.95 | PASS |
| W9 | 0.105 | 1.95 | PASS |
| W10 | 0.073 | 1.95 | PASS |
| W11 | 0.105 | 1.95 | PASS |
| W12 | 0.074 | 1.95 | PASS |

**Y-direction, Wind Loading**

| Load Case | Total Building Displacement (in) | Maximum Building Drift Allowed (in) | Pass |
|---|---|---|---|
| W1 | -0.048 | 1.95 | PASS |
| W2 | 0.142 | 1.95 | PASS |
| W3 | -0.008 | 1.95 | PASS |
| W4 | -0.065 | 1.95 | PASS |
| W5 | 0.043 | 1.95 | PASS |
| W6 | 0.169 | 1.95 | PASS |
| W7 | 0.070 | 1.95 | PASS |
| W8 | -0.142 | 1.95 | PASS |
| W9 | 0.121 | 1.95 | PASS |
| W10 | -0.016 | 1.95 | PASS |
| W11 | -0.038 | 1.95 | PASS |
| W12 | -0.175 | 1.95 | PASS |

EX B @ (-379.546, -319.250), trace Location 3

## Wind Building Drift - East End

$h_{building}$ = 65 ft

**X-direction, Wind Loading**

| Load Case | Total Building Displacement (in) | Maximum Building Drift Allowed (in) | Pass |
|---|---|---|---|
| W1 | 0.072 | 1.95 | PASS |
| W2 | 0.009 | 1.95 | PASS |
| W3 | 0.056 | 1.95 | PASS |
| W4 | 0.052 | 1.95 | PASS |
| W5 | 0.000 | 1.95 | PASS |
| W6 | 0.013 | 1.95 | PASS |
| W7 | 0.061 | 1.95 | PASS |
| W8 | 0.048 | 1.95 | PASS |
| W9 | 0.052 | 1.95 | PASS |
| W10 | 0.039 | 1.95 | PASS |
| W11 | 0.042 | 1.95 | PASS |
| W12 | 0.030 | 1.95 | PASS |

**Y-direction, Wind Loading**

| Load Case | Total Building Displacement (in) | Maximum Building Drift Allowed (in) | Pass |
|---|---|---|---|
| W1 | 0.051 | 1.95 | PASS |
| W2 | 0.059 | 1.95 | PASS |
| W3 | 0.010 | 1.95 | PASS |
| W4 | 0.067 | 1.95 | PASS |
| W5 | 0.144 | 1.95 | PASS |
| W6 | -0.056 | 1.95 | PASS |
| W7 | 0.083 | 1.95 | PASS |
| W8 | -0.006 | 1.95 | PASS |
| W9 | -0.035 | 1.95 | PASS |
| W10 | 0.158 | 1.95 | PASS |
| W11 | -0.101 | 1.95 | PASS |
| W12 | 0.092 | 1.95 | PASS |

EX C @ (-365.149, -844.326), trace location 4

## Wind Building Drift - East End

$h_{building}$ = 65 ft

**X-direction, Wind Loading**

| Load Case | Total Building Displacement (in) | Maximum Building Drift Allowed (in) | Pass |
|---|---|---|---|
| W1 | 0.125 | 1.95 | PASS |
| W2 | -0.071 | 1.95 | PASS |
| W3 | 0.065 | 1.95 | PASS |
| W4 | 0.123 | 1.95 | PASS |
| W5 | 0.048 | 1.95 | PASS |
| W6 | -0.155 | 1.95 | PASS |
| W7 | 0.041 | 1.95 | PASS |
| W8 | 0.147 | 1.95 | PASS |
| W9 | -0.067 | 1.95 | PASS |
| W10 | 0.129 | 1.95 | PASS |
| W11 | 0.013 | 1.95 | PASS |
| W12 | 0.208 | 1.95 | PASS |

**Y-direction, Wind Loading**

| Load Case | Total Building Displacement (in) | Maximum Building Drift Allowed (in) | Pass |
|---|---|---|---|
| W1 | -0.072 | 1.95 | PASS |
| W2 | 0.244 | 1.95 | PASS |
| W3 | -0.011 | 1.95 | PASS |
| W4 | -0.097 | 1.95 | PASS |
| W5 | 0.032 | 1.95 | PASS |
| W6 | 0.334 | 1.95 | PASS |
| W7 | 0.129 | 1.95 | PASS |
| W8 | -0.237 | 1.95 | PASS |
| W9 | 0.242 | 1.95 | PASS |
| W10 | -0.049 | 1.95 | PASS |
| W11 | -0.032 | 1.95 | PASS |
| W12 | -0.323 | 1.95 | PASS |

EX D @ (-556.445, -926.789), trace location 5

## APPENDIX C.3 – TORSIONAL IRREGULARITY AND SEISMIC AMPLIFICATION FACTOR

### Amplification Factor - West Side of Heifer International Center

**X-direction Seismic Loading**

| Level | δ EX A + Ext A (in) | δ EX B + Ext B (in) | δ Average (in) | δ Maximum (in) | $A_x$ | 1.2(δ Average | 1.4(δ Average | Irregularity Type 1a (Table 12.3-1) | Irregularity Type 1b (Table 12.3-1 |
|---|---|---|---|---|---|---|---|---|---|
| Story3 | 0.380 | 0.244 | 0.312 | 0.380 | 1.03 | 0.374 | 0.436 | NA | Type 1b |
| Story2 | 0.218 | 0.142 | 0.180 | 0.218 | 1.02 | 0.216 | 0.252 | NA | Type 1b |
| Story1 | 0.073 | 0.047 | 0.060 | 0.073 | 1.03 | 0.072 | 0.084 | NA | Type 1b |
| Controlling Case | E5 | | | | | | | | |

EX A @ (-156.198, -393.277), trace Location 1
EX B @ (-379.546, -319.250), trace Location 3

| Level | $A_x$ | $V_i$ (kips) | e (ft) | $M_z$ (k-ft) | $V_{apply}$ (kips |
|---|---|---|---|---|---|
| Story3 | 1.03 | 186.15 | 11.26 | 2162 | 191.97 |
| Story2 | 1.02 | 283.64 | 11.26 | 3266 | 290.03 |
| Story1 | 1.03 | 331.55 | 11.26 | 3840 | 341.03 |

Eccentrictity calculated by RAM Frame

Shear only from x-direction of case E5, conservative assumption

## Amplification Factor - West Side of Heifer International Center

**Y-direction Seismic Loading**

| Level | δ EY A + Ext A (in) | δ EY B + Ext B (in) | δ Average (in) | δ Maximum (in) | $A_x$ | 1.2(δ Average | 1.4(δ Average | Irregularity Type 1a (Table 12.3-1) | Irregularity Type 1b (Table 12.3-1 |
|---|---|---|---|---|---|---|---|---|---|
| Story3 | 0.454 | 0.104 | 0.279 | 0.454 | 1.84 | 0.335 | 0.390 | NA | NA |
| Story2 | 0.260 | 0.060 | 0.160 | 0.260 | 1.83 | 0.192 | 0.224 | NA | NA |
| Story1 | 0.091 | 0.017 | 0.054 | 0.091 | 1.99 | 0.065 | 0.075 | NA | NA |
| Controlling Case | E9 | | | | | | | | |

EY A @ (-156.198, -393.277), trace Location 1
EY B @ (-379.546, -319.250), trace Location 3

| Level | $A_x$ | $V_i$ (kips) | e (ft) | $M_z$ (k-ft) | $V_{apply}$ (kips |
|---|---|---|---|---|---|
| Story3 | 1.00 | 185.64 | 7.88 | 1463 | 185.64 |
| Story2 | 1.00 | 282.97 | 7.88 | 2230 | 282.97 |
| Story1 | 1.00 | 331.21 | 7.88 | 2610 | 331.21 |

Eccentrictity calculated by RAM Frame

Shear only from y-direction of case E9, conservative assumption

## Amplification Factor - East Side of Heifer International Center

**X-direction Seismic Loading**

| Level | δ EX C + Ext C (in) | δ EX D + Ext D (in) | δ Average (in) | δ Maximum (in) | $A_x$ | 1.2(δ Average | 1.4(δ Average | Irregularity Type 1a (Table 12.3-1) | Irregularity Type 1b (Table 12.3-1 |
|---|---|---|---|---|---|---|---|---|---|
| Story3 | 0.205 | 0.408 | 0.307 | 0.408 | 1.23 | 0.368 | 0.429 | NA | Type 1b |
| Story2 | 0.106 | 0.204 | 0.155 | 0.204 | 1.20 | 0.186 | 0.217 | NA | Type 1b |
| Story1 | 0.011 | 0.019 | 0.015 | 0.019 | 1.07 | 0.018 | 0.021 | NA | Type 1b |
| Controlling Case | E21 | | | | | | | | |

EX C @ (-365.149, -844.326), trace location 4
EX D @ (-556.445, -926.789), trace location 5

| Level | $A_x$ | $V_i$ (kips) | e (ft) | $M_z$ (k-ft) | $V_{apply}$ (kips |
|---|---|---|---|---|---|
| Story3 | 1.23 | 180.16 | 9.87 | 2188 | 221.73 |
| Story2 | 1.20 | 274.77 | 9.87 | 3249 | 329.23 |
| Story1 | 1.07 | 325.55 | 9.87 | 3431 | 347.62 |

Eccentrictity calculated by RAM Frame

Shear only from x-direction of case E21, conservative assumption

## Amplification Factor - East Side of Heifer International Center

**Y-direction Seismic Loading**

| Level | δ EY C + Ext C (in) | δ EY D + Ext D (in) | δ Average (in) | δ Maximum (in) | $A_x$ | 1.2(δ Average | 1.4(δ Average | Irregularity Type 1a (Table 12.3-1) | Irregularity Type 1b (Table 12.3-1 |
|---|---|---|---|---|---|---|---|---|---|
| Story3 | 0.252 | -0.219 | 0.236 | 0.252 | 1.00 | 1.252 | 0.744 | NA | Type 1b |
| Story2 | 0.125 | -0.101 | 0.113 | 0.125 | 1.00 | 1.125 | 0.619 | NA | Type 1b |
| Story1 | 0.010 | -0.007 | 0.008 | 0.010 | 1.00 | 1.010 | 0.509 | NA | Type 1b |
| Controlling Case | E21 | | | | | | | | |

EX C @ (-365.149, -844.326), trace location 4
EX D @ (-556.445, -926.789), trace location 5

| Level | $A_x$ | $V_i$ (kips) | e (ft) | $M_z$ (k-ft) | $V_{apply}$ (kips |
|---|---|---|---|---|---|
| Story3 | 1.00 | 180.16 | 5.63 | 1014 | 180.16 |
| Story2 | 1.00 | 274.77 | 5.63 | 1547 | 274.77 |
| Story1 | 1.00 | 325.55 | 5.63 | 1833 | 325.55 |

Eccentricity calculated by RAM Frame

Shear only from y-direction of case E21, conservative assumption

## APPENDIX C.4 – BUILDING OVERTURNING CHECK

### Overturning Moment and Base Shear - West End

Building Effective Weight = 4022.94 kips

**Wind Base Shear and Overturning Moment**

| Load Case | Level | Elevation (ft) | Base Shear Vx (kip) | Base Shear Vy (kip) | Overturning Moment Mx (kip-ft) | Overturning Moment My (kip-ft) |
|---|---|---|---|---|---|---|
| Wind X | Level 3 | 42 | 35.04 | 0 | | |
| | Level 2 | 28 | 67.36 | 0 | | |
| | Level 1 | 14 | 63.31 | 0 | 4,244.10 | - |
| Wind Y | Level 3 | 42 | 0 | 53.91 | | |
| | Level 2 | 28 | 0 | 103.94 | | |
| | Level 1 | 14 | 0 | 98.15 | - | 6,548.64 |

**Seismic Base Shear and Overturning Moment**

| Load Case | Level | Elevation (ft) | Base Shear Vx (kip) | Base Shear Vy (kip) | Overturning Moment Mx (kip-ft) | Overturning Moment My (kip-ft) |
|---|---|---|---|---|---|---|
| Seismic X | Level 3 | 42 | 184.71 | 0 | | |
| | Level 2 | 28 | 96.62 | 0 | | |
| | Level 1 | 14 | 48.55 | 0 | 11,142.88 | - |
| Seismic Y | Level 3 | 42 | 0 | 184.49 | | |
| | Level 2 | 28 | 0 | 96.67 | | |
| | Level 1 | 14 | 0 | 48.72 | - | 11,137.42 |

Maximum moment = 11,142.88 kip-ft experienced by building (assume worst case moment in either direction)
Resisting Moment = 60,800.03 kip-ft from the weight of the building (assuming smallest moment arm and factor of safety of 1.5)

Factor of Safety = 5.5

Overturning Passes

| | Weight (kips) | Mass (k-s2/ft) | Center of Mass X | Center of Mass Y | Building Edge X | Building Edge Y |
|---|---|---|---|---|---|---|
| Story 3 | 1560.4 | 48.46 | -260.6 | -385.83 | -155.803 | -392.882 |
| Story 2 | 1226.43 | 38.088 | -264.46 | -383.47 | -155.803 | -392.882 |
| Story 1 | 1236.11 | 38.388 | -265.33 | -382.93 | -155.803 | -392.882 |

| Distance for Measurement | Distance to Edge COM to N | Distance to Edge COM to S |
|---|---|---|
| 104.797 | 23.2 | 34.6 |
| 108.657 | 23.08 | 35.27 |
| 109.527 | 22.67 | 33.56 |

**Overturning Moment and Base Shear - East End**

Building Effective Weight = 3966.09 kips

**Wind Base Shear and Overturning Moment**

| Load Case | Level | Elevation (ft) | Base Shear | | Overturning Moment | |
|---|---|---|---|---|---|---|
| | | | Vx (kip) | Vy (kip) | Mx (kip-ft) | My (kip-ft) |
| Wind X | Level 3 | 42 | 35.04 | 0 | | |
| | Level 2 | 28 | 67.36 | 0 | | |
| | Level 1 | 14 | 63.31 | 0 | 4,244.10 | - |
| Wind Y | Level 3 | 42 | 0 | 47.25 | | |
| | Level 2 | 28 | 0 | 91.1 | | |
| | Level 1 | 14 | 0 | 86.02 | - | 5,739.58 |

**Seismic Base Shear and Overturning Moment**

| Load Case | Level | Elevation (ft) | Base Shear | | Overturning Moment | |
|---|---|---|---|---|---|---|
| | | | Vx (kip) | Vy (kip) | Mx (kip-ft) | My (kip-ft) |
| Seismic X | Level 3 | 42 | 178.93 | 0 | | |
| | Level 2 | 28 | 93.81 | 0 | | |
| | Level 1 | 14 | 52.48 | 0 | 10,876.46 | - |
| Seismic Y | Level 3 | 42 | 0 | 178.93 | | |
| | Level 2 | 28 | 0 | 93.81 | | |
| | Level 1 | 14 | 0 | 52.48 | - | 10,876.46 |

Maximum moment = 10,876.46 kip-ft experienced by building (assume worst case moment in either direction)
Resisting Moment = 40,136.83 kip-ft from the weight of the building (assuming smallest moment arm and factor of safety of 1.5)

Factor of Safety = 3.7

Overturning Passes

| | Weight (kips) | Mass (k-s2/ft) | Center of Mass | | Building Edge | |
|---|---|---|---|---|---|---|
| | | | X | Y | X | Y |
| Story 3 | 1487.45 | 46.194 | -471.97 | -875.62 | -364.201 | -844.61 |
| Story 2 | 1169.75 | 36.328 | -468.17 | -874.49 | -364.201 | -844.61 |
| Story 1 | 1308.89 | 40.649 | -465.25 | -875.26 | -364.201 | -844.61 |

| Distance for Measurement |
|---|
| 107.769 |
| 103.969 |
| 101.049 |

| Distance to Edge | |
|---|---|
| COM to N | COM to S |
| 15.18 | 43.36 |
| 15.25 | 44.19 |
| 16.93 | 42.03 |

## APPENDIX C.5 – LATERAL SYSTEM HAND CHECKS

LATERAL SYSTEM HAND CHECK

WHAT IS CONTROLLING LOAD COMBINATION?

(5) $1.2D + 1.0E + L + 0.2S$

(7) $0.9D + 1.0E$

where,

$D = 113.98^k$

$W = 133.77^k$ worst case

$E = Q_E = 406.05^k$ → PER § 12.4.2 $E = E_h \pm E_v$

(+) → (5)

(−) → (7)

$L = 2.75^k$

$E_h = \rho Q_E = (1.0)(406.05^k) = 406.05^k$

$\rho = 1.0$ b/c SDC C PER § 12.3.4.1

$E_v = 0.2 S_{DS} D = 0.2(0.328)(113.98) = 7.477^k$

$S_{DS} = 0.328$ FROM U.S.G.S

So, (5) $P_u = 1.2D + 1.0E_v + L + 0.2S$

$= 1.2(113.98) + 1.0(7.477) + 2.75 + \cancel{0.2S}$ DISCONT. FROM ROOF

$= 147.003^k$

$V_u = 1.0E_h$

$= 1.0(406.05)$

$= 406.05^k$

(7) $P_u = 0.9D + 1.0E_v$

$= 0.9(113.98) + 1.0(7.477)$

$= 110.059^k$

$V_u = 1.0E_h = 406.05^k$ (FROM ABOVE)

thus, CASE 5 CONTROLS

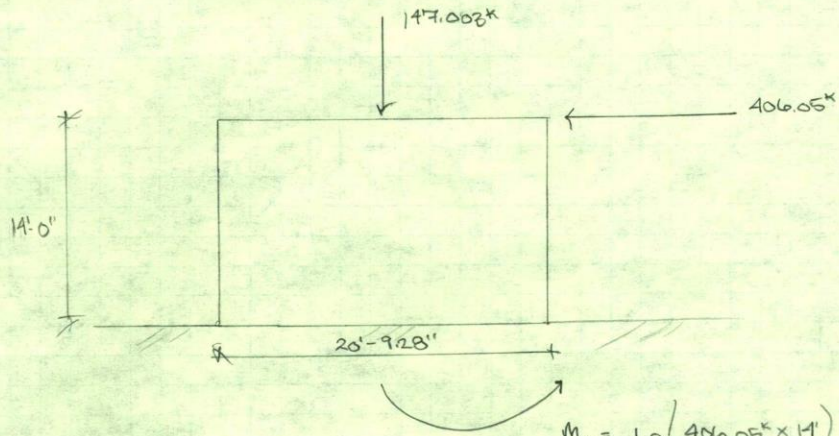


$$M_u = 1.0\left(406.05^k \times 14'\right)$$

$$= 5684.7'^k = M_u$$

CHECK CONCRETE SHEAR WALL

ENSURE, $\phi V_n > V_u = 406.05^k$

What is $V_c$?

PER ACI 318-11, CHAPTER 11

$$V_c = 3.3\lambda\sqrt{f'_c}\cdot h\cdot d + \frac{N_u\cdot d}{4\,l_w} \qquad \text{(eq. 11-27)}$$

$\lambda = 1.0$
$f'_c = 4000$ psi
$h = 8"$
$d = 0.8\,l_w = 0.8(20 + 9.28/12)\times 12 = 199.424"$
$N_u = 1.2(113.98) = 136.776^k$

so, $V_c = \left[3.3(1)\sqrt{4000}\cdot 8\cdot 199.424 + \left(\frac{136.776^k \cdot 199.424"}{4(20\times 12 + 9.28)}\right)\right]/1000$

$= 333.00^k$

ALSO CHECK,

$$V_c = \left[0.6\lambda\sqrt{f'_c} + \frac{l_w\cdot\left(1.25\lambda\sqrt{f'_c} + 0.2\frac{N_u}{l_w h}\right)}{\frac{M_u}{V_u} - \frac{l_w}{2}}\right]\cdot h\cdot d \qquad \text{(eq. 11-28)}$$

$$= \left[0.6(1)\sqrt{4000} + \frac{199.424\cdot\left(1.25(1)\sqrt{4000} + 0.2\cdot\frac{136.776}{(20\times 12+9.28)(8)}\right)}{\frac{5684.7\times 12^{"/'}}{406.05} - \frac{(20\times 12 + 9.28)}{2}}\right]\times\frac{8\times 199.424}{1000}$$

$= 785.77^k$

so, $V_c = \min \left| \begin{array}{l} 333 \\ 786^k \end{array} \right. \rightarrow V_c = 333^k$

$\phi V_n = 0.75(333) = 249.75^k < 406.05^k$

X INSUFFICIENT

what is $V_s$?

$V_s = \dfrac{A_v f_y d}{s}$ HORIZONTAL REINF: #4 @ 18" O.C.

$A_v = \left(\dfrac{14' \times 12"/'}{18"} + 1\right)(0.2)(2) = 4.13$

$f_y = 60$

$d = 199.424"$

so, $V_s = \dfrac{4.13(60)(199.424)}{18"} = 2747.6^k$

now, $\phi V_n = 0.75(333 + 2747.6) = \underline{2310^k > 406.05^k}$

✓ GOOD

DESIGN GENERATED
BY RAM SS ARE
SUFFICIENT...

RAM Concrete was used in the design of the shear walls for the Heifer International Center. SW 13 @ column 12 is shown below.

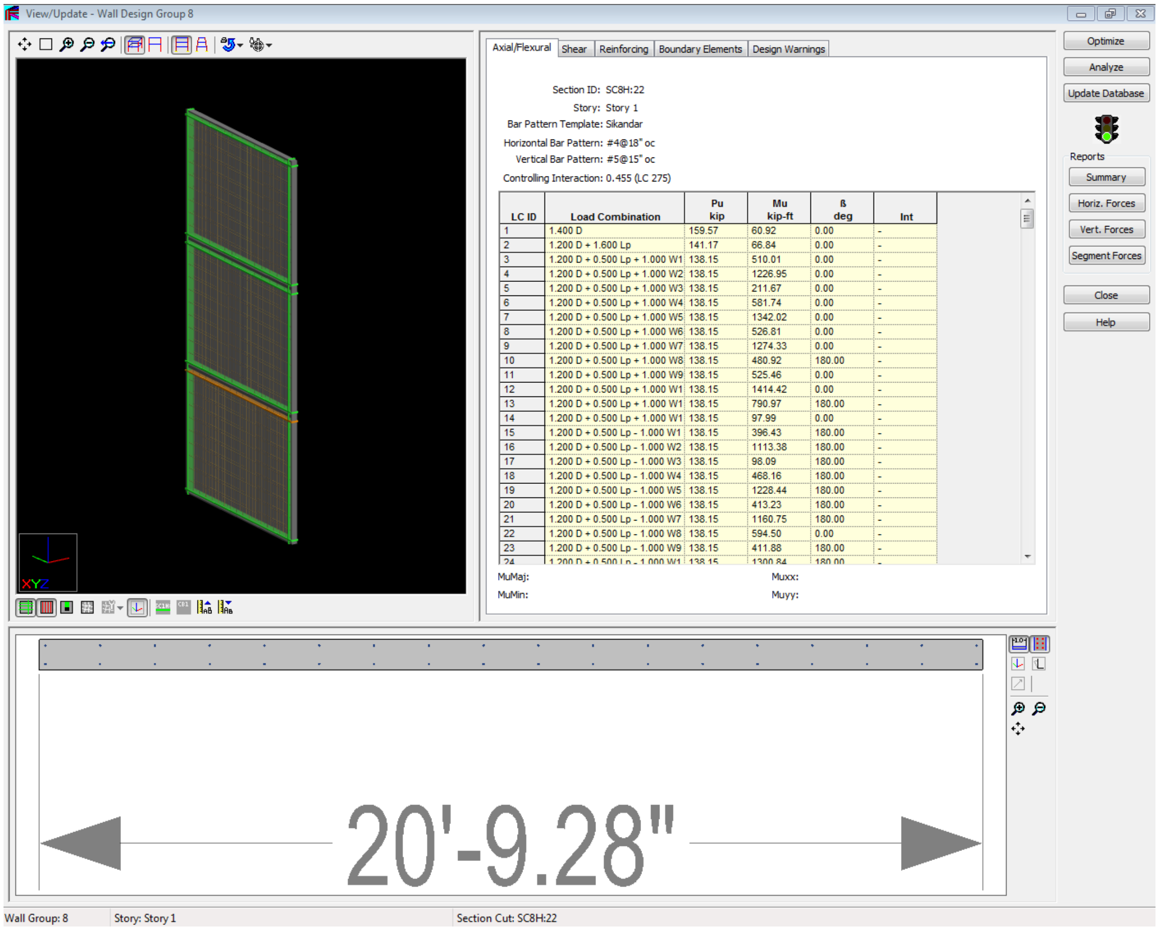

## APPENDIX C.6 – TRACE LOCATIONS

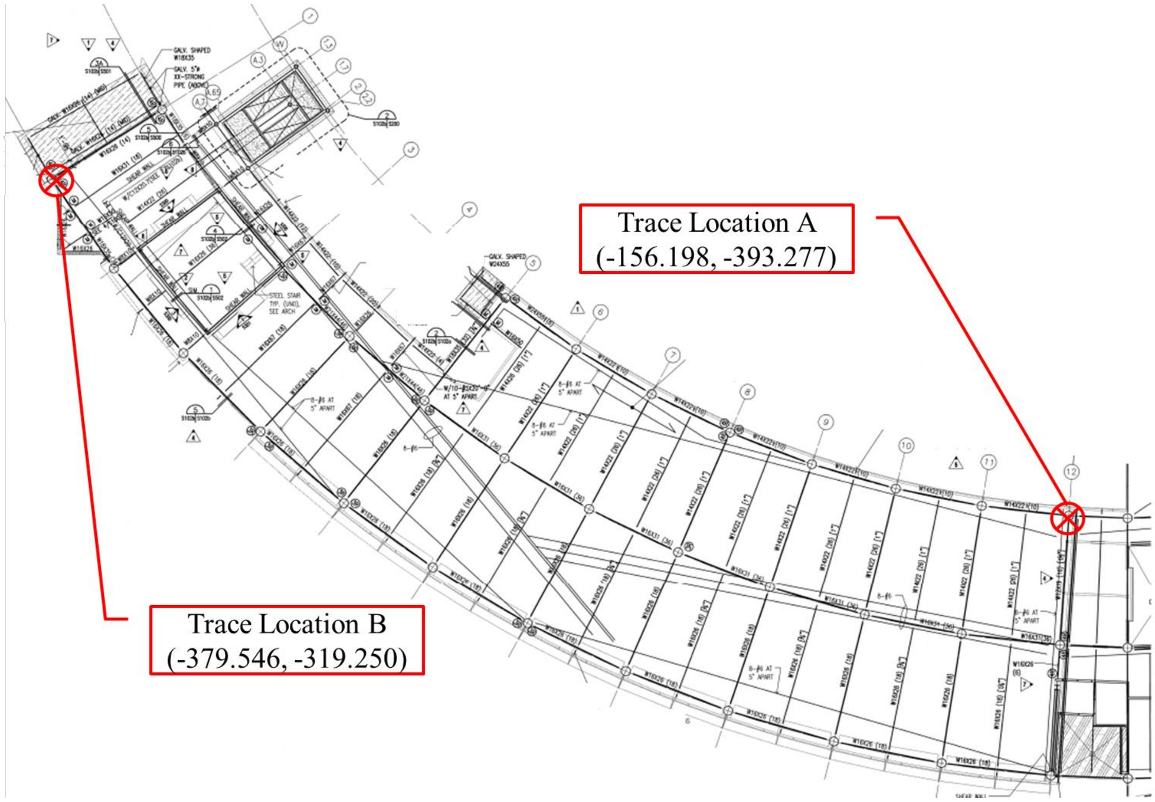


# APPENDIX D

## MECHANICAL AND ENVELOPE BREADTH

## APPENDIX D.1 – THERMAL BRIDGE STUDY

### Column Design

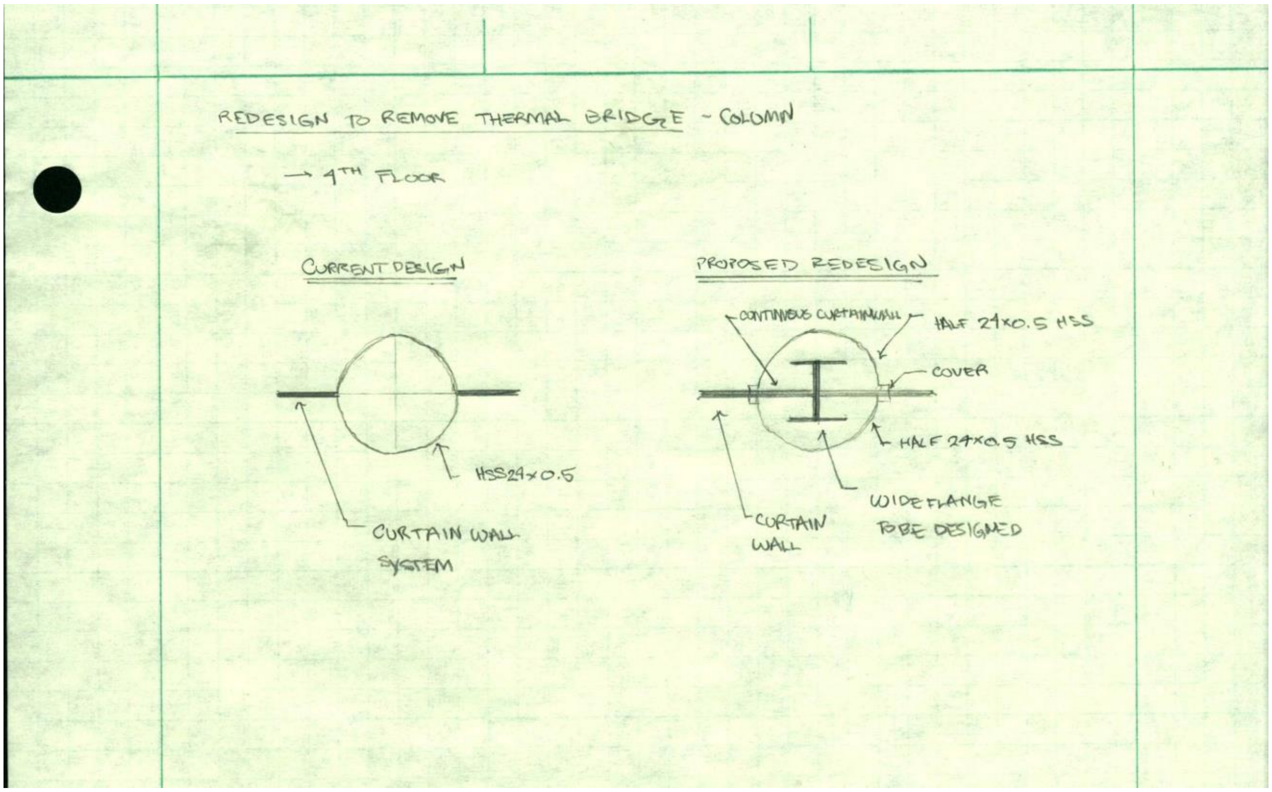

FROM PREVIOUS CALCS

PERIMETER BEAM 18.75K × 2 / FLOOR

QUEEN POST (ROOF) 14.5K

CONSERVATIVE CANTILEVERED AREA USED OF ROOF see below

CANTILEVERED ROOF LOADS (ASD)

30 PSF DL
20 PSF LL (SNOW) → 36 + 20 = 56 PSF

18.65' FOM ℄ COL. TO ℄ COL. → TRIB WIDTH ~19'

10' FOR LENGTH OF CANTILEVER

SO, 56 PSF × 19' = 1064 PLF ON CANTILEVER

R = V = wx = 1064 PLF × 10' = 10640 lb OR 10.64K FROM CANTILEVERED SECTION

NOW, 18.75K + 14.5K + 10.64K = 43.89K ~ 44K WITH AN UNBRACED LENGTH 10'

PER TABLE 4-1, W10x33 OR W12x40 @ 10' = $l_c$
220K (ASD) 265K (ASD)

WOULD BE SUFFICIENT → SMALLER WIDE FLANGES BUCKLE MORE EASILY AND WERE NOT CONSIDERED...

# Worst Case Thermal Gradient

## Worst Case Condition

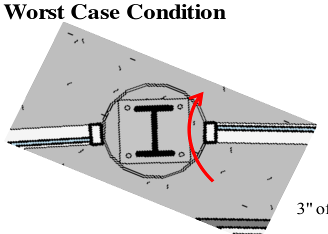

3" of insulation assumed

Let's say:

$T_i$ = 70
$T_o$ = 10
$T_i - T_o$ = 60
$T_{dp}$ = 14.69

**Redesigned System**

| | Material | Depth (in) | R (BTU-in/h-ft$^2$-°F) | U (1/R) | $\sum R_{o-x}$ | $T_x$ | Reference |
|---|---|---|---|---|---|---|---|
| 0 | Outside Air Film | - | 0.17 | 5.88 | 0.17 | 10.82 | |
| 0.5 | Aluminum Composite | 0.5 | 0.06 | 15.86 | 0.23 | 11.12 | Almaxco - Aluminum Compsite Panels |
| 3.5 | Batt Insulation | 3 | 11.45 | 0.09 | 11.69 | 66.41 | Owens Corning Insulation Systems, LLC |
| 4 | Aluminum Composite | 0.5 | 0.06 | 15.86 | 11.75 | 66.72 | Almaxco - Aluminum Compsite Panels |
| 4 | Inside Air Film | - | 0.68 | 1.47 | 12.43 | 70.00 | |
| | | Sum | 12.43 | 0.08 | | | |

**Existing System**ǂ

| | Material | Depth (in) | R (BTU-in/h-ft$^2$-°F) | U (1/R) | $\sum R_{o-x}$ | $T_x$ | Reference |
|---|---|---|---|---|---|---|---|
| 0 | Outside Air Film | - | 0.17 | 5.88 | 0.17 | 11.91 | |
| 0.5 | HSS Steel | 0.5 | 2.24 | 0.45 | 2.41 | 37.12 | Wolfram Alpha, LLC |
| 3.5 | Air | 23 | 0.00125 | 802.57 | 2.41 | 37.14 | Wolfram Alpha, LLC |
| 4 | HSS Steel | 0.5 | 2.24 | 0.45 | 4.65 | 62.35 | |
| 4 | Inside Air Film | - | 0.68 | 1.47 | 5.33 | 70.00 | Wolfram Alpha, LLC |
| | | Sum | 5.33 | 0.19 | | | |

ǂthis is really a thermal bridge

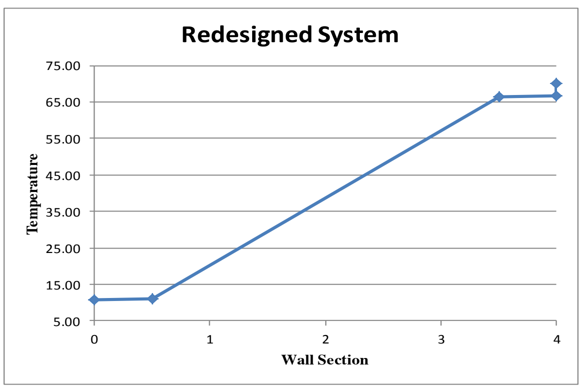


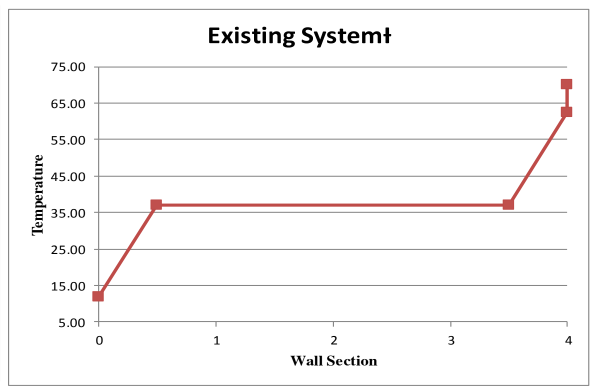

# Middle Case Thermal Gradient

**Middle Case Condition**

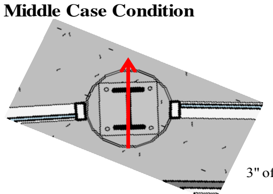

3" of insulation assumed

Let's say:

$T_i$ = 70
$T_o$ = 10
$T_i - T_o$ = 60
$T_{dp}$ = 14.69

**Redesigned System**

| | Material | Depth (in) | R (BTU-in/h-ft$^2$-°F) | U (1/R) | $\sum R_{o\text{-}x}$ | $T_x$ | Reference |
|---|---|---|---|---|---|---|---|
| 0 | Outside Air Film | - | 0.17 | 5.88 | 0.17 | 10.21 | |
| 0.5 | Aluminum Composite | 0.5 | 0.06 | 15.86 | 0.23 | 10.29 | Almaxco - Aluminum Compsite Panels |
| 6.5 | Batt Insulation | 6 | 22.91 | 0.04 | 23.14 | 38.32 | Owens Corning Insulation Systems, LLC |
| 17.5 | Wide Flange | 11 | 2.24 | 0.45 | 25.38 | 41.06 | |
| 23.5 | Batt Insulation | 6 | 22.91 | 0.04 | 48.29 | 69.09 | |
| 24 | Aluminum Composite | 0.5 | 0.06 | 15.86 | 48.35 | 69.17 | Almaxco - Aluminum Compsite Panels |
| 24 | Inside Air Film | - | 0.68 | 1.47 | 49.03 | 70.00 | |
| | | Sum | 49.03 | 0.02 | | | |

**Existing System‡**

| | Material | Depth (in) | R (BTU-in/h-ft$^2$-°F) | U (1/R) | $\sum R_{o\text{-}x}$ | $T_x$ | Reference |
|---|---|---|---|---|---|---|---|
| 0 | Outside Air Film | - | 0.17 | 5.88 | 0.17 | 11.91 | |
| 0.5 | HSS Steel | 0.5 | 2.24 | 0.45 | 2.41 | 37.12 | Wolfram Alpha, LLC |
| 23.5 | Air | 23 | 0.00125 | 802.57 | 2.41 | 37.14 | Wolfram Alpha, LLC |
| 24 | HSS Steel | 0.5 | 2.24 | 0.45 | 4.65 | 62.35 | |
| 24 | Inside Air Film | - | 0.68 | 1.47 | 5.33 | 70.00 | Wolfram Alpha, LLC |
| | | Sum | 5.33 | 0.19 | | | |

**‡this is really a thermal bridge**

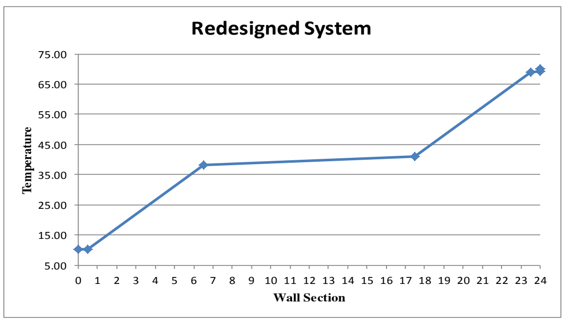


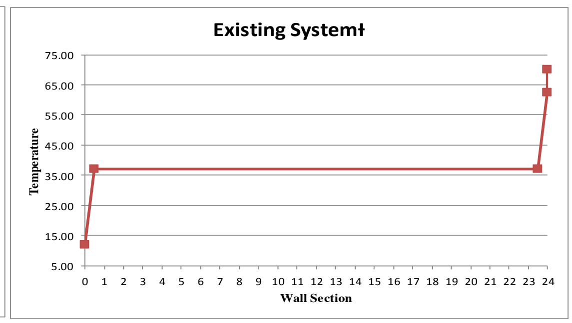

# ACADEMIC VITA

## SIKANDAR PORTER-GILL

1326 SOUTH PUGH ST,
STATE COLLEGE, PA 16801

sportergill@gmail.com | 240.505.4956

## EDUCATION

**The Pennsylvania State University** **University Park, PA**
*Integrated Bachelor and Master of Architectural Engineering* *Graduation, May 2014*
Structural Option | Five-year professional degree | ABET accredited
EIT Certified upon graduation | Schreyer Honors College

**The Tsinghua University** **Beijing, China**
*Summer School for International Construction* *Summer 2012*

**The University of Hong Kong** **Pokfulam, Hong Kong**
*The Department of Real Estate and Construction* *Summer 2012*

## WORK EXPERIENCE

**Penn State University** | Research and Education Institute **University Park, PA**
*Indeterminate Analysis and Computer Modeling Teaching Assistant* August 2013 – present

- Provide feedback to students by evaluating homework and exams

**Holbert Apple Associates, Inc.** | Structural Engineer Consultants **Washington D.C. Area**
*Engineering Intern* May 2013 – August 2013

- Performed analysis on existing framing and design of new framing, with limited site visits
- Reviewed shop drawings for concrete reinforcing and structural steel
- Prepared construction documents using AutoCAD and Revit
- Worked with RAM SBeam, spSlab, PROFIS, Enercalc and Decon STDesign

**Penn State University** | Research and Education Institute **University Park, PA**
*Undergraduate Researcher* | *Laboratory Scholar* January 2010 – May 2013

- Tested Structural Insulated Panels for intended wide spread use
- Examined formaldehyde reduction in buildings using gypsum dry board
- Engineered working models in RISA, ETABS and SAP 2000
- Managed ordering of project
- Conceptualized fuel cell productivity using printed biofilms on the electrode and examined immobilization of biofilms using latex substance

**Sustainable Design Group** | Design and Construction Firm **Gaithersburg, MD**
*Intern* May 2011 – August 2011

- Prepared construction documents for residential and business projects
- Evaluated sustainable design research for developing countries
- Oversaw permitting application for counties in Maryland and Virginia
- Worked with Graphisoft ArchiCAD 13/15, Photoshop CS.5, and Google Sketchup

## PUBLICATIONS

Wagner, R., Porter-Gill, S. “Immobilization of anode-attached microbes in a microbial fuel cell.” AMB Express. 2012.

Porter-Gill, S. “Overview of the Causes and Remediation of Sinkholes.” The American Society of Civil Engineers TCFE. 2013.